Agnieszka Ewa Smolińska

Opracowanie metody izolacji i długotrwałej hodowli subpopulacji pluripotencjalnych komórek macierzystych wywodzących się z mezenchymalnych komórek macierzystych/stromalnych izolowanych z galarety Whartona

Rozprawa na stopień naukowy doktora
w dziedzinie nauk medycznych i nauk o zdrowiu
w dyscyplinie nauki medyczne

Promotor: dr hab. Anna Sarnowska

Promotor pomocniczy: dr Marzena Zychowicz

Postępowanie w sprawie nadania stopnia doktora

w Instytucie Medycyny Doświadczalnej i Klinicznej
im. Mirosława Mossakowskiego PAN

Warszawa rok 2024

Niniejsza rozprawa doktorska nie powstałaby, gdyby nieoceniona pomoc wielu osób. Serdecznie chciałabym podziękować:

Dr hab. Annie Sarnowskiej,
za prowadzenie na naukowej ścieżce, poświęcony czas, mnóstwo rad oraz przekazaną wiedzę.

Dr Marzenie Zychowicz,
za cenne uwagi oraz pomoc w trakcie realizacji badań.

Ś.p. Prof. Krystynie Domańskiej-Janik,
za otrzymaną szansę pracy pod jej skrzydłami.

Koleżankom z Platformy Badań Translacyjnej,
za współpracę, miłą atmosferę oraz przyjemnie spędzony czas w Waszym towarzystwie.

Dr Wioletcie i Dr hab. Marcie z ZBKM oraz Koleżankom i Kolegom ze studiów doktoranckich IMDiK,
za okazane wsparcie i zrozumienie.

Przyjaciołom i wszystkim osobom życzliwym, które trzymały za mnie kciuki.

***Moim Najbliższym**: Mężowi, Rodzicom i Bratu.*

Za wszystko.

Bez Waszego wsparcia nie zaszłabym tak daleko.

Zbiór artykułów wchodzących w skład rozprawy doktorskiej:

I. Kaminska, A.; Wedzinska, A.; Kot, M.; Sarnowska, A. *Effect of Long-Term 3D Spheroid Culture on WJ-MSC*. Cells 2021, 10, 719. Doi: 10.3390/ cells10040719, 5-letni IF: 6.7.

II. Smolinska, A.; Chodkowska, M., Kominek, A.; Janiec, J.; Piwocka, K.; Sulejczak, D.; Sarnowska, A,. *Stemness properties of SSEA-4+ subpopulation isolated from heterogenous Wharton jelly mesenchymal stem/stromal cells*. Frontiers of Cell and Developmental Biology 2024, Doi: 10.3389/fcell.2024.1227034, 5-letni Imapct Factor: 6.079

III. Smolinska, A., Bzinkowska, A; Rybkowska, P.; Chodkowska, M.; Sarnowska, A.. *Promising markers in the context of mesenchymal stem/stromal cells subpopulations with unique properties*. Stem Cells International 2023, Doi: 10.1155/2023/1842958, 5-letni Impact Factor: 4,7

Badania, których wyniki przedstawiono w powyższych artykułach naukowych były finansowane w ramach następujących projektów naukowo-badawczych:

- grant OPUS finansowany przez Narodowe Centrum Nauki, nr 2018/31/B/NZ4/03172,
- grant PRELUDIUM finansowany przez Narodowe Centrum Nauki, nr 2022/45/N/NZ3/02564,
- środki z Programu Operacyjnego Wiedza Edukacja Rozwój 2014-2020 współfinansowanego ze środków EFS nr POWR.03.02.00-00-I028/17-00

NARODOWE CENTRUM NAUKI

Fundusze Europejskie Wiedza Edukacja Rozwój

Rzeczpospolita Polska

Unia Europejska Europejski Fundusz Społeczny

Spis treści

1. Wykaz skrótów

AD-MSC mezenchymalne komórki macierzyste/zrębowe pochodzące z tkanki tłuszczowej (*adipose derived mesenchymal stem/stromal cells);*

BDNF neurotroficzny czynnik pochodzenia mózgowego (*brain-derived neurotrophic factor*);

bFGF podstawowy czynnik wzrostu fibroblastów (*basal fibroblasts growth factor*);

BM-MSC mezenchymalne komórki macierzyste/zrębowe pochodzące ze szpiku kostnego (*bone marrow derived mesenchymal stem/stromal cells)*

CCL2 ligand chemokiny 2 (*chemokine ligand 2)*;

CFU jednostka tworząca kolonię (*colony forming unit*);

DFAT odróżnicowane komórki tłuszczowe (*dedifferentiated fat cells*);

EGF nabłonkowy czynnik wzrostu (*epitelial growth factor*);

EMT przejście nabłonkowo-mezenchymalne (*epithelial-to-mesenchymal transition*);

ESC zarodkowe komórki macierzyste (*embryonic stem cells*);

FACS sortowanie komórek aktywowane fluorescencyjnnie *(Fluorescence-Activated Cell Sorting)*;

GDNF czynnik wzrostu pochodzenia glejowego *(glial cell line-derived neurotrophic factor)*;

HGF czynnik wzrostu hepatocytów (*hepatocyte growth factor)*;

iPSC indukowane pluripotencjalne komórki macierzyste (*induced pluripotent stem cells*);

ISCT Międzynarodowe Towarzystwo Terapii Komórkowej (*International Society for Cellular and Gene Therapy*);

KM komórki macierzyste;

LPM somatyczna mezoderma boczna (*somatic lateral plate mesoderm*);

MACS sortowanie komórek aktywowane magnetycznie (*Magnetic Activated Cell Sorting*);

MET przejście mezenchymalne-nabłonkowe (*mesenchymal to epithelial transition*);

MSC mezenchymalne komórki macierzyste/zrębowe (*mesenchymal stem/stromal cells);*

MUSE Cells wieloliniowe komórki różnicujące się pod wpływem stresu (*multi-lineage differentiating stress enduring cells*);

NCSC komórki macierzyste pochodzące z grzebienia neuralnego (*neural crest derived stem cells*);

NSC neuralne komórki macierzyste (*neural stem cells*);

PDT czas podwojenia populacji *(population doubling time)*;

SRTF czynniki transkrypcyjne związane z macierzystością (*stemness-related transcritpion factors*);

SSEA swoisty powierzchniowy antygen zarodkowy (s*tage specific embryonic antigen*);

UC-MSC mezenchymalne komórki macierzyste/zrębowe pochodzące ze sznura pępowinowego (*umbilical cord derived mesenchymal stem cells)*;

VEGF czynnik wzrostu śródbłonka naczyniowego *(vascular endothelial growth factor*);

WJ-MSC mezenchymalne komórki macierzyste/zrębowe pochodzące z galarety Whartona (*Wharton Jelly derived mesenchymal stem cells)*;

2. Streszczenie polskojęzyczne

Komórki macierzyste (KM) stanowią podstawę tzw. terapii komórkowej stosowanej w medycynie regeneracyjnej. Jej pierwotnym założeniem miało być zastąpienie uszkodzonych komórek nowymi, wywodzącymi się z przeszczepionych KM, zdolnymi do funkcjonalnego różnicowania. Największą potencję w tym kierunku posiadają komórki o charakterze pluripotencjalnym, tzn. takie które wykazują zdolność od różnicowania w funkcjonalne komórki wywodzące się z wszystkich trzech listków zarodkowych (ektodermy, mezodermy oraz endodermy). Do komórek pluripotencjalnych należą zarodkowe komórki macierzyste (*embryonic stem cells*. ESC) oraz indukowane pluripotencjalne komórki macierzyste (*induced pluripotent stem cells,* iPSC). Jednakże ich szeroki potencjał do różnicowania wiąże się także ze zdolnością do nieograniczonej proliferacji, a co za tym idzie – ryzykiem tumorogenezy. Jako alternatywę proponuje się stosowanie dorosłych (somatycznych) KM, które niestety cechuje węższy potencjał do różnicowania, ograniczony zazwyczaj do jednego z listków zarodkowych. Jedną z szeroko badanych grup somatycznych KM są mezenchymalne komórki macierzyste/zrębowe (MSC). Są one klasyfikowane jako multipotencjalne ze względu na zdolność do różnicowania w komórki wywodzące się z mezodermalnego listka zarodkowego, tj. osteocyty, chondrocyty i adipocyty. Jednakże badacze donoszą o możliwości różnicowania MSC w komórki wywodzące się z innych listków zarodkowych, np. w neurony (wywodzące się z ektodermy) czy w hepatocyty (wywodzące się z endodermy). Dodatkowo, pod wpływem określonych warunków środowiskowych MSC wykazują ekspresję genów typowych dla komórek pluripotencjalnych, choć na znacznie niższym poziomie. Te nietypowe dla komórek multipotencjalnych cechy tłumaczone są wysoką heterogennością populacji MSC i obecnością komórek o bardzo różnym stopniu zróżnicowania. Inna z proponowanych teorii tłumaczy obserwowane zjawisko odmiennym pochodzeniem rozwojowym pojedynczych komórek w stosunku do całej populacji, które zasiedliły mezenchymę w wyniku migracji z innych struktur, np. cewy nerwowej.

W niniejszej rozprawie doktorskiej podjęto próbę zweryfikowania hipotezy badawczej dotyczącej obecności subpopulacji komórek o charakterze pluripotencjalnym w heterogennej populacji MSC. W ramach pracy analizowano czynniki pozwalające

na wyodrębnienie komórek przejawiających niezróżnicowany charakter, cechujących się wysokim potencjałem do proliferacji i samoodnowy, podwyższoną ekspresją genów pluripotencjalnych (*SOX2, OCT3/4, NANOG*) w stosunku do populacji wyjściowej MSC oraz zdolnością do różnicowania w kierunku komórek wywodzących się ze wszystkich trzech listków zarodkowych.

Głównym celem prowadzonych badań było wyznaczenie metody pozwalającej na izolację spośród MSC oraz dalszą hodowlę poszukiwanej subpopulacji. Jako źródło MSC wybrano tkankę popłodu – galaretę Whartona (WJ-MSC), stromę sznura pępowinowego, która jest rozwojowo młodą tkanką, traktowaną jako odpad medyczny.

Na podstawie literatury zdecydowano się uwzględnić dwie techniki uzyskiwania poszukiwanej subpopulacji. Pierwszą z nich była zmiana warunków przestrzennych hodowli z 2D na 3D. Zdolność do wzrostu i proliferacji w warunkach przestrzenna (w sferach) charakteryzuje m.in. komórki pluripotencjalne. Drugą stosowaną techniką była izolacja subpopulacji metodą sortowania, w której wykorzystano marker powierzchniowy SSEA-4, wybrany po pierwszym etapie badań i występujący na powierzchni komórek pluripotencjalnych.

W pierwszym etapie badań,WJ-MSC, standardowo hodowane w warunkach adhezyjnych (2D), zostały przeniesione do warunków 3D, modyfikując metodę stosowaną w hodowli neuralnych komórek macierzystych (NSC) w postaci sfer. Hodowlę 3D prowadzono przez 20 dni w celu wyodrębnienia komórek o lepszej zdolności do przeżycia i proliferacji, które potencjalnie mogłyby wykazywać cechy komórek pluripotencjalnych. Długotrwała hodowla WJ-MSC w warunkach 3D okazała się czynnikiem stresogennym, prowadzącym do zwiększonej śmiertelności komórek, spowolnienia ich proliferacji, spadku zdolności do tworzenia kolonii oraz przyspieszenia procesów starzenia. Nie zauważono wzrostu ekspresji genów pluripotencjalnych, natomiast obserwowano wzrost ekspresji genów oraz markerów neuralnych. Jednocześnie stwierdzono, że w trakcie długotrwałej hodowli 3D znacząco lepszą przeżywalność wykazała subpopulacja WJ-MSC ekspresjonująca antygen powierzchniowy SSEA-4.

W oparciu o uzyskane wyniki, w drugim etapie prowadzonych badań zdecydowano się wyizolować i scharakteryzować WJ-MSC wykazujące ekspresję SSEA-4 jako potencjalną

subpopulację komórek o szerszych zdolnościach do różnicowania. Poszukiwane komórki wyodrębniono z wykorzystaniem techniki sortowania komórek aktywowanego fluorescencyjnie (FACS). Otrzymana subpopulacja charakteryzowała się znacznie podwyższonym odsetkiem komórek SSEA-4+, który utrzymywał się przez 6 kolejnych pasaży hodowli komórkowej. Analiza subpopulacji SSEA-4+ wykazywała wyższą ekspresję genów pluripotencjalnych na początkowym etapie hodowli komórkowej w stosunku do populacji wyjściowej. Niestety, z czasem ekspresja tych genów spadła do poziomu obserwowanego w populacji niesortowanej. Przeanalizowano również właściwości funkcjonalne wyodrębnionej subpopulacji. Komórki SSEA-4+ przejawiały zdolność do tworzenia sfer, których średnica była mniejsza w stosunku do sfer utworzonych przez komórki populacji wyjściowej, a także zawierały znacząco więcej żywych komórek. Populacja SSEA-4+ nie różniła się zdolnością do różnicowania w kierunku trzech listków zarodkowych, tempem proliferacji oraz klonogennością od populacji niesortowanej oraz negatywnej (SSEA-4-). Zbadano również współwystępowanie SSEA-4 z innymi markerami kojarzonymi z właściwościami macierzystymi komórek, takimi jak: CD49F, CD133, CD146 czy CD271 - nie wykryto współzależności. Na podstawie otrzymanych wyników nie potwierdzono szerszego potencjału do różnicowania subpopulacji komórek SSEA-4+. Jednakże, otrzymana subpopulacja wyróżniała się odmiennym profilem sekrecyjnym w stosunku do populacji wyjściowej i populacji negatywnej, co może wskazywać na jej inne potencjalne wykorzystanie w medycynie regeneracyjnej.

Podsumowując, na podstawie zaproponowanych metod nie wyodrębniono subpopulacji komórek o cechach pluripotencjalnych. Otrzymane wyniki wskazują jednak na znaczną heterogenność morfologiczną i funkcjonalną populacji MSC. Wyodrębnianie poszczególnych grup komórek oraz szczegółowa analiza ich właściwości terapeutycznych wymagają dalszych badań.

3. Streszczenie angielskojęzyczne

Stem cells (SCs) are the basis of cellular therapies, widely used in regenerative medicine. Its main purpose is the replacement of injured cells by SCs provided with transplantation, that are capable to fully regenerate the tissue. The most desirable cells are pluripotent, i.e. those from which cells derived from all three embryonic germ layers can be derived, such as embryonic stem cells (ESCs) and induced pluripotent stem cells (iPSCs). However, observed wide differentiation potential is connected with limitless proliferation capacities and risks of tumorogenesis. Adult (somatic) SCs are proposed as an alternative, even though their narrow differentiation potential, usually limited to cells from one embryonic gem layer. Mesenchymal stem/stromal cells (MSCs) are one of frequently studied adults SCs group, classified as multipotent, due to differentiational potential toward mesodermal cells i.e. osteocytes, chondrocytes and adipocytes. However, researchers reported the possibility of MSCs differentiating into cells derived from other germ layers, such as neurons (ectoderm) or hepatocytes (endoderm). Furthermore, under specific environmental conditions, MSCs exhibit the expression of pluripotency-related genes, but observed levels are still lower than reported for ESCs or iPSCs. Due to the high heterogeneity of MSCs population, there could be found cells with different differentiation potentials. It is proposed that those undifferentiated cells possess different developmental origin, i.e. originate from neural crest, what would explain their unique properties.

Hereby, this dissertation attempted a verification whether MSCs could contain subpopulation exhibiting pluripotent characteristics. Conducted experiments examined different factors for separation of cells possessing undifferentiated potential, that exhibit high proliferation and self-renewal potentials, elevated pluripotent genes expression (*SOX2, OCT3/4, NANOG*) and differentiate toward cells from all three embryonic germ layers.

The main purpose of described research was the development of efficient method to isolation and further cell culture of potential subpopulation exhibiting pluripotent features from MSCs. MSCs were isolated from Wharton Jelly (WJ-MSCs) – a part of umbilical cord which is a commonly used MSCs source.

Based on the recent literature, two potential methods for separation were chosen to derive the desired subpopulation. First approach was to change spatial condition of cell culture from 2D to 3D, associated with sphere-forming ability of pluripotent cells. Second approach was to isolate subpopulation expressing surface antigen SSEA-4, occurring in pluripotent cells.

During the first stage of doctoral research, WJ-MSCs, usually propagated in adherent 2D conditions, were transferred to 3D conditions, by modification of culture method proposed for neural stem cells. 3D culture was conducted for about 20 days *in vitro* to select cells with better survivability in harsh conditions; such cells could exhibit properties of pluripotent cells. However, long-term 3D culture was stressogenic for WJ-MSC , leading to slowed cell division ratio, reduced colony forming frequency and acceleration of senescence processes. Increase of pluripotent gene expression was not observed, while expression of markers connected with neural tissue was elevated. There was also reported that SSEA-4-positive cells exhibited better survival under long-termed 3D culture condition.

Based on received results, WJ-MSC positive for SSEA-4 were isolated and characterized as a theoretic population with a wider potential, during the second stage of doctoral research. This subpopulation was selected with fluorescence-activated cell sorting (FACS). Received positive population (WJ-MSC-SSEA-4+) contained significantly more SSEA-4+ cells for the next 6 passages of further in vitro culture. WJ-MSC-SSEA-+ population exhibited transient increase of pluripotent genes, that was reported directly after separation but diminished with further cell culturing. Other functional properties of isolated subpopulation were analyzed as well. WJ-MSC-SSEA-4+ cells formed spheroids upon 3D initiating conditions, that were smaller and contained more number of alive cells, compared to unsorted and negative populations (WJ-MSC-SSEA-4-). WJ-MSC-SSEA-4+ cells did not differed with tri-germ layer differentiational potential, proliferation and clonogenicity from initial and negative populations. SSEA-4 expression was not associated with other stemness markers such as CD49F, CD133, CD146 and CD271. According to the received results, SSEA-4+ population's pluripotent character was not confirmed. However, studied subpopulation could be applied for other therapeutic purposes due to their unique secretome profile.

In summary, presence of pluripotent-like subpopulation in WJ-MSC was not confirmed by chosen methods. However, observed results indicated a wide heterogeneity and diversity of subpopulations constituting to MSCs. Selection and detailed analysis of specific cell groups demand further research to relate their therapeutic applications.

4. Innowacyjność rozprawy

Innowacyjność niniejszej rozprawy polega na próbie weryfikacji hipotezy dotyczącej obecności subpopulacji komórek o cechach pluripotencjalnych wśród mezenchymalnych komórek macierzystych/zrębowych (MSC). Hipoteza ta oparta jest na wysokiej heterogenności analizowanej populacji MSC, zawierającej komórki o różnym stopniu zróżnicowania – od komórek progenitorowych: preadipocytów i prechondro-osteoblastów po komórki niezróżnicowane, które zachowały macierzysty charakter. Jednym z proponowanych wyjaśnień hipotezy jest niejednorodne pochodzenie rozwojowe tej grupy komórek. Według doniesień literaturowych, MSC częściowo wywodzą się z somatycznej mezodermy bocznej i w trakcie rozwoju przechodzą rundy zmian, zwane przejściem nabłonkowo-mezenchymalnym, jak również i procesom odwrotnym, zwanym przejściem mezenchymalno-nabłonkowym. Dodatkowo, wśród MSC odnajduje się komórki o pochodzeniu ektodermalnym, wywodzące się prawdopodobnie z grzebienia nerwowego (*Neural Crest derived Stem Cells*, NCSC), które w trakcie rozwoju zarodkowego odbywają migrację z cewy nerwowej i rozprzestrzeniają się po całym organizmie. Obydwa zjawiska mogłyby tłumaczyć zdolność MSC do różnicowania się w komórki pochodzące z pozostałych listków zarodkowych.

Obecnie brakuje jednoznacznych markerów lub technik pozwalających na wyodrębnienie z MSC potencjalnej subpopulacji wykazującej cechy pluripotencjalne. Jednym z proponowanych podejść jest zmiana warunków środowiskowych z hodowli 2D na hodowlę 3D, która jest bliższa strukturze natywnej tkanki oraz powszechnie stosowana przy hodowli pluripotencjalnych komórek macierzystych. Innym podejściem jest wyodrębnienie markera, który umożliwiłby odróżnienie MSC o zachowanych cechach macierzystości od całej heterogennej populacji komórek zrębowych. Do takich kandydatów należą m.in.: antygeny z rodziny SSEA, CD271, CD146, CD133 czy CD49F.

W naszym projekcie rozpoczęliśmy doświadczenia od zmiany warunków przestrzennych hodowli MSC, aby wyselekcjonować komórki o odmiennych właściwościach, typowych dla komórek niezróżnicowanych. W tym celu opracowaliśmy metodę hodowli 3D opartą na tworzeniu sferoidów MSC. W kolejnym kroku przeanalizowaliśmy zmiany jakie zachodzą w populacji MSC w czasie jej długotrwałej hodowli przestrzennej. W wyniku doświadczeń wyodrębniliśmy populację komórek o wyższej przeżywalności w warunkach

3D. Komórki te wykazywały podwyższoną ekspresję markera SSEA-4. W oparciu o otrzymane wyniki, podjęto próbę izolacji i charakterystyki subpopulacji MSC SSEA-4+. Otrzymana subpopulacja MSC-SSEA-4+ bezpośrednio po wyizolowaniu wykazywała zwiększoną ekspresję genów typowych dla komórek pluripotencjalnych, natomiast w miarę prowadzenia hodowli komórkowej ekspresja tych genów malała do poziomu obserwowanego w heterogennej, wyjściowej populacji MSC. Ponadto komórki SSEA4-pozytywne nie wykazywały zdolności do różnicowania poza listek mezodermalny, ani podwyższonego potencjału proliferacyjnego i klonogennego. Czynnikiem wyróżniającym badaną subpopulację był profil wydzielniczy, odmienny w stosunku do populacji niesortowanej.

Rozprawę doktorską zamyka artykuł przeglądowy, zbierający najnowsze doniesienia dotyczące badań nad właściwościami terapeutycznymi poszczególnych subpopulacji, które można znaleźć wśród MSC. Znajduje się w nim obszerny podrozdział dotyczący markerów sugerujących niezróżnicowany charakter komórek, jak również podrozdział dotyczący markerów wskazujących na bardziej wyspecjalizowane funkcje komórek w populacji. Przegląd literatury wyraźnie wskazuje na potrzebę dalszych, pogłębionych badań w temacie analizy poszczególnych subpopulacji tworzących MSC.

5. Wstęp

5.1. Komórki macierzyste i terapia komórkowa

Poszukiwania metod leczenia trwałego uszkodzenia narządów i tkanek w wyniku urazów lub chorób przewlekłych i degeneracyjnych doprowadziły do rozpoczęcia stosowania komórek macierzystych (KM), zapoczątkowując medycynę regeneracyjną oraz inżynierię tkankową. KM charakteryzują się zdolnością do samoodnowy dzięki możliwości asymetrycznych podziałów komórkowych oraz zdolnością do różnicowania w inne typy komórek [1, 2]. Z powyższych powodów, terapie komórkowe mogą być alternatywą dla transplantologii, a także stanowić nowe podejście terapeutyczne np. w leczeniu chorób neurodegeneracyjnych. Ze względu na potencjał do różnicowania KM dzielimy na: totipotencjalne, pluripotencjalne, multipotencjalne i unipotencjalne (**Rycina 1**).

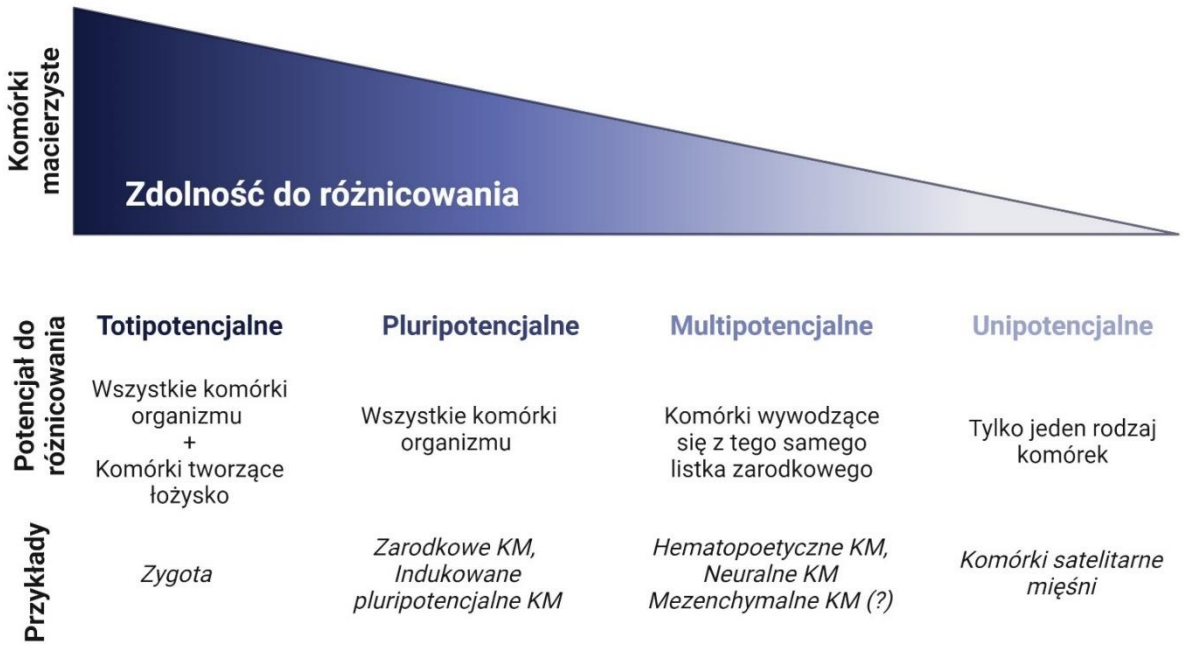

Rycina 1. *Podział komórek macierzystych (KM) pod kątem zdolności do różnicowania, tzw. potencjału.*

KM można również podzielić ze względu na źródło pochodzenia na zarodkowe i somatyczne. W dorosłym organizmie, w niszach poszczególnych tkanek, rezydują specyficzne somatyczne KM, zasiedlając je już podczas rozwoju płodowego [3–5]. Odpowiedzialne są one za endogenne procesy naprawcze i utrzymanie homeostazy w organizmie [4, 5]. Pozostają one w tzw. stanie uśpienia, a ich różnicowanie jest

wyzwalane w wyniku tkankowych sygnałów środowiskowych, prowadząc do zastąpienia utraconych, zróżnicowanych komórek [3]. Somatyczne KM (zwane też dorosłymi KM) mają ograniczony potencjał do różnicowania i zazwyczaj są multipotencjalne.

Niestety, w części przypadków klinicznych endogenne procesy zastępowania komórek są niewystarczające ze względu na zbyt rozległe uszkodzenia, niewielką pulę KM rezydujących w niszy lub ich utratę w wyniku choroby. Z tego powodu głównym celem terapii komórkowej jest dostarczenie nowej puli KM i wspomaganie endogennych procesów naprawczych. W tym celu najbardziej pożądane jest podanie komórek o cechach pluripotencjalnych, z których można uzyskać komórki wywodzące się z wszystkich trzech listków zarodkowych: ektodermy, mezodermy i endodermy, a co za tym idzie komórki dowolnej tkanki. Zalicza się do nich zarodkowe komórki macierzyste (*embryonic stem cells*. ESC) i indukowane pluripotencjalne komórki macierzyste (*induced pluripotent stem cells,* iPSC). Stosowanie ludzkich ESC jest mocno ograniczone m.in. z powodów etycznych [6, 7]. Z kolei proces uzyskiwania iPSC nadal pozostaje długi i kosztowny [2]. Ze względu na swój pluripotencjalny charakter, stosowanie w terapii ESC i iPSC bez zapewnienia ich pełnego zróżnicowania jest również obarczone ryzykiem nowotworzenia [7]. Pomimo rozpoczętych badań klinicznych z wykorzystaniem zróżnicowanych komórek iPSC [8], poszukuje się alternatywnych źródeł KM dla terapii komórkowych. Dużą uwagę badaczy skupiają somatyczne KM, izolowane z dorosłych tkanek organizmu, a jedną z proponowanych grup komórek są multipotencjalne mezenchymalne komórki macierzyste/zrębowe (MSC).

5.2. Mezenchymalne komórki macierzyste/zrębowe – definicja i właściwości

Początkowo MSC zostały zidentyfikowane w zrębie szpiku kostnego w 1968 roku przez Friedensteina i współpracowników [9], natomiast w 1991 roku Arnold Caplain po raz pierwszy nadał im obecnie stosowaną nazwę i zaproponował ich wykorzystanie w terapii [10]. Oprócz szpiku kostnego (BM-MSC), MSC zidentyfikowano m.in.: w tkance tłuszczowej (AD-MSC), miazdze zębowej, skórze właściwej, błonie maziowej stawów, mleku matczynym oraz w narządach okołoporodowych, takich jak sznur pępowinowy (UC-MSC), płyn owodniowy i łożysko [11]. Według zaleceń Międzynarodowego Towarzystwa Terapii Komórkowej (*International Society for Cellular and Gene Therapy*, ISCT) z roku 2010 MSC muszą charakteryzować się [12]:

- pozytywną ekspresją markerów powierzchniowych: CD73, CD90 i CD105 oraz negatywną ekspresją markerów powierzchniowych – CD34, CD45, CD11a, CD19 lub CD79α, CD14 lub CD11b i cząsteczek HLA-DR,
- zdolnością przylegania do powierzchni plastikowej oraz zdolnością tworzenia kolonii, których morfologia podobna jest do fibroblastów,
- zdolnością do różnicowania w warunkach *in vitro* w osteocyty, chondrocyty i adipocyty.

Obecnie toczą się spory w temacie nomenklatury MSC, czy faktycznie można zaliczyć je do komórek macierzystych. Zaproponowano, aby określać je mianem *zrębowych* bądź *stromalnych,* czyli wspierających tkankę [13]. ISCT w 2019 roku opublikowało sugestie, wedle których [14]:

- w charakterystyce komórek powinno zostać wspomniane tkankowe źródło pochodzenia komórek,
- stwierdzenie *macierzyste* powinno zostać wykorzystane tylko w przypadku dostarczenia dowodów na zdolność samoodnowy i różnicowania w warunkach *in vitro* i *in vivo,*
- zalecone zostało przeprowadzenie dodatkowych testów funkcjonalnych, które potwierdziłyby dodatkowe właściwości terapeutyczne MSC.

Z tego względu w niniejszej rozprawie w odniesieniu do badanych komórek mezenchymalnych użyto sformułowania *macierzyste/zrębowe*.

MSC znajdują się w kręgu zainteresowań badaczy głównie ze względu na silne właściwości immunomodulacyjne [15], zdolności wydzielnicze [16, 17] oraz zdolności do różnicowania. Jak wcześniej wspomniano, MSC różnicują w komórki tkanki łącznej (osteocyty, adipocyty oraz chondrocyty), ale udało się również uzyskać inne komórki o pochodzeniu mezodermalnym, takie jak komórki mięśni, ścięgien i więzadeł [17]. Mimo zaklasyfikowania MSC jako komórki multipotencjalne, doniesienia naukowe wskazują na ich zdolności do trans-różnicowania – różnicowania w komórki wywodzące się z innych listków zarodkowych, na przykład ektodermy (neurony) [18] czy endodermy (hepatocyty) [19] (**Rycina 2**).

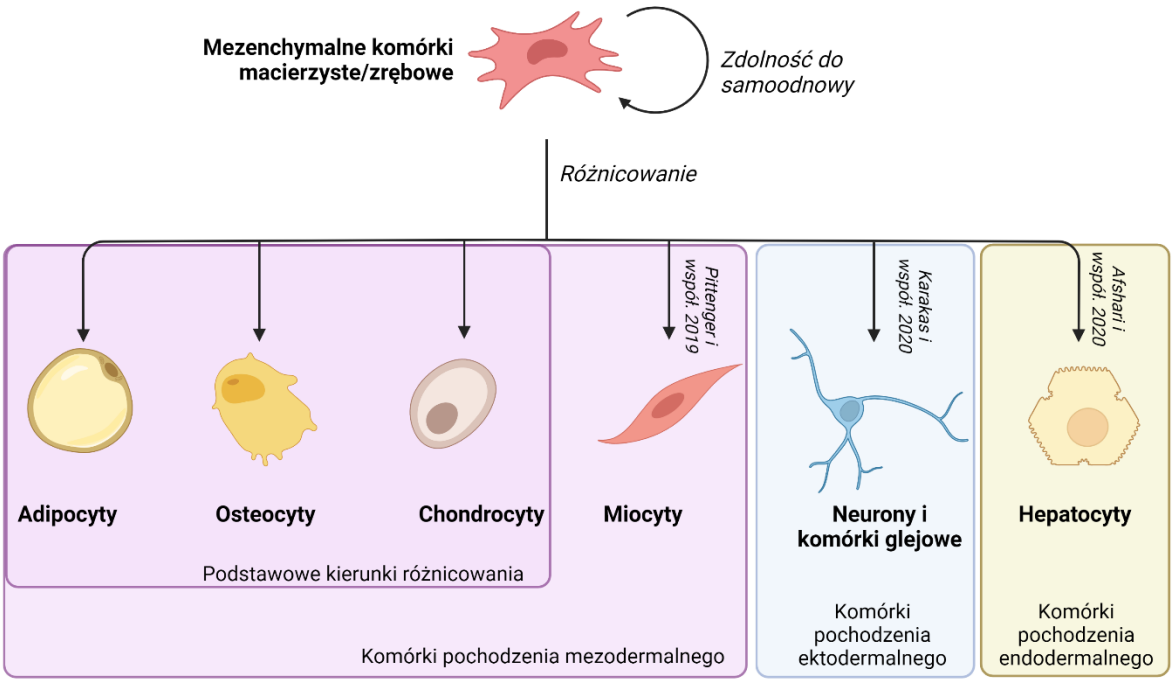

Rycina 2. *Możliwe kierunki różnicowania mezenchymalnych komórek macierzystych/zrębowych (MSC). Oprócz podstawowych kierunków różnicowania w komórki pochodzenia mezodermalnego, wymaganych przez ISCT, badacze wskazują na możliwość trans-różnicowania MSC w kierunku komórek wywodzących się z innych listków zarodkowych (źródła:*[17–19]*).*

5.3. Przesłanki świadczące o istnieniu subpopulacji MSC o cechach pluripotencjalnych

Wyjaśnienie fenomenu różnicowania MSC w komórki wywodzące się spoza mezodermy mogłoby umożliwić ich zastosowanie jako alternatywy dla komórek pluripotencjalnych w terapiach komórkowych. Wysoka heterogenność populacji MSC jest obserwowana na wielu poziomach i zależy od czynników zewnętrznych takich jak zmienność pomiędzy dawcami komórek, tkankami źródłowymi i sposobami hodowli komórkowej oraz czynników wewnętrznych takich jak obecność klonów o różnym profilu ekspresji genów czy plastyczność fenotypu MSC [20, 21]. Badania transkryptomu na poziomie pojedynczej komórki wykazały, że populacja MSC składa się z subpopulacji różniących się między sobą stopniem zróżnicowania – od komórek niezróżnicowanych do komórek progenitorowych: unipotentnych preadipocytów i bipotentnych prechondro-osteoblastów [22]. To właśnie te pierwsze z wymienionych, komórki wykazujące niezróżnicowany, prymitywny charakter, mogą posiadać zdolność do samoodnowy i różnicowania poza jeden listek zarodkowy w odróżnieniu od pozostałych komórek zrębowych tworzących populację MSC.

Powodem heterogenności MSC może być ich niejednorodne pochodzenie, które pozostaje niewyjaśnione mimo wielu lat badań. Według badaczy somatyczna mezoderma boczna (*somatic lateral plate mesoderm,* LPM) jest głównym źródłem MSC [23]. Komórki LPM przechodzą szereg zmian, zwanych przejściem nabłonkowo-mezenchymalnym (*epithelial-to-mesenchymal transition,* EMT) oraz przejściem mezenchymalno-nabłonkowym (*mesenchymal to epithelial transition*, MET) [23]. Komórki mogą przejść wiele rund EMT-MET zanim osiągną swój docelowy stan zróżnicowania. Istnieją również doniesienia wskazujące na inne pochodzenie MSC – z grzebienia neuralnego, który pojawia się w trakcie rozwoju cewy nerwowej [24]. W wyniku EMT, komórki grzebienia neuralnego, wykazujące ekspresję genów z rodziny *SOX*, *SNAIL* i *FOXD3* oddzielają się od fałdów nerwowych i migrują w rozwijającym się organizmie [25, 26]. Komórki macierzyste pochodzące z grzebienia neuralnego (*Neural Crest derived stem cells,* NCSC) różnicują w komórki neuralne, a potem neurony i komórki glejowe, a także komórki neuroendokrynne, melanocyty czy komórki szkieletu twarzoczaszki [27]. Zachodzące procesy rozwojowe mogłyby tłumaczyć obecność komórek o charakterystyce MSC

w ektodermalnej tkance miazgi zębowej [28]. Co więcej, NCSC zostały także zidentyfikowane w szpiku kostnym czy tkance tłuszczowej [27, 29], co sugeruje możliwość częściowego wywodzenia się subpopulacji MSC z grzebienia neuralnego. Opisywane zjawisko mogłoby tłumaczyć nietypowe właściwości MSC opisywane przez różne grupy badawcze, w tym różnicowanie w komórki ekto- i endodermy.

Przesłanką świadczącą o istnieniu komórek o charakterze pluripotencjalnym wśród MSC jest ekspresja markerów charakterystycznych dla komórek pluripotencjalnych, tzw. czynników transkrypcyjnych związanych z macierzystością (*Stemness-related transcrutpion factors,* SRTF) takich jak *SOX2, OCT3/4, NANOG* i *KLF4*, czy antygenów powierzchniowych z rodziny SSEA (*Specific Stage Embryonic Antigen*) np. SSEA-3 i SSEA-4 [30, 31]. MSC izolowane z tkanek młodszych rozwojowo, jak np. sznur pępowinowy, a zwłaszcza jego zrąb, tzw. galareta Whartona (WJ-MSC), charakteryzują się podwyższoną ekspresją wymienionych genów związanych z macierzystością oraz wyższym potencjałem proliferacyjnym i klonogennym [32–34]. Obserwowany w MSC poziom ekspresji tych markerów jest jednakże znacząco niższy niż prezentowany przez ESC czy iPSC [31, 35]. Korelując ekspresję opisywanych genów ze zdolnością komórek do różnicowania, poszukuje się czynników środowiskowych mogących zwiększyć lub utrzymać w trakcie hodowli tą ekspresję w komórkach somatycznych. Na utrzymanie ekspresji SRTF mogą mieć wpływ np. warunki hodowli *in vitro* takie jak obecność tlenu w stężeniu 5%, zbliżonym do panującego w wybranych narządach [30].

Innym, szeroko dyskutowanym sposobem na zwiększenie ekspresji SRTF jest zmiana środowiska przestrzennego hodowli komórkowej – ze standardowo stosowanych warunków 2D (tzw. hodowla adherenta) na warunki 3D [36]. Hodowla w formie agregatów zwanych sferami/sferoidami wpływa na zmianę morfologii komórki, reorganizację jej cytoszkieletu jak również wzrost ekspresji genów SRTF [36]. Zmianę warunków przestrzennych hodowli proponuje się jako sposób na utrzymanie komórek w stanie macierzystości lub selekcjowanie takich właśnie komórek spośród heterogennej populacji.

Również ogólnie zdefiniowane warunki stresogenne mogą przyczyniać się do wzrostu ekspresji SRTF. Potwierdzono ten efekt dla subpopulacji odróżnicowanych komórek tłuszczowych (*dedifferentiated fat cell,* DFAT), wyodrębnianych metodą hodowli odwrotnej/sufitowej [37]. Dla innych źródeł MSC nie udało się opisać metod uzyskiwania

odróżnicowanej populacji. Z tego powodu poszukuje się specyficznych markerów, preferencyjnie antygenów powierzchniowych, charakterystycznych dla komórek wczesnych rozwojowo, dzięki którym można byłoby wyodrębnić z ogólnej populacji subpopulację o wskazanym fenotypie za pomocą technik sortowania komórkowego.

Wśród markerów komórek o niezróżnicowanym charakterze proponowane są antygeny powierzchniowe z rodziny SSEA, które są obecne na powierzchni komórek w trakcie rozwoju zarodkowego [38]. Komórki SSEA-3+ izolowane z MSC i opisane przez grupę prof. M. Dezawy jako Muse cells (*Multi-lineage differentiating stress enduring cells*) wykazują ekspresję genów pluripotencjalnych oraz mają zdolność do różnicowania w komórki wszystkich listków zarodkowych zarówno w warunkach *in vitro* oraz *in vivo* [39, 40]. Jednocześnie, posiadając wielokierunkową zdolność do różnicowania, nie wykazują potencjału do nowotworzenia [40]. Jednakże populacja SSEA-3+ jest znikoma – waha się od 1 do 5% w zależności od źródła MSC. Alternatywnym markerem mógłby być antygen SSEA-4, który występuje liczniej w populacji MSC; w zależności od źródła komórek i warunków hodowli: od 5% do 85% [41–43]. Wykazano, że komórki SSEA-4+ wyodrębnione z populacji BM-MSC pochodzących od starszych pacjentów (powyżej 65 roku życia) posiadały cechy zbliżone do BM-MSC wyizolowanych od młodych dawców [44].

Dane literaturowe opisują obecność w populacji MSC również markera CD271 – receptora o niskim powinowactwie dla czynniku wzrostu nerwów [45], związanego z NCSC [27, 46]. W porównaniu do heterogennej populacji początkowej, MSC-CD271+ charakteryzują się się szybszym tempem proliferacji [42, 45], lepszą zdolnością do tworzenia kolonii i sfer [45, 47] oraz wykazują ekspresję genów pluripotentnych i neuralnych na wyższym poziomie [42, 48]. Część badaczy proponuje CD146 – cząsteczkę adhezji komórek czerniaka, jako poszukiwany marker. MSC-CD146+ izolowane z miazgi zębowej wykazują zwiększoną proliferację oraz lepszy potencjał do różnicowania [49]. Jednakże, inne badania pokazują, że marker CD146 może być związany z bardziej specyficzną subpopulacją MSC, odpowiedzialną za oddziaływania z komórkami śródbłonka naczyń oraz angiogenezą, a także odnową tkanki kostnej i remineralizacji [50–53]. Jako kandydaci dla markerów komórek niezróżnicowanych proponowane są także antygeny powierzchniowe, związane z innymi grupami komórek macierzystych

t.j.: CD49F – integryna α6 [54], CD349 – białko Frizzled-9 (ang. *frizzled* – kędzierzawy) [55], CD133 (prominina) [56] oraz Sca-1, który został zidentyfikowany tylko dla komórek mysich [57]. W przypadku MSC wykazujących obecność tych cząsteczek, obserwowano szybsze tempo proliferacji lub podwyższoną ekspresję genów SRTF. Potrzebne są jednak dokładniejsze analizy pomagające zweryfikować zdolność do wielokierunkowego różnicowania tych komórek. W ramach rozprawy doktorskiej zaprezentowano przegląd wyników uzyskanych przez inne zespoły badawcze w temacie poszukiwań dalszych potencjalnych antygenów powierzchniowych świadczących o unikalnych zdolnościach MSC, co zostało przedstawione w Artykule III [58].

W niniejszej rozprawie doktorskiej postanowiono zweryfikować hipotezę badawczą, która zakłada istnienie w heterogennej populacji mezenchymalnych komórek macierzystych/zrębowych subpopulacji komórek wykazujących zdolność do różnicowania w komórki wywodzące się z pozostałych listków zarodkowych. Zastosowanie wyselekcjonowanej subpopulacji o cechach pluripotencjalnych mogłoby stanowić przełom w medycynie regeneracyjnej. Potencjalna poszukiwana grupa komórek wykazywałaby lepszą klonogenność, wyższe tempo proliferacji, jak również zdolność do funkcjonalnego różnicowania w dowolną tkankę organizmu. Jednocześnie, w związku z późniejszym pochodzeniem ontogenetycznym niż zarodkowe, zdolność do wielokierunkowego różnicowania nie niosłaby ze sobą ryzyka nowotworzenia związanego z typową pluripotencjalnością. Ponieważ dotychczas nie udało się opracować metody izolacji komórek o charakterze niezróżnicowanym, uniwersalnej dla każdego źródła MSC, a także sposobu ich dalszego namnożenia, zagadnienie to zostało podjęte w niniejszej rozprawie.

6. Cel pracy doktorskiej

Głównym celem prowadzonych prac była identyfikacja, izolacja i charakterystyka subpopulacji wykazującej cechy pluripotencjalne, wywodzącej się z heterogennej populacji mezenchymalnych komórek macierzystych/zrębowych pochodzących z galarety Whartona.

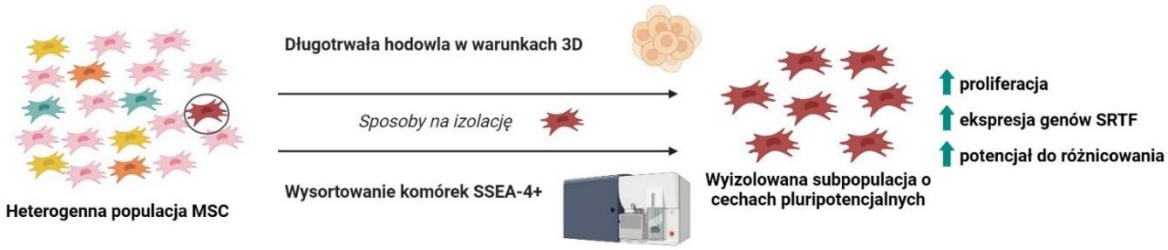

Rycina 3. *Schemat zaproponowanych podejść wyizolowania subpopulacji o cechach pluripotencjalnych spośród WJ-MSC, opisanych w ramach rozprawy doktorskiej.*

W przebiegu badań sformułowano następujące cele szczegółowe:

1. Wyodrębnienie i charakterystyka poszukiwanej subpopulacji w zmodyfikowanych przestrzennych warunkach środowiska (długotrwała hodowla 3D) (Artykuł I).

2. Wyodrębnienie i charakterystyka subpopulacji komórek wykazujących obecność swoistego powierzchniowego antygenu zarodkowego (SSEA-4) metodą sortowania komórkowego (Artykuł II).

3. Analiza potencjalnych właściwości pluripotencjalnych subpopulacji komórek SSEA-4-pozytywnych (Artykuł II).

7. Materiały i metody

Do przeprowadzenia zaplanowanych badań, jako źródło MSC wybrano galaretę Whartona. Jest to tkanka podporowa sznura pępowiny, traktowana jako odpad medyczny, zawierająca mezenchymalne komórki macierzyste/stromalne. W oparciu o wyniki wcześniej prowadzonych badań, MSC izolowano z galarety Whartona metodą mechaniczną [59], dzięki której uzyskane komórki wykazują wyższy potencjał proliferacyjny, wolniejsze tempo starzenia oraz wyjściowo wysoki potencjał klonogenny w porównaniu z komórkami otrzymanymi w procesie izolacji enzymatycznej. WJ-MSC wykorzystane w eksperymentach pochodziły z 3-5 pasażu hodowli komórkowej.

Badania do rozprawy doktorskiej zostały przeprowadzone w dwóch etapach:

1) W pierwszym etapie badań opracowano metodę hodowli WJ-MSC w formie sferoidów w celu wyodrębnienia komórek wykazujących lepszą zdolność do przeżycia w zmodyfikowanych warunkach środowiska. W tym celu zastosowano pożywkę hodowlaną wykorzystywaną do hodowli neuralnych komórek macierzystych (*neural stem cells,* NSC) oraz płytki o powierzchni antyadhezyjnej. Pożywka hodowlana nie zawierała lizatu płytkowego, ani innego źródła białka lub czynników troficznych, poza dodatkiem nabłonkowego czynnika wzrostu (*epitelial growth factor,* EGF) i podstawowego czynnika wzrostu fibroblastów (*basal fibroblasts growth factor,* bFGF). W 3 i 10 dniu hodowli przestrzennej oznaczono żywotność komórek. Po upływie 20 dni, przetrwałą populację WJ-MSC ponownie wysiano na powierzchnię 2D. W eksperymentach porównano: tempo proliferacji komórek (*population doubling time,* PDT), odsetek komórek tworzących kolonie (*colony forming unit,* CFU), proces starzenia komórkowego, ekspresję genów i białek typowych dla komórek pluripotencjalnych oraz neuralnych dla: heterogennej populacji wyjściowej WJ-MSC, populacji WJ-MSC stale hodowanej w warunkach adhezyjnych oraz subpopulacji WJ-MSC wyodrębnionej w czasie hodowli 3D (**Rycina 4**).

Materiały i metody wykorzystane w tym etapie badań zostały szczegółowo opisane w Artykule I.

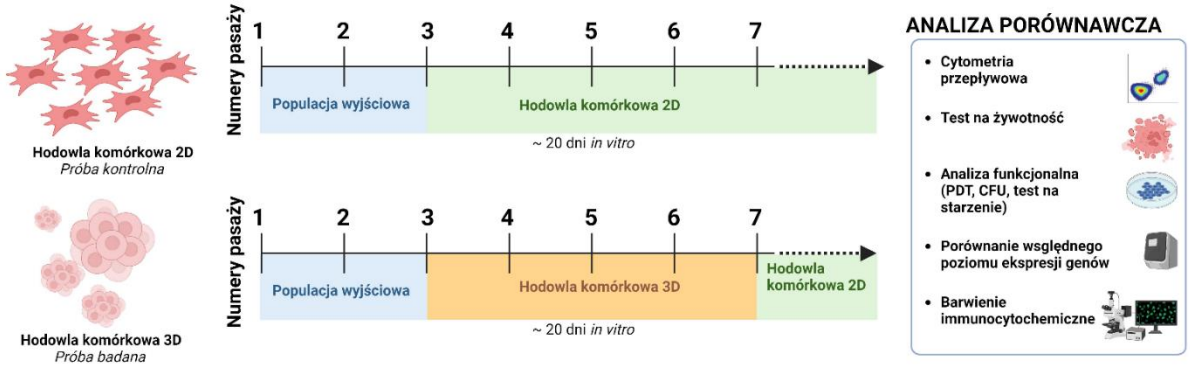

Rycina 4. *Schemat indukcji długotrwałej hodowli WJ-MSC w formie sferoidów. W prowadzonych doświadczeniach wykorzystano następujące grupy kontrolne: 1) populację wyjściową WJ-MSC, pochodzącą z 3 pasażu hodowli 2D, 2) populację WJ-MSC hodowaną w warunkach 2D do 7 pasażu (hodowla komórkowa 2D). Jako grupę badaną zastosowano 3) populację WJ-MSC hodowaną w formie sferoidów (hodowla komórkowa 3D). Po upływie 20 dni hodowli in vitro, WJ-MSC z warunków przestrzennych 3D były ponownie wysiewane do warunków 2D w celu porównania ich właściwości z populacjami kontrolnymi.*

2) Po pierwszym etapie badań, w którym wykazano lepszą przeżywalność komórek wykazujących ekspresję antygenu powierzchniowego SSEA-4, podjęto próbę scharakteryzowania tej subpopulacji pod kątem cech typowych dla komórek pluripotencjalnych. W celu doboru najbardziej optymalnej metody wyodrębniania populacji WJ-MSC-SSEA-4+ porównano sortowanie aktywowane magnetycznie (*Magnetic Activated Cell Sorting*, MACS) i sortowanie aktywowane fluorescencyjnie (*Fluorescence-Activated Cell Sorting*, FACS). Do dalszych badań wybrano technikę FACS. Po procesie sortowania oceniono utrzymywanie się ekspresji antygenu SSEA-4 w trakcie trwaniem hodowli dla populacji negatywnej i pozytywnej w 1, 2, 4 i 6 pasażu. W ramach charakterystyki subpopulacji WJ-MSC-SSEA-4+ porównano: tempo proliferacji (PDT), odsetek komórek klonogennych (CFU), zdolność do tworzenia sferoidów w krótkotrwałych warunkach hodowli 3D, poziom ekspresji genów pluripotencjalnych, charakterystycznych dla 3 listków zarodkowych oraz neuralnych, koekspresję antygenów powierzchniowych typowych dla innych komórek macierzystych oraz zdolności wydzielnicze. Uzyskane wyniki porównano z populacją wyjściową i populacją niewykazującą obecności SSEA-4 (**Rycina 5**).

Materiały i metody wykorzystane w tym etapie badań zostały szczegółowo opisane w Artykule II.

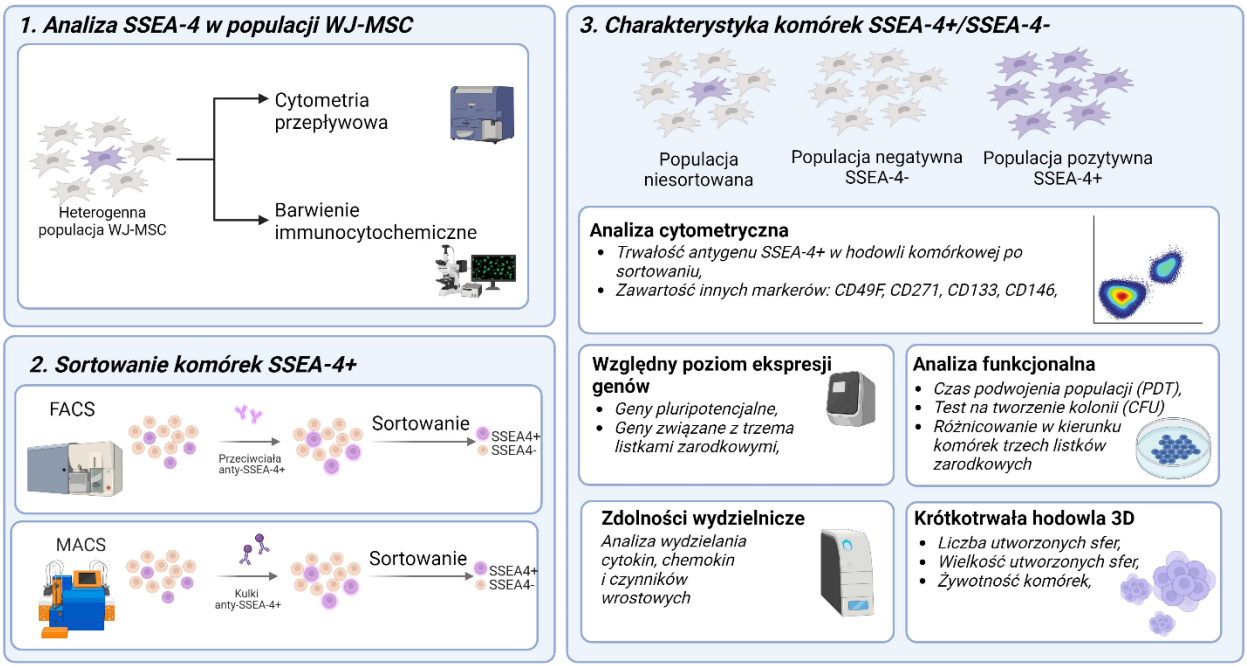

***Rycina* 5.** *Schemat izolacji i charakterystyki komórek WJ-MSC wykazujących ekspresję SSEA-4. Dla heterogennej populacji WJ-MSC oznaczono odsetek komórek SSEA-4+, i wybrano najbardziej optymalną metodę wysortowania tej subpopulacji. Następnie przeprowadzono charakterystykę porównawczą, w której poddano analizom następujące grupy komórek: 1) populację niesortowaną, 2) populację negatywną SSEA-4- i 3) populację pozytywną SSEA-4+.*

8. Podsumowanie najważniejszych wyników

8.1. Analiza WJ-MSC hodowanych w warunkach 3D

Opisywane wyniki przedstawiono w Artykule I [60].

8.1.1. W odpowiednich warunkach hodowlanych WJ-MSC stworzyły sfery.

WJ-MSC, mimo silnych właściwości adhezyjnych, stworzyły agregaty komórek zwane sferoidami, po zastosowaniu powierzchni antyadhezyjnej oraz pożywki hodowlanej typowej dla NSC (Artykuł I, Fig. 1.B). W trakcie prowadzenia hodowli 3D zauważono zmianę morfologii komórek tworzących sferę, potwierdzoną przez analizę cytometryczną. W dniu 3 hodowli 3D dominowały komórki mniejsze i bardziej okrągłe w stosunku do hodowli 2D, natomiast w dniu 10 hodowli 3D obserwowano wzrost udziału liczby komórek o większej średnicy. W przypadku hodowli 2D nie obserwowano zmian rozmiarów komórek (Artykuł I, Fig. 1.C). Pomimo długotrwałej hodowli w warunkach 3D, WJ-MSC dalej wykazywały właściwości adhezyjne po ponownym wysianiu do warunków 2D. Większość komórek, po przeniesieniu z warunków przestrzennych do warunków 2D, ponownie zmieniła morfologię na typową, fibroblastopodobną. Jednakże, wśród nich zauważono również wyodrębnienie się subpopulacji komórek o wydłużonym ciele i dwubiegunowym kształcie oraz komórek o kształcie ameboidalnym, typowym dla komórek starzejących się (Artykuł I, Fig. 1.D).

Hodowla w formie 3D wpłynęła negatywnie na żywotność WJ-MSC, co wykazano barwieniem przyżyciowym (Artykuł I, Fig. 2). Odsetek komórek martwych zmniejszał się wraz z trwaniem hodowli 3D. Otrzymane wyniki sugerują, że pierwsze 3 dni są najbardziej krytyczne dla przeżycia w warunkach przestrzennych/stresogennych heterogennej populacji MSC lub, że jest to okres w którym przeżywa pewna subpopulacji komórek o odmiennych właściwościach (Artykuł I, Fig. 2.C).

8.1.2. Długotrwała hodowla 3D wpłynęła negatywnie na aktywność fizjologiczną WJ-MSC.

WJ-MSC przeprowadzone przez etap hodowli przestrzennej, po powrocie do warunków standardowych charakteryzowały się zmniejszonym tempem proliferacji (Artykuł I, Fig. 3.A,B) i niższą klonogennością w stosunku do populacji początkowej (Artykuł I, Fig. 3. D). Zaobserwowano także większy odsetek komórek starzejących się, wykazujących aktywność β-galaktozydazy, (Artykuł I, Fig. 3.C) w stosunku do komórek pozostających stale w warunkach hodowli 2D.

W celu analizy wpływu warunków 3D na ekspresję genów pluripotencjalnych oraz neuralnych wybrano dwa punkty czasowe, w których pobierano materiał RNA: moment zakończenia hodowli 3D (materiał zebrano ze stadium sferoidów) oraz 48 godzin po ponownym wysianiu do warunków 2D. Zauważono, że WJ-MSC w stadium sfer charakteryzowały się wyższą ekspresją genów *OCT3/4* i *SOX2* oraz niższą ekspresją *NANOG* w stosunku do populacji wyjściowej oraz komórek ponownie wysianych do warunków 2D. Niestety, z powodu dużych odchyleń w poziomach ekspresji pomiędzy próbami badanymi, uzyskane różnice nie były istotne statystycznie. Jednakże zmiana wzoru ekspresji genów między dwoma czasami analizy może sugerować, że hodowla 3D wywiera efekt przejściowy na ekspresję genów SRTF (Artykuł I, Fig. 6, Fig. S3).

WJ-MSC hodowane w warunkach 3D, w pożywce dedykowanej hodowli NSC z dodatkiem EGF i bFGF wykazywały predyspozycje do różnicowania w kierunku neuroektodermy. Zaobserwowano obecność markerów neuralnych takich jak Nestyna, β-III-Tubulina i A2B5 (Artykuł I, Fig. 4). Po ponownym wysianiu do warunków 2D, komórki wykazywały większą ekspresję Nestyny i β-III-Tubuliny w stosunku do populacji wyjściowej, jak również hodowanej stale w warunkach 2D (Artykuł I, Fig. 5. A, B). Hodowla 3D wpłynęła również na przejściowy wzrost ekspresji genu *NESTYNA* (Artykuł I, Fig. S3). Zarówno długotrwała hodowla w warunkach przestrzennych, jak również ponowne wysianie do warunków 2D nie indukowały wzrostu ekspresji markerów związanych z różnicowaniem w neurony: NF200 czy NeuN w stosunku do populacji stale hodowanej w warunkach adhezyjnych (Artykuł I, Fig. 4, Fig. 5. A, B).

8.1.3. Pod wpływem hodowli 3D zwiększył się odsetek komórek SSEA-4+ w populacji WJ-MSC.

Przestrzenna hodowla heterogennej populacji WJ-MSC prowadziła do selekcji komórek. W trakcie takiej hodowli zaobserwowano zwiększenie udziału komórek wykazujących obecność antygenu powierzchniowego SSEA-4 - jednego z zarodkowych antygenów powierzchniowych mogących świadczyć o zdolności komórek do wielokierunkowego różnicowania (Artykuł I, Fig. 4). W celu potwierdzenia żywotności tych komórek zastosowano barwienie przeciwko kaspazie 3. Barwienie wykazało, że komórki SSEA-4+ znajdujące się głównie w rdzeniu sfery pozostawały żywe (Artykuł I, Fig. S2). Wzrost ekspresji SSEA-4 utrzymywał się również po ponownym wysianiu komórek do warunków 2D (Artykuł I, Fig. 5). Na podstawie zaobserwowanych wyników stwierdzono, że długotrwała hodowla 3D promuje przeżycie komórek wykazujących na swojej powierzchni antygen SSEA-4.

8.2. Analiza populacji WJ-MSC-SSEA-4+

Wyniki uzyskane w trakcie pierwszego etapu badań wskazujące na unikalne cechy komórek SSEA-4-pozytywnych skłoniły do kontynuacji badań w kierunku pogłębionej analizy wyodrębnionej subpopulacji. Przedstawione wyniki przedstawiono w Artykule II [61].

8.2.1. Metoda FACS pozwoliła na uzyskanie zwiększonego odsetka komórek SSEA-4+ w populacji WJ-MSC w stosunku do metody MACS.

Ekspresja SSEA-4 w MSC różniła się znacząco w zależności od tkanki źródłowej oraz zastosowanych warunków hodowlanych. WJ-MSC wyizolowane z tkanki wczesnej rozwojowo, tkanki popłodu, zawierały znacznie większy odsetek komórek SSEA-4+ niż AD-MSC pobrane z tkanki pochodzącej od osoby dorosłej (Artykuł II, Fig. 1.B). Odsetek komórek SSEA-4+ w WJ-MSC nie zmieniał się istotnie między pasażami: 1, 3 i 5 (Artykuł II, Fig. 1.D), natomiast zmieniał się znacząco w zależności od zastosowanego w hodowli źródła czynników troficznych (lizatu płytkowego). W obecności lizatu płytkowego MultiPL'30 charakteryzującego się niższym stężeniem składników osocza w produkcie odsetek komórek SSEA-4+ w populacji wynosił około 35%, natomiast w obecności lizatów

płytkowych bogatych w osocze (MultiPL'100 i PLTGold – blisko 100% w produkcie) odsetek ten wzrastał w populacji do około 70% (Artykuł II, Fig. 1.E). Uzyskane wyniki wskazują na istotną rolę białek i czynników troficznych obecnych w środowisku na ekspresję SSEA-4 w populacji WJ-MSC. W oparciu o powyższe obserwacje, w dalszych eksperymentach wykorzystano WJ-MSC z pasażu 3, hodowane w pożywce z dodatkiem ludzkiego lizatu płytkowego PLTGold.

W celu doboru optymalnej metody izolacji subpopulacji SSEA-4+ porównano dwie techniki separacji komórkowej: MACS (metodzie wykorzystującej kulki magnetyczne powleczone przeciwciałami monoklonalnymi skierowanymi swoiście przeciwko wybranym antygenom) oraz FACS (wykorzystującej specyficzne przeciwciała, w oparciu o cytometrię przepływową). Jako, że publikacje porównujące obydwie techniki stoją ze sobą w sprzeczności oraz wykorzystują różne kryteria do opisania wydajności, postanowiono porównać wybrane parametry: odzysk (ang. *recorvery*), przeżywalność (ang. *survival*) i wydajność (ang. *yield*). Odzysk wyrażono jako stosunek liczby komórek uzyskanych we frakcji pozytywnej do liczby komórek wykorzystanych do sortowania. Przeżywalność oznaczono jako odsetek komórek żywych po sortowaniu. Wydajność wyrażono jako stosunek odsetka komórek pozytywnych przed i po sortowaniu, do czego wykorzystano analizę cytometryczną. FACS charakteryzował się znacząco lepszym odzyskiem w stosunku do MACS (Artykuł II, Fig. 2.A). Nie zaobserwowano istotnych różnic statystycznych w przypadku przeżywalności oraz wydajności obydwu rodzajów separacji (Artykuł II, Fig. 2.B, C, D). Na podstawie zaobserwowanych parametrów i przeważająco lepszemu odzyskowi komórek, w dalszych badaniach zdecydowano się na zastosowanie metody FACS.

W wyniku sortowania FACS uzyskano dwie populacje: pozytywną (WJ-MSC-SSEA-4+) oraz negatywną (WJ-MSC-SSEA-4-). Bezpośrednio po sortowaniu zbadano ponownie obecność komórek SSEA-4+: dla populacji pozytywnej odsetek wynosił 87,4%, a dla populacji negatywnej 1,2% (Artykuł II, Fig. 3.A, B). Z racji ograniczeń technicznych obydwu technik sortowania, nie jest możliwe odnotowanie 100% komórek SSEA-4+ w populacji pozytywnej i 0% w populacji negatywnej. W populacji negatywnej zauważono stopniowy wzrost liczby komórek SSEA-4+ w miarę prowadzenia dalszej hodowli komórkowej. Analizę prowadzono do 6 pasażu komórkowego, to jest do momentu, kiedy

przestano obserwować istotne różnice w wielkości populacji SSEA-4+ między obydwoma grupami badanymi (Artykuł II, Fig. 3.B, C).

8.2.2. Subpopulacja WJ-MSC-SSEA-4+ wykazywała przejściowo zwiększoną ekspresję genów pluripotencjalnych, co nie przełożyło się na inne cechy komórek pluripotencjalnych.

Bezpośrednio po sortowaniu, WJ-MSC-SSEA-4+ wykazywały podwyższoną ekspresję genów pluripotencjalnych *NANOG* oraz *OCT4*. Jednakże, wraz z czasem prowadzenia hodowli komórkowej, zauważono spadek poziomu ekspresji wspomnianych genów (Artykuł II, Fig. 4.A). Jednocześnie, w subpopulacji WJ-MSC-SSEA-4+ uzyskanej bezpośrednio po sortowaniu zauważono wzrost spontanicznej ekspresji genów związanych z tkanką nerwową, w tym z neuronami i komórkami glejowymi (*NESTYNA*, *H3TUBULINA*, *GFAP*). Podwyższona ekspresja dla genów *NESTYNA* i *H3TUBULINA* utrzymała się przez kolejny pasaż (Artykuł II, Fig. 4. B). Nasze wyniki wskazują na lepszy spontaniczny potencjał do różnicowania neuralnego subpopulacji WJ-MSC-SSEA-4+, co może być związane z ich przejściowym charakterem niezróżnicowanym.

Przeanalizowano również potencjał do różnicowania subpopulacji WJ-MSC-SSEA-4+ w kierunku komórek wywodzących się z trzech listków zarodkowych: ektodermy, mezodermy i endodermy. Zarówno w populacji pozytywnej jak i negatywnej zauważono tendencję wzrostową w ekspresji genu kodującego *BRACHYURY* – markera mezodermalnego, ale uzyskane wyniki nie były istotne statystycznie. Brachyury wykryto także na poziomie białka w barwieniu immunocytochemicznym (Artykuł II, Fig. 4 C, D). Nie udało się potwierdzić skutecznego różnicowania subpopulacji WJ-MSC-SSEA-4+ i WJ-MSC-SSEA-4- w kierunku komórek ektodermy (*OTX2* i *H3TUBULINA*) i endodermy (*SOX17* i *FOX2A*) (Artykuł II, Fig. 4. C, D).

Badana subpopulacja WJ-MSC-SSEA-4+ nie wyróżniała się tempem podziałów komórkowych oraz zdolnością do tworzenia kolonii w stosunku do populacji WJ-MSC-SSEA-4- i populacji wyjściowej (Artykuł II, Fig. 4.D, E).

8.2.3. Sferoidy utworzone przez WJ-MSC-SSEA-4+ wykazywały się mniejszą średnicą oraz większą przeżywalnością.

Jako kolejną cechę komórek o charakterze pluripotencjalnym, porównano zdolność badanych subpopulacji do tworzenia sfer. Zauważono, że wszystkie 3 badane populacje WJ-MSC tworzyły sfery podczas krótkotrwałej hodowli 3D (Artykuł II, Fig. 7). Liczba uzyskanych sfer była zbliżona w badanych populacjach i spadała wraz z czasem trwania hodowli (Artykuł II, Fig. 7.B). Jednakże sfery utworzone przez populację WJ-MSC-SSEA-4+, choć wykazywały mniejszą średnicę w stosunku do pozostałych wariantów (Artykuł II, Fig. 9.C-E), zawierały również mniej komórek martwych (Artykuł II, Fig. 8).

Podsumowując uzyskane wyniki stwierdzono, że pomimo przejściowego wzrostu ekspresji genów pluripotencjalnych, zdolności do tworzenia sfer oraz przeżycia w warunkach hodowli przestrzennej, marker SSEA-4+ nie może być jedynym wyznacznikiem subpopulacji wykazującej cechy pluripotencjalne.

8.2.4. SSEA-4 nie jest powiązany z innymi antygenami powierzchniowymi związanymi z macierzystością.

W związku z wynikami uzyskanymi w pierwszym etapie badań oraz odmiennymi cechami subpopulacji wykazującej obecność antygenu SSEA-4, przeprowadzono analizę piśmiennictwa w celu wyodrębnienia innych markerów, potencjalnie związanych z unikatowymi zdolnościami do wielokierunkowego różnicowania MSC (Artykuł III). W oparciu o zgromadzone dane literaturowe, oznaczono w populacji WJ-MSC ekspresję następujących antygenów powierzchniowych: CD271, CD49F, CD146 i CD133. W kolejnym kroku podjęto próbę powiązania ich występowania z ekspresją antygenu SSEA-4. Odnotowano jednak, że poziomy ekspresji analizowanych markerów nie różniły się znacząco między populacjami: niesortowaną, SSEA-4+ i SSEA-4- (Artykuł II, Fig. 5). Uzyskane wyniki wskazują na brak wzajemnego związku pomiędzy współwystępowaniem w komórkach markera SSEA-4, a innymi markerami świadczącymi o macierzystości MSC.

8.2.5. Subpopulacja WJ-MSC-SSEA-4+ wykazuje odmienny profil sekrecyjny.

W związku z obserwowaną unikatowością subpopulacji SSEA-4+, która nie wiązała się z cechami do pluripotencji, a wpływała na lepszą przeżywalnością w stresowych warunkach, zdecydowano się na analizę jej profilu sekrecyjnego w 3 i 5 dniu po sortowaniu FACS (Artykuł II, Fig. 6). Wyniki porównano do populacji wyjściowej oraz negatywnej w kierunku antygenu SSEA4. Populacja niesortowana odznaczała się wyższym wydzielaniem neurotroficznego czynnika pochodzenia mózgowego (BDNF), czynnika wzrostu hepatocytów (HGF) i czynnika wzrostu pochodzenia glejowego (GDNF) w stosunku do pozostałych grup badanych analizowanych 3 dni po sortowaniu. Z kolei, w 5 dniu po sortowaniu, populacja WJ-MSC-SSEA-4+ charakteryzowała się najwyższym wydzielaniem ligandu chemokiny 2 (*chemokine ligand 2,* CCL2) oraz obniżonym wydzielaniem czynnika wzrostu śródbłonka naczyniowego (*vascular endothelial growth factor,* VEGF-c). Biorąc pod uwagę udział chemokiny CCL2 w procesie repolaryzacji makrofagów w kierunku przeciwzapalnego fenotypu M2, a także wpływ na przyspieszenie gojenia się ran [62], możliwe wydaje się terapeutyczne wykorzystanie badanej subpopulacji SSEA-4+ w wymienionych procesach.

9. Wnioski

1. Zastosowanie długotrwałej hodowli komórkowej w zmodyfikowanych warunkach przestrzennych (3D) umożliwia wyizolowanie z heterogennej populacji WJ-MSC subpopulacji o zwiększonej przeżywalności, wykazującej wczesnorozwojowy marker SSEA-4. Jednakże hodowla w warunkach 3D skutkuje ogólną zmniejszoną przeżywalnością komórek, obniżonym tempem proliferacji i zdolnościami klonogennymi oraz przyspieszeniem procesów starzenia w porównaniu z hodowlą prowadzoną w warunkach 2D.

2. Technika FACS umożliwia skuteczniejsze wyodrębnienie subpopulacji SSEA-4-pozytywnej z heterogennej populacji WJ-MSC w porównaniu do techniki MACS. Jednakże, udział procentowy komórek wyrażających SSEA-4 zmniejsza się w populacji pozytywnej w trakcie prowadzenia hodowli komórkowej.

3. Subpopulacja SSEA-4-pozytywna wykazuje przejściową, zwiększoną ekspresję genów pluripotencjalnych w stosunku do populacji wyjściowej i negatywnej, tworzy sferoidy o mniejszej średnicy i wyższej przeżywalności, a także charakteryzuje się odmiennymi właściwościami sekrecyjnymi. Jednakże, w stosunku do populacji wyjściowej oraz negatywnej nie wykazuje różnic w potencjale proliferacyjnym, klonogennym, w zdolności do różnicowania w komórki trzech listków zarodkowych, a także ekspresji antygenów powierzchniowych związanych z innymi subpopulacjami o możliwych właściwościach pluripotencjalnych.

10. Bibliografia

1. Loya K. Stem Cells. Handb Pharmacogenomics Stratif Med. 2014;:207–31.

2. Szabłowska-Gadomska I, Bużańska L, Małecki M. Właściwości komórek macierzystych, regulacje prawne oraz zastosowanie w medycynie. Postepy Hig Med Dosw. 2017;71:1216–30.

3. de Lucas B, Pérez LM, Gálvez BG. Importance and regulation of adult stem cell migration. J Cell Mol Med. 2018;22:746–54.

4. Smart N, Riley PR. The Stem Cell Movement. Circ Res. 2008;102:1155–68.

5. Tweedell KS. The Adaptability of Somatic Stem Cells: A Review. J Stem Cells Regen Med. 2017;13:3.

6. King NMP, Perrin J. Ethical issues in stem cell research and therapy. Stem Cell Res Ther. 2014;5:1–6.

7. Lowenthal J, Sugarman J. Ethics and Policy Issues for Stem Cell Research and Pulmonary Medicine. Chest. 2015;147:824.

8. Kim JY, Nam Y, Rim YA, Ju JH. Review of the Current Trends in Clinical Trials Involving Induced Pluripotent Stem Cells. Stem Cell Rev Reports. 2022;18:142.

9. Friedenstein AJ, Petrakova KV, Kurolesova AI, Frolova GP. Heterotopic of bone marrow. Analysis of precursor cells for osteogenic and hematopoietic tissues. Transplantation. 1968;6:230–47.

10. Caplan AI. Mesenchymal stem cells. J Orthop Res. 1991;9:641–50.

11. Macrin D, Joseph JP, Pillai AA, Devi A. Eminent Sources of Adult Mesenchymal Stem Cells and Their Therapeutic Imminence. Stem Cell Rev Reports 2017 136. 2017;13:741–56.

12. Dominici M, Le Blanc K, Mueller I, Slaper-Cortenbach I, Marini FC, Krause DS, et al. Minimal criteria for defining multipotent mesenchymal stromal cells. The International Society for Cellular Therapy position statement. Cytotherapy. 2006;8:315–7.

13. Lindner U, Kramer J, Rohwedel J, Schlenke P. Mesenchymal Stem or Stromal Cells: Toward a Better Understanding of Their Biology? Transfus Med Hemotherapy. 2010;37:75.

14. Viswanathan S, Shi Y, Galipeau J, Krampera M, Leblanc K, Martin I, et al. Mesenchymal stem versus stromal cells: International Society for Cell & Gene Therapy (ISCT®) Mesenchymal Stromal Cell committee position statement on nomenclature. Cytotherapy. 2019;21:1019–24.

15. Zhao Q, Ren H, Han Z. Mesenchymal stem cells: Immunomodulatory capability and clinical potential in immune diseases. Journal of Cellular Immunotherapy. 2016;2:3–20.

16. Naji A, Eitoku M, Favier B, Deschaseaux F, Rouas-Freiss N, Suganuma N. Biological functions of mesenchymal stem cells and clinical implications. Cell Mol Life Sci 2019 7617. 2019;76:3323–48.

17. Pittenger MF, Discher DE, Péault BM, Phinney DG, Hare JM, Caplan AI.

Mesenchymal stem cell perspective: cell biology to clinical progress. npj Regen Med 2019 41. 2019;4:1–15.

18. Karakaş N, Bay S, Türkel N, Öztunç N, Öncül M, Bilgen H, et al. Neurons from human mesenchymal stem cells display both spontaneous and stimuli responsive activity. PLoS One. 2020;15.

19. Afshari A, Shamdani S, Uzan G, Naserian S, Azarpira N. Different approaches for transformation of mesenchymal stem cells into hepatocyte-like cells. Stem Cell Res Ther. 2020;11:1–14.

20. Rennerfeldt DA, Van Vliet KJ. Concise Review: When Colonies Are Not Clones: Evidence and Implications of Intracolony Heterogeneity in Mesenchymal Stem Cells. Stem Cells. 2016;34:1135–41.

21. Levy O, Kuai R, Siren EMJ, Bhere D, Milton Y, Nissar N, et al. Shattering barriers toward clinically meaningful MSC therapies. Sci Adv. 2020;6.

22. Wang Z, Chai C, Wang R, Feng Y, Huang L, Zhang Y, et al. Single-cell transcriptome atlas of human mesenchymal stem cells exploring cellular heterogeneity. Clin Transl Med. 2021;11:11.

23. Sheng G. The developmental basis of mesenchymal stem/stromal cells (MSCs). 2015. https://doi.org/10.1186/s12861-015-0094-5.

24. Coste C, Neirinckx V, Sharma A, Agirman G, Rogister B, Foguenne J, et al. Human bone marrow harbors cells with neural crest-associated characteristics like human adipose and dermis tissues. PLoS One. 2017;12:e0177962.

25. Simões-Costa M, Bronner ME. Establishing neural crest identity: a gene regulatory recipe. Development. 2015;142:242.

26. Martik ML, Bronner ME. Regulatory logic underlying diversification of the neural crest. Trends Genet. 2017;33:715.

27. Dupin E, Sommer L. Neural crest progenitors and stem cells: From early development to adulthood. Dev Biol. 2012;366:83–95.

28. Ledesma-Martínez E, Mendoza-Núñez VM, Santiago-Osorio E. Mesenchymal Stem Cells Derived from Dental Pulp: A Review. Stem Cells Int. 2016;2016.

29. Niibe K, Zhang M, Nakazawa K, Morikawa S, Nakagawa T, Matsuzaki Y, et al. The potential of enriched mesenchymal stem cells with neural crest cell phenotypes as a cell source for regenerative dentistry. Japanese Dental Science Review. 2017;53:25–33.

30. Drela K, Sarnowska A, Siedlecka P, Szablowska-Gadomska I, Wielgos M, Jurga M, et al. Low oxygen atmosphere facilitates proliferation and maintains undifferentiated state of umbilical cord mesenchymal stem cells in an hypoxia inducible factor-dependent manner. Cytotherapy. 2014;16:881–92.

31. Musiał-Wysocka A, Kot M, Sułkowski M, Badyra B, Majka M. Molecular and Functional Verification of Wharton's Jelly Mesenchymal Stem Cells (WJ-MSCs) Pluripotency. Int J Mol Sci. 2019;20:1807.

32. Drela K, Lech W, Figiel-Dabrowska A, Zychowicz M, Mikula M, Sarnowska A, et al. Enhanced neuro-therapeutic potential of Wharton's Jelly-derived mesenchymal stem cells in comparison with bone marrow mesenchymal stem cells culture. Cytotherapy. 2016;18:497–509.

33. Paladino FV, De Rodrigues JM, Da Silva A, Goldberg AC. The Immunomodulatory Potential of Wharton's Jelly Mesenchymal Stem/Stromal Cells. Stem Cells Int. 2019;2019.

34. El Omar R, Beroud J, Stoltz JF, Menu P, Velot E, Decot V. Umbilical Cord Mesenchymal Stem Cells: The New Gold Standard for Mesenchymal Stem Cell-Based Therapies? https://home.liebertpub.com/teb. 2014;20:523–44.

35. Pennock R, Bray E, Pryor P, James S, McKeegan P, Sturmey R, et al. Human cell dedifferentiation in mesenchymal condensates through controlled autophagy. Sci Rep. 2015;5:13113.

36. Jauković A, Abadjieva D, Trivanović D, Stoyanova E, Kostadinova M, Pashova S, et al. Specificity of 3D MSC Spheroids Microenvironment: Impact on MSC Behavior and Properties. Stem Cell Reviews and Reports. 2020;16:853–75.

37. Figiel-Dabrowska A, Radoszkiewicz K, Rybkowska P, Krzesniak NE, Sulejczak D, Sarnowska A. Neurogenic and Neuroprotective Potential of Stem/Stromal Cells Derived from Adipose Tissue. Cells 2021, Vol 10, Page 1475. 2021;10:1475.

38. Henderson JK, Draper JS, Baillie HS, Fishel S, Thomson JA, Moore H, et al. Preimplantation Human Embryos and Embryonic Stem Cells Show Comparable Expression of Stage-Specific Embryonic Antigens. Stem Cells. 2002;20:329–37.

39. Kuroda Y, Kitada M, Wakao S, Nishikawa K, Tanimura Y, Makinoshima H, et al. Unique multipotent cells in adult human mesenchymal cell populations. Proc Natl Acad Sci U S A. 2010;107:8639–43.

40. Ogura F, Wakao S, Kuroda Y, Tsuchiyama K, Bagheri M, Heneidi S, et al. Human Adipose Tissue Possesses a Unique Population of Pluripotent Stem Cells with Nontumorigenic and Low Telomerase Activities: Potential Implications in Regenerative Medicine. Stem Cells Dev. 2014;23:717–28.

41. Petrenko Y, Vackova I, Kekulova K, Chudickova M, Koci Z, Turnovcova K, et al. A Comparative Analysis of Multipotent Mesenchymal Stromal Cells derived from Different Sources, with a Focus on Neuroregenerative Potential. Sci Rep. 2020;10.

42. Kawamura H, Nakatsuka R, Matsuoka Y, Sumide K, Fujioka T, Asano H, et al. TGF-β Signaling Accelerates Senescence of Human Bone-Derived CD271 and SSEA-4 Double-Positive Mesenchymal Stromal Cells. Stem Cell Reports. 2018;10:920–32.

43. Selle M, Koch JD, Ongsiek A, Ulbrich L, Ye W, Jiang Z, et al. Influence of age on stem cells depends on the sex of the bone marrow donor. J Cell Mol Med. 2022;26:1594–605.

44. Block TJ, Marinkovic M, Tran ON, Gonzalez AO, Marshall A, Dean DD, et al. Restoring the quantity and quality of elderly human mesenchymal stem cells for autologous cell-based therapies. Stem Cell Res Ther. 2017;8:239.

45. Mikami Y, Ishii Y, Watanabe N, Shirakawa T, Suzuki S, Irie S, et al. CD271/p75NTR inhibits the differentiation of mesenchymal stem cells into osteogenic, adipogenic, chondrogenic, and myogenic lineages. Stem Cells Dev. 2011;20:901–13.

46. Vidal A, Redmer T. Decoding the Role of CD271 in Melanoma. Cancers (Basel). 2020;12:1–19.

47. Barilani M, Banfi F, Sironi S, Ragni E, Guillaumin S, Polveraccio F, et al. Low-affinity Nerve Growth Factor Receptor (CD271) Heterogeneous Expression in Adult and Fetal Mesenchymal Stromal Cells. Sci Rep. 2018;8:1–11.

48. González-Garza MT, Cruz-Vega DE, Cárdenas-Lopez A, de la Rosa RM, Moreno-Cuevas JE. Comparing stemness gene expression between stem cell subpopulations from peripheral blood and adipose tissue. Am J Stem Cells. 2018;7:38–47.

49. Ma L, Huang Z, Wu D, Kou X, Mao X, Shi S. CD146 controls the quality of clinical grade mesenchymal stem cells from human dental pulp. Stem Cell Res Ther. 2021;12:1–16.

50. Espagnolle N, Guilloton F, Deschaseaux F, Gadelorge M, Sensébé L, Bourin P. CD146 expression on mesenchymal stem cells is associated with their vascular smooth muscle commitment. J Cell Mol Med. 2014;18:104–14.

51. Wangler S, Menzel U, Li Z, Ma J, Hoppe S, Benneker LM, et al. CD146/MCAM distinguishes stem cell subpopulations with distinct migration and regenerative potential in degenerative intervertebral discs. Osteoarthr Cartil. 2019;27:1094–105.

52. Harkness L, Zaher W, Ditzel N, Isa A, Kassem M. CD146/MCAM defines functionality of human bone marrow stromal stem cell populations. Stem Cell Res Ther. 2016;7:1–14.

53. Matsui M, Kobayashi T, Tsutsui TW. CD146 positive human dental pulp stem cells promote regeneration of dentin/pulp-like structures. Hum Cell. 2018;31:127–38.

54. Yang Z, Ma S, Cao R, Liu L, Cao C, Shen Z, et al. CD49f high Defines a Distinct Skin Mesenchymal Stem Cell Population Capable of Hair Follicle Epithelial Cell Maintenance. J Invest Dermatol. 2020;140:544-555.e9.

55. Battula VL, Treml S, Abele H, Bühring HJ. Prospective isolation and characterization of mesenchymal stem cells from human placenta using a frizzled-9-specific monoclonal antibody. Differentiation. 2008;76:326–36.

56. Glumac PM, LeBeau AM. The role of CD133 in cancer: a concise review. Clin Transl Med. 2018;7:18.

57. Baustian C, Hanley S, Ceredig R. Isolation, selection and culture methods to enhance clonogenicity of mouse bone marrow derived mesenchymal stromal cell precursors. Stem Cell Res Ther. 2015;6.

58. Smolinska A, Bzinkowska A, Rybkowska P, Chodkowska M, Sarnowska A. Promising Markers in the Context of Mesenchymal Stem/Stromal Cells Subpopulations with Unique Properties. Stem Cells Int. 2023;2023.

59. Lech W, Figiel-Dabrowska A, Sarnowska A, Drela K, Obtulowicz P, Noszczyk BH, et al. Phenotypic, Functional, and Safety Control at Preimplantation Phase of MSC-Based Therapy. Stem Cells Int. 2016;2016:2514917.

60. Kaminska A, Wedzinska A, Kot M, Sarnowska A. Effect of Long-Term 3D Spheroid Culture on WJ-MSC. Cells. 2021;10:719.

61. Smolinska A, Chodkowska M, Kominek A, Janiec J, Piwocka K, Sulejczak D, et al. Stemness properties of SSEA-4+ subpopulation isolated from heterogenous Wharton's jelly mesenchymal stem/stromal cells. Front Cell Dev Biol. 2024;12:1227034.

62. Whelan DS, Caplice NM, Clover AJP. Mesenchymal stromal cell derived CCL2 is required for accelerated wound healing. Sci Rep. 2020;10.

11. Kopie publikacji tworzące rozprawę

11.1. Artykuł I

cells

MDPI

Article

Effect of Long-Term 3D Spheroid Culture on WJ-MSC

Agnieszka Kaminska [1], Aleksandra Wedzinska [1], Marta Kot [2] and Anna Sarnowska [1,2,*]

[1] Mossakowski Medical Research Centre, Translational Platform for Regenerative Medicine, Polish Academy of Science, 02-106 Warsaw, Poland; akaminska@imdik.pan.pl (A.K.); awedzinska@imdik.pan.pl (A.W.)
[2] Mossakowski Medical Research Centre, Department of Stem Cell Bioengineering, Polish Academy of Sciences, 02-106 Warsaw, Poland; mkot@imdik.pan.pl
* Correspondence: asarnowska@imdik.pan.pl; Tel.: +48-22-6086598

Abstract: The aim of our work was to develop a protocol enabling a derivation of mesenchymal stem/stromal cell (MSC) subpopulation with increased expression of pluripotent and neural genes. For this purpose we used a 3D spheroid culture system optimal for neural stem cells propagation. Although 2D culture conditions are typical and characteristic for MSC, under special treatment these cells can be cultured for a short time in 3D conditions. We examined the effects of prolonged 3D spheroid culture on MSC in hope to select cells with primitive features. Wharton Jelly derived MSC (WJ-MSC) were cultured in 3D neurosphere induction medium for about 20 days in vitro. Then, cells were transported to 2D conditions and confront to the initial population and population constantly cultured in 2D. 3D spheroids culture of WJ-MSC resulted in increased senescence, decreased stemness and proliferation. However long-termed 3D spheroid culture allowed for selection of cells exhibiting increased expression of early neural and SSEA4 markers what might indicate the survival of cell subpopulation with unique features.

Keywords: mesenchymal stem cells; mesenchymal stromal cells; 3D culture; neurospheres; spheroids; pluripotency; neural; quiescence

Citation: Kaminska, A.; Wedzinska, A.; Kot, M.; Sarnowska, A. Effect of Long-Term 3D Spheroid Culture on WJ-MSC. *Cells* **2021**, *10*, 719. https://doi.org/10.3390/cells10040719

Academic Editor: Joni H. Ylostalo

Received: 2 March 2021
Accepted: 22 March 2021
Published: 24 March 2021

1. Introduction

Mesenchymal stromal/stem cells (MSC) were discovered by Friedenstein in 1966 [1] and since that time most of the researchers have used 2D culture condition to expand this population. The adherence is listed as one of the criteria to revise cells as MSC [2]. Monolayer culture system allows MSC to attach to the surface just like in natural environment and to expand in two dimensions. In spite of its widespread, this method has multiple limitations, and it is discussed how close is to the natural cell environment of MSC [3,4].

Currently, cell cultures are cultivated more and more often in 3D conditions as an alternative for 2D conditions. Spheroid culture, one from the multiple solutions, provides cell-to-cell contacts and intercellular signaling what resembles the environment of tissue [5]. Moreover, such a method of culture is also supposed to imitate the natural cell niche with the stem cells preserved in it.

Spheroid is the floating aggregate of cells with visible changes across its structure. The core consists of proliferating cells, whereas cells from external layer might differentiate and migrate. In order to mimic the natural conditions, MSC has also started to be cultured as 3D aggregates. MSC spheres are described to be formed by using different protocols including low attachment surface [6,7], hanging drop culture [8,9], scaffolds [10], and even the bioreactors [11]. Few research groups tested also neurosphere assay, proposed for neural stem cells (NSC) [12,13] to achieve MSC spheroids. Culture media for neurospheres contain epithelial growth factors (EGF) and basal fibroblast growth factor (bFGF) but no serum.

Most of the experiments conducted with MSC-neurospheres were focused on acquisition of neural phenotype. it was suggested that 3D culture condition could improve

neural differentiation of MSC. In spite of improvement of neural differentiation under 3D conditions, evidences of receiving fully functional neuronal cells from MSC populations are limited. Still there is a demand for efficient protocol, which could be used in clinic. Except analysis of neural phenotype, other aspects such as proliferation, senescence and stemness were not so broadly taken into consideration during research. Moreover, majority of MSC spheroids experiments were a short-term—3D cultured did not last up to seven days in vitro of culture (div) [4] and results were obtained usually during first three div. There were little evidences whether observed effects were transient or constant whether how cells would react for prolonged 3D conditions. Even less is known about the influence of 3D condition on stem cell niche: effect on surface markers expression, commitment of specific type of MSC or interaction between cells. That would explain why some cells survive in 3D conditions and how we could select with better properties.

In the present study, Wharton Jelly derived (WJ)-MSC were cultured in two different culture conditions as the standard, monolayer 2D culture or as 3D culture. Both cultures were conducted parallel for about 20 div—the time required to achieve three passages during standard 2D MSC culture. Cells derived from spheroid culture were compared to those cultured as monolayer regarding such properties as cell senescence, rate of proliferation, capability to form the colonies, and pluripotent and neural gene expression.

2. Materials and Methods

2.1. WJ-MSC Isolation and Primary Culture

Human umbilical cords were acquired from full-term deliveries with the written consent of mother according to the Ethics Committee of Warsaw Medical University guideline (KB/213/2016). Cords (15–20 cm) transported in phosphate buffer saline (PBS) solution (PBS; Sigma-Aldrich, Saint Louis, MO, USA) with mix of Penicillin-Streptomycin-Amphotericin B (1:100, Gibco, Thermo Fisher Scientific, Waltham, MA, USA) were cut with lancet to 2–3 mm in thickness slices. The cylindrical fragments of Wharton Jelly (WJ) of 2–3 mm diameter were obtained from the slices of umbilical cord using the diameter biopsy punch (Miltex, GmbH, Viernheim, Germany). Explants were transferred to six well cultured plates and culture in the standard cell culture medium for WJ-MSC: DMEM (Gibco), 10% human platelet cell lysate (Macopharma, Tourcoing, France), mix of penicillin, streptomycin amphotericin B (1:100; Gibco, Thermo Fisher Scientific), 2 µg/mL heparin (Sigma-Aldrich). Conditions for cell culture were following adherent surface, 37 °C temperature, 95% of humidity, 5% concentration of CO_2, and 5% concentration of O_2. The culture medium was replaced every 2 days for 14 div. When the cells migrated out of the explant and the culture reached semiconfluence, the cells were detached with Accutase Cell Detachment Solution (Beckton Dickinson, Franklin Lakes, NJ, USA) and counted.

WJ-MSC were cultured in conditions described above until the end of 3 passage (initial population of WJ-MSC). After the 3rd passage, cells were collected and divided into two group—part of them was cultured as a spheroids (3D cultured WJ-MSC) and the rest were continually cultured in previous cell culture conditions until the 7th passage (2D cultured WJ-MSC).

2.2. Spheroid Culture

WJ-MSC from the 3rd passage were collected and seeded on anti-adhesive 6 well plates (Nunclon Sphera, Thermo Fischer Scientific, Waltham, MA, USA) at the high density of $30 \times 10^3/cm^2$ in 5% O_2. Cells were cultured in medium DMEM/F12 (Gibco) containing mix of penicillin, streptomycin, amphotericin B (1:100) (Gibco), L-Glutamine 200 mM (1:100) (Gibco), N2 supplement (1:100; Biotechne, Minneapolis, MN, USA) and EGF (20 ng/mL; PeproTech, London, UK). In 3 div, Medium was replaced, and new medium was started to use from this point of culture—Neurobasal Medium (Gibco, Thermo Fischer Scientific) with mix of penicillin, streptomycin, amphotericin B (1:100; Gibco, Thermo Fischer Scientific), L-Glutamine 200 mM (1:100; Gibco, Thermo Fischer

Scientific), B27 supplement (1:50; Gibco, Thermo Fischer Scientific), EGF (20 ng/mL; PeproTech) and bFGF (20 ng/mL; PeproTech).

WJ-MSC spheres were cultured in parallel to standard 2D culture—until the standard culture acquire the 7th passage (about 20 div of culture). After that time spheroids were dissociated to obtain single cells with Accutase Cell Detachment Solution (Becton Dickinson) and seeded again to the 2D culture in standard medium. Reseeded cells were used to measure colony forming unit frequency (CFU-F), population doubling time (PDT), senescence processes, gene expression level, and to perform immunocytochemistry staining.

2.3. Flow Cytometry Analysis

Cells were detached with Accutase Cell Detachment Solution (Beckton Dickinson) and washed in PBS. Required cell number (1×10^6) was resuspend in cold Stain Buffer (Beckton Dickinson) and used for further flow cytometry analysis. Cell markers were analyzed with Human MSC Analysis Kit (Beckton Dickinson) containing antibodies conjugated with fluorochrome against following antigens: CD73, CD90, CD105 (positive markers), CD11b, CD19, CD34, CD45, and PE (negative markers) (Table 1). Cells were incubated in diluted antibodies in the dark for 30 min. After incubation, cells were washed twice with Stain Buffer (Beckton Dickinson) and resuspend in Stain Buffer. Resuspended cells were analyzed using FACS Canto II (Beckton Dickinson) with FACSDiva Software (Beckton Dickinson) and FlowJo 10 (Beckton Dickinson).

Table 1. List of antibodies used for flow cytometry—Human mesenchymal stem/stromal cell (MSC) Analysis Kit (Beckton Dickinson) (cat. nr 562245).

	Antigen	Fluorochrome
Positive cocktail	CD73	APC
	CD90	FITC
	CD105	PerCP-Cy5.5
Negative cocktail	CD11b	PE
	CD19	
	CD34	
	CD49	
	HLA-DR	

In 3rd and 10th div of 3D culture, spheroids were dissociated and resuspended in Stain Buffer. Before running the sample, cells were filtered through 30 µm filter (Miltenyi Biotec, Bergisch Gladbach, Germany) to avoid dublets. Cells were analyzed to compare the change in size with flow cytometry FACS Canto II (Beckton Dickinson) with FACSDiva Software (Beckton Dickinson) and FlowJo 10 (Beckton Dickinson).

2.4. Live-Dead Staining

Aggregates were stained with mix of ethidium homodimer-1 (8 µM, EthD-1) and Calcein AM (Cal-AM) (0.1 µM, Invitrogen, Thermo Fischer Scientific, Waltham, MA, USA) to confirm the viability of cells in spheroids. Spheroids or single cells derived from spheroids were incubated with staining mixture for 45 min in room temperature in a darkness. Stained cells were observed in fluorescence microscope Axio Vert.A1 (Carl Zeiss, Oberkochen, Germany).

2.5. CFU Assay

WJ-MSC from initial population, 2D culture and 3D culture were seeded on 6-well plate in the amount of 100 cells per well. Cells were cultured for 10 div in standard conditions. Then, cells were washed with PBS, fixed with 4% PFA for 15 min and again washed with PBS. Fixed cells were stained with 0.5% toluidine blue for 20 min and washed with distilled water after staining. The number of colonies containing 50 cells or more were counted, and CFU-F was calculated as a percentage of seeded cells.

2.6. Senescence Assay

The cells senescence was analyzed with Senescence Cells Histochemical Staining Kit (Sigma-Aldrich) in initial population, 2D culture, and 3D culture of WJ-MSC. Cells from 2D cultures grew until the confluence reached 50–60% while the cells from dissociated spheroids were cultured 48 h in standard conditions and then the assay was performed.

Cells were washed with 1×PBS and then fixed with Fixation Buffer (provided with kit) for 6–7 min in room temperature. Then, cells were washed 3 times with 1×PBS. After washing, cells were incubated overnight in 37 °C with Staining Solution (prepared according to the protocol). Next day, total cell number was count as well as blue-stained cell number. The percentage of β-galactosidase positive cells was calculated.

2.7. Proliferation Analysis

The cell proliferation was analyzed in the initial population, 2D culture, and 3D culture. WJ-MSC were seeded at a density 2000 cells/cm^2 and cultured in standard conditions until the 80% confluence was reached. Then cells were collected, counted, and re-seeded again at initial density. PDT and cumulative population doublings (cPD) were calculated for the next 4 passages, based on total cell number at each passage. The PDT value was calculated with the following formula:

$$PDT = ((t - t_0) \times \log 2)/(\log N - \log N_0)$$

where N is the number of cells obtained at the end of the passage, N_0 is the initial number of seeded cells, and $t - t_0$ is the duration of passage (counted in days).

2.8. Cryostat Sectioning

Spheroids were collected, fixed in 4% PFA for 15 min and washed twice with PBS. Then, PBS was replaced with 7.5% sucrose solution and incubated overnight. Next day, solution was replaced with 15% sucrose solution and 30% sucrose solution. Then, spheroids were embedded in medium for frozen tissue specimen (OCT Sakura Tissue-Tek, Sakura Finetek Europe, Alphen aan den Rijn, The Netherlands) and moved to −80 °C. Spheroids were cut with cryostat for the 20–30 µm thickness sections. Sections were collected on APTEX (3-Aminopropyl) triethoxysilane) coated glass microscope slides, stored in −20 °C and used for immunocytochemical staining.

2.9. Immunocytochemistry

Immunocytochemistry was performed to detect pluripotency and early neural markers in initial population, 2D culture and 3D culture of WJ-MSC. WJ-MSC were washed with PBS and fixed in 4% PFA for 15 min. Samples were permeabilized with 0.2% Triton X-100 (Sigma-Aldrich) for 15 min and then washed with PBS. After incubation with 10% Goat Serum (Sigma-Aldrich) for 1 h primary antibodies were applied for 24 h in 4 °C (Table 2). Next day, cells were washed with PBS and then incubated with the secondary antibodies conjugated with fluorochrome for 1 h (Supplementary Table S1, Supplementary Figure S1). Cell nuclei were stained with Hoechst 33342 dye (1 µg/mL; Sigma-Aldrich). The analysis was performed using confocal microscope Zeiss LSM780 (Carl Zeiss).

Table 2. List of primary antibodies used for immunocytochemistry.

Antigen	Source	Isotype	Dilution	Company	Catalogue Number
Nestin	Mouse monoclonal	IgG1	1:500	Merck Millipore	MAB5326
β-III-Tubulin	Mouse monoclonal	IgG2B	1:500	Sigma-Aldrich	T8660
Neurofilament 200 (NF-200)	Mouse monoclonal	IgG1	1:400	Merck Millipore	N042
NeuN	Mouse monoclonal	IgG1	1:100	Merck Millipore	MAB377
A2B5	Mouse monoclonal	IgM	1:700	Merck Millipore	MAB312R
Ki67	Rabbit polyclonal	IgG(L+H)	1:1000	Abcam	AB15580
SSEA4	Mouse monoclonal	IgG3	1:400	Merck Millipore	MAB4304

2.10. Real Time-Quantitative Polymerase Chain Reaction (RT-qPCR)

Total RNA was isolated from initial, 2D populations, and 3D cultured population using the following kits: Total RNA Mini Plus kit (A&A Biotechnology, Gdynia, Poland) and Total RNA Mini Plus Concentrator (A&A Biotechnology) according to the manufacturer's protocols.

RNA was eluted with 20 µL of RNase-free H_2O (Sigma Aldrich). The quantity and the quality of RNA were assessed using a NanoDrop 2000 spectrophotometer (Thermo Scientific). The elimination of genomic DNA (gDNA) contamination in all RNA samples was performed using a Clean up RNA Concentrator (A&A Biotechnology).

RNA samples were stored at −80 °C until were further used. A complementary strand of DNA (cDNA) from RNA was generated using a High-Capacity RNA-to-cDNA™ Kit (Applied Biosystems, Thermo Fischer Scientific, Waltham, MA, USA) according to the manufacturer's instructions. Following the reverse transcription, samples were diluted in RNase-free water and stored at −20 °C until subsequent testing.

Quantitative polymerase chain reactions were performed using SYBR green Master Mix (Applied Biosystems) and specific primers (Table 3) with the 7500 Real Time PCR System (Applied Biosystems). The relative amount of RNA was calculated with the comparative delta-delta Ct method ($2^{-\Delta\Delta Ct}$) and gene expression was normalized using β-actin (ACTB). Gene expression was compared with the mean level of the corresponding gene expression in cells from initial population (3rd passage of WJ-MSC culture) and expressed as n-fold ratio.

Table 3. List of primers used for Real Time-Quantitative Polymerase Chain Reaction (RT-qPCR).

Gene	NCBI Reference Sequence	Product Size	Primer Sequence (5′ -> 3′)
β-Actin	NM_001101.5	250 bp	F: CATGTACGTTGCTATCCAGGC R: CTCCTTAATGTCACGCACGAT
Nestin1	NM_006617.2	64 bp	F: GGGAAGAGGTGATGGAACCA R: AAGCCCTGAACCCTCTTTGC
β-Tubulin III	NM_001197181.2	126 bp	F: GGAAGAGGGCGAGATGTACG R: GGGTTTAGACACTGCTGGCT
MAP-2	NM_001375545.1	99 bp	F: TTGGTGCCGAGTGAGAAGA R: GTCTGGCAGTGGTTGGTTAA
GFAP	NM_001363846.2	100 bp	F: CCGACAGCAGGTCCATGT R: GTTGCTGGACGCCATTG
Sox2	NM_003106.4	93 bp	F: GTGGAAACTTTTGTCGGAGA R: TTATAATCCGGGTGCTCCTT
Rex1	NM_001304358.2	107 bp	F: GCTCCCTTGAATGTTCTTTG R: GCCTGTCATGTACTCAGAAT
Nanog	NM_024865.4	103 bp	F: GAACCTCAGCTACAAACAGG R: CGTCACACCATTGCTATTCT
Oct3/4 (Pou5F1)	NM_001285986.2	331 bp	F: CCTGAAGCAGAAGAGGATCACC R: AAAGCGGCAGATGGTCGTTTGG

2.11. Statistics

Two-group comparisons were performed with Student's test, whereas multiple groups used one-way analysis of variance (ANOVA). The results are presented as mean values of 3 independent experiments ± SD (* < 0.05, ** < 0.01, *** < 0.001, **** < 0.0001), each experiment was performed with cells obtained from one donor. Statistical analysis was conducted with GraphPad Prism v. 7.00 software.

3. Results

3.1. Characteristics of WJ-MSC Cultured in 2D and 3D Conditions

WJ-MSC chosen for experiments exhibited characteristic features of MSC such as morphology and expression of markers. Cells were adherent to the surface and presented

spindle, fibroblast-like morphology. Flow cytometry analysis revealed that cells expressed specific mesenchymal markers (CD73, CD90, and CD105). Less than 1% of WJ-MSC expressed negative markers for MSC (CD34, CD11b, CD19, CD45, and HLA-DR) (Figure 1A). Above described features are accordant with the minimal criteria for MSC established by The International Society for Cellular Therapy.

WJ-MSC were cultured until the third passage in the monolayer with standardly used culture medium. Then, collected cells were divided into two groups: first group was cultured constantly as monolayer (2D cultured), while the second—as spheroids (3D culture) (Figure 1B). Both cultures were conducted for time required for three passages (about 20 div). Then spheroids were dissociated and seeded again to 2D conditions—to observe changes of WJ-MSC. In further analysis, following populations were compared: initial population—third passage of standard WJ-MSC culture; 2D culture—seventh passage of standard WJ-MSC culture; and 3D culture—WJ-MSC cultured as spheroids for 20 div and then reseeded to standard conditions.

Applied 3D method, slightly modified in our laboratory succeeded in sphere formation by WJ-MSC. WJ-MSC were cultured on anti-adhesive surface with the presence of supplements and mitogens (EGF and bFGF)—similarly to the neurospheres formed by NSC. Diameter of WJ-MSC spheroids varied from 20 µm to even 500 µm; however, average size oscillated between 40 and 120 µm. Spheres were cultured up to 20 div; however, the best morphology was observed in the first five div of 3D culture—in later stages spheres spontaneously disintegrated.

Flow cytometry analysis revealed the change in size of single cells—differences were noticed during the cultivation time, as well as between 2D and 3D culture models (Figure 1C). In young spheroids (three div) small, round cells predominated, compared to parallelly cultured 2D cells, whereas in old spheroids (10 div) we could distinguish an increase in the number of large cells. During 2D culture, the ratio of both cells subpopulations (small and large) did not change remarkably.

Adherent properties in WJ-MSC were still detectable after long-term 3D. Although cell morphology was similar to those acquired during standard culture, some differences occurred more frequently (Figure 1D). After 3D culture, we distinguished three subpopulation of cells—standard fibroblast-like cells similar to standard 2D culture; narrow and spindle cells with improved neural potential; and very broad cells indicating senescent morphology.

Live-dead staining using EthD-1 and Cal AM revealed that most of the cells cultured in monolayer were alive (98.91% $\pm$ 0.26) (Figure 2A), whereas spheroids contained significantly more dead cells inside (Figure 2B,C). Number of alive cells was reduced to 55.9% $\pm$ 6.18 and 72.87% $\pm$ 5.29 in 3 and 10 div respectively (Figure 2C). The increase in viability between early and late stage of spheroid culture was also significant.

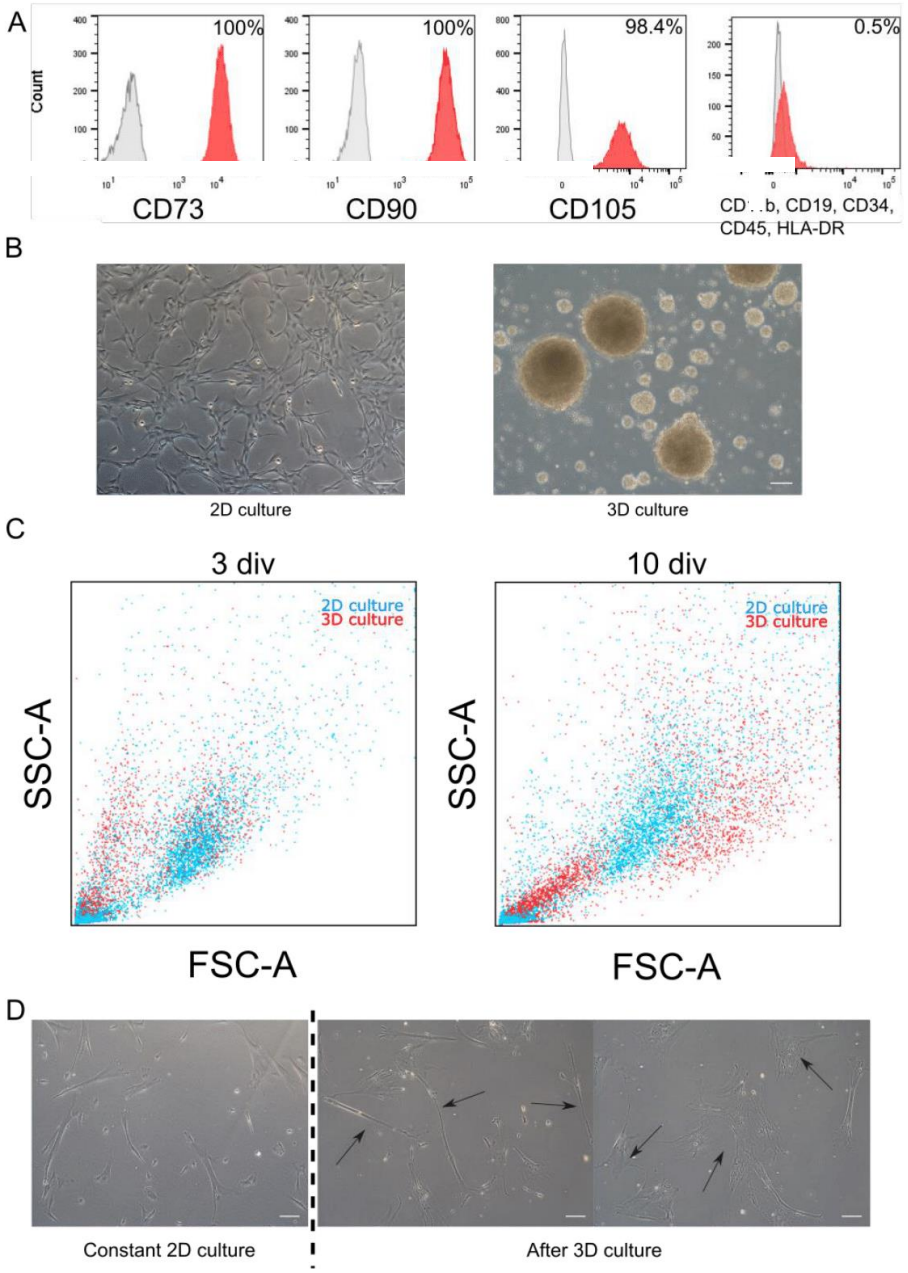

Figure 1. Morphology and phenotype of WJ-MSC cultured in monolayer and as spheroids. (**A**). Flow cytometry analysis. Initial population of WJ-MSC used to experiments expressed specific MSC markers (CD73, CD90, and CD105) and less than 1% of WJ-MSC expressed negative markers (CD11b, CD19, CD34, CD45, and HLA-DR). Red histogram—analyzed marker, grey histogram—isotype control. (**B**). Morphology of 2D and 3D cultured WJ-MSC—monolayer culture of WJ-MSC from 4th passage (up) and WJ-MSC 4 div after formed spheroids (down). (**C**). Flow cytometry—Forward scatter (FSC) and Side scatter (SSC) analysis for 3D culture (spheroids) and 2D (monolayer). Three days in vitro (div) and 10 div after sphere induction, there were differences in size of cells between 2D and 3D culture. (**D**). Different morphology of cells cultured as spheroids after reseeding into 2D conditions. Right: WJ-MSC cultured constantly in 2D for 8 passages. Center and left: WJ-MSC from 3D reseeded to 2D condition—visible two different types of morphology: narrow and small (center) and flat and broad (left) cells. White scalebars represent 100 μm.

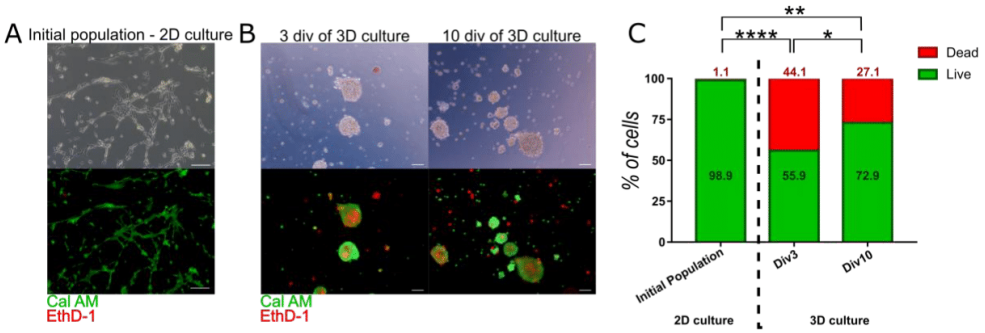

Figure 2. Viability of 3D cultured WJ-MSC—Calcein AM (Cal AM) and Ethidium homodimer-1 (EthD-1) staining. Cal AM stains live cells in green, while EthD-1 stains dead cells in red. Double stained cells are early apoptotic cells. (**A**) Initial population of WJ-MSC contained live cells with almost no dead cells. Scale bars: 100 µm. (**B**) Viability of cells in spheroids—after 3 and 10 div (day in vitro) of 3D culture. Observed darker shade in the contrast phase corresponds to dead cells visible. Scale bars: 100 µm. (**C**) Analysis of live, dead, and early apoptotic cells in initial population and 3D cultured population for 3rd and 10th (div). The results are presented as mean values of 3 experiments ± SD, for * < 0.05, ** <0.01, **** < 0.0001.

3.2. Physiological Properties of WJ-MSC Cultured in 3D Conditions

Spheroids culture conditions change not only the morphology of WJ-MSC, but also influence on the physiological features of the cells. We compared culture features such as: doubling ratio of cells, induction of senescence process and content of stem fraction in population. For this purpose, WJ-MSC spheroids were dissociated to the single cells after 20 div of culture and reseeded to monolayer culture conditions. Results of assays obtained from 3D cultured WJ-MSC were compared to those observed in the initial population of WJ-MSC (from passage 3) and WJ-MSC continuously cultured in 2D conditions (from passage 7).

WJ-MSC were monitored after reseeding to monolayer conditions to calculate Population Doubling Time (PDT) required for each of next four passages. During first passage after 3D cultured, cell proliferation decreased compared to cells constantly cultured in monolayer (Figure 3A). In further passages, 3D cultured WJ-MSC restored the doubling rate and divided in the same ratio as 2D cultured WJ-MSC (Supplementary Table S2). There is a shift between passages of 2D and 3D cultured populations when cumulative value is analyzed (Figure 3B).

To evaluate the effect of the culture method on cell senescence, the β-galactosidase activity was measured. Spheroid-cultured WJ-MSC exhibited significantly higher activity of β-galactosidase (49.04 ± 10.72) than initial population of WJ-MSC (1.24 ± 0.59) and WJ-MSC continuously cultured as monolayer (1.84 ± 0.93) (Figure 3C).

ISCT recommends the Colony forming unit frequency assay (CFU-F) to confirm the stemness of MSC and estimate the fraction of stem/progenitor cells in the population. The values of CFU-F from initial population of WJ-MSC (19.63± 9.5) and 2D cultured WJ-MSC (12.78 ± 5.02) does not differ significantly. However, 3D cultured WJ-MSC indicated significantly reduced CFU-F than initial population (5.11 ± 6.95) (Figure 3D).

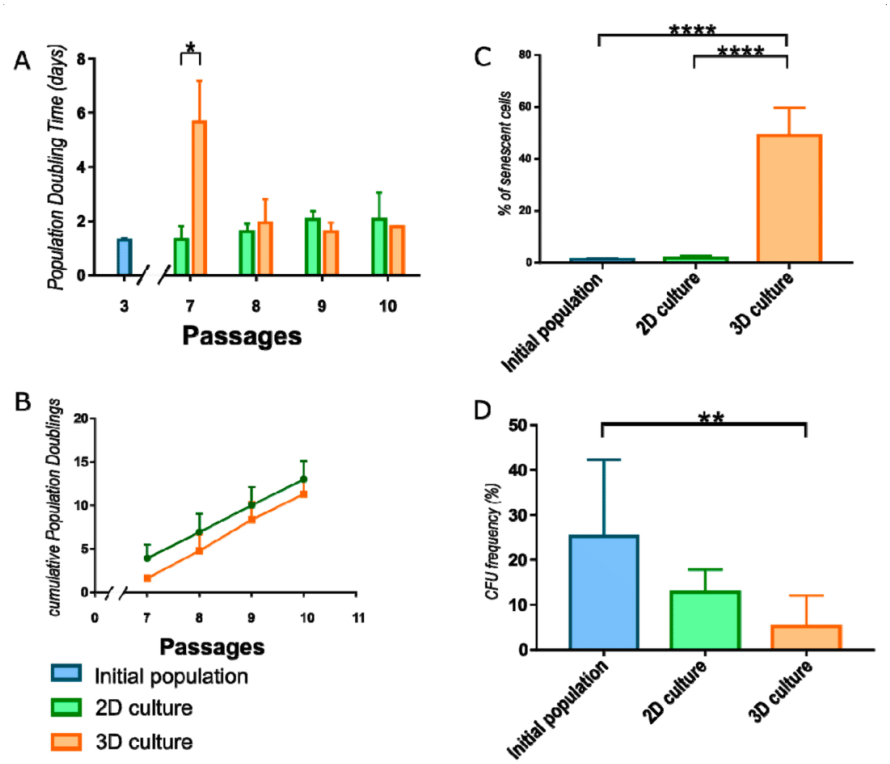

Figure 3. Characteristic of WJ-MSC cultured in different conditions. (**A**) Population doubling time (PDT) for WJ-MSC cultured in 2D and 3D. 3D cultured WJ-MSC divided more slowly than 2D cultured WJ-MSC during the first passage. However, there are observed no differences in next 3 passages. (**B**) Cumulative Population Doublings calculation revealed shift between 2D and 3D cultured populations. (**C**) Senescence process analysis. Number of cells expressing β-galactosidase was significantly higher in 3D cultured WJ-MSC than in initial and 2D cultured populations. (**D**) Colony forming unit (CFU) frequency reduced significantly during 3D culture of WJ-MSC. Following populations of WJ-MSC were used: from 3rd passage (initial populations), from 7th passage (2D culture) and cultured as spheroids (3D culture). The results are presented as mean values of 3 experiments ± SD. For * < 0.05, ** <0.01, **** < 0.0001.

3.3. Neural and Pluripotent Markers Expression in 3D Cultured WJ-MSC

To find out whether 3D culture condition predisposes to increase expression of early neural as well as pluripotent markers, immunocytochemical analysis was performed. Staining of sectioned spheroids revealed the presence in the sphere the early neural markers: Nestin and β-III-Tubulin, early oligodendrocyte marker A2B5 as well as pluripotent surface marker SSEA4. However, we did not observe more mature markers as NF200 or NeuN inside the sphere (Figure 4). Double staining for SSEA4 and Caspase-3 showed that most of SSEA-4 positive cells remained alive (Supplementary Figure S2).

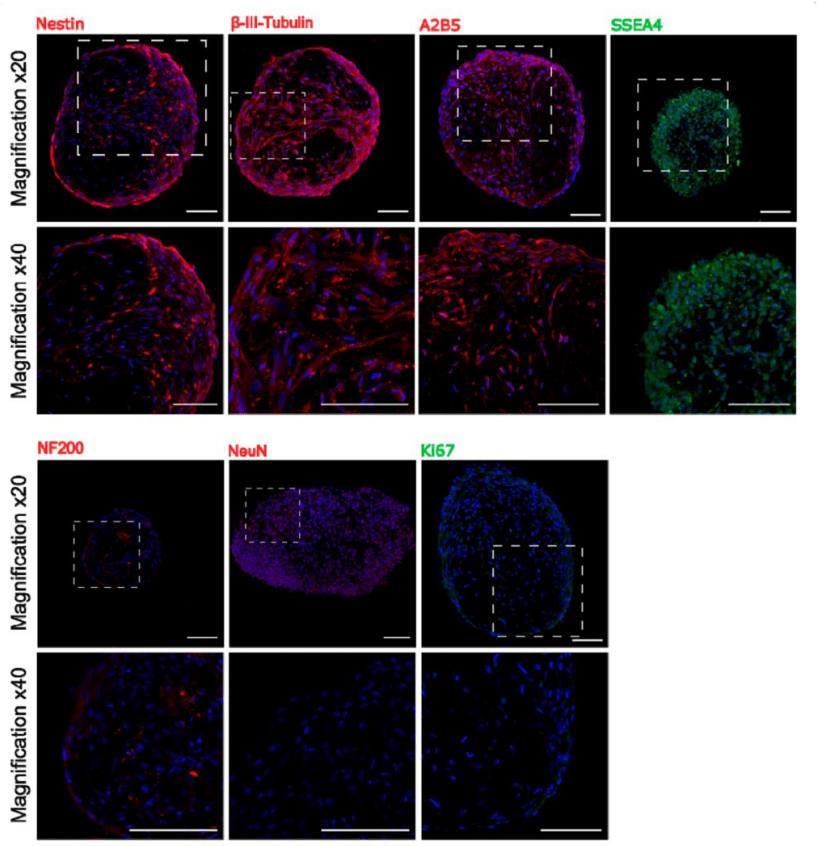

Figure 4. Immunocytochemistry staining of neural and pluripotent markers in sectioned WJ-MSC spheroids in two different magnifications. Early neural markers are also expressed inside the sphere, whereas more mature neural markers were not detected. Spheroids were collected between 10 and 20 day in vitro of 3D culture. Scale bars: 100 μm.

3D population seeded again on the monolayer also displayed early neural and oligodendrocyte markers—the expression was compared to initial population and 2D constantly cultured WJ-MSC (Figure 5, Supplementary Table S3). Expression of Ki67—proliferation marker—was decreased in 3D cultured WJ-MSC compared to initial and 2D cultures, what confirms previously described PDT and CFU-F observations. Early neural markers—Nestin and β-III-Tubulin—were presented more frequently in 3D cultured WJ-MSC than in 2D cultured WJ-MSC. β-III-Tubulin expression in 3D WJ-MSC was even higher than in initial population. However, 3D cell culture conditions did not increase the expression of more mature markers NF-200 and NeuN. Changed culture condition did not affect the expression of A2B5. Expression of SSEA4—pluripotent surface glycosphingolipid—was increased in 3D cultured WJ-MSC, what may indicate that SSEA4-positive cells more favorably survives during long-termed 3D culture.

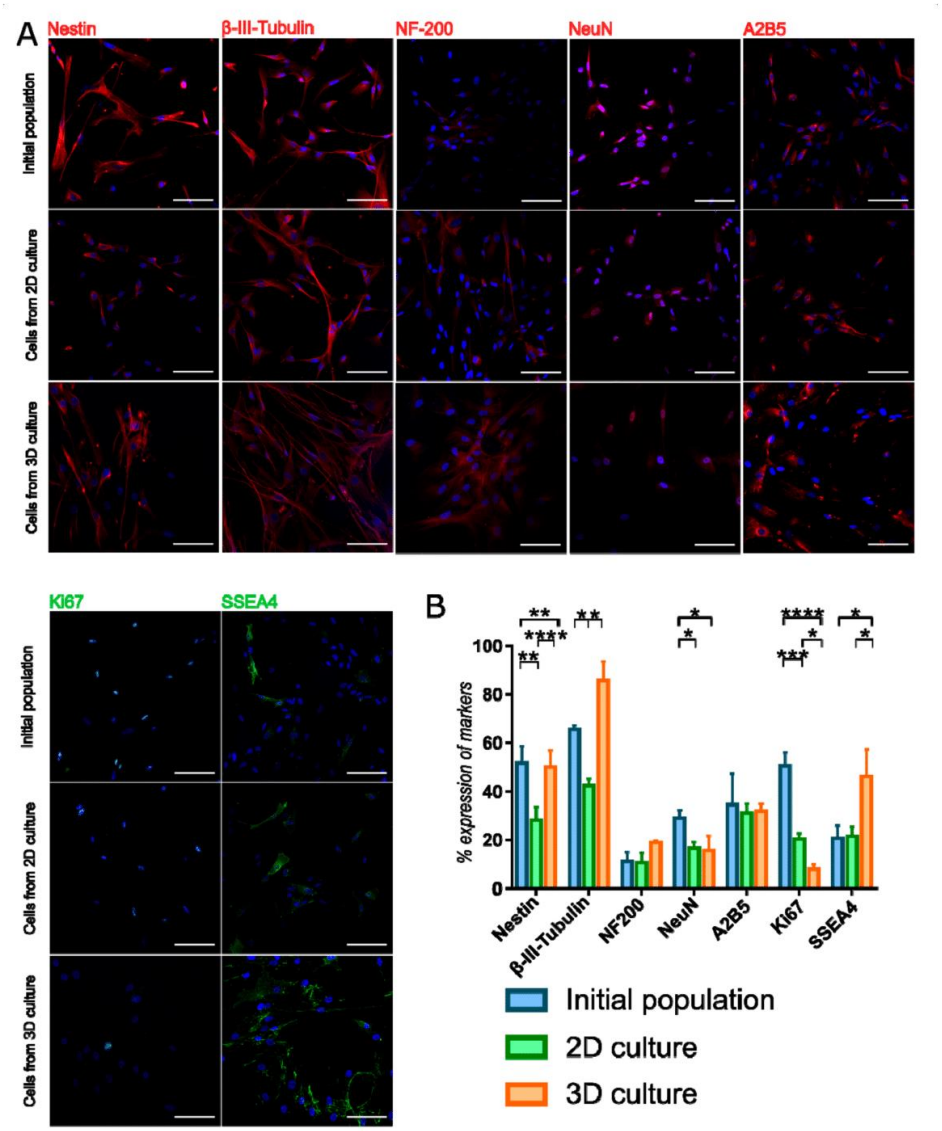

Figure 5. Immunocytochemistry staining of neural and pluripotent markers in WJ-MSC cultured in different conditions. (**A**) 3D cultures changes the expression of some neural and pluripotent markers what is observed even after reseeding to 2D culture. Scale bars: 100 µm. (**B**) Analysis of marker expression in WJ-MSC populations. Following populations of WJ-MSC were used: cells from 3rd passage (initial populations), cells from 7th passage (2D culture) and cells cultured as spheroids after reseeding to 2D (3D culture). The results are presented as mean values of 3 experiments ± SD. For * < 0.05, ** <0.01, *** < 0.001, **** < 0.0001.

3D culture influence was also assessed by the expression changes in genes characteristic for neural or pluripotent phenotype (Figure 6, Supplementary Table S4). Due to the huge fluctuations between genetic material from different isolations we did not reported significant changes upon a long-term 3D cells culture when it comes to early neural marker Nestin and pluripotency genes Nanog, Sox2, Oct3/4, and Rex1. Tendency of increased expression of Nestin and Nanog genes may indicate the maintenance of early undifferentiated state of cells during 3D cell culture. Other analyzed markers—H3Tubulin (early

neural marker), MAP2 (mature neural marker) and GFAP (astroglial marker) revealed some changes between initial population and two methods of further culturing. 2D conditions was more favorable for expression of MAP2 and GFAP. Results obtained from gene expression and immunocytochemistry analysis are not fully consistence, however it may be connected with differences between transcriptional and protein level of analyzed markers. We also performed gene expression analysis for RNA isolated directly from 3D spheroids—without reseeding to 2D (Figure S3). We observed the changes between two timepoints of analysis—Nestin was expressed on higher level in 3D spheroids than 48 h after reseeding to 2D culture. We observed this tendency also for other genes; however, differences were not significantly important.

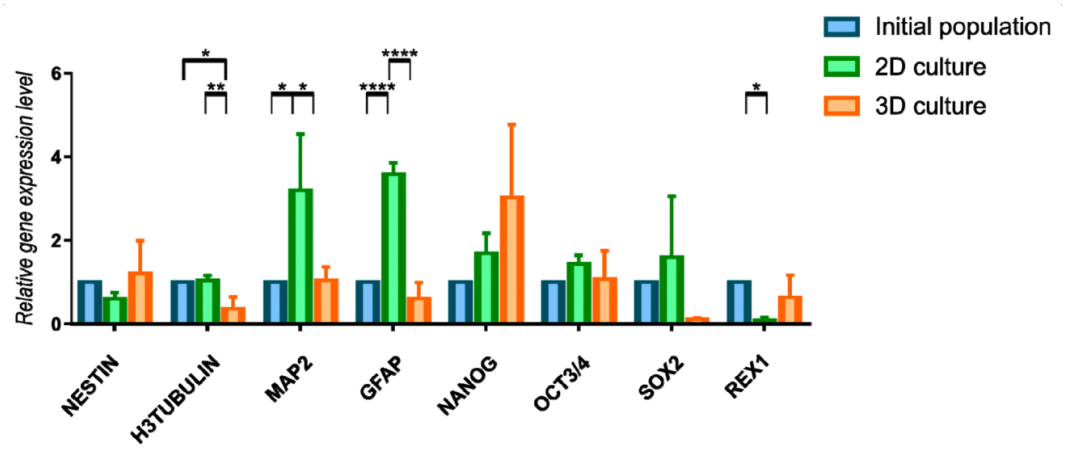

Figure 6. Relative gene expression level (fold change, mean ± SD) of neural and pluripotency phenotype in 2D and 3D WJ-MSC cultures. Quantitation of these genes was determined relative to ACTB as a housekeeping gene by quantitative real-time PCR. Changes in gene expression in WJ-MSC cells cultured in 2D and 3D conditions are shown relative to that in cells grown in the initial population. Following populations of WJ-MSC were used: from 3rd passage (initial populations), from 7th passage (2D culture), cultured as spheroids and transferred to 2D (3D culture). Results shown are the mean of 3 independent RNA isolations, for * < 0.05, ** <0.01, **** < 0.0001.

4. Discussion

Umbilical cord contains Wharton Jelly, which is commonly used source of MSC in stem cell research [14,15]. Different factors and culture conditions are proposed to improve either stemness properties or differentiation potential of WJ-MSC. Our group is especially interested in establishment of protocol inducing differentiation of WJ-MSC toward neural lineage—due to limited alternatives for regeneration of neural system. Although neural differentiation of MSC is controversial, due to the lack functional evidence in vivo, our group confirmed the presence of voltage-sensitive and ligand-gated channels in differentiating neural stem-like cells derived from the nonhematopoietic fraction of human umbilical cord blood [16]. As MSC populations is highly heterogenous [17], we assume initial selection of pro-neural or undifferentiated cells would improve the effect of further neural differentiation. We continued in targeting our research on WJ-MSC and looked for the manner of increasing their neural/undifferentiated potential as we had reported in WJ-MSC spontaneous expression of neuroglial markers such as β-III-Tubulin, GFAP, NF-200 probably due to their premature origin [18]. Change of culture spatial structure appeared to be promising factor that we would like to confront.

The present studies were focused on the effect of prolonged 3D culture system of MSC. We tried to find out if applied culture conditions would result in obtaining population with better proliferation potential, younger phenotype or increased clonogenic abilities

like in the cell niche. What is more, we examined the influence on gene expression and presence of markers responsible for neural or pluripotent phenotype—which direction cells would follow after 3D culture. WJ-MSC were cultured as spheroids in long termed culture for about 20 div to examine physiological changes. We compared features of 3D cultured cells with initial population derived from early passage (third passage) as well as population cultured constantly in monolayer up to the seventh passage. Clonogenicity, proliferation potential, senescence, and expression of neural and pluripotency markers were analyzed to confirm whether long-term 3D conditions are favorable for MSC.

We confirmed that despite their adherent properties, WJ-MSC can be directed to form the spheres in culture medium dedicated for NSC formed neurospheres. Spheroids can be generated also from other tissues containing MSC such as bone marrow [19], adipose tissue [20], or dental pulp [21] as well as other [21–24]. Main purpose of 3D neurosphere culture is to selectively isolate and culture the subpopulation of cells with higher neural differentiation capacities.

WJ-MSC in spheroids still exhibited strong adhesive properties—even undissociated spheres in standard culture medium settled down and attached to surface. 3D culture also did not change expression of typical MSC markers (CD73, CD90, and CD105) and multipotent differentiation into mesodermal lines [25,26]. Some research groups observed even enhanced mesodermal differentiation after 3D culture [7,26]. Spheroid culture led to morphology changes, visible especially during the first passage after reseeding on 2D [6,8,11,27]. Except WJ-MSC with characteristic fibroblast-like morphology, we observed more small cells with round or spindle shape. Acquisition of round shape and then elongation is typical for neural cell maturation from progenitors to immature neurons [28]. Morphological changes were also observed in non-neural cells undergoing neuronal differentiation [29]. Small size of cells after 3D culture could be also the effect of cell reorganization in spheroids and decreased packing density [11,27]. Unfortunately, we also noticed more large, flat cells connected with the loss of stemness state and higher senescence process [30,31]. We speculate that 3D culture could promote the survival of quiescent cell subpopulation.

3D cultured WJ-MSC significantly differed in cell division ratio than initial WJ-MSC population and 2D cultured WJ-MSC. What is more, immunochemistry staining for Ki67—proliferation marker—confirmed smaller fraction of dividing cells after 3D culture. Ki67 staining in AD-MSC neurospheres revealed that more than 80% of cells remains in quiescent phase [32]. Reduced proliferation of cells in spheroids suggested arrest in Go/G1 phase [7,8,26,33–35]. This observation could be connected with reduced CFU frequency indicating smaller number of clonogenic cells presented in 3D cultured population. However, many groups noticed better CFU frequency after transferring cells from spheres to 2D conditions [6,36]. Bartosh and colleagues published observations similar to ours, that CFU and population doubling values decreased directly after seeding cells derived from spheres. However, in further passages those features were similar or even higher than in a standard adherent culture [8]. Additionally, AD-MSC cultured as spheres expanded more rapidly than 2D cultured cells, but the difference was visible after 42 div of 2D culture [10]. Some research group did not observe the differences in CFU frequency between 2D and 3D cell culture [7].

Senescence was more pronounced in 3D cultured WJ-MSC. Increased β-galactoside activity was detected in almost a half of population just after changing the environment from 2D to 3D. To the contrast, other research groups reported that population after 3D culture contains less amount of senescent cells [6]. AD-MSC from spheroids contained more senescent cells in longer 3D culture, but still less than cells cultured on monolayer [10]. Differences in senescent processes between the results may arise from the source of MSC. In our experiments MSC were isolated from afterbirth tissue—part of umbilical cord. The initial population of WJ-MSC contained small number of senescent cells (less than 1%) and senescence process did not increase with further passages (up to 5% of senescent cells) [37], whereas for tissues from adult patients percentage of senescent cells was higher:

for BM-MSC about 22,5% [6], for AD-MSC about 10% [10]. In our opinion, changing the culture conditions to less physiological for adherent cells (stress factor) accelerates senescence. Despite that, the other subpopulation that remains in the culture over time—those cells either have greater stress resistance or are developmentally younger and do not necessarily require adhesion for proper function.

These observations are consistent with changes in cell survival. In the majority of published experiments, 3D culture is a transient stage which last usually up to three div, no longer than seven div—especially when it comes to the use of low-attachment surface [4] among others because of poor MSC survival in 3D conditions. In our experiments 3D culture also reduced cell viability. Calcein AM and Ethidium Homodimer-1 staining pointed huge proportion of dead cells inside spheroid, which usually was placed in dark core. We noticed huge fraction of double stained cells, which was counted as dead—those cells were permeabilized with residual activity of esterases. Such situation was reported in other publication, using propidium iodide which has the same properties and emission spectrum as EthD-1 [38]. According to Peng, apoptosis rate in sphere reaches up to 20% of cells [39]. The most visible shift we noticed between third and fourth div of 3D culture. This change in viability was reported also by other research groups [8,32]. Even 3D cultures performed with other method, such as hanging drop, underwent the reduction in viability [8]. However, the spheroid culture contained more alive cells in 10 div of culture than in 3 div. With the duration of 3D cell culture, cellular composition of spheres had to change as the number of dead cells declined. This confirms our assumptions that during 3D culture, spheroid is decomposed, while population is segregated spontaneously—survived cells are more resistant to stress conditions, with slightly different properties than typical adult mesenchymal cells. Decreased viability might be also connected with size and insufficient transportation of nutrients and oxygen to all cells in bigger spheroids. For ESC embryoid bodies, oxygen concentration in the center can vary depends on the structure's radius. In larger aggregates (400 μm radius) was lower than in smaller aggregates (200 μm radius) [40]. For 100 μm sphere diameter, the concentration of glucose and glutamine is 36,38 and 1,33 mmol/L—those values are insufficient, and cells begin to die in spheres core [41]. However, MSC spheroids are usually smaller. Hypoxic core, which could be responsible for increased cell deaths, was observed only in large spheroids consisting of 250,000 cells or more [27]. In smaller spheres oxygen gradient varied less than 10% across the aggregate layers. Decreased packing density might be the other mechanism that enable penetration of nutrients and oxygen to sphere core [27]. Observed population of smaller cells in 3D culture supported the evidence for change in cell densities and morphology in spheroids. Despite that, caspase activity confirmed that viability of cells decrease with sphere size [27]. Other used technique—thermal lifting in 3D culture was reported not only to lower apoptosis processes but also ischemic stress which is another relevant factor [36]. Cells in 3D culture were characterized by metabolism changes such as lower glucose consumption, lower L-lactase production [6,27], as well as changes in mitochondria [6]. Although lowered metabolism rate, there were observed higher level of mitochondrial and total reactive oxide species [6], what might be responsible for lowered viability and increased senescence during long-term 3D culture of MSC.

Except the changes of cell morphology, physiology and viability, 3D culture stimulates the acquisition of unique phenotype by cells. RNA-sequencing revealed the unique transcriptional profile of UC-MSC neurospheres, containing the features of NSC and MSC [42]. In our experiments, immunocytochemistry staining confirmed increased presence of early neural markers such as Nestin and β-III-Tubulin. 3D culture probably improve only the early stages of acquiring neural phenotype—NF-200 and NeuN expression was weak and did not changed between 2D and 3D culture. Yang and colleagues reported similar effect of 3D culture—cells from neurospheres expressed more Nestin after exposition to neural differentiation conditions, but any mature markers such as NeuN, MAP2, or glial marker GFAP [32]. However, 3D culture stage effected on future neural differentiation. Neurosphere culture of UC-MSC increased expression of neural [43] or both neural and glial [44]

markers during neural differentiation. According to some reports, neurosphere culture of MSC improved neural differentiation potential [44]. Especially, Feng and colleagues claimed to have obtained even nerve-like cells with properties of astrocytes, neurons, and oligodendrocytes [45]. 3D culture could be an initial step preceding the neural differentiation under the specific differentiation conditions.

Stemness-related transcription factors (SRTF)—Sox2, Nanog, Rex1, Oct3/4, Klf4, are involved in cell divisions during embryonic development. Pluripotency and differentiation of MSC into all germ layers is broadly discussed. Oct3/4 was observed in WJ-MSC cultured in 5% oxygen concentration [46]. Nanog was detected in AD-MSC and BM-MSC, but not Sox-2 and Oct3/4 [47]. Although the discoveries of pluripotency genes in MSC, their expression is much weaker than in ESC [47] or iPSC [48]. 3D culture is proposed as a method to increase the expression of pluripotent genes by MSC. However, we did not observe the change of SRTF genes expression between 2D and 3D culture conditions what is not consistent with observations from other research groups. Pluripotent marker expression in MSC-neurospheres was observed by others in neurosphere-forming media [39,42,44] as well as in other sphere-inducing conditions [6,9,10,33]. Except the increased expression of SRTF, there were also observed epigenetic changes gene promotors and miRNAs responsible for pluripotency [9]. However, some research also did not report increased expression of stem cell markers in MSC-neurospheres—Bonilla-Porras and colleagues observed lower levels of Nanog, Oct4 and Sox2 in cells from WJ-MSC neurospheres than from 2D cultured WJ-MSC [43]. Dromard and colleagues did not notice the significant differences in expression of Nanog and Oct3/4 between spheres and monolayer [7]. The differences in above discussed results may be explained with the time of material collection. Cells in sphere did not exhibit pluripotency during whole period of 3D culture—expression was the highest between 3 and 5 div, after six div it drops [34]. We observed that even short time of adhesion change the RNA expression (Supplementary materials). Other authors reported that during 48 h after spheres return to 2D conditions, pluripotent expression decreases to the level presented in cultured monolayer cells [34]. Unfortunately, expression of pluripotent genes in MSC 3D still was significantly lower than in ESC [34].

It is discussed whether described effects are exaggerated by 3D conditions or could be influence by source of MSC. The comparative analysis are limited. WJ-MSC and BM-MSC generated secondary spheres after dissociation, while AD-MSC did not. What is more, secretomes profile of spheres were different—WJ-MSC secreted more neurotrophic factors. Protein level of neural markers inside sphere and under neural differentiation conditions also varied between different tissues. According to these observations, authors strongly suggested that WJ has better neurogenic potential than other sources [49]. In addition, Peng and colleagues performed identical analysis on MSC-spheres derived from two tissues—adipose and umbilical cord. The relative gene expression was similar, although the time of increase in gene expression differed. For some genes, such as Sox2 or Olig2 for UC-MSC spheres expression reached the maximum in second div, while for AD-MSC the peak was in seventh div [39,42]. It indicates that choice of MSC source be relevant.

Immunostaining revealed increased presence of surface marker SSEA4—glycosphingolipid which is included as a one of pluripotency markers. SSEA4 and SSEA3—other molecule from the same family—are characteristic for ESC cells [50]. SSEA3 is earlier in development—SSEA3 expression is the highest between four and eight cell stages of embryo, whereas SSEA4—morula and early blastocyst stages [51,52]. SSEA4 is also detected in early neuroepithelium [53,54] SSEA4-positive NSC can form neurospheres and SSEA4 expression remains sustained during 3 passages of NSC cultures [55]. Role of SSEA4 in NSC cells still remains unknown [51]. SSEA4 is also detected on MSC surface [18,56,57]. SSEA4 is presented during the MSC culture up to the ninth passage of WJ-MSC culture, while expression of SSEA3 is the highest directly after isolation and is detected only up to fifth passage [56]. SSEA4-positive BM-MSC population characterizes with better clonogenity [57]. SSEA4 together with small cell size are proposed as prognostic markers to distinguish young and old cells, which can be isolated with FACS [58]. SSEA4 expression

may depend on cell culture conditions—it was correlated with medium serum concentration [56]. SSEA4, even counted as pluripotency marker, does not always coexist with other pluripotency genes what was shown on population of limbal stem cells (which resembled MSC) [59]. Similar situation was observed in MSC—SSEA4-positive WJ-MSC expressed SRTF genes on the same level as SSEA-4-negative cells [56]. Increased detection of SSEA4 in 3D cultured population might suggest acquiring this marker during spheroids culture or better survival of SSEA4-positive cells. Double staining for SSEA4 and Caspase-3 confirmed that apoptosis did occur only in a small fraction of SSEA-4-positive cells (Supplementary Materials). We rather assume that SSEA4-positve cells are more favorable to endure harsh conditions of neurosphere formation. The presence of SSEA4 positive cells could correspond with their undifferentiated state. According to Arrora and colleagues, undifferentiated state of cells in unfavorable conditions could be connected with quiescence [60]. Stress conditions such as loss of adhesion and high cell density lead to the quiescent state of MSC. Described earlier hypoxia and oxidative stress linked with sphere size [27] seems to be also responsible for cell persistent in a quiescent state in order to be available for further tissue repair and regeneration in beneficial [61].

In accordance with suggested neuroectodermal origin of distinct subpopulation of MSC [62], existing subpopulation of small cells and increased containment of early neural markers Nestin and β-III-Tubulin indicate that prolonged 3D culture enable to select cells with higher neural potential. Especially, very interesting for us was expression of Nestin, which may indicate the other explanation. Even though, quiescent NSC are negative for Nestin, active NSC express Nestin—importantly to mention, active NSC is the population which forms neurospheres, whereas quiescent NSC do not [63]. When it comes to MSC, Nestin may be the key explaining neurosphere formation—Nestin-negative cells do not form spheroids [64,65]. Nestin expression and sphere-forming capacities suggest neuroectodermal origin of this population [64]. Nestin-positive population derived from rat bone marrow contains MSC and Neural Crest Stem Cells as well [66]. During development, cells from neural crest which are not committed to glial lineage yet may migrate along nerves to bone marrow and there reside for the rest of life [67]. Those cells create a niche for hematopoietic stem cells (HSC) and remains quiescent in adulthood [64,65]. Under spheroids culture formed by magnetic levitation, increased Nestin expression is explained as quiescent state of such cells [67]. Neural crest-derived cells occur not only in bone marrow but also in other tissues containing MSC such as adipose [68,69]. Human umbilical cord blood contains neural crest-like progenitor cells which express Nestin, form neurospheres and can differentiate into neuronal and glial lineages [70]. Interestingly, we also reported more SSEA4-positive cells after long 3D cell culture. High content of SSEA3 and SSEA4 was observed during cell progeny activated by antibody mimicking Interferon-I [71]. Taking together, increased levels of Nestin and SSEA4 suggest quiescence of cells which remained over 20 div of 3D culture. Quiescent state can be the factor that enables survival of MSC during long-termed non-adherent conditions.

5. Conclusions

We confirmed that WJ-MSC can be cultured as spheroids on low-attachment surface with culture medium dedicated for neurospheres for at least 20 div. This type of culture characterizes with increased cell death after first three div, but then, viability stabilizes in later stage. Long-termed 3D culture of WJ-MSC as spheroids did not improved the cell condition. In fact, it reduced stemness and increased senescence process. However, it improved the occurrence of early neural markers what might indicate the survival of cell subpopulation with unique features, such as SSEA4 expression and possible quiescent state.

Supplementary Materials: The following are available online at https://www.mdpi.com/2073-4409/10/4/719/s1, Table S1: List of secondary antibodies used for immunocytochemistry, Figure S1: Secondary antibody staining controls for 2D and 3D conditions, Table S2: Population doubling time values (days) for 2D and 3D cultured WJ-MSC, Table S3: Quantitative data of immunocytochemistry staining analysis, Figure S2: Immunocytochemistry double staining for SSEA4 and Cleaved caspase-3

in WJ-MSC spheroid, Table S4: Relative gene expression level quantitative data. Figure S3: Extended analysis for relative gene expression level (fold change, mean ± SD) of neural and pluripotency phenotype in 2D and 3D WJ-MSC. Table S5: Relative gene expression level quantitative data for RNA collected directly from free floating spheroids.

Author Contributions: Conceptualization, A.K. and A.S.; methodology, A.K., M.K., and A.S.; software, A.K.; validation, A.K, A.W., and M.K.; formal analysis, A.K., A.W., and M.K.; investigation, A.K.; resources, A.K.; data curation, A.K. and A.S.; writing—original draft preparation, A.K.; writing—review and editing, A.S.; visualization, A.K.; supervision, M.K. and A.S.; project administration, A.S.; funding acquisition, A.S. All authors have read and agreed to the published version of the manuscript.

Funding: This research was funded by The National Center for Research Grant NCN 2018/31/B/NZ4/03172, and ESF, POWR.03.02.00-00-I028/17-00.

Institutional Review Board Statement: The study was conducted according to the guidelines of the Declaration of Helsinki, and approved by the Ethics Committee of Warsaw Medical University guideline (KB/213/2016).

Informed Consent Statement: Informed consent was obtained from all subjects involved in the study.

Data Availability Statement: The data presented in this study are available on request from the corresponding author.

Acknowledgments: We are thankful to Laboratory of Advanced Microscopy Techniques for assistance with Confocal Microscopy imaging, and colleagues from Translational Platform for Regenerative Medicine and Department of Stem Cell Bioengineering for supporting during research.

Conflicts of Interest: The authors declare no conflict of interest.

References

1. Friedenstein, A.J.; Piatetzky-Shapiro, I.I.; Petrakova, K.V. Osteogenesis in transplants of bone marrow cells. *Development* **1966**, *16*, 381–390.
2. Dominici, M.; Le Blanc, K.; Mueller, I.; Slaper-Cortenbach, I.; Marini, F.C.; Krause, D.S.; Deans, R.J.; Keating, A.; Prockop, D.J.; Horwitz, E.M. Minimal criteria for defining multipotent mesenchymal stromal cells. The International Society for Cellular Therapy position statement. *Cytotherapy* **2006**, *8*, 315–317. [CrossRef] [PubMed]
3. Sart, S.; Tsai, A.C.; Li, Y.; Ma, T. Three-dimensional aggregates of mesenchymal stem cells: Cellular mechanisms, biological properties, and applications. *Tissue Eng. Part B Rev.* **2014**, *20*, 365–380. [CrossRef] [PubMed]
4. Jauković, A.; Abadjieva, D.; Trivanović, D.; Stoyanova, E.; Kostadinova, M.; Pashova, S.; Kestendjieva, S.; Kukolj, T.; Jeseta, M.; Kistanova, E.; et al. Specificity of 3D MSC Spheroids Microenvironment: Impact on MSC Behavior and Properties. *Stem Cell Rev. Rep.* **2020**, *16*, 853–875. [CrossRef]
5. Knight, E.; Przyborski, S. Advances in 3D cell culture technologies enabling tissue-like structures to be created in vitro. *J. Anat.* **2015**, *227*, 746–756. [CrossRef] [PubMed]
6. Liu, Y.; Muñoz, N.; Tsai, A.C.; Logan, T.M.; Ma, T. Metabolic Reconfiguration Supports Reacquisition of Primitive Phenotype in Human Mesenchymal Stem Cell Aggregates. *Stem Cells* **2017**, *35*, 398–410. [CrossRef]
7. Dromard, C.; Bourin, P.; André, M.; de Barros, S.; Casteilla, L.; Planat-Benard, V. Human adipose derived stroma/stem cells grow in serum-free medium as floating spheres. *Exp. Cell Res.* **2011**, *317*, 770–780. [CrossRef]
8. Bartosh, T.J.; Ylöstalo, J.H.; Mohammadipoor, A.; Bazhanov, N.; Coble, K.; Claypool, K.; Lee, R.H.; Choi, H.; Prockop, D.J. Aggregation of human mesenchymal stromal cells (MSCs) into 3D spheroids enhances their antiinflammatory properties. *Proc. Natl. Acad. Sci. USA* **2010**, *107*, 13724–13729. [CrossRef]
9. Guo, L.; Zhou, Y.; Wang, S.; Wu, Y. Epigenetic changes of mesenchymal stem cells in three-dimensional (3D) spheroids. *J. Cell. Mol. Med.* **2014**, *18*, 2009–2019. [CrossRef]
10. Cheng, N.-C.; Chen, S.-Y.; Li, J.-R.; Young, T.-H. Short-Term Spheroid Formation Enhances the Regenerative Capacity of Adipose-Derived Stem Cells by Promoting Stemness, Angiogenesis, and Chemotaxis. *Stem Cells Transl. Med.* **2013**, *2*, 584–594. [CrossRef]
11. Frith, J.E.; Thomson, B.; Genever, P.G. Dynamic three-dimensional culture methods enhance mesenchymal stem cell properties and increase therapeutic potential. *Tissue Eng. Part C Methods* **2010**, *16*, 735–749. [CrossRef]
12. Vescovi, A.L.; Parati, E.A.; Gritti, A.; Poulin, P.; Ferrario, M.; Wanke, E.; Frölichsthal-Schoeller, P.; Cova, L.; Arcellana-Panlilio, M.; Colombo, A.; et al. Isolation and Cloning of Multipotential Stem Cells from the Embryonic Human CNS and Establishment of Transplantable Human Neural Stem Cell Lines by Epigenetic Stimulation. *Exp. Neurol.* **1999**, *156*, 71–83. [CrossRef]
13. Reynolds, B.A.; Weiss, S. Generation of neurons and astrocytes from isolated cells of the adult mammalian central nervous system. *Science* **1992**, *255*, 1707–1710. [CrossRef] [PubMed]

14. Forraz, N.; Mcguckin, C.P. The umbilical cord: A rich and ethical stem cell source to advance regenerative medicine. *Cell Prolif.* **2011**, *44*, 60–69. [CrossRef]
15. Pirjali, T.; Azarpira, N.; Ayatollahi, M.; Aghdaie, M.H.; Geramizadeh, B.; Talai, T. Isolation and Characterization of Human Mesenchymal Stem Cells Derived from Human Umbilical Cord Wharton's Jelly and Amniotic Membrane. *Int. J. Organ Transplant. Med.* **2013**, *4*, 111–116. [PubMed]
16. Sun, W.; Buzanska, L.; Domanska-Janik, K.; Salvi, R.J.; Stachowiak, M.K. Voltage-Sensitive and Ligand-Gated Channels in Differentiating Neural Stem-Like Cells Derived from the Nonhematopoietic Fraction of Human Umbilical Cord Blood. *Stem Cells* **2005**, *23*, 931–945. [CrossRef]
17. Li, Z.; Zhang, C.; Weiner, L.P.; Zhang, Y.; Zhong, J.F. Molecular characterization of heterogeneous mesenchymal stem cells with single-cell transcriptomes. *Biotechnol. Adv.* **2013**, *31*, 312–317. [CrossRef]
18. Drela, K.; Lech, W.; Figiel-Dabrowska, A.; Zychowicz, M.; Mikula, M.; Sarnowska, A.; Domanska-Janik, K. Enhanced neurotherapeutic potential of Wharton's Jelly-derived mesenchymal stem cells in comparison with bone marrow mesenchymal stem cells culture. *Cytotherapy* **2016**, *18*, 497–509. [CrossRef] [PubMed]
19. Somoza, R.; Conget, P.; Rubio, F.J. Neuropotency of Human Mesenchymal Stem Cell Cultures: Clonal Studies Reveal the Contribution of Cell Plasticity and Cell Contamination. *Biol. Blood Marrow Transplant.* **2008**, *14*, 546–555. [CrossRef] [PubMed]
20. Choi, S.A.; Lee, J.Y.; Wang, K.-C.; Phi, J.H.; Song, S.H.; Song, J.; Kim, S.-K. Human adipose tissue-derived mesenchymal stem cells: Characteristics and therapeutic potential as cellular vehicles for prodrug gene therapy against brainstem gliomas. *Eur. J. Cancer* **2012**, *48*, 129–137. [CrossRef]
21. Pisciotta, A.; Bertoni, L.; Riccio, M.; Mapelli, J.; Bigiani, A.; La Noce, M.; Orciani, M.; de Pol, A.; Carnevale, G. Use of a 3D Floating Sphere Culture System to Maintain the Neural Crest-Related Properties of Human Dental Pulp Stem Cells. *Front. Physiol.* **2018**, *9*, 547. [CrossRef] [PubMed]
22. Abe, S.; Yamaguchi, S.; Sato, Y.; Harada, K. Sphere-Derived Multipotent Progenitor Cells Obtained From Human Oral Mucosa Are Enriched in Neural Crest Cells. *Stem Cells Transl. Med.* **2016**, *5*, 117–128. [CrossRef]
23. Lee, S.-T.; Chu, K.; Jung, K.-H.; Song, Y.-M.; Jeon, D.; Kim, S.U.; Kim, M.; Lee, S.K.; Roh, J.-K. Direct Generation of Neurosphere-Like Cells from Human Dermal Fibroblasts. *PLoS ONE* **2011**, *6*, e21801. [CrossRef]
24. Yang, R.; Xu, X. Isolation and culture of neural crest stem cells from human hair follicles. *J. Vis. Exp.* **2013**, *6*, e3194. [CrossRef]
25. Fu, L.; Zhu, L.; Huang, Y.; Lee, T.D.; Forman, S.J.; Shih, C.C. Derivation of neural stem cells from mesenchymal stem cells: Evidence for a bipotential stem cell population. *Stem Cells Dev.* **2008**, *17*, 1109–1121. [CrossRef] [PubMed]
26. Baraniak, P.R.; McDevitt, T.C. Scaffold-free culture of mesenchymal stem cell spheroids in suspension preserves multilineage potential. *Cell Tissue Res.* **2012**, *347*, 701–711. [CrossRef] [PubMed]
27. Murphy, K.C.; Hung, B.P.; Browne-Bourne, S.; Zhou, D.; Yeung, J.; Genetos, D.C.; Leach, J.K. Measurement of oxygen tension within mesenchymal stem cell spheroids. *J. R. Soc. Interface* **2017**, *14*, 20160851. [CrossRef]
28. Vieira, M.S.; Santos, A.K.; Vasconcellos, R.; Goulart, V.A.M.; Parreira, R.C.; Kihara, A.H.; Ulrich, H.; Resende, R.R. Neural stem cell differentiation into mature neurons: Mechanisms of regulation and biotechnological applications. *Biotechnol. Adv.* **2018**, *36*, 1946–1970. [CrossRef] [PubMed]
29. Jurga, M.; Forraz, N.; Basford, C.; Atzeni, G.; Trevelyan, A.J.; Habibollah, S.; Ali, H.; Zwolinski, S.A.; McGuckin, C.P. Neurogenic properties and a clinical relevance of multipotent stem cells derived from cord blood samples stored in the biobanks. *Stem Cells Dev.* **2012**, *21*, 923–936. [CrossRef]
30. Wagner, W.; Ho, A.D.; Zenke, M. Different facets of aging in human mesenchymal stem cells. *Tissue Eng. Part B Rev.* **2010**, *16*, 445–453. [CrossRef] [PubMed]
31. Gu, Y.; Li, T.; Ding, Y.; Sun, L.; Tu, T.; Zhu, W.; Hu, J.; Sun, X. Changes in mesenchymal stem cells following long-term culture in vitro. *Mol. Med. Rep.* **2016**, *13*, 5207–5215. [CrossRef] [PubMed]
32. Yang, E.; Liu, N.; Tang, Y.; Hu, Y.; Zhang, P.; Pan, C.; Dong, S.; Zhang, Y.; Tang, Z. Generation of neurospheres from human adipose-derived stem cells. *BioMed Res. Int.* **2015**, *2015*, 743714. [CrossRef] [PubMed]
33. Zhang, Q.; Nguyen, A.L.; Shi, S.; Hill, C.; Wilder-Smith, P.; Krasieva, T.B.; Le, A.D. Three-dimensional spheroid culture of human gingiva-derived mesenchymal stem cells enhances mitigation of chemotherapy-induced oral mucositis. *Stem Cells Dev.* **2012**, *21*, 937–947. [CrossRef] [PubMed]
34. Pennock, R.; Bray, E.; Pryor, P.; James, S.; McKeegan, P.; Sturmey, R.; Genever, P. Human cell dedifferentiation in mesenchymal condensates through controlled autophagy. *Sci. Rep.* **2015**, *5*, 13113. [CrossRef]
35. Santos, J.M.; Camões, S.P.; Filipe, E.; Cipriano, M.; Barcia, R.N.; Filipe, M.; Teixeira, M.; Simões, S.; Gaspar, M.; Mosqueira, D.; et al. Three-dimensional spheroid cell culture of umbilical cord tissue-derived mesenchymal stromal cells leads to enhanced paracrine induction of wound healing. *Stem Cell Res. Ther.* **2015**, *6*, 1–19. [CrossRef] [PubMed]
36. Kim, J.; Ma, T. Endogenous extracellular matrices enhance human mesenchymal stem cell aggregate formation and survival. *Biotechnol. Prog.* **2013**, *29*, 441–451. [CrossRef]
37. Lech, W.; Figiel-Dabrowska, A.; Sarnowska, A.; Drela, K.; Obtulowicz, P.; Noszczyk, B.H.; Buzanska, L.; Domanska-Janik, K. Phenotypic, Functional, and Safety Control at Preimplantation Phase of MSC-Based Therapy. *Stem Cells Int.* **2016**, *2016*, 2514917. [CrossRef] [PubMed]
38. Hiraoka, Y.; Kimbara, K. Rapid assessment of the physiological status of the polychlorinated biphenyl degrader Comamonas testosteroni TK102 by flow cytometry. *Appl. Environ. Microbiol.* **2002**, *68*, 2031–2035. [CrossRef] [PubMed]

39. Peng, C.; Lu, L.; Li, Y.; Hu, J. Neurospheres Induced from Human Adipose-Derived Stem Cells as a New Source of Neural Progenitor Cells. *Cell Transplant.* **2019**, *28*, 66S–75S. [CrossRef]
40. van Winkle, A.P.; Gates, I.D.; Kallos, M.S. Mass transfer limitations in embryoid bodies during human embryonic stem cell differentiation. *Cells Tissues Organs* **2012**, *196*, 34–47. [CrossRef] [PubMed]
41. Ge, D. Effect of the neurosphere size on the viability and metabolism of neural stem/progenitor cells. *Afr. J. Biotechnol.* **2012**, *11*, 3976–3985. [CrossRef]
42. Peng, C.; Li, Y.; Lu, L.; Zhu, J.; Li, H.; Hu, J. Efficient One-Step Induction of Human Umbilical Cord-Derived Mesenchymal Stem Cells (UC-MSCs) Produces MSC-Derived Neurospheres (MSC-NS) with Unique Transcriptional Profile and Enhanced Neurogenic and Angiogenic Secretomes. *Stem Cells Int.* **2019**, *2019*, 9208173. [CrossRef]
43. Bonilla-Porras, A.R.; Velez-Pardo, C.; Jimenez-Del-Rio, M. Fast transdifferentiation of human Wharton's jelly mesenchymal stem cells into neurospheres and nerve-like cells. *J. Neurosci. Methods* **2017**, *282*, 52–60. [CrossRef] [PubMed]
44. Mukai, T.; Nagamura-Inoue, T.; Shimazu, T.; Mori, Y.; Takahashi, A.; Tsunoda, H.; Yamaguchi, S.; Tojo, A. Neurosphere formation enhances the neurogenic differentiation potential and migratory ability of umbilical cord-mesenchymal stromal cells. *Cytotherapy* **2016**, *18*, 229–241. [CrossRef]
45. Feng, N.; Han, Q.; Li, J.; Wang, S.; Li, H.; Yao, X.; Zhao, R.C. Generation of highly purified neural stem cells from human adipose-derived mesenchymal stem cells by Sox1 activation. *Stem Cells Dev.* **2014**, *23*, 515–529. [CrossRef]
46. Drela, K.; Sarnowska, A.; Siedlecka, P.; Szablowska-Gadomska, I.; Wielgos, M.; Jurga, M.; Lukomska, B.; Domanska-Janik, K. Low oxygen atmosphere facilitates proliferation and maintains undifferentiated state of umbilical cord mesenchymal stem cells in an hypoxia inducible factor-dependent manner. *Cytotherapy* **2014**, *16*, 881–892. [CrossRef]
47. Pierantozzi, E.; Gava, B.; Manini, I.; Roviello, F.; Marotta, G.; Chiavarelli, M.; Sorrentino, V. Pluripotency regulators in human mesenchymal stem cells: Expression of NANOG but not of OCT-4 and SOX-2. *Stem Cells Dev.* **2011**, *20*, 915–923. [CrossRef]
48. Musiał-Wysocka, A.; Kot, M.; Sułkowski, M.; Badyra, B.; Majka, M. Molecular and Functional Verification of Wharton's Jelly Mesenchymal Stem Cells (WJ-MSCs) Pluripotency. *Int. J. Mol. Sci.* **2019**, *20*, 1807. [CrossRef]
49. Balasubramanian, S.; Thej, C.; Venugopal, P.; Priya, N.; Zakaria, Z.; SundarRaj, S.; Majumdar, A. Sen Higher propensity of Wharton's jelly derived mesenchymal stromal cells towards neuronal lineage in comparison to those derived from adipose and bone marrow. *Cell Biol. Int.* **2013**, *37*, 507–515. [CrossRef]
50. Kallas, A.; Pook, M.; Maimets, M.; Zimmermann, K.; Maimets, T. Nocodazole Treatment Decreases Expression of Pluripotency Markers Nanog and Oct4 in Human Embryonic Stem Cells. *PLoS ONE* **2011**, *6*, e19114. [CrossRef]
51. Itokazu, Y.; Yu, R.K. Glycolipid Antigens in Neural Stem Cells. In *Neural Surface Antigens: From Basic Biology Towards Biomedical Applications*; Elsevier Inc.: Amsterdam, The Netherlands, 2015; pp. 91–102. ISBN 9780128011263.
52. Fenderson, B.A.; Eddy, E.M.; Hakomori, S.-I. Glycoconjugate expression during embryogenesis and its biological significance. *BioEssays* **1990**, *12*, 173–179. [CrossRef]
53. Barraud, P.; He, X.; Caldwell, M.A.; Franklin, R.J. Secreted factors from olfactory mucosa cells expanded as free-floating spheres increase neurogenesis in olfactory bulb neurosphere cultures. *BMC Neurosci.* **2008**, *9*, 24. [CrossRef] [PubMed]
54. Piao, J.-H.; Odeberg, J.; Samuelsson, E.-B.; Kjældgaard, A.; Falci, S.; Seiger, Å.; Sundström, E.; Åkesson, E. Cellular composition of long-term human spinal cord- and forebrain-derived neurosphere cultures. *J. Neurosci. Res.* **2006**, *84*, 471–482. [CrossRef] [PubMed]
55. Barraud, P.; Stott, S.; Møllgård, K.; Parmar, M.; Björklund, A. In vitro characterization of a human neural progenitor cell coexpressing SSEA4 and CD133. *J. Neurosci. Res.* **2007**, *85*, 250–259. [CrossRef]
56. He, H.; Nagamura-Inoue, T.; Tsunoda, H.; Yuzawa, M.; Yamamoto, Y.; Yorozu, P.; Agata, H.; Tojo, A. Stage-Specific Embryonic Antigen 4 in Wharton's Jelly—Derived Mesenchymal Stem Cells Is Not a Marker for Proliferation and Multipotency. *Tissue Eng. Part A* **2014**, *20*, 1314–1324. [CrossRef] [PubMed]
57. Lai, Y.; Sun, Y.; Skinner, C.M.; Son, E.L.; Lu, Z.; Tuan, R.S.; Jilka, R.L.; Ling, J.; Chen, X.-D. Reconstitution of Marrow-Derived Extracellular Matrix Ex Vivo: A Robust Culture System for Expanding Large-Scale Highly Functional Human Mesenchymal Stem Cells. *Stem Cells Dev.* **2010**, *19*, 1095–1107. [CrossRef] [PubMed]
58. Block, T.J.; Marinkovic, M.; Tran, O.N.; Gonzalez, A.O.; Marshall, A.; Dean, D.D.; Chen, X.D. Restoring the quantity and quality of elderly human mesenchymal stem cells for autologous cell-based therapies. *Stem Cell Res. Ther.* **2017**, *8*, 239. [CrossRef]
59. Lim, M.N.; Hussin, N.H.; Othman, A.; Umapathy, T.; Baharuddin, P.; Jamal, R.; Zakaria, Z. Ex vivo expanded SSEA-4+ human limbal stromal cells are multipotent and do not express other embryonic stem cell markers. *Mol. Vis.* **2012**, *18*, 1289–1300. [PubMed]
60. Arora, R.; Rumman, M.; Venugopal, N.; Gala, H.; Dhawan, J. Mimicking muscle stem cell quiescence in culture: Methods for synchronization in reversible arrest. In *Methods in Molecular Biology*; Humana Press Inc.: Totowa, NJ, USA, 2017; Volume 1556, pp. 283–302.
61. Demaria, M.; Campisi, J. Matters of life and breath: A role for hypoxia in determining cell state. *Aging* **2012**, *4*, 523–524. [CrossRef]
62. Niibe, K.; Zhang, M.; Nakazawa, K.; Morikawa, S.; Nakagawa, T.; Matsuzaki, Y.; Egusa, H. The potential of enriched mesenchymal stem cells with neural crest cell phenotypes as a cell source for regenerative dentistry. *Jpn. Dent. Sci. Rev.* **2017**, *53*, 25–33. [CrossRef] [PubMed]
63. Codega, P.; Silva-Vargas, V.; Paul, A.; Maldonado-Soto, A.R.; DeLeo, A.M.; Pastrana, E.; Doetsch, F. Prospective Identification and Purification of Quiescent Adult Neural Stem Cells from Their In Vivo Niche. *Neuron* **2014**, *82*, 545–559. [CrossRef]

64. Méndez-Ferrer, S.; Michurina, T.V.; Ferraro, F.; Mazloom, A.R.; MacArthur, B.D.; Lira, S.A.; Scadden, D.T.; Ma'ayan, A.; Enikolopov, G.N.; Frenette, P.S. Mesenchymal and haematopoietic stem cells form a unique bone marrow niche. *Nature* **2010**, *466*, 829–834. [CrossRef]
65. Isern, J.; García-García, A.; Martín, A.M.; Arranz, L.; Martín-Pérez, D.; Torroja, C.; Sánchez-Cabo, F.; Méndez-Ferrer, S. The neural crest is a source of mesenchymal stem cells with specialized hematopoietic stem cell niche function. *eLife* **2014**, *3*, e03696. [CrossRef]
66. Wislet-Gendebien, S.; Laudet, E.; Neirinckx, V.; Alix, P.; Leprince, P.; Glejzer, A.; Poulet, C.; Hennuy, B.; Sommer, L.; Shakhova, O.; et al. Mesenchymal stem cells and neural crest stem cells from adult bone marrow: Characterization of their surprising similarities and differences. *Cell. Mol. Life Sci.* **2012**, *69*, 2593–2608. [CrossRef]
67. Lewis, E.E.L.; Wheadon, H.; Lewis, N.; Yang, J.; Mullin, M.; Hursthouse, A.; Stirling, D.; Dalby, M.J.; Berry, C.C. A Quiescent, Regeneration-Responsive Tissue Engineered Mesenchymal Stem Cell Bone Marrow Niche Model via Magnetic Levitation. *ACS Nano* **2016**, *10*, 8346–8354. [CrossRef]
68. Coste, C.; Neirinckx, V.; Sharma, A.; Agirman, G.; Rogister, B.; Foguenne, J.; Lallemend, F.; Gothot, A.; Wislet, S. Human bone marrow harbors cells with neural crest-associated characteristics like human adipose and dermis tissues. *PLoS ONE* **2017**, *12*, e0177962. [CrossRef]
69. Sowa, Y.; Imura, T.; Numajiri, T.; Takeda, K.; Mabuchi, Y.; Matsuzaki, Y.; Nishino, K. Adipose stromal cells contain phenotypically distinct adipogenic progenitors derived from neural crest. *PLoS ONE* **2013**, *8*, e84206. [CrossRef]
70. Al-Bakri, Z.; Ishige-Wada, M.; Fukuda, N.; Yoshida-Noro, C.; Nagoshi, N.; Okano, H.; Mugishima, H.; Matsumoto, T. Isolation and characterization of neural crest-like progenitor cells in human umbilical cord blood. *Regen. Ther.* **2020**, *15*, 53–63. [CrossRef]
71. Hatzfeld, A.; Eid, P.; Peiffer, I.; Li, M.L.; Barbet, R.; Oostendorp, R.A.J.; Haydont, V.; Monier, M.N.; Milon, L.; Fortunel, N.; et al. A sub-population of high proliferative potential-quiescent human mesenchymal stem cells is under the reversible control of interferon α/β. *Leukemia* **2007**, *21*, 714–724. [CrossRef]

cells

MDPI

Table S1. List of secondary antibodies used for immunocytochemistry.

Antibody	Conjugate	Dilution	Company	Catalogue number
Goat anti-mouse IgG1	Alexa Fluor 546	1:1000	Invitrogen	A21123
Goat anti-mouse IgG2B	Alexa Fluor 546	1:1000	Invitrogen	A21143
Goat anti-mouse IgGM	Alexa Fluor 546	1:1000	Invitrogen	A21045
Goat anti-mouse IgG3	Alexa Fluor 488	1:1000	Invitrogen	A21151
Goat anti-rabbit IgG (H+L)	Alexa Fluor 488	1:1000	Jakcson ImmunoResearch	111-545-144

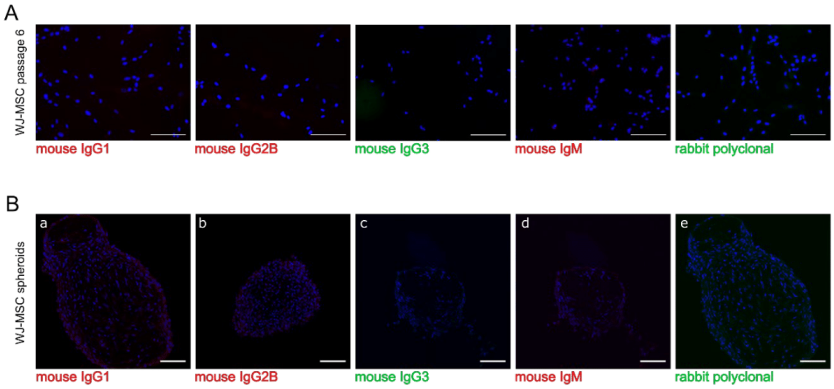

Figure S1. Secondary antibody staining controls for 2D (A) and 3D conditions (B). Following secondary antibodies were applies: goat anti-mouse IgG1 (a), goat anti-mouse IgG2B (b), Goat anti-mouse IgG3 (c), Goat anti-mouse IgM (d), Goat anti-rabbit IgG polyclonal (e). Following conjugates were applied: Alexa Fluor 488 – green label, Alexa Fluor 546 – red label. Antibodies were provided by Invitrogen, except goat anti-rabbit IgG (manufacturer: Jackosn ImmunoResearch). Cells used for control stainings: WJ-MSC from 6th passage (A) and WJ-MSC spheroids from 10th div (B). Scale bars: 100 µm.

Table S2. Population doubling time values (days) for 2D and 3D cultured WJ-MSC.

Passage n_o	Group	PDT values (days)	SD
3	Initial	1.29	0.08
7	2D culture	1.32	0.5
	3D culture	5.65	1.55
8	2D culture	1.6	0.3
	3D culture	1.94	0.88
9	2D culture	2.06	0.32
	3D culture	1.6	0.35
10	2D culture	2.06	1
	3D culture	1.78	0.03

Following groups of WJ-MSC were used: initial - 3rd passage WJ-MSC, 2D culture – 7th passage WJ-MSC, 3D culture – WJ-MSC cultured as spheres for 20 div. The results are presented as mean values of 3 experiments with standard deviation.

Table S3. Quantitative data of immunocytochemistry staining analysis.

Marker	Characteristic	Group	% of positive cells	SD
Nestin	Early neural	Initial	51.6	7.09
		2D culture	28.04	5.56
		3D culture	50.06	6.86
β-III-Tubulin	Early neural	Initial	65.55	1.66
		2D culture	42.28	2.84
		3D culture	85.66	7.9
NF-200	Neuronal	Initial	11	4.06
		2D culture	10.6	4.31
		3D culture	18.87	0.74
NeuN	Neuronal	Initial	28.88	3.5
		2D culture	16.56	2.66
		3D culture	15.7	5.95
A2B5	Glial	Initial	34.47	12.92
		2D culture	31.08	3.87
		3D culture	31.91	3.05
Ki67	Proliferative	Initial	50.55	5.48
		2D culture	20.31	2.39
		3D culture	7.88	2.05
SSEA4	Pluripotent/ embryonic	Initial	20.53	5.4
		2D culture	21.49	4.01
		3D culture	46.06	11.34

Following groups of WJ-MSC were used: initial - 3rd passage WJ-MSC, 2D culture – 7th passage WJ-MSC, 3D culture – WJ-MSC cultured as spheres for 20 div. The results are presented as mean values of 3 experiments with SD

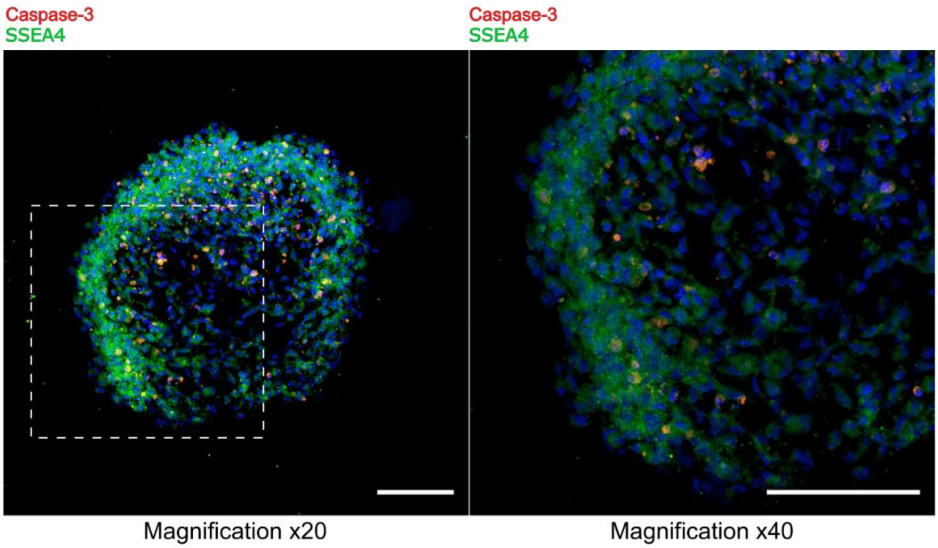

Figure S2. Immunocytochemistry double staining for SSEA4 and Cleaved caspase-3 in WJ-MSC spheroid. Population of SSEA-4 stem cells consists on both alive and dead cells, according to respectively positive and negative signals for Caspase-3, apoptotic marker. For Cleaved caspase-3 detection following antibodies were used: rabbit IgG polyclonal antibody (Cell Signaling Technology, cat. number 9661S) as primary antibody, Cy™3-conjugated goat-anti rabbit IgG polyclonal (Jackson ImmunoResearch, cat. number 111-165-144) as secondary antibody. Spheroid was collected in 10th div. Scale bars: 100 μm.

Table S4. Relative gene expression level quantitative data.

Gene	Characteristic	Group	RQ	SD
NESTIN	Early neural	Initial	1	0
		2D culture	0.6	0.16
		3D culture after 48 h	1.12	0.79
H3TUBULIN	Early neural	Initial	1	0
		2D culture	1.042	0.12
		3D culture after 48 h	0.37	0.28
MAP2	Neuronal	Initial	1	0
		2D culture	3.2	1.35
		3D culture after 48 h	1.05	0.32
GFAP	Glial	Initial	1	0
		2D culture	3.59	0.28
		3D culture after 48 h	0.6	0.38
NANOG	Pluripotent	Initial	1	0
		2D culture	1.69	0.48
		3D culture after 48 h	3.04	1.7
OCT3/4	Pluripotent	Initial	1	0
		2D culture	1.48	0.21
		3D culture after 48 h	1.07	0.7
SOX2	Pluripotent	Initial	1	0
		2D culture	1.63	1.46
		3D culture after 48 h	0.12	0.02
REX1	Pluripotent	Initial	1	0
		2D culture	0.09	0.07
		3D culture after 48 h	0.64	0.54

RQ – relative quantification of gene expression level. Following groups of WJ-MSC were used: **initial** - 3rd passage WJ-MSC, **2D culture** – 7th passage WJ-MSC, **3D culture spheroid** – WJ-MSC cultured as spheres for 20 div and then RNA was collected, **3D culture after 48 h** - WJ-MSC cultured as spheres for 20 div, transferred for 48 hours and then RNA was collected . For Rex1 3D spheroid group amplification after 40 PCR cycle was not observed in any experiment. Gene expression was normalized using β-actin (ACTB) and compared with the mean level of the corresponding gene expression in cells from initial population (3rd passage WJ-MSC). The results are presented as mean values of 3 experiments with standard deviation (SD).

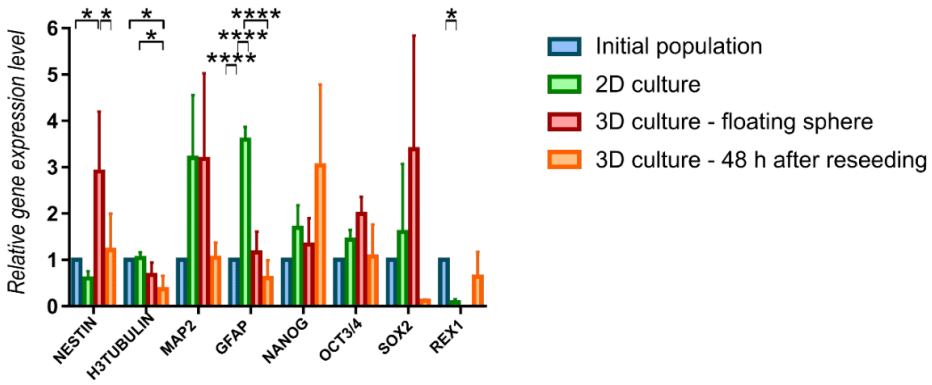

Figure S3. Extended analysis for relative gene expression level (fold change, mean ± SD) of neural and pluripotency phenotype in 2D and 3D WJ-MSC. Except initial population (passage 3rd) and 2D constantly 2D culture (passage 7th), we compared results for RNA collected directly from free floating spheroids and spheroid cultured for 48h in 2D conditions. Quantitation of these genes was determined relative to ACTB as a housekeeping gene by quantitative real-time PCR. Changes in gene expression in WJ-MSC cells cultured in 2D and 3D conditions are shown relative to that in cells grown in the initial population . Results shown are the mean of 3 independent RNA isolations, for * <0.05, ** <0.01,****<0.0001.

For 3D culture we wanted to examine differences between two timepoints of RNA collections – directly from floating spheroids and after more than 48 hours after transfer of spheroids to 2D culture conditions. We observed differences in results in both variants. We detected significant increase of Nestin expression in 3D spheroids – however, its expression decreased after return to 2D culture. This tendency was observed in other genes: for MAP2, Oct3/4 and Sox2. Interestingly, for Nanog situation is reversed: expression tended to increase in 48 h after reseeding spheroids to 2D conditions. To the contrary, level of Rex1 was for floating spheres were not determined – Ct value was greater than cut-off value for real-time amplification assays. Due to huge fluctuations between genetic material from different isolations we hardly reported any relevant statistical differences between all analysed groups in pluripotency genes. Change of expression pattern suggests that 3D culture effect might be transient or conditions modification drastically effect on cell characteristics. That effect was also observed by Pennock and colleagues, which measured pluripotent expression level in 5, 24 and 48 h after transferring spheres to 2D conditions (Pennock et al. 2015).

Table S5. Relative gene expression level quantitative data for RNA collected directly from free floating spheroids.

Gene	Characteristic	RQ	SD
NESTIN	Early neural	2.9	1.3
H3TUBULIN	Early neural	0.68	0.27
MAP2	Neuronal	3.18	1.8
GFAP	Glial	1.161	0.4451
NANOG	Pluripotent	1.33	0.57
OCT3/4	Pluripotent	1.993	0.37
SOX2	Pluripotent	3.387	2.45
REX1	Pluripotent	*undetermined*	-

RQ – relative quantification of gene expression level. For Rex1 3D spheroid group amplification after 40 PCR cycle was not observed in any experiment. Gene expression was normalized using β-actin (ACTB) and compared with the mean level of the corresponding gene expression in cells from initial population (3rd passage WJ-MSC). The results are presented as mean values of 3 experiments with standard deviation (SD).

11.2. Artykuł II

frontiers | Frontiers in Cell and Developmental Biology

TYPE Original Research
PUBLISHED 22 February 2024
DOI 10.3389/fcell.2024.1227034

OPEN ACCESS

EDITED BY
Selim Kuci,
University Hospital Frankfurt, Germany

REVIEWED BY
Tokiko Nagamura-Inoue,
The University of Tokyo, Japan
Ajoy Aloysius,
University of Kentucky, United States

*CORRESPONDENCE
Anna Sarnowska,
asarnowska@imdik.pan.pl,

RECEIVED 23 May 2023
ACCEPTED 17 January 2024
PUBLISHED 22 February 2024

CITATION
Smolinska A, Chodkowska M, Kominek A, Janiec J, Piwocka K, Sulejczak D and Sarnowska A (2024), Stemness properties of SSEA-4+ subpopulation isolated from heterogenous Wharton's jelly mesenchymal stem/stromal cells.
Front. Cell Dev. Biol. 12:1227034.
doi: 10.3389/fcell.2024.1227034

Stemness properties of SSEA-4+ subpopulation isolated from heterogenous Wharton's jelly mesenchymal stem/stromal cells

Agnieszka Smolinska[1], Magdalena Chodkowska[1], Agata Kominek[2], Jakub Janiec[2], Katarzyna Piwocka[2], Dorota Sulejczak[3] and Anna Sarnowska[1]*

[1]Translational Platform for Regenerative Medicine, Mossakowski Medical Research Institute, Polish Academy of Sciences, Warsaw, Poland, [2]Laboratory of Cytometry, Nencki Institute of Experimental Biology, Polish Academy of Sciences, Warsaw, Poland, [3]Department of Experimental Pharmacology, Mossakowski Medical Research Institute, Polish Academy of Sciences, Warsaw, Poland

Background: High heterogeneity of mesenchymal stem/stromal cells (MSCs) due to different degrees of differentiation of cell subpopulations poses a considerable challenge in preclinical studies. The cells at a pluripotent-like stage represent a stem cell population of interest for many researchers worldwide, which is worthy of identification, isolation, and functional characterization. In the current study, we asked whether Wharton's jelly-derived MSCs (WJ-MSCs) which express stage-specific embryonic antigen-4 (SSEA-4) can be considered as a pluripotent-like stem cell population.

Methods: SSEA-4 expression in different culture conditions was compared and the efficiency of two cell separation methods were assessed: Magnetic Activated Cell Sorting (MACS) and Fluorescence Activated Cell Sorting (FACS). After isolation, SSEA-4+ cells were analyzed for the following parameters: the maintenance of the SSEA-4 antigen expression after cell sorting, stem cell-related gene expression, proliferation potential, clonogenicity, secretome profiling, and the ability to form spheres under 3D culture conditions.

Results: FACS allowed for the enrichment of SSEA-4+ cell content in the population that lasted for six passages after sorting. Despite the elevated expression of stemness-related genes, SSEA-4+ cells neither differed in their proliferation and clonogenicity potential from initial and negative populations nor exhibited pluripotent differentiation repertoire. SSEA-4+ cells were observed to form smaller spheroids and exhibited increased survival under 3D conditions.

Abbreviations: AD-MSCs, adipose-derived mesenchymal stem/stromal cells; BDNF, brain-derived neurotrophic factor; bFGF, basic fibroblast growth factor; Cal-AM, Calcein AM; CCL2, chemokine ligand 2; CFU, colony forming unit; EGF, epithelial growth factor; ESC, embryonic stem cells; EthD-1, Ethidium homodimer-1; FACS, Fluorescence Activated Cell Sorting (FACS); GDNF, glial cell line-derived neurotrophic factor; ICAM-1, intercellular adhesion molecule 1; iPSCs, induced pluripotent stem cells; LIF, leukemia inhibitory factor; MACS, Magnetic Activated Cell Sorting (MACS); MSCs, mesenchymal stem/stromal cells; PDT, population duplication time; RT-qPCR, Real Time-Quantitative Polymerase Chain Reaction; SSEA-4, Specific stage embryonic antigen-4; UC-MSCs, umbilical cord-derived mesenchymal stem/stromal cells; VEGF-c, vascular endothelial growth factor-c; WJ-MSCs, Wharton jelly mesenchymal stem/stromal cells; WJ-MSC-SSEA-4 +, SSEA-4-positive WJ-MSC population; WJ-MSC-SSEA-4-, SSEA-4-negative WJ-MSC population.

Conclusion: Despite the transient expression of stemness-related genes, our findings could not fully confirm the undifferentiated pluripotent-like nature of the SSEA-4+ WJ-MSC population cultured *in vitro*.

KEYWORDS

mesenchymal stem/stromal cells, SSEA-4, stemness, pluripotent, FACS, MACs, heterogeneity

1 Introduction

According to the guidelines published in 2006 by the International Society for Cell & Gene Therapy, mesenchymal stem/stromal cells (MSCs) are multipotent adult cells that differentiate toward mesodermal lineage tissues: osteocytes, chondrocytes, and adipocytes (Dominici et al., 2006). However, many research groups suggested a wider MSC differentiation potential by providing protocols to obtain other cells such as neurons or hepatocytes (Zhao et al., 2016). Some researchers went even further and claimed that MSCs might manifest the properties of pluripotent-like cells by the expression of stemness-related transcription factors (such as Sox2, Nanog, and Oct4) and differentiation toward cells from all three germ layers. Even though the reported observations are controversial and disputable, the observed discrepancies between research groups can be explained by MSC heterogeneity.

Heterogeneity poses a serious issue for further research as only a small fraction of cells in MSC populations appear to fulfill functional criteria for stem cells (Ivanovic, 2023). The existence of surface antigens associated with other cell types is one of the observed aspects of MSC heterogeneity. Researchers propose numerous candidates for a genuine stem population to improve the efficiency of MSC therapies (Lv et al., 2014) based on induced pluripotent stem (iPS) and embryonic stem cell studies. Cells positive for SSEA-3, an early embryonic antigen, were confirmed to differentiate toward cells from all three germ layers (Kuroda et al., 2010) although they were present in the initial population in a negligible percentage, which does not correspond to the plasticity of MSCs. MSCs positive for CD271, an antigen typical of neural crest-derived cells, proliferated more rapidly and contained more cells capable of forming colonies (Mikami et al., 2011; Barilani et al., 2018). MSCs expressing CD146, an antigen associated with endothelial cells, exhibited a greater ability to migrate to damaged tissue (Wangler et al., 2019). CD133, a surface antigen associated with glioblastoma cells, was also suggested as a potential marker of stemness population in umbilical cord-derived MSCs (UC-MSCs) and MSCs derived from adipose tissue (AD-MSCs) (Doshmanziari et al., 2021). Another iPS- and embryonic stem cell (ESC)-expressed marker found in a much higher proportion of MSCs is stage-specific embryonic antigen-4 (SSEA-4).

SSEA-4 appears during early embryonic development (Henderson et al., 2002) but is also found on undifferentiated cells such as embryonic stem cells (ESCs) (Draper et al., 2002; Kallas et al., 2011), induced pluripotent stem cells (iPSCs) (Ojima et al., 2015), and various types of tumor cells (Sivasubramaniyan et al., 2015; Nakamura et al., 2019; Lee et al., 2021). Many publications reported the expression of SSEA-4 within MSC populations within the range of 30%–90% (Drela et al., 2016; Musiał-Wysocka et al., 2019). Despite the abundance of evidence on pluripotent-like properties of SSEA-3, researchers debate whether SSEA-4 may also be a prognostic marker for genuine stem cell populations (Gang et al., 2007; Kawanabe et al., 2012). Targeting SSEA-4 is a strategy for stem population selection in undifferentiated ESCs from differentiated derivatives (Fong et al., 2009) and neural stem/progenitor cells from the human embryonic forebrain (Barraud et al., 2007). SSEA-4 was also suggested as an identifier of tumor-initiating subpopulations and proposed as a target for the therapies (He and Garcia, 2004; Sivasubramaniyan et al., 2015; Soliman et al., 2020). In our previous paper, long-term 3D culture was observed to increase the content of SSEA-4+ cells, thereby suggesting that SSEA-4 could help toward survival under harsh 3D conditions (Kaminska et al., 2021).

This study was carried out to determine the therapeutic benefits of the SSEA-4-positive cells from Wharton's jelly MSCs (WJ-MSCs) as a potential pluripotent-like stem cell population responsible for so-called "MSCs plasticity" with restorative (replacing injured cells) properties. To identify the MSC-SSEA-4 + subpopulation's unique properties, it was compared both to the negative population, without SSEA-4, (WJ-MSC-SSEA-4-) and to the heterogenous MSC populations (unsorted WJ-MSC) (experimental steps explained in Supplementary Figure S1). Our experiments allowed us to establish the most favorable conditions for SSEA-4 expression and separation while the positive subpopulation analyses provided full characteristics of stemness-related properties.

2 Materials and methods

2.1 WJ-MSCs isolation and primary culture

Human umbilical cords were acquired from full-term deliveries with the written consent of the mother according to the Warsaw Medical University Ethics Committee Guidelines (KB/213/2016). The cords (15–20 cm long) were first transported in phosphate-buffer saline solution (PBS; Sigma-Aldrich, Saint Louis, MO, United States) with a mixture of penicillin-streptomycin-amphotericin B (1:100, Gibco, Thermo Fisher Scientific, Walthman, United States) and then cut into slices with a lancet (slice thickness: 2–3 mm). Wharton's jelly cylindrical fragments of 2–3 mm in diameter were obtained from the umbilical cord using the diameter biopsy punch (Miltex, GmbH, Viernheim, Germany). The explants were transferred to 6-well culture plates and cultured in the following medium standard for WJ-MSC culture: DMEM (Gibco), 5% human platelet cell lysate (Mill Creek Life Sciences, Rochester, MN, United States), and penicillin-streptomycin-amphotericin B (1:100; Gibco). The following cell culture conditions were applied: adherent surface, 37°C temperature,

TABLE 1 List of antibodies used in flow cytometry analysis.

Specificity	Fluorochrome	Isotype	Company	Catalog number
SSEA-4	PerCP-Cy5.5	Mouse IgG3 κ	BD	561565
Isotype control	PerCP-Cy5.5	Mouse IgG3 κ	BD	561572
CD271	PE	Mouse IgG1 κ	BD	560927
CD146	PE	Mouse IgG1 κ	BD	550315
Isotype control	PE	Mouse IgG1 κ	BD	555749
CD133	Brilliant Violet 421	Mouse IgG2B κ	BD	566598
Isotype control	Brilliant Violet 421	Mouse IgG2B κ	BD	562748
CD49F	PE	Rat IgG2A κ	ThermoFischer Scientific	12-0495-81
Isotype control	PE	Rat IgG2A κ	ThermoFischer Scientific	12-4321-80

95% humidity, 5% CO_2 concentration, and 5% O_2 concentration. The culture medium was replaced every 2 days for 14 days *in vitro*. The cells were cultured until they migrated out of the explant and the culture reached semiconfluence; then the cells were detached with Accutase Cell Detachment Solution (Beckton Dickinson, Franklin Lakes, NJ, United States) and counted.

We compared SSEA-4 expression in populations cultured with different human platelet cell lysates such as PLTGold Clinical Grade (Mill Creek Life Sciences), MultiPL'30 (Macopharma), and MultiPL'100 (Macopharma, Tourcoing, France). In further experiments, PLT Gold Clinical Grade was used as a lysate. The WJ-MSCs were cultured under the conditions described above for three passages. The cells were collected and cell sorting was performed.

2.2 Flow cytometry

The cells were detached with Accutase Cell Detachment Solution (BD), washed in PBS, and resuspended in Stain Buffer (BD). Flow cytometry analyses were performed with antibodies listed in Table 1. The cells were incubated in diluted antibodies in the dark for 30 min. After incubation, the cells were washed twice with Stain Buffer (BD) and resuspended in Stain Buffer. The resuspended cells were analyzed using FACS Canto II (BD) with FACSDiva software (BD) and FlowJo 10 (BD). The following laser configurations were applied: violet - 407 nm (detectors: 510/50, 450/50), blue - 488 nm (detectors: 488,10, 530/30, 585/42, 670LP, 780/60), and red - 633 nm (detectors: 660/20, 780/60). The gating strategy was presented in online resources (Supplementary Figure S2).

2.3 AD-MSCs culture

AD-MSCs isolation and culture were accepted by the Bioethical Committee at the Centre of Postgraduate Medical Education (No. 63/PB/2013) on 25 September 2013, according to the guidelines of the Declaration of Helsinki. Adipose tissue was collected during liposuction in the Plastic Surgery Department at Orlowski's Clinical Hospital in Warsaw. The AD-MSCs were isolated according to the previously described protocol (Figiel-Dabrowska et al., 2021; Rybkowska et al., 2023). The isolated AD-MSCs were in MEM α (Gibco), 5% human platelet lysate (Mill Creek Life Sciences), and 1% penicillin-streptomycin-amphotericin B (1:100; Gibco). The following cell culture conditions were applied: adherent surface, 37°C temperature, 95% humidity, 5% CO_2 concentration, and 5% O_2 concentration. The culture medium was changed every 2–3 days and AD-MSCs were passaged when the culture reached semiconfluence. AD-MSCs from the third passage were detached with Accutase Cell Detachment Solution and washed with PBS twice. AD-MSCs were used for flow cytometry and prepared in the manner described above.

2.4 Magnetic activated cell sorting (MACS) isolation of SSEA-4+ cells

The WJ-MSCs from the third passage were used for MACS separation of WJ-MSC-SSEA-4+ cells. WJ-MSCs were detached and counted. The collected cells (~2-10 × 10^6) were incubated with magnetic beads using an anti-SSEA-4 MicroBead kit for 20 min in the dark. Then, the cells were washed with PBS. The cells were resuspended in PBS with 1% BSA and loaded into the autoMACS Pro Separator (Miltenyi Biotec, Bergisch Gladbach, Germany). The cells were run through the magnetic field with the Possel S. For further analysis, we used a positive cell population retained within the column and eluted as the second fraction was collected. After MACS sorting, the cells were counted with Trypan Blue on a hemocytometer to calculate the total cell number and cell viability. Then, the cells were subcultured for further experiments as described above.

2.5 Fluorescence-activated cell sorting (FACS) isolation of SSEA-4+ cells

The WJ-MSCs from the third passage were used for FACS separation of WJ-MSC-SSEA-4+ cells. The cells were stained as was the case in flow cytometry staining described in Section 2.2. After incubation and washing, the cells were sorted using FACS Aria IIu (BD) in the Laboratory of Cytometry, Nencki Institute of Experimental Biology, Warsaw. The following laser

TABLE 2 List of antibodies used for immunocytochemistry.

Antigen	Isotype	Dilution	Company	Applied secondary antibody	Secondary antibody fluorochrome
SSEA-4	Mouse IgG3	1:200	Merck	Goat anti-IgG3	Alexa Fluor 488
CD90	Mouse IgG1	1:200	Santa Cruz	Goat anti-IgG1	Alexa Fluor 546
SOX17	Goat IgG H + L	1:100	R&D	Donkey anti-IgG	Alexa Fluor 488
Otx2	Goat IgG H + L	1:100	R&D	Donkey anti-IgG	Alexa Fluor 488
Brachyury	Goat IgG H + L	1:100	R&D	Donkey anti-IgG	Alexa Fluor 488

configurations were applied: violet - 407 nm (detectors: 450/40, 530/30), blue - 488 nm (detectors: 488/10, 530/30, 585/42, 616/23, 695/40, 780/60), and red - 633 nm (detectors: 660/20, 780/60). The gating strategy is presented in online resources (Supplementary Figure S3). The cells were collected from both populations, SSEA-4- and SSEA-4+, and resuspended in the cell culture medium. Directly after FACS sorting, the obtained population was analyzed with FACS Aria again to confirm the purity of sorting. Then, the cells were transported to our laboratory where we counted the total cell number and viability with Trypan Blue on a hemocytometer. Then, the cells were seeded in a culture dish and subcultured for further experiments as described above.

2.6 Parameters of cell sorting

The following parameters of MACS and FACS sorting, which are recovery, survival, and yield, were compared in order to determine a more efficient method of SSEA-4+ cell separation. Recovery was expressed as the ratio of the number of cells obtained in the positive fraction to the number of cells used in the sorting. To calculate recovery, we counted cells prior to sorting and in post-sorting fractions. To describe survival, we investigated the mortality of cells in samples received after cell separation with Trypan Blue staining. The yield was expressed as the ratio of positive cell content before and after cell separation. Purity was described as the percentage of SSEA-4+ cells received in a positive population sample. To estimate yield, the samples were analyzed with flow cytometry.

2.7 Immunocytochemistry

Immunocytochemistry was performed to detect SSEA-4 and CD90, one of the surface antigen characteristics of MSCs, for the following populations: unsorted WJ-MSC, WJ-MSC-SSEA-4-, and WJ-MSC-SSEA-4+. WJ-MSCs were washed with PBS and fixed in 4% PFA for 15 min. The samples were incubated with a blocking mixture consisting of 10% Goat Serum (Sigma Aldrich) and 1% bovine serum albumin (Sigma Aldrich) for 1 h at room temperature (RT). In the next step, primary antibodies were applied for 24 h at 4°C (Table 2). The next day, the cells were washed with PBS and then incubated with secondary antibodies conjugated with fluorochrome for 1 h (Table 2). Finally, the samples were mounted with Fluoromont-G with DAPI (Gibco) that stained cell nuclei. The analysis was performed using a confocal microscope (Zeiss, Oberkochen, Germany).

2.8 Real time-quantitative polymerase chain reaction (RT-qPCR)

Total RNA was isolated from the following groups: unsorted WJ-MSCs, negative and positive populations after FACS sorting (WJ-MSC-SSEA-4- p0 and WJ-MSC-SSEA4+ p0, respectively), and negative and positive fractions cultured for 1 passage *in vitro* (WJ-MSC-SSEA-4- p1 and WJ-MSC-SSEA4+ p1, respectively). RNA isolation was performed using the following kits depending on the cell number: Total RNA Mini Plus kit (A&A Biotechnology, Gdynia, Poland) and Total RNA Mini Plus Concentrator (A&A Biotechnology) according to the manufacturer's protocols. After isolation, the RNA was eluted with 20 µL of RNase-free H_2O (Sigma Aldrich). The quantity and quality of RNA were assessed using a NanoDrop 2000 spectrophotometer (Thermo Scientific). Genomic DNA (gDNA) contamination was eliminated in all RNA samples using a Clean-up RNA Concentrator (A&A Biotechnology, Thermo Fisher Scientific, Walthman, United States).

The reverse transcription process was generated using a High-Capacity RNA-to-cDNA™ Kit (Applied Biosystems) according to the manufacturer's instructions. After receiving complementary strand DNA (cDNA), the samples were diluted in RNase-free water. Quantitative polymerase chain reactions were performed using SYBR green Master Mix (Applied Biosystems) and specific primers (Supplementary Table S1) with the 7,500 Real-Time PCR System (Applied Biosystems). The relative amount of RNA was calculated using the comparative delta-delta Ct method ($2^{-\Delta\Delta CT}$) and gene expression was normalized using β-actin (ACTB), while the unsorted population was used as a reference group. Gene expression was compared with the mean level of corresponding gene expression in cells of the unsorted population and expressed as an n-fold ratio. Gene expression was compared with the mean level of corresponding gene expression in cells of the unsorted population and expressed as an n-fold ratio.

2.9 Three germ layer differentiation potential evaluation

Three germ layer differentiation potential was determined for unsorted, positive, and negative populations. After FACS separation, the cells were seeded on a 6-well plate and cultured in a standard culture medium with the addition of basic fibroblast growth factor (bFGF) (Gibco) until they reached 70%–80% confluency. Differentiation assay was performed with the Human Pluripotent Stem Cell Functional Identification Kit (Biotechne, R&D Systems,

Minneapolis, MN, United States), which is dedicated to the differentiation of iPSCs. The cells were cultured according to the manufacturer's protocol, with a culture medium based on DMEM. After 4 days of *in vitro* culture, the cells were collected for RNA isolation and evaluation for gene expression of OTX2, Brachyury, and SOX17 (scheme of the experiment presented in Supplementary Figure S4; primers sequences can be found in Supplementary Table S1).

2.10 Colony forming unit (CFU) assay

To perform the CFU assay, unsorted WJ-MSCs, WJ-MSC-SSEA-4-, and WJ-MSC-SSEA-4 + were seeded on a 6-well plate, 10 cells per well. The cells were cultured for 10 days *in vitro* under standard conditions. The cells were washed with PBS, fixed with 4% PFA for 15 min, and washed with PBS again. The fixed cells were stained with 0.5% toluidine blue for 20 min and washed with distilled water after staining. The number of colonies containing 50 cells or more was counted and fibroblast colony-forming units (CFU-F) were calculated as a percentage of seeded cells.

2.11 Proliferation analysis

Cell proliferation was estimated as population duplication time (PDT) for four passages after cell sorting for the following populations: unsorted WJ-MSC, WJ-MSC-SSEA-4-, and WJ-MSC-SSEA-4+. The cells from each group were counted in Trypan Blue, seeded at a density of 2000 cells/cm2, and cultured under standard conditions. After 5 days of *in vitro* culture, the cells were collected, counted, and reseeded again at initial density. The PDT value was calculated according to the following equation: $PDT = \frac{(t-t_0) \times log\,2}{logN - log\,N_0}$, where N is the number of cells obtained at the end of the passage, N_0 is the initial number of the seeded cells and $t\text{-}t_0$ is the duration of the passage (counted in days).

2.12 Soluble secretome analysis

Soluble secretome was analyzed with human Magnetic Luminex Assay (R&D Systems, Minneapolis, MN, United States) for unsorted, positive, and negative populations. For this purpose, the cells after FACS sorting were seeded at a density of 2,000 cells per cm^2. The medium from the cell culture was collected at two time points: 3 days and 5 days *in vitro* after FACS sorting. The standard culture medium was used as a negative control. The levels of the following molecules were measured: epithelial growth factor (EGF), bFGF, glial cell line-derived neurotrophic factor (GDNF), brain-derived neurotrophic factor (BDNF), chemokine ligand 2 (CCL2), leukemia inhibitory factor (LIF), angiogenin, vascular endothelial growth factor-c (VEGF-c), and intercellular adhesion molecule 1 (ICAM-1). The actual levels of secreted factors were determined by subtraction of the negative control values from the obtained results. Luminex assay was performed according to the manufacturer's protocol and measured in Bio-Plex 200 System (Bio-Rad Bio-Rad, Hercules, CA, United States).

2.13 3D culture of WJ-MSCs

Unsorted WJ-MSCs from the third passage and WJ-MSCs directly after cell sorting (WJ-MSC-SSEA-4- and WJ-MSC-SSEA-4+) were collected, counted, and seeded in antiadhesive 6-well plates (Nunclon Sphera, Thermo Fischer Scientific) at a density of 10^5 cells per 1 mL. The cells were cultured as spheroids in culture medium and the conditions described above for 72 h *in vitro*. The diameters and numbers were measured after 24, 48, and 72 h of 3D culture. After 72 h of 3D culture, spheroids were collected and dissociated with Accutase Cell Detachment Solution (BD) for further viability analysis.

2.14 Viability test after 3D culture

To estimate the number of alive and dead cells after 3D culture, a viability test was performed using a mix of ethidium homodimer-1 (8 µM, EthD-1, Invitrogen) Calcein AM (Cal-AM) (0,1 µM, Invitrogen) and Hoechst 33,342 dye (1 µg/mL; Sigma Aldrich). Spheroids or single cells derived from dissociated spheroids were incubated with a staining mixture for 45 min at room temperature in darkness. The stained cells were observed in the Axio Vert.A1 fluorescence microscope (Zeiss). Dead and alive cells were calculated automatically with the ZEISS ZEN 2.0 Blue Edition software.

2.15 Statistics

The experiments were performed on the cells obtained from at least three WJ donors ($n \geq 3$). Normality was examined with the Shapiro-Wilk normality test. The unpaired t-student test was used for the data from two groups with normal distribution. The data from multiple groups with normal distribution were analyzed by using a one-way analysis of variance (ANOVA), followed by Tuckey's multiple comparison test. For the non-moral distribution, the data was analyzed using the Kruskal–Wallis test, followed by Dunn's multiple comparison test. The results are presented as mean ± standard deviation (SD) for parametric tests or as median ±95% confidence interval (95% CI) for non-parametric tests. The results were considered statistically significant when the *p*-value was higher than 0.05. Statistical analysis was conducted with the GraphPad Prism 7 software.

3 Results

3.1 Expression of SSEA-4 in the heterogenous WJ-MSCs population

WJ-MSCs used for the experiments exhibited surface antigens recommended by *The International Society for Cell & Gene Therapy* for MSC characteristics (Supplementary Figure S5; Supplementary Table S2) and differentiated toward mesodermal lineage cells: osteocytes, adipocytes, and chondrocytes (Supplementary Figure S6). All MSC-SSEA-4+ cells expressed the CD90, which is one of the recommended MSC antigens (Figure 1A; negative controls are

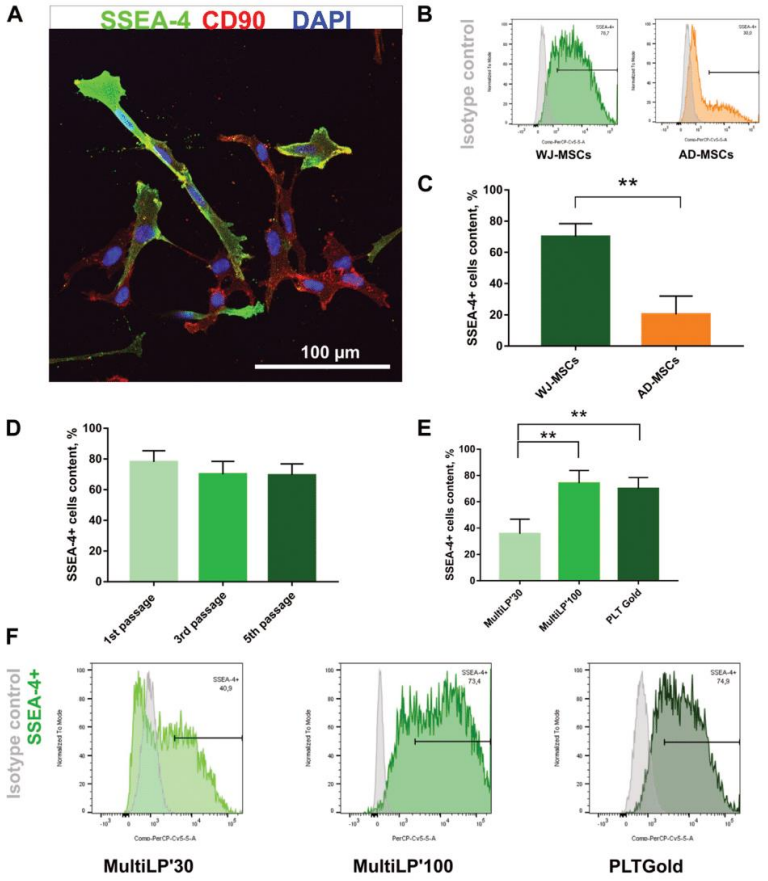

FIGURE 1
SSEA-4+ cells content in the heterogenous population of WJ-MSCs. **(A)** SSEA-4 surface antigen together with CD90 in the heterogenous WJ-MSC populations; immunocytochemical staining. The white scale bar indicates 100 µm. **(B)** Representative histograms from flow cytometry analysis for SSEA-4+ population in WJ-MSCs and AD-MSCs. **(C)** Comparison of SSEA-4+ cells in MSCs isolated from different sources: Wharton's Jelly (WJ-MSCs) and adipose tissue (AD-MSCs). Passage number of analyzed cells: third passage; applied lysate platelet: PLTGold. **(D)** SSEA-4+ cell content in the WJ-MSCs from first, third, and fifth passage of cell culture; flow cytometry. **(E)** SSEA-4+ cell content in the WJ-MSC populations cultured with different platelet lysates: MultiLP'30 (Macopharma), MultiLP'100 (Macopharma), and PLTGold (Mill Creek Life Sciences); flow cytometry analysis. **(F)** Representative histograms from flow cytometry analysis for the SSEA-4+ population from WJ-MSCs cultured in different platelet lysates: MultiLP'30, MultiLP'100, and PLTGold. For **(B)**, **(D)**, and **(E)** results are presented as mean values of three experiments ±SD. *p*-value for ** <0.01.

presented in online resources: Supplementary Figure S7). To establish the most favorable conditions, SSEA-4+ cells present in heterogenous MSCs were estimated with regard to i) the source of tissue, ii) the passage number, and iii) the culture medium. SSEA-4+ cell content was compared in two MSC populations derived from different tissues: Wharton's jelly and adipose tissue (Figures 1B,C). Nearly 3.5 times more SSEA-4+ cells were detected in WJ-MSCs than in AD-MSCs (70% ± 8.3% and 20.3% ± 11.7, respectively). No significant changes were observed in SSEA-4 expression in WJ-MSCs obtained from the first, third, and fifth passage of *in vitro* culture (Figure 1D). To choose the most optimal culture medium composition, three commercially available platelet lysates were compared as a source of proteins and tropic factors: MultiLP'30, MultiLP'100, and PLTGold Clinical Grade (Figures 1E,F). MultiLP'100 and PLT Gold lysates were more abundant in growth factors than MultiLP'30. The proportion of positive cells was the lowest under cell culture with MultiLP'30 lysate (35.7% ± 11.1), while it was found to increase in cultures using MultiLP'100 and PLTGold lysates (74% ± 9.7% and 70% ± 8.3, respectively) (Figure 1F). The application of a higher concentration of platelet lysate was also observed to increase the content of double-positive SSEA-4+ CD271+ cells in WJ-MSC populations (Supplementary Figure S8). Although almost all WJ-MSC-SSEA-4+ cultured with lysates at a higher concentration expressed CD271, a similar analysis in AD-MSC populations revealed that it was CD271+ cells that were a separate subpopulation of SSEA-4+ cells (Supplementary Figure S6D). Consequently, WJ-MSCs from the third passage, cultured with PLTGold human platelet lysate, were selected for further experiments and analysis.

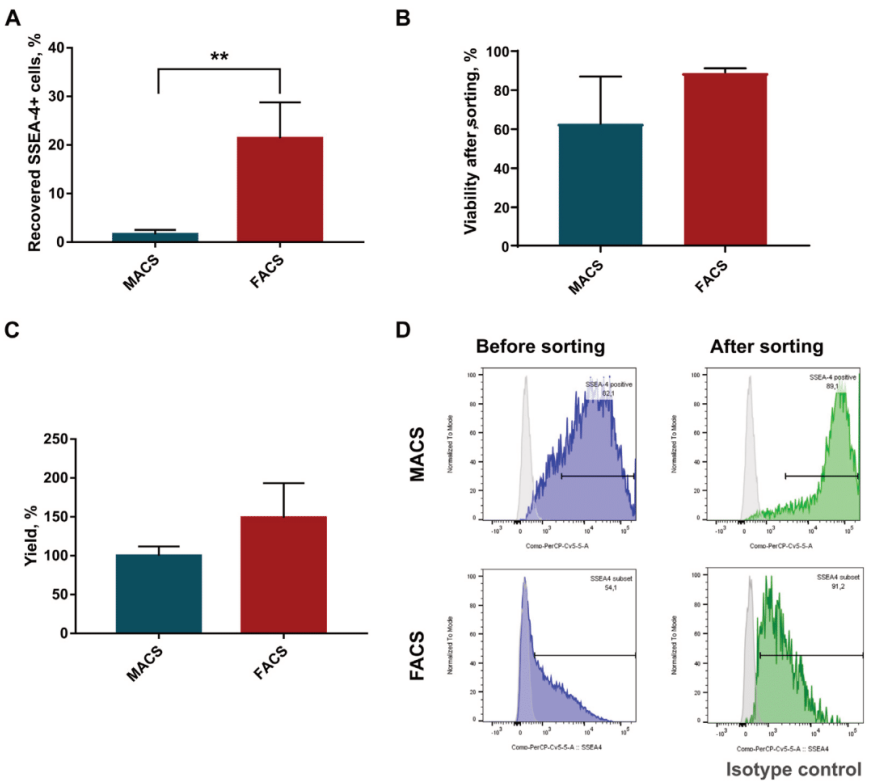

FIGURE 2
Parameter comparison of sorting methods: Magnetic Activated Cell Sorting (MACS) and Fluorescence Activated Cell Sorting (FACS). **(A)** Percent of recovered SSEA-4+ cells after cell sorting; *p*-value for **<0.01. **(B)** Viability of cells in population after cell sorting. **(C)** Sorting yield expressed as a change in SSEA-4+ cell content calculated before and after sorting. **(D)** Representative histograms from flow cytometry analyses of SSEA-4 cell content before and after sorting for MACS and FACS were used to calculate yield. For **(B)** and **(D)** results are presented as mean values of at least four experiments ±SD. *p*-value for ** <0.01.

3.2 Comparison of sorting methods for WJ-MSC-SSEA-4+ cell separation

To choose a more optimal WJ-MSC-SSEA-4+ cell separation method, MACS and FACS were considered. The following parameters were compared: recovery, which was expressed as the ratio of the positive cell numbers obtained to the cell number used in sorting; survival, which was expressed as cell mortality and yield and as the ratio of positive cells before and after sorting. FACS allowed us to obtain more than 13 times as many cells as with MACS(MACS: 1.6% ± 0.9 vs. FACS: 21.4% ± 7.4) (Figure 2A). We observed a decrease in the cell viability after MACS sorting, but the differences were not statistically significant due to substantial discrepancies in the values obtained in MACS sorting (MACS: 62.75% ± 24.3 vs. FACS: 89% ± 2) (Figure 2B). Our calculations performed with Trypan Blue staining were also supported by EthD-1 staining used in the pilot experiment (Supplementary Figure S9). A slightly higher yield was recorded for the FACS method, with the differences being statistically insignificant (MACS: 99.9% ± 11.9 vs. FACS: 148.9% ± 44.4) (Figure 2C). SSEA-4+ cell content recorded before and after sorting was compared to calculate yield value (Figure 2D). Overall, FACS sorting was selected for our further experiments as the method showed superior cell recovery and tendencies toward decreased mortality and increased yield.

Figure 2D shows a significant difference in SSEA4 expression in the initial population, which resulted from the difference in the cytometer assigned to the method. MACS sorting was analyzed using FACS Canto. For FACS sorting, we used the integrated FACS Aria IIu (BD), which differed in the detector settings (as described in the materials and method section). The results obtained may explain the discrepancies in the SSEA4 expression of the different study groups. Nevertheless, the same cytometer was always used in our further experiments, such as the persistence of SSEA-4+ cells after sorting or co-expression of other surface antigens.

3.3 SSEA-4+ cells after FACS separation

As a result of FACS, two groups of cells were received, which are the negative subpopulation (WJ-MSC-SSEA-4-) and the positive

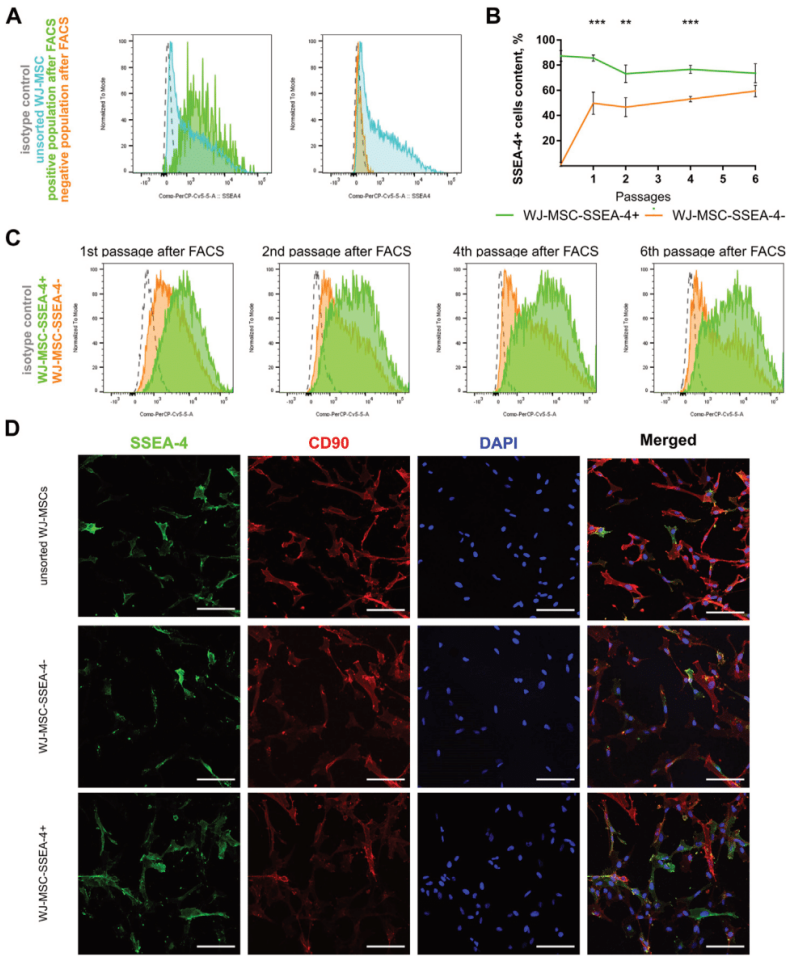

FIGURE 3
Persistence of SSEA-4+ cells after FACS in WJ-MSC populations: unsorted WJ-MSCs, WJ-MSC-SSEA-4+, and WJ-MSC-SSEA-4-. **(A)** Purity and yield of FACS—the comparison of unsorted WJ-MSCs before FACS and in positive and negative populations after FACS; representative histograms. **(B)** SSEA-4+ cells content dynamics during cell culture after FACS. The results are presented as mean values of three experiments ±SD, *p*-value for ** <0.01 and *** <0.001. **(C)** SSEA-4+ cell content changes after 1, 2, 4, and 6 passages after FACS; representative histograms. **(D)** SSEA-4 co-expression with CD90 for unsorted populations and positive and negative populations at the end of the first passage after FACS. White scale bars indicate 100 µm.

subpopulation (WJ-MSC-SSEA-4+) (Figure 3). The content in the unsorted population before FACS and in populations received after FACS was measured to examine purity and yield (Figure 3A). The FACS method resulted in 87.4% ± 4.3 of SSEA-4+ cells in the positive population, while the negative population contained 1.2% ± 1.6 of SSEA-4+ cells (Figure 3B). SSEA-4+ cell content in positive and negative populations was monitored for the next six passages (Figures 3B,C). For the first four passages, both populations differed significantly in SSEA-4+ percentage. SSEA-4+ cell content was observed to increase in the negative population. In the sixth passage after FACS, no differences between the analyzed populations were recorded. Immunocytochemical staining revealed notably more SSEA-4+ cells in the positive population after FACS separation (Figure 3D).

3.4 Pluripotent-like properties of WJ-MSC-SSEA-4+ subpopulation

The expression of genes associated with pluripotent stem cells (Nanog, Oct4, and Sox2) was compared to confirm the undifferentiated state of the SSEA-4+ population (Figure 4A). RNA was collected directly after cell sorting (p0) and after one passage of *in vitro* cell culture (p1) for the populations received with FACS. WJ-MSC-SSEA-4- + population exhibited increased expression of Nanog and Oct4 directly after cell sorting, which decreased with cell culture. The expression of early neural genes connected with the ectoderm germ layer was also analyzed (Figure 4B). An increased expression of H3TUBULIN, NESTIN,

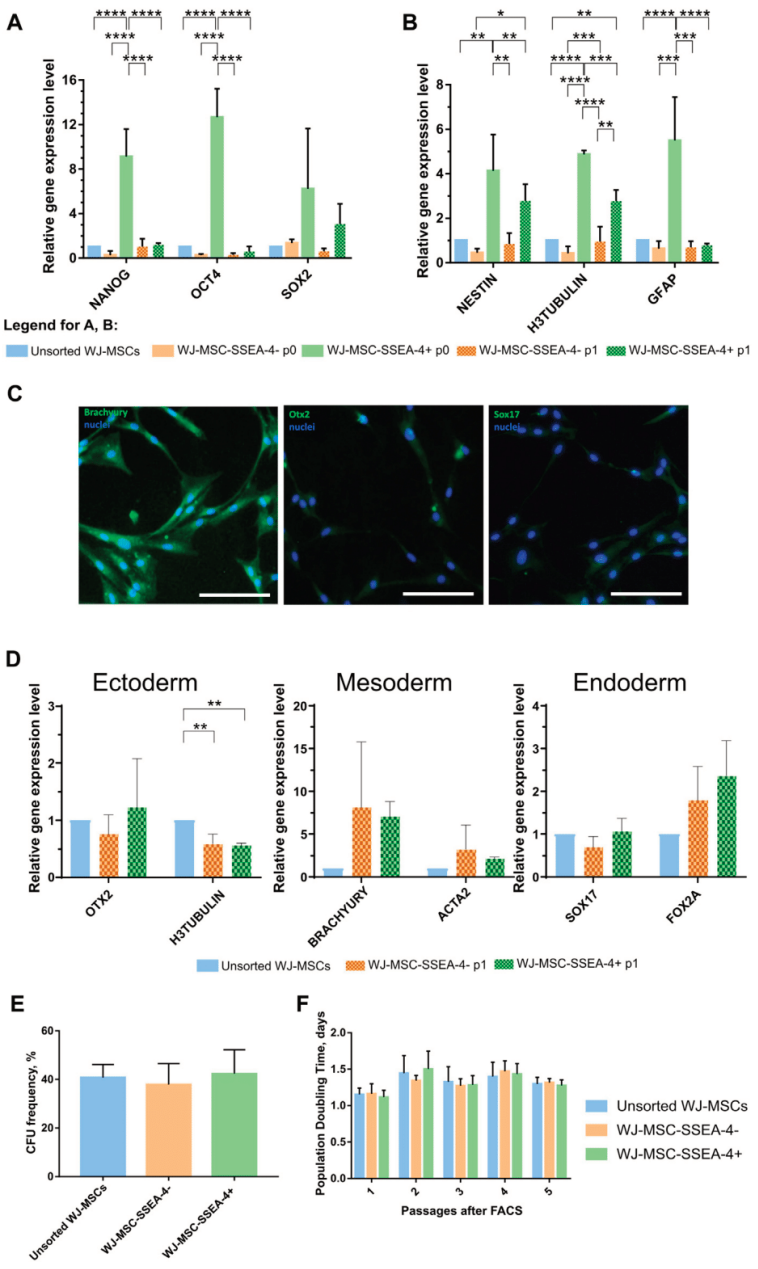

FIGURE 4
Stemness properties of WJ-MSC populations. **(A, B)** Relative gene expression level (fold change, mean ± SD) of pluripotency **(A)** and neural **(B)** associated genes. Quantitation was determined relative to ACTB by quantitative real-time PCR. Changes in gene expression are shown relative to the unsorted WJ-MSC populations (value = 1). The expression of the following groups was analyzed: unsorted WJ-MSCs, negative fraction collected directly after sorting (WJ-MSC-SSEA-4- p0), positive fraction collected directly after sorting (WJ-MSC-SSEA-4+ p0), negative fraction cultured for one passage *in vitro* (WJ-MSC-SSEA-4- p1), and positive fraction cultured for one passage *in vitro* (WJ-MSC-SSEA-4+ p1). The results shown are the mean of three independent RNA isolations, with the *p*-value of * <0.05, ** <0.01, ***<0.001, and ****<0.0001. **(C)** Immunocytochemical analysis of Brachyury, Otx2, and Sox17 (green) expression. Nuclei were counterstained with DAPI (blue). Scale bar = 100 µm. **(D)** The relative gene expression level (fold change, mean ± SD) of genes associated with specific germ layers, OTX2 (ectoderm), BRACHYURY (mesoderm), and SOX17 (endoderm), after differentiation. Quantitation was determined relative to ACTB by quantitative real-time PCR. Changes in gene expression are shown relative to the unsorted WJ-MSC populations (value = 1). The results shown are the mean of three independent RNA isolations. **(E)** Colony forming unit (CFU) frequency assay. **(F)** Population Doubling Time (PDT). The results are presented as mean values of three experiments ±SD.

and GFAP was observed in the positive population directly after FACS sorting; the expression of H3TUBULIN was still elevated after one passage of cell culture.

Subsequently, the potential to differentiate toward cells derived from three germ layers was compared between unsorted and sorted populations (Figures 4C,D; Supplementary Figure S4). Final effects were evaluated with the measurement of specific gene expression–OTX2 for ectodermal differentiation, BRACHYURY for mesodermal differentiation, and SOX17 for endodermal differentiation–and visualized with immunocytochemical staining. Both populations received in FACS sorting, WJ-MSC-SSEA-4+, and WJ-MSC-SSEA-4- exhibited increased expression of BRACHYURY, compared to the unsorted population, but the differences were not statistically significant. Unchanged OTX2 and SOX17 expression indicated that the WJ-MSC-SSEA-4+ population lacked pluripotent potential (Figure 4D). The immunocytochemical analysis confirmed the abovementioned results: high expression for the mesodermal marker (Brachyury) and no clear expression for ectodermal and endodermal lineage. No difference between all three populations was observed (Figure 4C). Additionally, the observed mesodermal differentiation capacity toward osteocytes, adipocytes, and chondrocytes was similar for both analyzed populations (Supplementary Figure S10).

The physiological properties of the analyzed subpopulations–clonogenicity and proliferation–between passages were also investigated. Clonogenicity was examined with the CFU assay (Figure 4E). Proliferation was described as the PDT for five passages after FACS (Figure 4F). No significant differences were recorded between unsorted, negative, and positive subpopulations in the CFU assay and PDT measurements. With regard to proliferation and clonogenicity, the SSEA-4+ population propagated in the *in vitro* culture as was the case in the negative and initial populations.

3.5 Expression of other surface antigens within WJ-MSC populations after SSEA-4+ enrichment

We examined whether the SSEA-4+ cell enrichment influenced the expression of other surface antigens associated with other stem cells still found within MSC populations, which are CD49F, CD133, CD146, and CD271 (Figure 5). We did not observe significant changes in the percentage of the surface antigens before and after cell sorting. WJ-MSC subpopulations contained 84%–94% of CD49F + cells (Figures 5A,B), 1.4%–3.5% of CD133+ cells (Figures 5C,D), 74%–79% of CD146+ cells (Figures 5E,F), and 2.4%-4% of CD271+ cells (Figures 5G,H). For each antigen, the fold in expression was calculated in relation to the unsorted population (Figure 5I). The most significant changes were observed for antigens that were sparse in population, such as CD133 and CD271. However, we did not record any statistically significant differences again, potentially due to considerable discrepancies between samples received from different donors. Additionally, the same analysis was performed for AD-MSCs isolated from adult donors and a significantly lower number of CD49F cells (34.2% ± 14.5) was found, while the CD271+ subpopulation was more numerous than in the WJ-MSCs (32.4% ± 7.8) (Supplementary Figure S11). Our surface antigen analysis revealed that the SSEA-4+ population could hardly be connected with other unique subpopulations.

3.6 Secretory profiles of subpopulations

In the next step, we compared the secretory profiles of unsorted WJ-MSCs, WJ-MSC-SSEA-4-, and WJ-MSC-SSEA-4+ subpopulations on days 3 and 5 *in vitro* after FACS sorting (Figure 6). We measured the levels of selected trophic factors (EGF, bFGF, GDNF, and BDNF), cytokines and chemokines (CCL2 and LIF), and vascular factors (angiogenin, VEGF-c, and ICAM-1). The unsorted population exhibited an increased secretion of BDNF, HGF, and GDNF on the third day of our observation. The WJ-MSC-SSEA-4- population secreted less VEGF-c on the third day after FACS sorting. The secretion profile slightly differed on the fifth day after FACS sorting. The WJ-MSC-SSEA-4- population secreted higher levels of bFGF and LIF, compared to other variants. The WJ-MSC-SSEA-4+ population secreted a higher level of CCL2 and a lower level of VEGF-c. Except for soluble molecules described above, no significant differences in secretion of other factors were recorded between compared groups while the levels of EGF were found to be lower than the levels observed in the culture media of negative controls (Supplementary Figure S12).

3.7 Sphere formation ability in the WJ-MSC-SSEA-4+ population

Finally, we analyzed the influence of WJ-MSC-SSEA-4+ enrichment on the sphere formation ability in the 3D culture. The 3D culture was carried out with anti-adherent culture plates for 72 h *in vitro*. All the analyzed populations were observed to form spheroids with a small diameter (15–50 µm) (Figure 7A). For each day, we counted the cell number per 10,000 seeded cells (Figure 7B) and measured their diameters (Figures 7C–E); spheroids were grouped according to their size: small spheres (smaller than 20 µm), medium spheres (20–50 µm), and large spheres (larger than 50 µm) (Figures 7F–H). A decrease in spheroid number was observed in 3D culture (Figure 7B). After the first 24 h, WJ-MSC-SSEA-4- cells formed significantly smaller spheroids than the unsorted subpopulation (95% CI, 25.3–27.6 vs. 29.15–32.4, respectively), while WJ-MSC-SSEA-4+ cells were found to form the smallest spheroids (95% CI range: 23.4–25.6 µm) (Figure 7C). After 48 h of 3D culture, unsorted WJ-MSCs formed significantly bigger spheres than negative and positive populations (95% CI ranges, 35.89–39.47 vs. 31.41–34.82 vs. 31.65–34.03, respectively) (Figure 7D). After 72 h, no significant differences were detected in the diameter of the spheroid between the analyzed variants (Figure 7E). The medium-sized spheroid predominated in all the compared groups in 3D culture (Figures 7F,G). The percentage of spheres of different sizes varied over time. A significantly larger number of small spheroids was identified in negative and positive subpopulations during the first 24 h than in subsequent days of 3D culture. Similarly, we observed fewer medium-size spheres in the positive subpopulations and larger spheres in unsorted and negative subpopulations. WJ-MSC-SSEA-4+ cells formed smaller spheres during the first 24 h of 3D culture; however, the differences diminished with the duration of 3D culture.

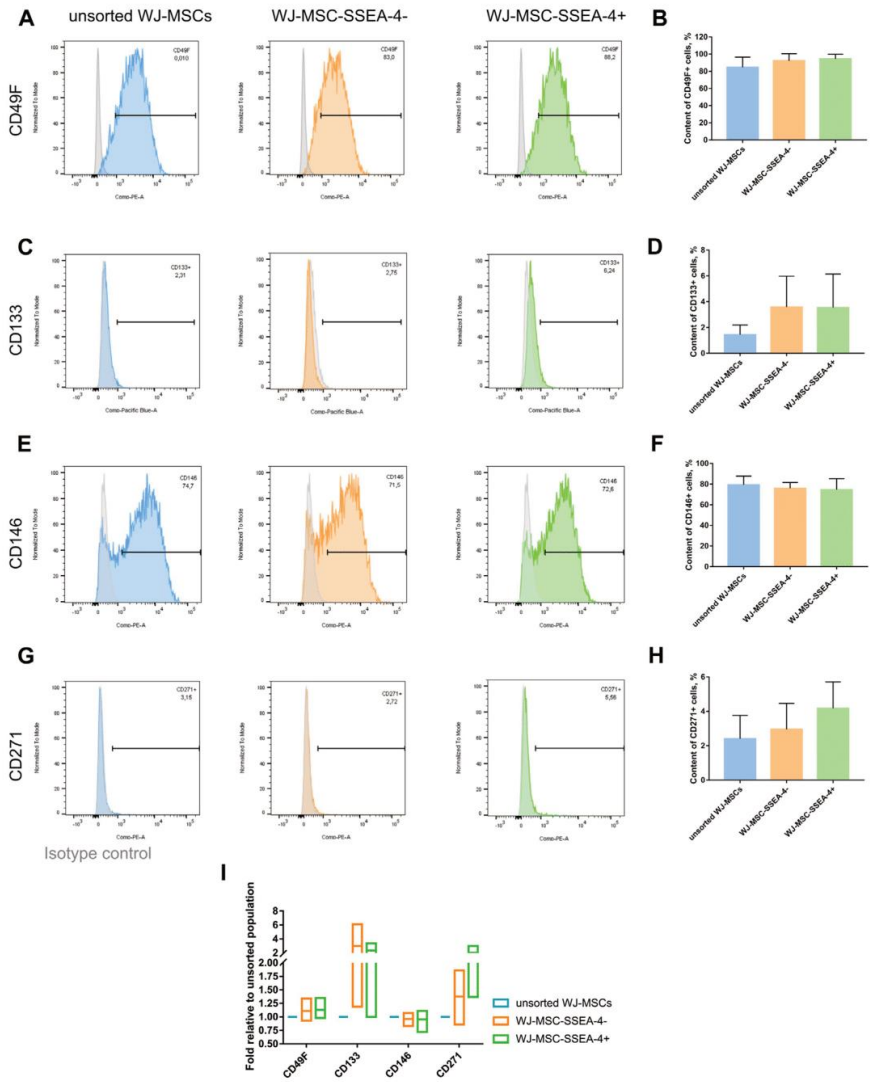

FIGURE 5
Unique surface antigens before and after FACS for the following populations: unsorted WJ-MSCs, WJ-MSC-SSEA-4- and WJ-MSC-SSEA-4+. **(A–H)**. Flow cytometry analyses – representative histograms and gathered results for CD49F **(A, B)**, CD133 **(C, D)**, CD146 **(E, F)**, CD271 **(G, H)**. Grey histogram – isotype control. **(I)**. Change in the content of the analyzed antigens after cell sorting compared to the content observed in the unsorted population. For **(B, D, F, H and I)** the results are presented as mean values of 3 experiments ± SD.

The viability of cells after 3D culture was evaluated with live-dead staining using Cal AM, EthD-1, and Hoechst after 72 h of 3D culture (Figure 8A). Cal AM-stained live cells in green, while EthD-1 bonded with nucleic acid, indicating dead cells. Dead cells were mostly observed in the spheroid core. WJ-MSC-SSEA-4+ subpopulation contained significantly fewer dead cells than unsorted and negative subpopulations (6.6 ± 1.7 for WJ-MSC-SSEA-4+ vs. 8.4 ± 2.7 for unsorted WJ-MSCs vs. 11.4 ± 2.8 for WJ-MSC-SSEA-4-) (Figure 8B). Our experiments revealed that SSEA-4+ cells formed smaller spheres during the first 24 h of 3D culture; WJ-MSC-SSEA-4+ cells were characterized with better survival during 3D culture.

4 Discussion

The heterogeneity of the MSCs arises from multiple factors ranging from differences between donors, isolation sites, and

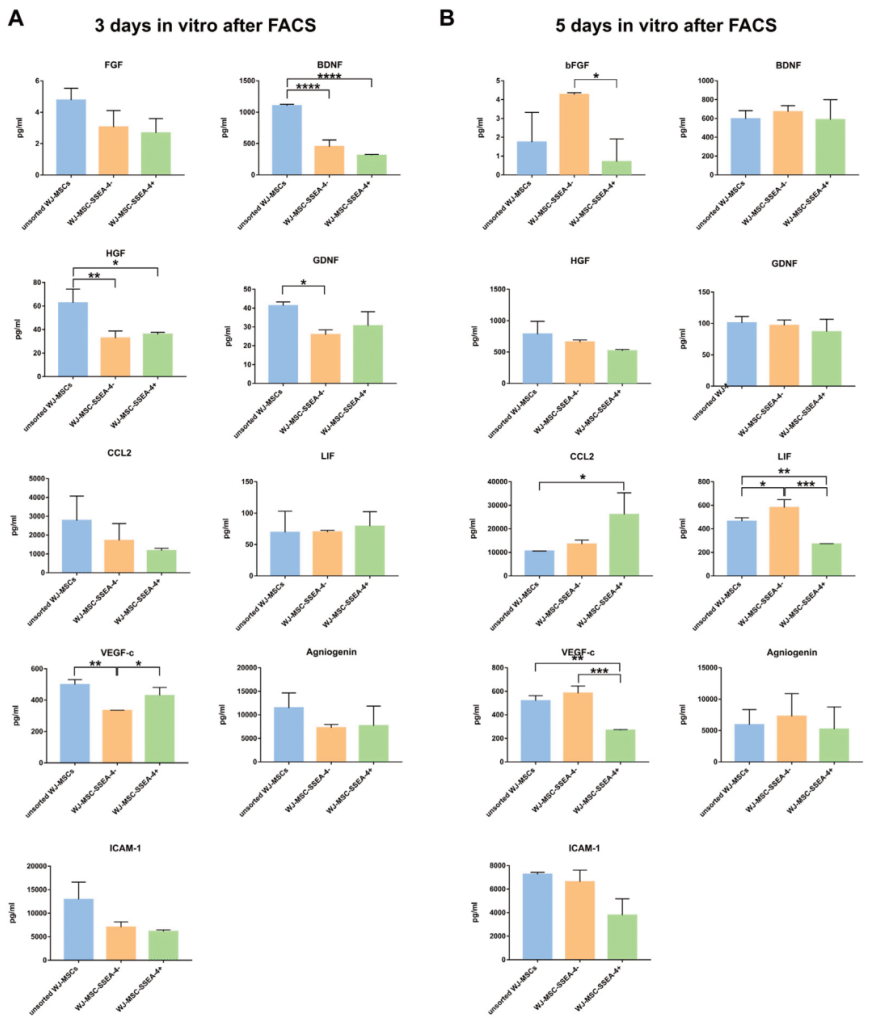

FIGURE 6
Secretory profiles 3 days *in vitro* **(A)** and 5 days *in vitro* **(B)** after FACS. The following groups were analyzed: unsorted WJ-MSCs, negative population (WJ-MSC-SSEA-4-), and positive population (WJ-MSC-SSEA-4+). The results are presented as mean values ±SD of three experiments. *p*-value for * <0.05, ** <0.01, *** <0.001, and **** <0.0001.

methods to a variety of proposed culture conditions (Lech et al., 2016; Costa et al., 2021; Wedzinska et al., 2021). Moreover, the heterogeneity issue is even more multifaceted as the cells within an established *in vitro* culture differ in morphology, size, phenotype, and differentiation potency (Sun et al., 2020; Wang et al., 2021; Zhang et al., 2022). Confirmed differentiation of multipotent MSCs toward neuron-like cells could result from intrinsic cell plasticity or contamination by cells of different origins (Somoza et al., 2008). The heterogeneity of MSCs causes a serious limitation in the translation of MSC studies for further clinical research. The application of a homogeneous subpopulation of morphologically similar cells would not only overcome this problem but would also result in better therapeutic outcomes as separated cells could exhibit outstanding properties such as faster proliferation (Kawamura et al., 2018) or unique differentiation directions (Khaki et al., 2018). Separation by surface antigen is one of the ideas in search of such a promising subpopulation, especially because MSCs present a variety of markers associated with other cell types. This study investigated whether SSEA-4+ could distinguish genuine (pluripotent-like) stem cells within MSC populations, especially in light of our previous studies, in which this subpopulation survived significantly longer in 3D culture (in spheres) (Kaminska et al., 2021).

Heterogenous MSC populations can be divided at least into two distinct classes that differ significantly in terms of ontogenetic origin and relatedly basic biological characteristics. MSCs isolated from perinatal tissues, i.e., umbilical cord, umbilical cord blood, placenta,

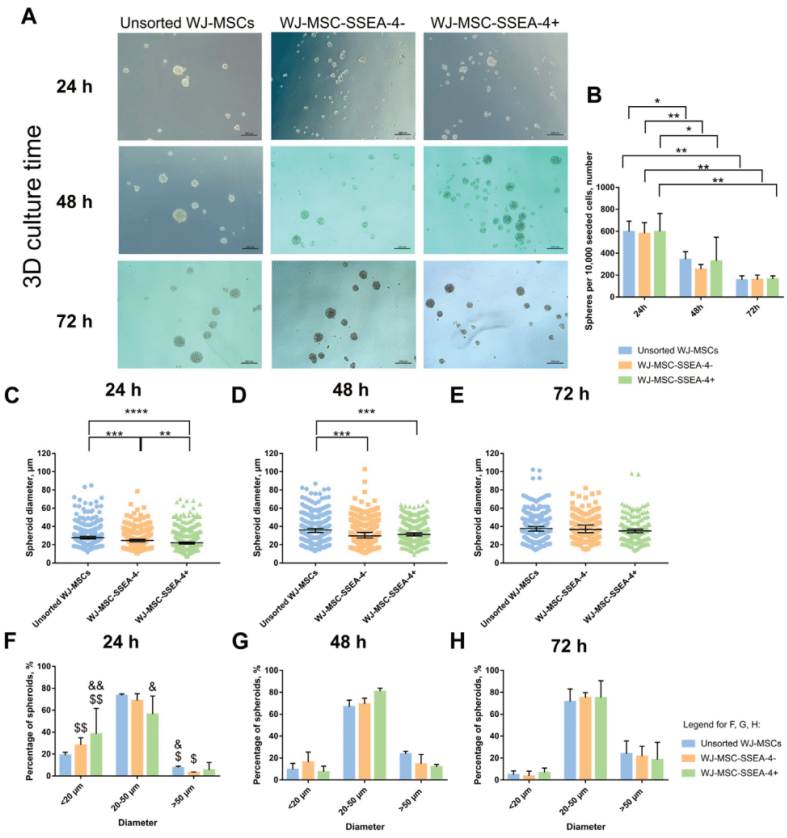

FIGURE 7
3D spheroid culture for unsorted WJ-MSCs, negative population (WJ-MSC-SSEA-4-), and positive population (WJ-MSC-SSEA-4+): time characteristics. **(A)** Morphology during the first 72 h of spheroid culture. Black scale bars represent 100 µm. **(B)** The number of spheroids formed from 10,000 cells during the first 72 h of spheroid culture. **(C–E)**: spheroid diameter during 24, 48, and 72 h of 3D culture, respectively. **(F–H)**: percentage of spheroids depending on the diameter during 24, 48, and 72 h of 3D culture, respectively. The results are presented as mean values ±SD **(B, F, G, and H)** or median values ±95% Confidence Interval **(C–E)** of three experiments. *p*-value for * <0.05, ** <0.01, *** <0.001, and **** <0.0001; significant differences for **(F–H)**: & - 24 h vs. 48 h, for $ - 24 h vs. 72 h, single symbol – *p*-value <0.05, double symbol – *p*-value <0.01.

or amniotic fluid, are related to the early stages of fetal development and their spectrum of differentiation seems to be broader. The second class represents MSCs isolated from the adult tissue, e.g., bone marrow or adipose tissue, with lower clonogenic and proliferative potential (Drela et al., 2016). MSCs from neonatal and mid-gestational fetal tissues exhibit extremely low immunogenicity; they are more plastic and grow faster. WJ-MSCs also possess the spontaneous potential to express neural markers, which have almost been undetected in BMSC. The ontogenetic origin of "primitive" MSCs was described by Takashima et al. (Takashima et al., 2007), who used Cre recombinase-mediated lineage tracing analysis which revealed that a primitive class of immature somatic progenitors with pluripotent potential and a preference for neuronal differentiation may originate from the embryonic neural crest neuroepithelium. After undergoing the first developmental epithelial-mesenchymal transition (EMT), these cells could form a cohort of primitive mesenchymal cells (pre-MSCs) that transiently populate all fetal tissue niches and then are gradually replaced by the mesoderm-recruited, post-gastrulation, adult MSCs.

Based on the above data, in order to find the marker of "primitive MSCs", we selected an ontogenetically younger mesenchymal stem/stromal cell source, i.e., umbilical cord stroma (Wharton's jelly). WJ-MSCs used in our experiments expressed surface antigen characteristics of MSCs and possessed multipotent capacities to differentiate toward mesodermal cells (Supplementary Materials). On the basis of previous studies (Musiał-Wysocka et al., 2019), despite reports of slightly lower SSEA4 expression in 5% oxygen concentration, we decided to apply hypoxic/physioxic conditions that are considered closer to physiological conditions within the cell niche than atmospheric 21% concentration (Ivanovic, 2009). Following the flow cytometry analysis performed for MSCs derived from different tissues and passages, and cultured in different media, we decided to apply WJ-MSCs from the third passage cultured in platelet lysate with a higher concentration. The estimations of SSEA-4 expression in MSC populations vary

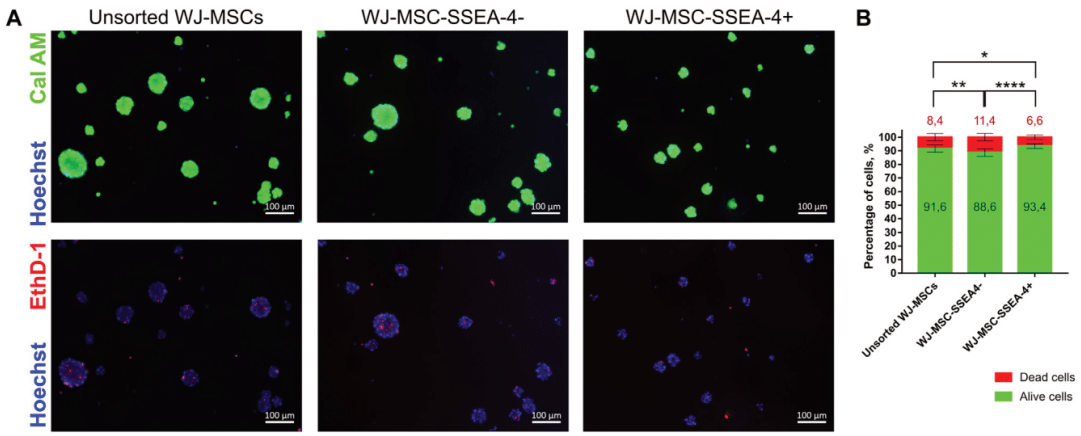

FIGURE 8
Viability of populations: unsorted WJ-MSCs, WJ-MSC-SSEA-4-, and WJ-MSC-SSEA-4+ after 72 h of 3D spheroid culture. **(A)** Calcein AM (Cal AM), ethidium homodimer-1 (EthD-1), and Hoechst staining. Green signals indicate alive cells (Cal AM), red signals indicate dead cells (EthD-1), and blue signals indicate nuclei (Hoechst). White scale bars represent 100 µm. **(B)** Analysis of dead and alive cell percentage in populations from CalAM-EthD-1 staining. The results are presented as mean values of three experiments ±SD. *p*-value for * <0.05, ** <0.01, and **** <0.0001.

across scientific literature and depend on several factors. Petrenko et al. reported differences between SSEA-4-cell percentage values observed in different MSC sources: 10% for AD-MSCs, 55% for bone marrow-derived MSCs (BM-MSCs), and 60% for WJ-MSCs (Petrenko et al., 2020). BM-MSCs from younger donors contained more SSEA-4+ cells (5.2% vs. 4% for elderly donors) (Kawamura et al., 2018) while MSCs isolated from female donors expressed fewer SSEA-4+ cells (72% vs. 79.8% observed in male donors) (Selle et al., 2022).

The available literature and our observations strongly suggest that the initial optimization should be vital for SSEA-4+ expression determination in MSC populations. Culture media components were also reported to affect SSEA-4 expression (He et al., 2014). He et al. confirmed that a higher concentration of fetal bovine serum increased SSEA-4+ cell content for WJ-MSC and BM-MSC (He et al., 2014), which is in agreement with our observation. It is especially important to emphasize this observation because sera and platelet lysates do differ between manufacturers and even batches. For the described experiments, we used PLT Gold for cell culture even though the analysis of its influence on MSC characteristics is lacking in scientific literature. However, studies performed for the older generations of this platelet lysate showed that it did not alter MSC characterization such as cell morphology, expression of MSC markers (CD73, CD90, and CD105), multipotent differentiation capacity, and proliferation ratio when compared with other human platelet lysates (Juhl et al., 2016; Lensch et al., 2018; Bhat et al., 2021). Low oxygen concentration is another factor that could reduce SSEA-4 expression (Musiał-Wysocka et al., 2019).In addition to environmental factors and the cell source, the technique of isolation may also be crucial. When isolating MSCs from WJ, the non-enzymatic method was reported to be the optimal one to obtain cells with higher clonogenic and proliferative potential expressing spontaneous neural markers (Lech et al., 2016). Unfortunately, this method applied in our experiments did not allow for an assessment of SSEA4 expression in freshly isolated, uncultured cells.

With our non-enzymatic method, it was not possible to analyze WJ-MSC without culture. To obtain the cells straight from the tissue, it would have been necessary to use the enzymatic method which does not seem to be optimal for UC-MSCs (Lech et al., 2016). In our so-called "0 passage" culture, the number of SSEA4+ cells varied and ranged from 30% to 90%. Other researchers reported that they isolated WJ-MSC from three patients and SSEA4+ cells accounted for 51%, 67%, and 70%, respectively (Musiał-Wysocka et al., 2019).

Furthermore, it is still debated whether MACS or FACS is a better sorting option to favorably affect the process efficiency and the cell quality. Some researchers reported that MACS allowed for the isolation of positive populations with reduced cell stress and increased yield (Bowles et al., 2019), while others found FACS-based selection less variable (Muratore et al., 2014; Cheng et al., 2017). FACS was shown to produce better outcomes in SSEA-4+ cell isolation from ESC populations (Fong et al., 2009). Sutermaster and Darling observed inefficient cell sorting and high false-negative rates when MACS was used according to the manufacturer's protocols (antibody and microbead concentration). After optimization, however, comparable MACS and FACS outcomes were obtained (Sutermaster and Darling, 2019). A dual MACS-FACS sorting procedure was recorded as the most effective (Kerényi et al., 2016). Our study demonstrated that FACS resulted in a more satisfactory recovery. In our study, reduced mortality of cells and better yield after FACS sorting were recorded but the observed differences were not statistically significant. Ultimately, FACS processing was selected to separate SSEA-4+ cells as the method proved to result in better recovery of positive cells.

In this study, two populations were received with FACS separation: negative (WJ-MSC-SSEA-4-) and positive (WJ-MSC-

SSEA-4+), and both were compared to unsorted WJ-MSCs. Post-sorting cytometric analysis to assess the purity was performed immediately after isolation. Increased values of SSEA-4+ percentage were recorded in the positive population and almost no SSEA-4+ cells were detected in the negative population directly after FACS. The purity of the following subpopulations was examined until the sixth passage of cell culture when we did not observe differences in the content of SSEA-4 + cells between the groups. Other research groups also reported the presence of SSEA-4+ cells in the negative population after cell sorting (Rosu-Myles et al., 2013; He et al., 2014). Although He et al. confirmed the purity of the negative population directly after cell sorting, they observed the SSEA-4 expression on similar levels both in positive and negative populations (He et al., 2014). Induction of SSEA-4 in a negative population could be associated with serum/platelet lysate concentration; this probably could provide an SSEA-4 substrate for cells. Rosu-Myles et al. reported a decrease in SSEA-4+ number during 28 days (approximately four passages) of culture in unsorted WJ-MSCs and both positive and negative subpopulations (Rosu-Myles et al., 2013). Glycosphingolipids, as well as other lipids, are not encoded by genes, while lipid cell composition is usually defined by enzymes involved in metabolic pathways (Dowhan, 2009). To detect SSEA-4 expression by qPCR, other studies used gene encoding sialyltransferase ST3GAL3 (ST3 beta-galactoside alpha-2,3-sialyltransferase 3) that is necessary for SSEA-4 synthesis (Hatzfeld et al., 2007). However, the main disadvantage of this approach is that it does not allow for direct measurement of SSEA-4 levels in cells.

Our quantitative PCR analysis revealed an increased expression of such stemness-related transcription factors as Oct4 and Nanog, which are associated with pluripotency. Small CD105+ SSEA-4+ cells isolated from bovine embryonic fibroblasts expressed pluripotent markers and differentiated toward cells from all three germ layers (Pan et al., 2015). He et al. did not observe an increased expression of pluripotency genes in the sorted SSEA-4+ subpopulation (He et al., 2014). In our earlier studies, we observed a spontaneous neural differentiation of MSCs manifested in the presence of genes and proteins associated with early neurons and glial cells (Figiel-Dabrowska et al., 2021; Tomecka et al., 2021). The SSEA-4+ population also exhibited increased expression of H-III-Tubulin, Nestin, and GFAP, thereby suggesting a better potential for ectoneural differentiation through their undifferentiated state. However, WJ-MSC-SSEA-4+ cells were incapable of efficient differentiation toward cells from all three germ layers, which definitely contradicts their pluripotent potential. Multipotential differentiation toward mesodermal lineage (osteocytes, adipocytes, and chondrocytes) was also performed by other researchers, but no notably significant differences were recorded in differentiation between cells from unsorted, positive, and negative populations (Rosu-Myles et al., 2013; He et al., 2014). He et al. did not only observe differences in proliferation between SSEA-4+ and SSEA-4- populations but also reported that SSEA-4+ expression was not correlated with cell proliferation (He et al., 2014). Furthermore, in our study, neither better proliferation nor colony-forming capacities by SSEA-4+ cells were detected, which is also consistent with other reports (He et al., 2014; Matsuoka et al., 2015). In contrast, Rosu-Myles et al. reported increased proliferation and clonogenicity potential for SSEA-4+ cells (Rosu-Myles et al., 2013). Interestingly, SSEA-4- subpopulation derived from limbal epithelial cells exhibited better clonogenicity than SSEA-4+ cells (Truong et al., 2011).

As MSCs are a highly heterogenous cell group, we investigated the impact of SSEA-4+ sorting on the expression of other surface antigens which have not been typically referred to by other researchers so far. We also assessed the expression of the markers in cells from two different sources: Wharton's jelly and adipose tissue. Following the latest literature, the following markers were selected to be analyzed: CD49F, CD133, CD146, and CD271 (Bakondi et al., 2009; Krebsbach and Villa-Diaz, 2017; Wangler et al., 2019). The distribution of CD49F (integrin α6) in various stem cell populations suggests its involvement in the stemness (pluripotent) maintenance; it was identified on the surface of, i.a., embryonic stem cells, hair follicle stem cells, hematopoietic stem cells, neural stem cells, and some cancer stem cells (Krebsbach and Villa-Diaz, 2017). AD-MSC-CD49F + exhibited a greater proliferation and mesenchymal differentiation potential. In one of the available studies, mouse and rat AD-MSCs were found to contain a maximum of 30% CD49F + cells, depending on the culture of the passage (Zha et al., 2021). Contrastingly, in our study, almost 90% of the cells in WJ-MSC populations were CD49F while AD-MSCs contained only approximately 17% of CD49F + cells. To our knowledge, this is the first paper to report CD49F+ in the human MSC populations derived from neonatal sources. CD133 (prominin 1) is another surface antigen not only associated with cancer stem cells but also found on the surface of hematopoietic stem cells and neural stem cells (Glumac and LeBeau, 2018). CD133+ cells isolated from MSCs derived from peripheral blood and adipose tissue-derived MSCs were already reported to express pluripotent markers at a higher level than unsorted MSCs (González-Garza et al., 2018). In our study, CD133+ appeared sparse for both WJ-MSCs and AD-MSCs. The expression of CD146 (melanoma cell adhesion molecule - MCAM) is associated with vascular smooth muscle cell lineage commitment (Espagnolle et al., 2014). We observed a higher percentage of CD146+ cells in WJ-MSC populations than in AD-MSCs. Finally, we investigated the expression of CD271 (low affinity nerve growth factor receptor—LANGFR/p75), which indicates cells of neuroectodermal, neural crest origin (Sowa et al., 2013; Coste et al., 2017). CD271+ cells were self-renewed and differentiated into neurons and glial cells after transplantation *in vivo* (Morrison et al., 1999). MSC-CD271+ cells were found to exhibit faster proliferation and better clonogenicity and expression of pluripotent and neural genes (Mikami et al., 2011; González-Garza et al., 2018; Kawamura et al., 2018). Originally, we also intended to separate CD271 + subpopulation. However, the number of CD271+ within the WJ-MSC populations was not sufficiently high for all the planned analyses to be made. We found that SSEA-4+ enrichment enhanced the CD271+ cell population, but the differences between the groups were not statistically significant. SSEA-4+ sorting was not found to significantly affect the expression of the surface antigens, which could be explained by extensive deviations between cells isolated from different donors.

Secretory properties of MSCs have been widely investigated in the context of therapeutic application but a limited number of reports focused on the secretion abilities of specific MSC subpopulations. We tested the hypothesis that surface markers

are strictly connected with stromal cell function by tuning the cytokines released (Islam et al., 2019) and modulating the tissue microenvironment. Here, we compared the correlation between the presence/lack of the SSEA4 marker and the levels of secreted, different regeneration-related molecules such as trophic factors, cytokines, chemokines, and factors associated with vasculogenesis. The secretion profiles were found to differ between the third and fifth day of the experiment. Reduced levels of some molecules (HGF, BDNF, and GDNF) observed in both sorted populations on the third day suggested the impact of FACS on the cells' condition. On the fifth day after FACS, for some trophic factors, the highest levels of secretion were observed in the negative population and the lowest levels were recorded in the positive population, which suggests that the SSEA-4-deficient cells may be the population that is more specialized in the secretion of trophic factors. However, the large standard deviations imply that the factors secretion could be more of an individual matter, as reported in our other paper (Sypecka et al., 2022).

Our study also examined whether the WJ-MSC-SSEA-4+ population would exhibit better survival in 3D conditions. According to the latest literature, 3D conditions could resemble the native niche of MSCs more accurately than standardly used 2D culture systems and could be more effective in stemness maintenance (Jauković et al., 2020; Rybkowska et al., 2023). Our previous paper confirmed that long-term spheroid culture affected WJ-MSCs' survival, proliferation, and senescence, as well as increased SSEA-4+ expression (Kaminska et al., 2021). In this study, we cultured WJ-MSCs from the analyzed groups for 3 days *in vitro* as spheroids and compared the number, diameter, and cell viability of the spheroids. Changes in diameter were recorded between variants for the first 48 h of 3D culture. The spheres formed with WJ-MSC-SSEA-4+ cells were the smallest in the first 24 h. At the endpoint, the differences between the groups ceased to be noticeable. SSEA-4+ cells derived from different tissues were also reported to form spheres (Barraud et al., 2007; Lopez-Lozano et al., 2022). SSEA-4+ isolated from the bovine embryonic fibroblast population formed larger spheres after the seventh day of 3D culture than SSEA-4 cells (Pan et al., 2015). The viability assay revealed that our WJ-MSC-SSEA-4+ subpopulation exhibited the lowest number of dead cells after 3D culture.

It would be an interesting aspect of the project if the differentiation potential of all analyzed populations cultured in 3D conditions could be assessed. Unfortunately, long-term 3D spheroids culture resulted in increased senescence and led to sphere disintegration of heterogenous WJ-MSCs (Kaminska et al., 2021).

Finally, the association of SSEA-4 with pluripotency was the last aspect we addressed in this study. Derivation of iPSCs from SSEA-3/4 knockout mice raised the question of whether SSEA-4 was essential (Hamamura et al., 2020). Moreover, the increased transient expression of pluripotent genes by the WJ-MSC-SSEA-4+ subpopulation did not affect the proliferation and colony-forming capacity. In fact, two states of pluripotency can be distinguished: naïve (observed for embryonic cells before implantation into the uterus) and primed (observed for cells after implantation) (Weinberger et al., 2016; Nishihara, 2017). SSEA-3 and SSEA-4 were associated only with primed pluripotency while SSEA-1 was observed in the naïve state (Nishihara, 2017). In both states, the cells were observed to express Nanog, Sox2, and Oct4 genes, and they did differentiate toward cells from all three germ layers and form teratomas *in vivo* (Nishihara, 2017). Knockout of B3GALT5, an enzyme involved in SSEA-3/4 synthesis, was reported to facilitate the transition of human ESCs from primed to naïve state (Lin et al., 2020). Contrastingly, SSEA-3+ cells isolated from the amniotic membrane appeared to represent a naïve state of pluripotency, which was confirmed by the presence of SSEA-1 and expression of KLF4—a gene characteristic only of this state (Ogawa et al., 2022). However, those observations were not confirmed in the SSEA-3+ population derived from other tissue sources. It remains debatable whether the presence of two states explains the observed results in the WJ-MSC-SSEA-4+ population.

Some limitations of this study should be acknowledged. A decrease in the cell viability observed in both methods of cell sorting is a downside of the methodology used. Slightly higher viability of cells from unsorted populations could influence the outcomes received in PDT and CFU assays. To minimize this effect, unsorted cells were transported to the sorting facility in similar conditions applied for both positive and negative subpopulations. Furthermore, if indeed the sorting procedure had such a profound effect on the condition of the cells, differences between passages in cell culture would have been noticed. The next limitation concerns the similarity of SSEA-4+ cell content between unsorted and positive populations. Most researchers report the results observed in positive and negative populations. We decided to analyze the outcomes from the initial population to confirm whether SSEA-4 enrichment indeed impacted WJ-MSC populations. Nevertheless, if SSEA-4 surface antigen had such a huge impact, we would have observed significantly different results at least in the negative population. In fact, some of the analyzed aspects such as proliferation, CFU, and expression of other surface antigens were almost similar in all study groups.

5 Conclusion

This study described the characteristics of SSEA-4+ cells separated from the heterogenous WJ-MSC populations. WJ-MSCs contained approximately 35%–70% SSEA-4+ cells, depending on the applied culture condition. The environment richer in proteins and trophic factors appeared to be more favorable for SSEA-4 cell enrichment probably due to providing the essential substrate for synthesis. FACS allowed for the selection of positive SSEA-4+ cells and its number increased during the further *in vitro* culture. Elevated relative expression of the investigated stemness-related genes suggested an undifferentiated state of the WJ-MSC-SSEA-4 + subpopulation, which could also affect the differentiation potential toward ectoneural cells. However, this effect was transient and diminished with further cell culture, which could account for the unchanged pluripotent differentiation potential, proliferation ratio, and colony-forming capacities observed in the positive population. The SSEA-4+ population was not found to be associated with other potential stemness surface antigens. SSEA-4 enrichment influenced such aspects of 3D culture as diameter during the first 24 h and viability of cells inside the spheres. Our hypothesis that WJ-MSC-SSEA-4+ cells could be a more favorable subpopulation due to unique pluripotent-like features and restorative/replacing properties could not be confirmed as no unequivocal results were obtained. However, the search for such a marker is an important direction for further research on mesenchymal stem cells.

Data availability statement

The datasets presented in this article are not readily available because of privacy issues to make sure that confidentiality of tissue's donor is preserved. Requests to access the datasets should be directed to Anna Sarnowska (contact: asarnowska@imdik.pan.pl)

Ethics statement

The studies involving human participants were reviewed and approved by Ethics Committee of Warsaw Medical University (date: 11 October 2016, no. KB/213/2016) and Bioethical Committee at the Centre of Postgraduate Medical Education (date: 8 October 2013, No. 63/PB/2013). The patients provided their written informed consent to participate in this study.

Author contributions

ASm was responsible for designing the study, performing experiments, analyzing data and writing the manuscript; AK, JJ and KP performed FACS sorting and analyzed data; MC performed experiments with AD-MSCs and analyzed data; DS performed Luminex assay and analyzed data; ASa designed the studies, supervised experiments, analyzed data and reviewed the manuscript. All authors contributed to the article and approved the submitted version.

Funding

This study was funded by National Science Centre grant NCN 2018/31/B/NZ4/03172, statutory funds to Mossakowski Medical Research Institute and ESF, POWR.03.02.00-00-I028/17-00.

Acknowledgments

We would like to thank Natalia Krześniak from the Prof. W. Orlowski Memorial Hospital in Warsaw for providing the adipose tissue for ADSCs isolation, the Laboratory of Advanced Microscopy Techniques for assistance with Confocal Microscopy imaging, and the Laboratory of Cytometry from Nencki Institute of Experimental Biology for their advice and help regarding flow cytometry. Finally, we are thankful to our colleagues from Translational Platform for Regenerative Medicine.

Conflict of interest

The authors declare that the research was conducted in the absence of any commercial or financial relationships that could be construed as a potential conflict of interest.

Publisher's note

All claims expressed in this article are solely those of the authors and do not necessarily represent those of their affiliated organizations, or those of the publisher, the editors and the reviewers. Any product that may be evaluated in this article, or claim that may be made by its manufacturer, is not guaranteed or endorsed by the publisher.

Supplementary material

The Supplementary Material for this article can be found online at: https://www.frontiersin.org/articles/10.3389/fcell.2024.1227034/full#supplementary-material

References

Bakondi, B., Shimada, I. S., Perry, A., Munoz, J. R., Ylostalo, J., Howard, A. B., et al. (2009). CD133 identifies a human bone marrow stem/progenitor cell sub-population with a repertoire of secreted factors that protect against stroke. *Mol. Ther.* 17, 1938–1947. doi:10.1038/mt.2009.185

Barilani, M., Banfi, F., Sironi, S., Ragni, E., Guillaumin, S., Polveraccio, F., et al. (2018). Low-affinity nerve growth factor receptor (CD271) heterogeneous expression in adult and fetal mesenchymal stromal cells. *Sci. Rep.* 8, 9321–9411. doi:10.1038/s41598-018-27587-8

Barraud, P., Stott, S., Møllgård, K., Parmar, M., and Björklund, A. (2007). *In vitro* characterization of a human neural progenitor cell coexpressing SSEA4 and CD133. *J. Neurosci. Res.* 85, 250–259. doi:10.1002/jnr.21116

Bhat, S., Viswanathan, P., Chandanala, S., Prasanna, S. J., and Seetharam, R. N. (2021). Expansion and characterization of bone marrow derived human mesenchymal stromal cells in serum-free conditions. *Sci. Rep.* 11, 3403–3418. doi:10.1038/s41598-021-83088-1

Bowles, K. R., Julia, T. C. W., Qian, L., Jadow, B. M., and Goate, A. M. (2019). Reduced variability of neural progenitor cells and improved purity of neuronal cultures using magnetic activated cell sorting. *PLoS One* 14, e0213374. doi:10.1371/journal.pone.0213374

Cheng, C., Fass, D. M., Folz-Donahue, K., MacDonald, M. E., and Haggarty, S. J. (2017). Highly expandable human iPS cell–derived neural progenitor cells (NPC) and neurons for central nervous system disease modeling and high-throughput screening. *Curr. Protoc. Hum. Genet.* 92, 1–21. doi:10.1002/cphg.33

Costa, L. A., Eiro, N., Fraile, M., Gonzalez, L. O., Saá, J., Garcia-Portabella, P., et al. (2021). Functional heterogeneity of mesenchymal stem cells from natural niches to culture conditions: implications for further clinical uses. *Cell Mol. Life Sci.* 78, 447–467. doi:10.1007/s00018-020-03600-0

Coste, C., Neirinckx, V., Sharma, A., Agirman, G., Rogister, B., Foguenne, J., et al. (2017). Human bone marrow harbors cells with neural crest-associated characteristics like human adipose and dermis tissues. *PLoS One* 12, e0177962. doi:10.1371/journal.pone.0177962

Dominici, M., Le Blanc, K., Mueller, I., Slaper-Cortenbach, I., Marini, F. C., Krause, D. S., et al. (2006). Minimal criteria for defining multipotent mesenchymal stromal cells. The International Society for Cellular Therapy position statement. *Cytotherapy* 8, 315–317. doi:10.1080/14653240600855905

Doshmanziari, M., Shirian, S., Kouchakian, M. R., Moniri, S. F., Jangnoo, S., Mohammadi, N., et al. (2021). Mesenchymal stem cells act as stimulators of neurogenesis and synaptic function in a rat model of Alzheimer's disease. *Heliyon* 7, e07996. doi:10.1016/j.heliyon.2021.e07996

Dowhan, W. (2009). Molecular genetic approaches to defining lipid function. *J. Lipid Res.* 50 (1), S305–S310. doi:10.1194/jlr.R800041-JLR200

Draper, J. S., Pigott, C., Thomson, J. A., and Andrews, P. W. (2002). Surface antigens of human embryonic stem cells: changes upon differentiation in culture. *J. Anat.* 200, 249–258. doi:10.1046/j.1469-7580.2002.00030.x

Drela, K., Lech, W., Figiel-Dabrowska, A., Zychowicz, M., Mikula, M., Sarnowska, A., et al. (2016). Enhanced neuro-therapeutic potential of Wharton's Jelly-derived mesenchymal stem cells in comparison with bone marrow mesenchymal stem cells culture. *Cytotherapy* 18, 497–509. doi:10.1016/j.jcyt.2016.01.006

Espagnolle, N., Guilloton, F., Deschaseaux, F., Gadelorge, M., Sensébé, L., and Bourin, P. (2014). CD146 expression on mesenchymal stem cells is associated with their vascular smooth muscle commitment. *J. Cell Mol. Med.* 18, 104–114. doi:10.1111/jcmm.12168

Figiel-Dabrowska, A., Radoszkiewicz, K., Rybkowska, P., Krzesniak, N. E., Sulejczak, D., and Sarnowska, A. (2021). Neurogenic and neuroprotective potential of stem/stromal cells derived from adipose tissue. *Cells* 10, 1475. doi:10.3390/cells10061475

Fong, C. Y., Peh, G. S. L., Gauthaman, K., and Bongso, A. (2009). Separation of SSEA-4 and TRA-1-60 labelled undifferentiated human embryonic stem cells from a heterogeneous cell population using magnetic-activated cell sorting (MACS) and fluorescence-activated cell sorting (FACS). *Stem Cell Rev. Rep.* 5, 72–80. doi:10.1007/s12015-009-9054-4

Gang, E. J., Bosnakovski, D., Figueiredo, C. A., Visser, J. W., and Perlingeiro, R. C. R. (2007). SSEA-4 identifies mesenchymal stem cells from bone marrow. *Blood* 109, 1743–1751. doi:10.1182/blood-2005-11-010504

Glumac, P. M., and LeBeau, A. M. (2018). The role of CD133 in cancer: a concise review. *Clin. Transl. Med.* 7, 18. doi:10.1186/s40169-018-0198-1

González-Garza, M. T., Cruz-Vega, D. E., Cárdenas-Lopez, A., de la Rosa, R. M., and Moreno-Cuevas, J. E. (2018). Comparing stemness gene expression between stem cell subpopulations from peripheral blood and adipose tissue. *Am. J. Stem Cells* 7, 38–47.

Hamamura, K., Hotta, H., Murakumo, Y., Shibuya, H., Kondo, Y., and Furukawa, K. (2020). Ssea-3 and 4 are not essential for the induction or properties of mouse ips cells. *J. Oral Sci.* 62, 393–396. doi:10.2334/josnusd.19-0513

Hatzfeld, A., Eid, P., Peiffer, I., Li, M. L., Barbet, R., Oostendorp, R. A. J., et al. (2007). A sub-population of high proliferative potential-quiescent human mesenchymal stem cells is under the reversible control of interferon alpha/beta. *Leukemia* 21, 714–724. doi:10.1038/sj.leu.2404589

He, H., Nagamura-Inoue, T., Tsunoda, H., Yuzawa, M., Yamamoto, Y., Yorozu, P., et al. (2014). Stage-specific embryonic antigen 4 in wharton's jelly-derived mesenchymal stem cells is not a marker for proliferation and multipotency. *Tissue Eng. - Part A* 20, 1314–1324. doi:10.1089/ten.TEA.2013.0333

He, X. L., and Garcia, K. C. (2004). Structure of nerve growth factor complexed with the shared neurotrophin receptor p75. *Science* 304, 870–875. doi:10.1126/science.1095190

Henderson, J. K., Draper, J. S., Baillie, H. S., Fishel, S., Thomson, J. A., Moore, H., et al. (2002). Preimplantation human embryos and embryonic stem cells show comparable expression of stage-specific embryonic antigens. *Stem Cells* 20, 329–337. doi:10.1634/stemcells.20-4-329

Islam, A., Urbarova, I., Bruun, J. A., and Martinez-Zubiaurre, I. (2019). Large-scale secretome analyses unveil the superior immunosuppressive phenotype of umbilical cord stromal cells as compared to other adult mesenchymal stromal cells. *Eur. Cell Mater* 37, 153–174. doi:10.22203/eCM.v037a10

Ivanovic, Z. (2009). Hypoxia or *in situ* normoxia: the stem cell paradigm. *J. Cell Physiol.* 219, 271–275. doi:10.1002/jcp.21690

Ivanovic, Z. (2023). Mesenchymal – stem and non-Stem – cells: the name of the rose. *Transfus. Clin. Biol.* 30, 305–306. doi:10.1016/J.TRACLI.2023.03.006

Jauković, A., Abadjieva, D., Trivanović, D., Stoyanova, E., Kostadinova, M., Pashova, S., et al. (2020). Specificity of 3D MSC spheroids microenvironment: impact on MSC behavior and properties. *Stem Cell Rev. Rep.* 16, 853–875. doi:10.1007/s12015-020-10006-9

Juhl, M., Tratwal, J., Follin, B., Søndergaard, R. H., Kirchhoff, M., Ekblond, A., et al. (2016). Comparison of clinical grade human platelet lysates for cultivation of mesenchymal stromal cells from bone marrow and adipose tissue. *Scand. J. Clin. Lab. Invest.* 76, 93–104. doi:10.3109/00365513.2015.1099723

Kallas, A., Pook, M., Maimets, M., Zimmermann, K., and Maimets, T. (2011). Nocodazole treatment decreases expression of pluripotency markers Nanog and Oct4 in human embryonic stem cells. *PLoS One* 6, e19114. doi:10.1371/journal.pone.0019114

Kaminska, A., Wedzinska, A., Kot, M., and Sarnowska, A. (2021). Effect of long-term 3D spheroid culture on WJ-MSC. *Cells* 10, 719. doi:10.3390/cells10040719

Kawamura, H., Nakatsuka, R., Matsuoka, Y., Sumide, K., Fujioka, T., Asano, H., et al. (2018). TGF-B signaling accelerates senescence of human bone-derived CD271 and SSEA-4 double-positive mesenchymal stromal cells. *Stem Cell Rep.* 10, 920–932. doi:10.1016/j.stemcr.2018.01.030

Kawanabe, N., Murata, S., Fukushima, H., Ishihara, Y., Yanagita, T., Yanagita, E., et al. (2012). Stage-specific embryonic antigen-4 identifies human dental pulp stem cells. *Exp. Cell Res.* 318, 453–463. doi:10.1016/j.yexcr.2012.01.008

Kerényi, F., Tarapcsák, S., Hrubi, E., Baráthne, S. A., Hegedüs, V., Balogh, S., et al. (2016). Comparison of sorting of fluorescently and magnetically labelled dental pulp stem cells. *Fogorvosi Szle.* 109 (1), 29–33. Available at: https://www.nlclibrary.ca/eds/detail?db=cmedm&an=27188159 (Accessed January 17, 2023).

Khaki, M., Salmanian, A. H., Abtahi, H., Ganji, A., and Mosayebi, G. (2018). Mesenchymal stem cells differentiate to endothelial cells using recombinant vascular endothelial growth factor -A. *Rep. Biochem. Mol. Biol.* 6, 144–150.

Krebsbach, P. H., and Villa-Diaz, L. G. (2017). The role of integrin α6 (CD49f) in stem cells: more than a conserved biomarker. *Stem Cells Dev.* 26, 1090–1099. doi:10.1089/scd.2016.0319

Kuroda, Y., Kitada, M., Wakao, S., Nishikawa, K., Tanimura, Y., Makinoshima, H., et al. (2010). Unique multipotent cells in adult human mesenchymal cell populations. *Proc. Natl. Acad. Sci. U. S. A.* 107, 8639–8643. doi:10.1073/pnas.0911647107

Lech, W., Figiel-Dabrowska, A., Sarnowska, A., Drela, K., Obtulowicz, P., Noszczyk, B. H., et al. (2016). Phenotypic, functional, and safety control at preimplantation phase of MSC-based Therapy. *Stem Cells Int.* 2016, 2514917. doi:10.1155/2016/2514917

Lee, R. H., Wang, Y. J., Lai, T. Y., Hsu, T. L., Chuang, P. K., Wu, H. C., et al. (2021). Combined effect of anti-SSEA4 and anti-globo H antibodies on breast cancer cells. *ACS Chem. Biol.* 16, 1526–1537. doi:10.1021/acschembio.1c00396

Lensch, M., Muise, A., White, L., Badowski, M., and Harris, D. (2018). Comparison of synthetic media designed for expansion of adipose-derived mesenchymal stromal cells. *Biomedicines* 6, 54. doi:10.3390/biomedicines6020054

Lin, R.-J., Kuo, M.-W., Yang, B.-C., Tsai, H.-H., Chen, K., Huang, J.-R., et al. (2020). B3GALT5 knockout alters gycosphingolipid profile and facilitates transition to human naïve pluripotency. *Proc. Natl. Acad. Sci. U. S. A.* 117, 27435–27444. doi:10.1073/pnas.2003155117

Lopez-Lozano, A. P., Arevalo-Niño, K., Gutierrez-Puente, Y., Montiel-Hernandez, J. L., Urrutia-Baca, V. H., Del Angel-Mosqueda, C., et al. (2022). SSEA-4 positive dental pulp stem cells from deciduous teeth and their induction to neural precursor cells. *Head. Face Med.* 18, 9. doi:10.1186/s13005-022-00313-6

Lv, F. J., Tuan, R. S., Cheung, K. M. C., and Leung, V. Y. L. (2014). Concise review: the surface markers and identity of human mesenchymal stem cells. *Stem Cells* 32, 1408–1419. doi:10.1002/stem.1681

Matsuoka, Y., Nakatsuka, R., Sumide, K., Kawamura, H., Takahashi, M., Fujioka, T., et al. (2015). Prospectively isolated human bone marrow cell-derived MSCs support primitive human CD34-negative hematopoietic stem cells. *Stem Cells* 33, 1554–1565. doi:10.1002/stem.1941

Mikami, Y., Ishii, Y., Watanabe, N., Shirakawa, T., Suzuki, S., Irie, S., et al. (2011). CD271/p75NTR inhibits the differentiation of mesenchymal stem cells into osteogenic, adipogenic, chondrogenic, and myogenic lineages. *Stem Cells Dev.* 20, 901–913. doi:10.1089/scd.2010.0299

Morrison, S. J., White, P. M., Zock, C., and Anderson, D. J. (1999). Prospective identification, isolation by flow cytometry, and *in vivo* self-renewal of multipotent mammalian neural crest stem cells. *Cell* 96, 737–749. doi:10.1016/s0092-8674(00)80583-8

Muratore, C. R., Srikanth, P., Callahan, D. G., and Young-Pearse, T. L. (2014). Comparison and optimization of hiPSC forebrain cortical differentiation protocols. *PLoS One* 9, e105807. doi:10.1371/journal.pone.0105807

Musiał-Wysocka, A., Kot, M., Sułkowski, M., Badyra, B., and Majka, M. (2019). Molecular and functional verification of wharton's jelly mesenchymal stem cells (WJ-MSCs) pluripotency. *Int. J. Mol. Sci.* 20, 1807. doi:10.3390/ijms20081807

Nakamura, Y., Miyata, Y., Matsuo, T., Shida, Y., Hakariya, T., Ohba, K., et al. (2019). Stage-specific embryonic antigen-4 is a histological marker reflecting the malignant behavior of prostate cancer. *Glycoconj J.* 36, 409–418. doi:10.1007/s10719-019-09882-2

Nishihara, S. (2017). Glycans define the stemness of naïve and primed pluripotent stem cells. *Glycoconj J.* 34, 737–747. doi:10.1007/s10719-016-9740-9

Ogawa, E., Oguma, Y., Kushida, Y., Wakao, S., Okawa, K., and Dezawa, M. (2022). Naïve pluripotent-like characteristics of non-tumorigenic Muse cells isolated from human amniotic membrane. *Sci. Rep.* 12, 17222–17317. doi:10.1038/s41598-022-22282-1

Ojima, T., Shibata, E., Saito, S., Toyoda, M., Nakajima, H., Yamazaki-Inoue, M., et al. (2015). Glycolipid dynamics in generation and differentiation of induced pluripotent stem cells. *Sci. Rep.* 5, 14988–15013. doi:10.1038/srep14988

Pan, S., Chen, W., Liu, X., Xiao, J., Wang, Y., Liu, J., et al. (2015). Application of a novel population of multipotent stem cells derived from skin fibroblasts as donor cells in bovine SCNT. *PLoS One* 10, e0114423. doi:10.1371/journal.pone.0114423

Petrenko, Y., Vackova, I., Kekulova, K., Chudickova, M., Koci, Z., Turnovcova, K., et al. (2020). A comparative analysis of multipotent mesenchymal stromal cells derived from different sources, with a focus on neuroregenerative potential. *Sci. Rep.* 10, 4290. doi:10.1038/s41598-020-61167-z

Rosu-Myles, M., McCully, J., Fair, J., Mehic, J., Menendez, P., Rodriguez, R., et al. (2013). The globoseries glycosphingolipid SSEA-4 is a marker of bone marrow-derived clonal multipotent stromal cells *in vitro* and *in vivo*. *Stem Cells Dev.* 22, 1387–1397. doi:10.1089/scd.2012.0547

Rybkowska, P., Radoszkiewicz, K., Kawalec, M., Dymkowska, D., Zabłocka, B., Zabłocki, K., et al. (2023). The metabolic changes between monolayer (2D) and three-dimensional (3D) culture conditions in human mesenchymal stem/stromal cells derived from adipose tissue. *Cells* 12, 178. doi:10.3390/cells12010178

Selle, M., Koch, J. D., Ongsiek, A., Ulbrich, L., Ye, W., Jiang, Z., et al. (2022). Influence of age on stem cells depends on the sex of the bone marrow donor. *J. Cell Mol. Med.* 26, 1594–1605. doi:10.1111/jcmm.17201

Sivasubramaniyan, K., Harichandan, A., Schilbach, K., Mack, A. F., Bedke, J., Stenzl, A., et al. (2015). Expression of stage-specific embryonic antigen-4 (SSEA-4) defines spontaneous loss of epithelial phenotype in human solid tumor cells. *Glycobiology* 25, 902–917. doi:10.1093/glycob/cwv032

Soliman, C., Chua, J. X., Vankemmelbeke, M., McIntosh, R. S., Guy, A. J., Spendlove, I., et al. (2020). The terminal sialic acid of stage-specific embryonic antigen-4 has a crucial role in binding to a cancer-targeting antibody. *J. Biol. Chem.* 295, 1009–1020. doi:10.1074/jbc.RA119.011518

Somoza, R., Conget, P., and Rubio, F. J. (2008). Neuropotency of human mesenchymal stem cell cultures: clonal studies reveal the contribution of cell plasticity and cell contamination. *Biol. Blood Marrow Transpl.* 14, 546–555. doi:10.1016/j.bbmt.2008.02.017

Sowa, Y., Imura, T., Numajiri, T., Takeda, K., Mabuchi, Y., Matsuzaki, Y., et al. (2013). Adipose stromal cells contain phenotypically distinct adipogenic progenitors derived from neural crest. *PLoS One* 8, e84206. doi:10.1371/journal.pone.0084206

Sun, C., Wang, L., Wang, H., Huang, T., Yao, W., Li, J., et al. (2020). Single-cell RNA-seq highlights heterogeneity in human primary Wharton's jelly mesenchymal stem/stromal cells cultured *in vitro*. *Stem Cell Res. Ther.* 11, 149. doi:10.1186/s13287-020-01660-4

Sutermaster, B. A., and Darling, E. M. (2019). Considerations for high-yield, high-throughput cell enrichment: fluorescence versus magnetic sorting. *Sci. Rep.* 9, 227–229. doi:10.1038/s41598-018-36698-1

Sypecka, M., Bzinkowska, A., Sulejczak, D., Dabrowski, F., and Sarnowska, A. (2022). Evaluation of the optimal manufacturing protocols and therapeutic properties of mesenchymal stem/stromal cells derived from wharton's jelly. *Int. J. Mol. Sci.* 24, 652. doi:10.3390/ijms24010652

Takashima, Y., Era, T., Nakao, K., Kondo, S., Kasuga, M., Smith, A. G., et al. (2007). Neuroepithelial cells supply an initial transient wave of MSC differentiation. *Cell* 129, 1377–1388. doi:10.1016/j.cell.2007.04.028

Tomecka, E., Lech, W., Zychowicz, M., Sarnowska, A., Murzyn, M., Oldak, T., et al. (2021). Assessment of the neuroprotective and stemness properties of human wharton's jelly-derived mesenchymal stem cells under variable (5% vs. 21%) aerobic conditions. *Cells* 10, 717. doi:10.3390/cells10040717

Truong, T. T., Huynh, K., Nakatsu, M. N., and Deng, S. X. (2011). SSEA4 is a potential negative marker for the enrichment of human corneal epithelial stem/progenitor cells. *Invest. Ophthalmol. Vis. Sci.* 52, 6315–6320. doi:10.1167/iovs.11-7518

Wang, Z., Chai, C., Wang, R., Feng, Y., Huang, L., Zhang, Y., et al. (2021). Single-cell transcriptome atlas of human mesenchymal stem cells exploring cellular heterogeneity. *Clin. Transl. Med.* 11, e650. doi:10.1002/ctm2.650

Wangler, S., Menzel, U., Li, Z., Ma, J., Hoppe, S., Benneker, L. M., et al. (2019). CD146/MCAM distinguishes stem cell subpopulations with distinct migration and regenerative potential in degenerative intervertebral discs. *Osteoarthr. Cartil.* 27, 1094–1105. doi:10.1016/j.joca.2019.04.002

Wedzinska, A., Figiel-Dabrowska, A., Kozlowska, H., and Sarnowska, A. (2021). The effect of proinflammatory cytokines on the proliferation, migration and secretory activity of mesenchymal stem/stromal cells (Wj-mscs) under 5% o2 and 21% o2 culture conditions. *J. Clin. Med.* 10, 1813. doi:10.3390/jcm10091813

Weinberger, L., Ayyash, M., Novershtern, N., and Hanna, J. H. (2016). Dynamic stem cell states: naive to primed pluripotency in rodents and humans. *Nat. Rev. Mol. Cell Biol.* 17, 155–169. doi:10.1038/nrm.2015.28

Zha, K., Li, X., Tian, G., Yang, Z., Sun, Z., Yang, Y., et al. (2021). Evaluation of CD49f as a novel surface marker to identify functional adipose-derived mesenchymal stem cell subset. *Cell Prolif.* 54, e13017. doi:10.1111/cpr.13017

Zhang, C., Han, X., Liu, J., Chen, L., Lei, Y., Chen, K., et al. (2022). Single-cell transcriptomic analysis reveals the cellular heterogeneity of mesenchymal stem cells. *Genomics Proteomics Bioinforma.* 20, 70–86. doi:10.1016/j.gpb.2022.01.005

Zhao, Q., Ren, H., and Han, Z. (2016). Mesenchymal stem cells: immunomodulatory capability and clinical potential in immune diseases. *J. Cell. Immunother.* 2, 3–20. doi:10.1016/j.jocit.2014.12.001

frontiers

Supplementary Material

Stemness properties of SSEA-4+ subpopulation isolated from heterogenous Wharton jelly mesenchymal stem/stromal cells First

Agnieszka Smolinska, Magdalena Chodkowska, Agata Kominek, Jakub Janiec, Katarzyna Piwocka, Dorota Sulejczak, Anna Sarnowska*.

*** Correspondence:** Corresponding Author: asarnowska@imdik.pan.pl

1 Supplementary materials and methods

Materials and methods S1. Flow cytometry analysis of MSCs specific surface antigens. For estimation of surface antigens content recommended by The International Society for Cellular Therapy, we used Human MSC Analysis Kit (BD) containing following anti-human antibodies: CD73-APC, CD90-FITC, CD105-PerCP-Cy5.5 (positive cocktail), CD11b-PE, CD19-PE, CD34-PE, CD45-PE (negative cocktail). According to the manufacturer protocols, cells were detached with Accutase Cell Detachment Solution (BD) and washed in PBS. Required cell number (1*106) was resuspend in cold Stain Buffer (BD) and then incubated with antibodies in the dark for 30 minutes. After incubation, cells were washed twice with Stain Buffer (BD) and resuspend in Stain Buffer. Resuspended cells were analysed using FACS Canto II (BD) with FACSDiva Software (BD) and FlowJo 10 (BD).

Materials and methods S2. MSCs multipotent differentiation assay. To verify the multipotency of WJ-MSCs used for experiments, mesodermal lineage differentiation was tested. Osteogenic, chondrogenic and adipogenic differentiation was induced with commercial differentiation media (Gibco, Thermo Fischer Scientific). Induction of adipogenesis and chondrogenesis was conducted for 14 days and induction for osteogenesis was conducted for 21 days. Then, cells were fixed in 4% PFA and then stained with histochemical dyes; osteogenesis was evaluated with 2% alizarin red S, chondrogenesis was evaluated with 1% alcian blue, adipogenesis was evaluated with 0,5% Oil Red.

Supplementary Table S1. List of primers used for RT-qPCR

Gene	NCBI Reference Sequence	Product size	Primer sequence (5′ -> 3′)
β-Actin	NM_001101.5	250 bp	F: CATGTACGTTGCTATCCAGGC R: CTCCTTAATGTCACGCACGAT
Nanog	NM_024865.4	103 bp	F: GAACCTCAGCTACAAACAGG R: CGTCACACCATTGCTATTCT
Oct3/4 (Pou5F1)	NM_001285986.2	331 bp	F: CTGAAGCAGAAGAGGATCACC R: AAAGCGGCAGATGGTCGTTTGG

Sox2	NM_003106.4	93 bp	F: GTGGAAACTTTTGTCGGAGA R: TTATAATCCGGGTGCTCCTT
Nestin1	NM_006617.2	64 bp	F: GGGAAGAGGTGATGGAACCA R: AAGCCCTGAACCCTCTTTGC
β-Tubulin III	NM_001197181.2	126 bp	F: GGAAGAGGGCGAGATGTACG R: GGGTTTAGACACTGCTGGCT
GFAP	NM_001363846.2	100 bp	F: CCGACAGCAGGTCCATGT R: GTTGCTGGACGCCATTG
OTX2	NM_001270523.2	98 bp	F: TTCATGCGAGAGGAGGTGGCA R: TGCTGTTGTTGGCGGCACTT
Brachyuri	NM_001379200.1	104 bp	F:ACGGCCACATTATTCTGAAT R:GAAGTTCTCCTCGGCATATT
ACTA2	NM_001141945.2	99 bp	F: CATCATGCGTCTGGATCTG R: TCACGCTCAGCAGTAGTA
SOX17	NM_022454.4	110 bp	F:AACTATCCTGACGTGTGACA R:CAAAAACCCAGGAGTCTGAG
FOX2A	NM_021784.5	89 bp	F: GGGAGCGGTGAAGATGGA R: TCATGTTGCTCACGGAGGAGTA

2 Supplementary figures

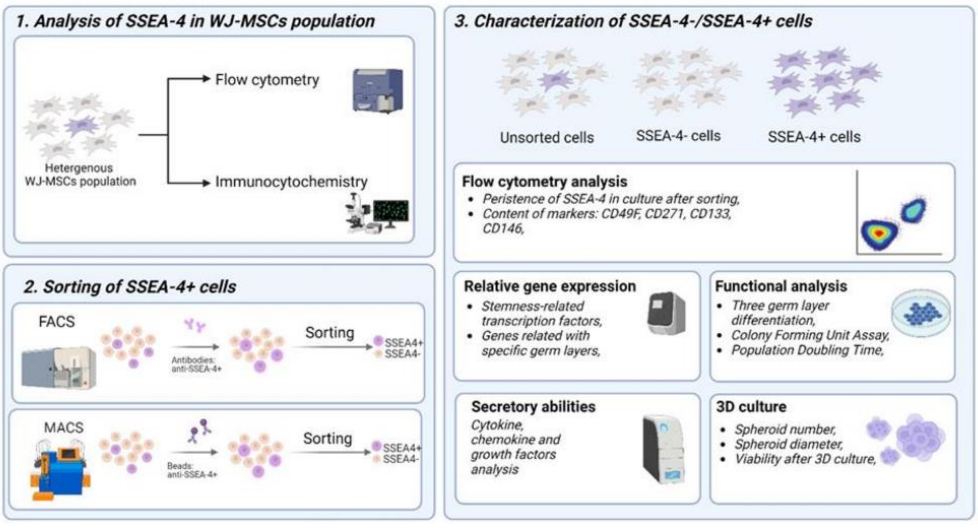

2

Supplementary Figure 1. General overview of experimental steps. First, SSEA-4 expression was analyzed within WJ-MSCs population. Then, two separation methods, Fluorescence Activated Cell Sorting (FACS) and Magnetic Activated Cell Sorting (MACS), were compared. Finally, SSEA-4+ population was characterized in comparison to the initial unsorted population and the negative population. The figure was created in BioRender (assessed date: 10.07.2023).

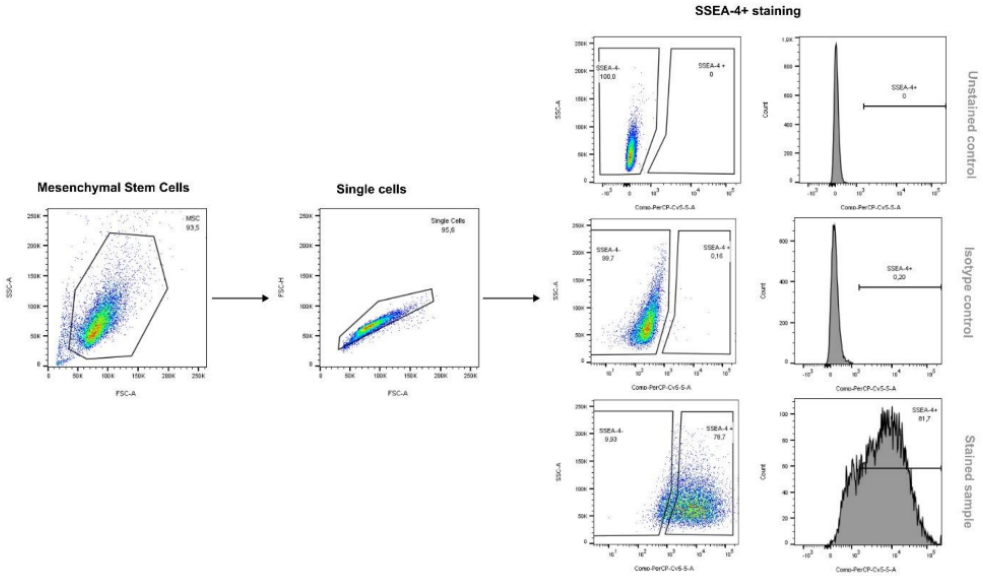

Supplementary Figure 2. Strategy gating for detection of SSEA-4+ cells in WJ-MSCs for unstained control, isotype control and stained sample; flow cytometry, FACSCanto II.

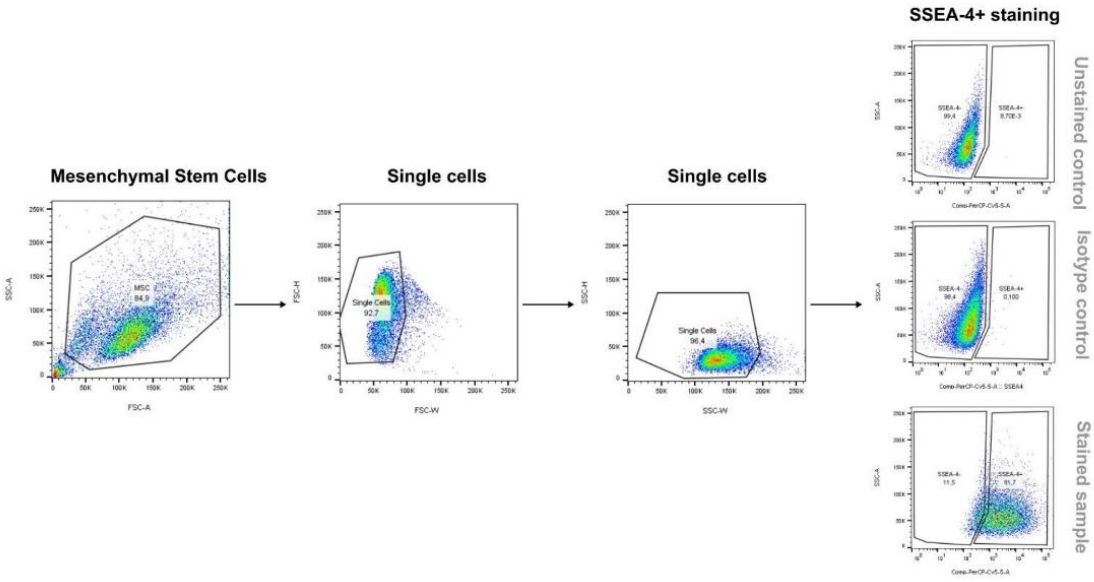

Supplementary Figure 3. Strategy gating for sorting of SSEA-4+ cells in WJ-MSCs for unstained control, isotype control and stained sample; flow cytometry, FACSAria II.

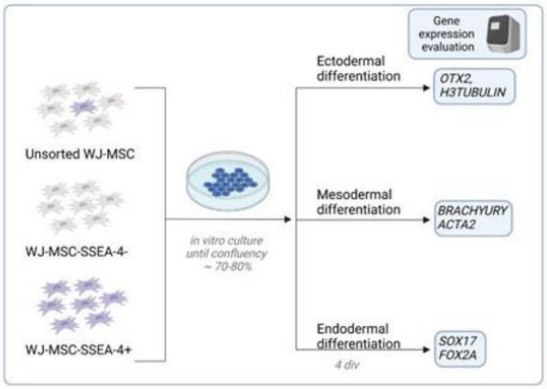

Supplementary Figure 4. Scheme of 3 germ layer differentiation. Cells from different variants were cultured until 70-80% confluency and then, culture medium was replaced with specific differentiation media. Then, the cells were cultured for 4 days in vitro (div) and then RNA was collected for gene expression analysis.

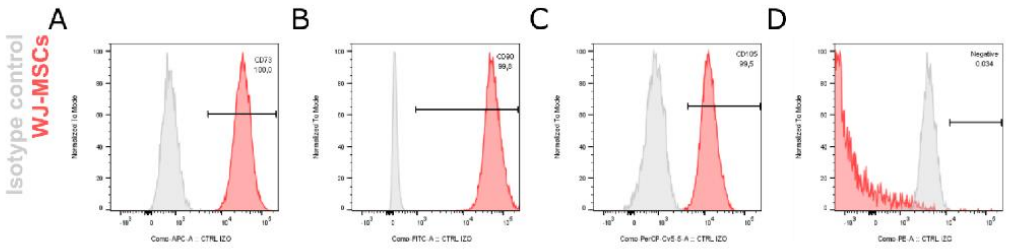

Supplementary Figure 5. Flow cytometry analysis of surface antigens recommended by *The International Society for Cellular Therapy* for MSCs characteristics – CD73 (A), CD90 (B), CD105 (C) and negative mix (CD11b, CD19, CD34, CD45 and HLA-DR).

Supplementary Table 2. Expression of surface antigens recommended by *The International Society for Cellular Therapy* for MSCs characteristics

Marker	Positive cells, % Mean	Standard deviation
CD73	99.7	0.40
CD90	99.8	0.08
CD105	97.4	1.90
CD11b, CD19, CD34, CD45, HLA-DR	0.2	0.26

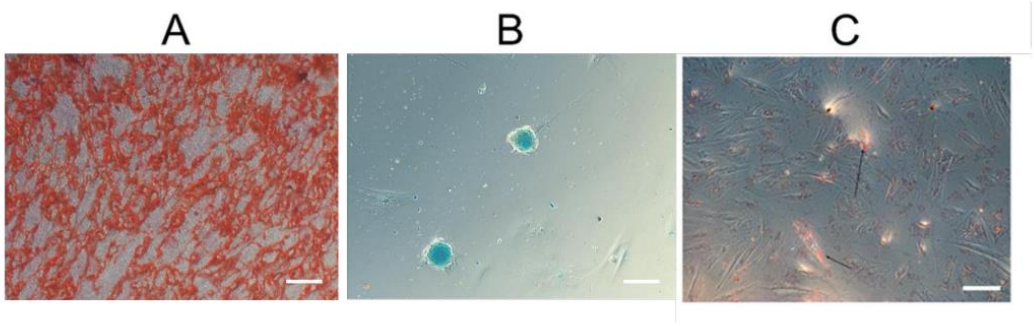

Supplementary Figure 6. Multipotent differentiation of WJ-MSC toward osteocytes (A), chondrocytes (B) and adipocytes (C). A. Calcium deposits characteristic for osteocytes were identified with alizarin red. B. Glycosaminoglycans characteristic for chondrocytes were identified with alcian blue. C. Lipid drops (black arrows) characteristic for adipocytes were identified with red oil. Scale bars: 100 µm.

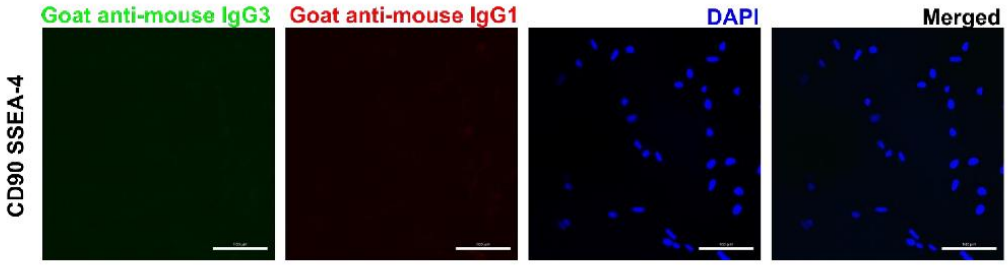

Supplementary Figure 7. Secondary antibody staining controls for Fig. 2.A. Following secondary antibodies were applied: goat anti-mouse IgG3 conjugated with Alexa Fluor 488 for SSEA-4, goat anti-mouse IgG1 conjugated with 546 for CD90. Cell nuclei were stained with DAPI. Scale bars: 100 µm.

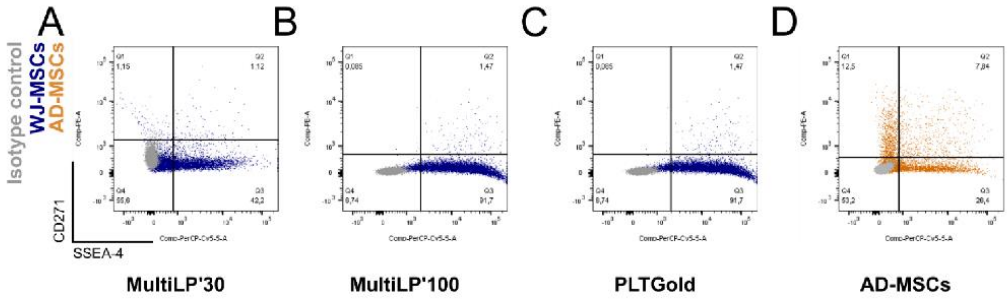

Supplementary Figure 8. SSEA-4 and CD271 coexpression, flow cytometry analysis. WJ-MSCs were cultured with following platelet lysates: MultiLP'30 (A) , MultiLP'100 (B) and PLTGold (C). AD-MSCs were cultured in PLTGold platelet lysate.

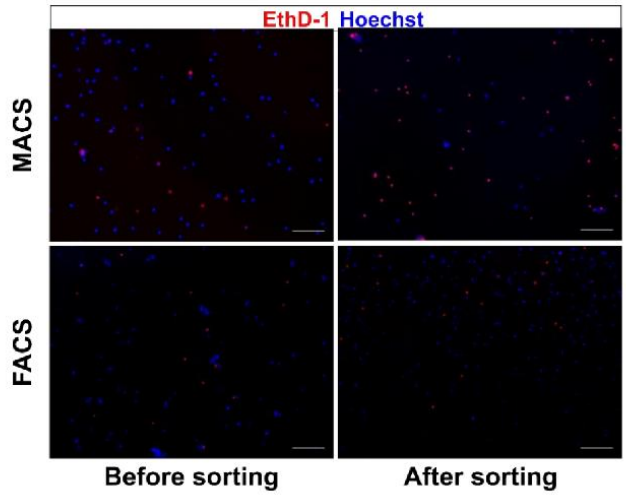

Supplementary Figure 9. Ethidium homodimer-1 (EthD-1) mortality staining for cells before and after cell sorting with MACS and FACS. Cell nuclei were stained with DAPI. Scale bars: 100 µm.

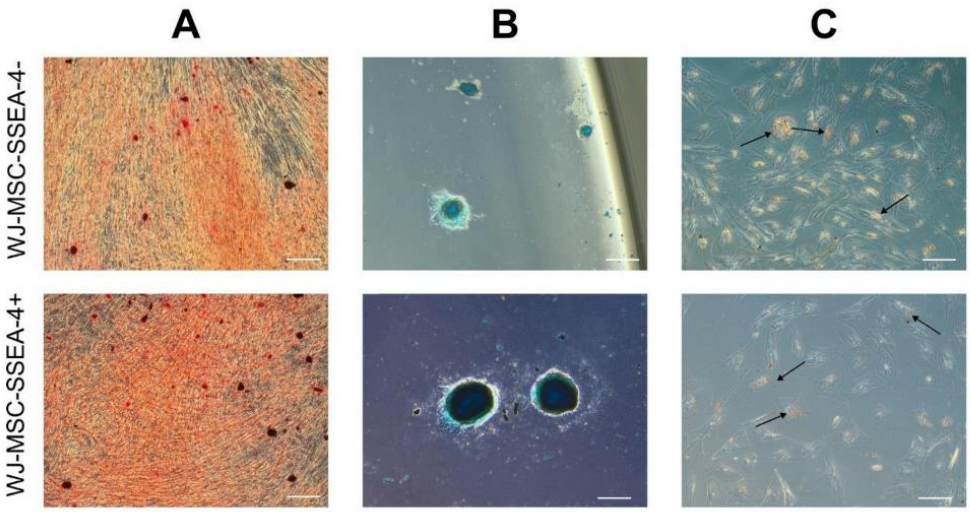

Supplementary Figure 10. Multipotent differentiation of SSEA-4 negative (WJ-MSC-SSEA-4-) and SSEA-4 positive WJ-MSC (WJ-MSC-SSEA-4+) populations toward osteocytes (A), chondrocytes (B) and adipocytes (C). Scale bars: 100 µm.

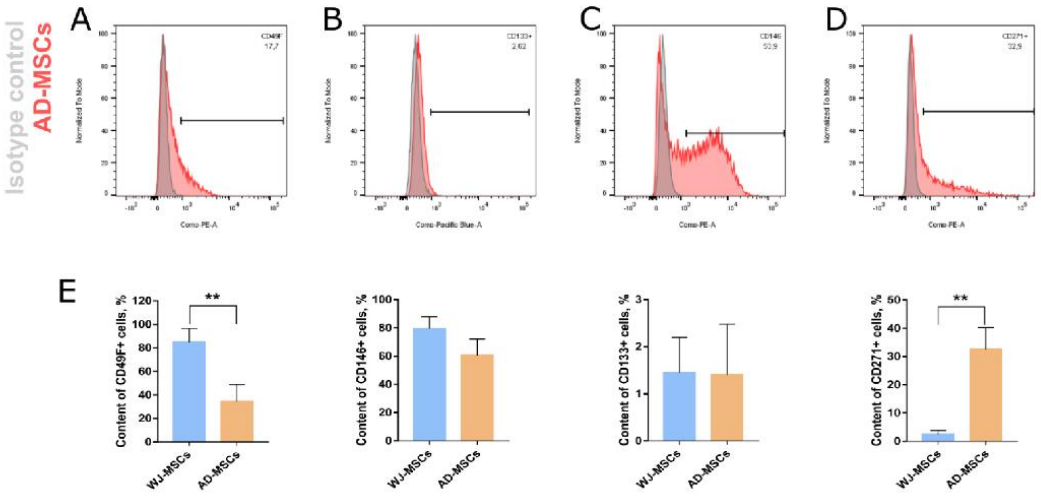

Supplementary Figure 11. Expression of surface antigens CD49F (A), CD133 (B), CD146 (C) and CD271 (D) for AD-MSCs; flow cytometry. (E) Expression comparison of CD49F, CD133, CD146 and

CD271 between WJ-MSCs and Adipose derived MSC (AD-MSCs). The results are presented as mean values of 3 experiments ± SD. P-value for ** <0.01,

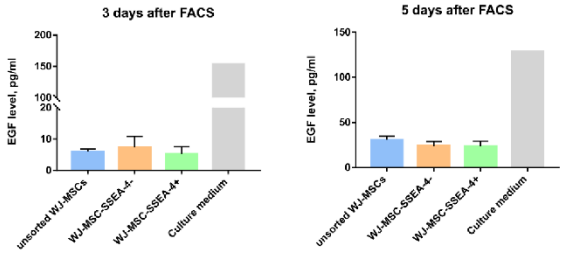

Supplementary Figure 12. EGF secretion analysis in 3rd and 5th day in vitro after FACS sorting for unsorted WJ-MSCs, negative population (WJ-MSC-SSEA-4-), positive population (WJ-MSC-SSEA-4+) and in culture medium. EGF levels detected during cell culture were below levels detected in culture medium.

11.3. Artykuł III

Hindawi
Stem Cells International
Volume 2023, Article ID 1842958, 21 pages
https://doi.org/10.1155/2023/1842958

Review Article

Promising Markers in the Context of Mesenchymal Stem/Stromal Cells Subpopulations with Unique Properties

Agnieszka Smolinska, Aleksandra Bzinkowska, Paulina Rybkowska, Magdalena Chodkowska, and Anna Sarnowska

Translational Platform for Regenerative Medicine, Mossakowski Medical Research Institute, Polish Academy of Sciences, 02-106, Warsaw, Poland

Correspondence should be addressed to Anna Sarnowska; a_sarnowska@tlen.pl

Agnieszka Smolinska and Aleksandra Bzinkowska contributed equally to this work.

Received 3 April 2023; Revised 11 August 2023; Accepted 25 August 2023; Published 20 September 2023

Academic Editor: Pasquale Marrazzo

The heterogeneity of the mesenchymal stem/stromal cells (MSCs) population poses a challenge to researchers and clinicians, especially those observed at the population level. What is more, the lack of precise evidences regarding MSCs developmental origin even further complicate this issue. As the available evidences indicate several possible pathways of MSCs formation, this diverse origin may be reflected in the unique subsets of cells found within the MSCs population. Such populations differ in specialization degree, proliferation, and immunomodulatory properties or exhibit other additional properties such as increased angiogenesis capacity. In this review article, we attempted to identify such outstanding populations according to the specific surface antigens or intracellular markers. Described groups were characterized depending on their specialization and potential therapeutic application. The reports presented here cover a wide variety of properties found in the recent literature, which is quite scarce for many candidates mentioned in this article. Even though the collected information would allow for better targeting of specific subpopulations in regenerative medicine to increase the effectiveness of MSC-based therapies.

1. Introduction

Mesenchymal stem/stromal cells (MSCs) attract an interest of researchers due to their wide potential applications in medicine. Multiple therapeutic properties of MSCs are thoroughly described: differentiation capacities toward mesodermal tissues, secretion of trophic factors supporting regeneration, immunosuppression, and homing functions [1]. Many clinical trials are currently conducted to confirm the safety and efficacy of MSCs treatment [1]. However, a lot of proposed therapies did not proceed to registration in the pharmaceutical market due to small success in preclinical studies or lack of progress in later stages of clinical trials [2]. A possible explanation for the insufficient efficiency of MSCs application in human studies is suggested by several causes; heterogeneity is one of them [2, 3].

MSCs heterogeneity is explored at multiple levels; variability between cells derived from different donors, sources, and isolation methods are listed as an extrinsic causes [4–6]. Even the complexity of the tissue could affect the properties of MSCs. Although the overall characteristic remains similar, the cells from different isolation sites may differ in more specific functions such as factors secretion, differentiation potential, or immunomodulatory properties, which was described for MSC isolated from adult tissues such as bone marrow or adipose tissue [7, 8]. In terms of perinatal tissues, it should be noted that even MSC of maternal and fetal origin influenced cell characteristics, such as osteogenic potential, proliferation, and immunomodulatory properties [9–11]. The variety of culture conditions and medium compositions amplifies the heterogeneity issue—applied methods differ even between good manufacturing practice facilities [12]. Described factors could be minimized with standardization of protocols and better criteria for the choice of cell source and donor, but the internal heterogeneity poses a more complex problem to solve. The development of multiomic approaches realized that many

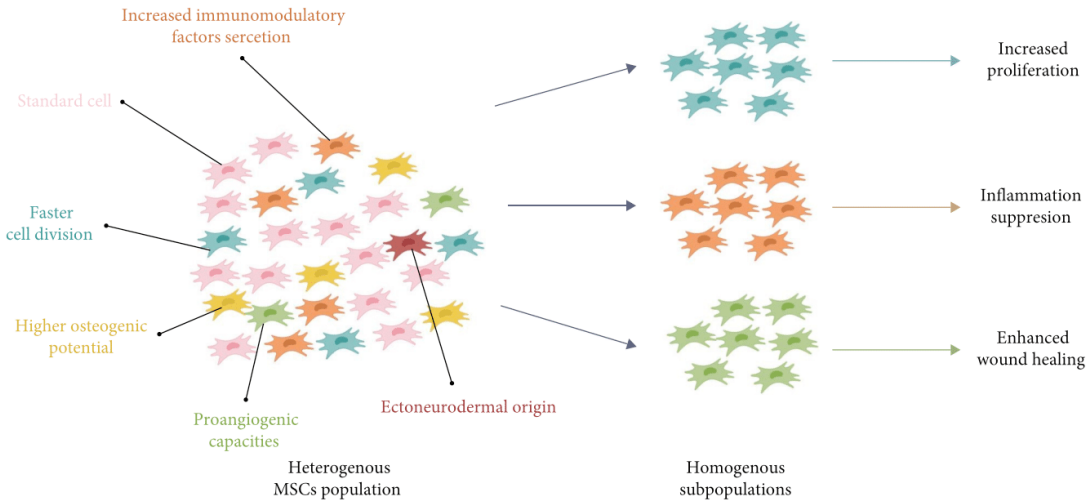

FIGURE 1: Heterogenous vs. homogenous MSCs population. MSCs population consist of distinct clones that could be separated, expanded in *in vitro* culture and applied for more specific therapeutic purposes.

subpopulations sharing distinct gene expression profiles might exist within one population [13]. Multicolor barcode labeling revealed that the apparently homogenous MSCs population consists of several subpopulations [14]. Heterogeneity observed *in vitro* could be a result of heterogeneity *in vivo*, caused potentially by numerous mechanisms such as phenotype plasticity, transcriptional fluctuations in gene expression, proliferation ratios of different clones, and cellular senescence [15], and probably imperative one: the diverse origin of MSCs cells.

Except the identification of MSCs in a fetal liver in 7-week human embryo [16], the earlier stages of MSCs development remain rather enigmatic. Researchers propose several possible pathways of MSC formation. Somatic lateral plate mesoderm (LPM) is suggested as a major source of MSCs cells, mainly based on the described exhibition of specific markers and differentiation directions [17]. During the development, cells located in the LPM layer as a result of the epithelial-to-mesenchymal transition (EMT), originally constituting as a homogeneous population. Then, LPM cells undergo the reverse process—the mesenchymal to epithelial transition. Many cells go through multiple rounds of EMT/MET before the acquisition of their final differentiation state, adding to the complexity of the LPM environment [17]. Part of MSCs could be derived from vascular endothelial cells through the EMT process [16]. Partial origin from another germ layer is also not excluded—neural crest, a transient structure located at the neural tube, also contributes to the MSCs' origin [16–18]. Neural crest-derived stem cells undergo EMT processes, resulting in their delamination and migration to further tissues [18]—they are found in neural and nonneural tissues—craniofacial skeleton and adipose tissue are listed as one of them [18]. Potential neuroectodermal origin could explain the observed neuronal and glial markers expression by MSCs from different sources [19, 20].

The different possible origins of the cells from the heterogeneous MSCs population constitute the variety exhibited therapeutic properties such as differentiation potential, proliferation rate, secretory profile, or angiogenesis capacity (Figure 1). Among MSCs, there could be found clones showing different degrees of specialization—from line-specific progenitors to the undifferentiated stem cells that give arise into cells from all three germ layers [21, 22]. Application of selected subpopulations could increase the therapeutic efficiency and reduce observed discrepancies. However, the optimal strategy for identifying potential promising subpopulations from other morphologically similar cells still remains to be explored.

The main aim of this review is to collect available information about markers suggesting the distinct subpopulations existing within the heterogeneous MSCs population. Here, we specified two groups of markers, depending on the application: those suggesting the stem, undifferentiated character of the population, and those indicating more specified progenitors. The first group would enhance cellular therapies by providing a pool of self-renewal, proliferating stem cells. The second group could be helpful in more specific areas of regenerative medicine, such as wound healing, proangiogenesis, or anti-inflammatory agents. Expression of described markers could depend on different factors—culture condition and media composition, source of origin, donors' age and/or gender, and even more specific intercellular interactions such as a phase of the cell cycle [23]. We decided not only to compile a recent literature in this topic but also to incorporate and refresh some older evidences that could be lost and forgotten among the plethora of reports in MSCs topic.

2. Markers for Stem Population within MSCs

Highly heterogenous MSCs population contains subsets of cells exhibiting different stages of differentiation—stem-like cells, multipotent progenitors, and more differentiated precursors [24].

The selection of a genuine stem cell population could improve the manufacturing of MSCs. Some authors proposed even existence of pluripotent-like stem cells that would exhibit expression of characteristic genes (Oct4, Sox2, Nanog, etc.) and differentiation toward cells from all three germ layers [22]. In the topic of the search for a universal stem cell, there are still many uncertainties to be resolved, especially in the understanding of intracellular mechanisms. According to recent reports, even the phase of the cell cycle can influence the potential for cell differentiation [23]. In this section, we will focus on markers predicting the potential stem character of subpopulations. We have gathered here the information on the availability of the described subpopulations in MSC tissues (Table 1) and their observed properties (Table 2).

2.1. SSEA-3. Specific stage embryonic antigens (SSEA) are glycosphingolipids appearing during embryonic development. SSEA3 and SSEA4 especially aroused the researchers' interest. Both antigens occur in an earlier stage of mouse embryonic development—SSEA3 peaks in the 2–8 cell stage, while SSEA4 in the morula [56]—and then disappears [57]. For human embryos, SSEA3 and SSEA4 are detected after blastocyst formation and only in inner cell mass [57]. Although SSEA3 and SSEA4 are found on the surface of embryonic stem cells (ESCs) [58, 59] and induced pluripotent stem cells [60], their association with pluripotency is discussed. Knockout of gene B3GALT5, involved in SSEA-3/4 synthesis, drived human ESCs from primed toward naive pluripotent state [61], while iPSCs were successfully established from fibroblasts derived from SSEA3/4-depleted mice [62].

SSEA-3+ population is rather sparse within MSCs; its percentage fluctuates around 5%, depending on the sources (Table 1). SSEA-3+ cells were identified for bone marrow, adipose tissue, Wharton Jelly, and dermis [42–45, 63, 64]. Long exposition to tripsine, as well as sphere-inducing conditions, seemed to increase the SSEA-3+ cell percentage in the MSCs population [65], while a higher concentration of FBS in media decreased the SSEA-3 expression in WJ-MSCs [34].

SSEA-3+ MSCs are intensively explored in a topic of MUSE cells—multilineage differentiating stress enduring cells [22]. SSEA-3+-MUSE cells formed spheroids that were self-renewal and exhibited pluripotency—differentiated toward cells from all three germ layers upon *in vitro* culture and after *in vivo* transplantation [21, 42, 43, 66]. SSEA-3+ cells were confirmed to differentiate *in vitro* toward cells from different germ layers, such as insulin-producing cells or neural precursor cells [67, 68]. Blocking SSEA-3 in the MUSE population reduced proliferation, clonogenicity, expression of pluripotent genes SOX2 and OCT3/4, as well as differentiation toward cells from three germ layers [66]. It was suggested that SSEA-3 is involved in stemness maintenance as a coreceptor for a fibroblast growth factor (FGF-2) through the PI3K pathway [66].

The efficiency of SSEA-3+ cells was confirmed also *in vivo* in multiple animal models [52, 68–72]. SSEA-3+-MUSE cells integrated into a host tissue and differentiated into neural cells after transplantation, which facilitated neural reconstruction in an animal model of lacunar stroke [72]. A similar effect was observed in the animal model of liver fibrosis and in human liver transplantation—transplanted cells integrated into a regenerated area and spontaneously differentiated into cells associated with major liver components [52, 73]. Differentiation toward specific tissues was observed in the treatment of aneurysm and acute myocardial infarction [71, 74]. Despite different places of cell injection tested in preclinical studies, MUSE cells were identified mostly in the damaged tissues due to their unique homing capacity [52, 71]. Injection of SSEA-3+ cells was safe—no tumors nor adverse effects occurred during the long-term follow-up period [52, 72, 75]. Human trials involving patients with myocardial infarction showed the efficiency and safety of intravenous administration of MUSE cells [76]. Currently, the phase 1 clinical trial is evaluating the safety and tolerance of MUSE cells in the treatment of neonatal hypoxic encephalopathy (NCT04261335) [77].

2.2. SSEA-4. SSEA-4 is synthesized from SSEA-3 by ST3GAL2-enzyme β-galactoside α2,3-sialyltransferase 2 [78], and its structure contains terminal sialic acid [78]. SSEA-4+ population within MSCs is more numerous than SSEA-3, but still, different authors report different values (Table 1). SSEA-4 numbers depend on the culture medium composition [34], source of tissue [29], and donor's age [31] or gender [46]. Neonatal tissues appeared to be more abundant in SSEA-4+ cells source of MSCs than adult tissues [29] (in submission). Long-term culture as neurospheres increased the content of SSEA-4+ cells [79].

SSEA-4 was proposed as a marker to distinguish physiologically younger cells within a population obtained from elderly donors [80]. However, it is debated whether SSEA-4 is genuinely a stemness marker. Rosu-Mylers et al. [54] reported higher proliferation ratios and colony-forming capacities of SSEA-4+ cells. SSEA-4+ cells exhibited better adipogenic differentiation [33], while SSEA-4+ cells from adipose-derived MSC (AD-MSCs) generated mature endothelial cells with microvascular patterns [81]. Other authors did not observe any differences in proliferation ratio, pluripotency genes expression, and osteogenic and adipogenic differentiation between SSEA-4+ and SSEA-4− cells [34]. Interestingly, we observed increased expression of genes associated with pluripotent cells and early neuroglial cells directly after cell sorting, but it returned to the previous state after further *in vitro* culture. Similarly to He et al. [34], our group did not observe changes in proliferation and clonogenicity (in submission). So far, studies targeting SSEA-4 in MSCs population have not progressed beyond the *in vitro* phase. Despite potential embryonic origin, provided biased evidences impede classification whether SSEA-4+ subpopulation outstands from the heterogenous MSCs population.

2.3. CD271. CD271, also known as low-affinity nerve growth factor (NGF) receptor or p75NTR, is a neurotrophin receptor binding NGF, brain-derived neurotrophic factor (BDNF), neurotrophin-3 and 4 as well as precursors: proNGF and proBDNF [82–84]. CD271 plays a role in neurotrophins

Table 1: Expression of markers for potential stem cells in different MSC sources.

Marker	MSCs source	% of cells	Comments	Reference
CD49f	BM	(1) 66.5 (2) 11	(1) Fetal BM (2) Adult BM -Loss CD49f expression during culture -Differences between donors	[25]
CD49f	BM	22.2%	-Passage 1 -Loss during culture passages -Differences between sources	[26]
CD49f	DM	6.68	-Passage 0 -Together with CD146 high expression	[27]
CD49f	(1) mouse AT (2) rat AT	(1): 17.7 (2): 27.2	-Passage 2 -CD49f expression decreased after TNF and IFN treatment -CD49f expression decreased with passage number	[28]
CD133	AT	12		[29]
CD133	BM	15		[29]
CD133	WJ	Less than 2		[29]
CD271	AFC	Less than 0.5		[30]
CD271	AT	8.4		[30]
CD271	AT	5		[29]
CD271	BM	(1) 22.3 (2) 10.1	(1) Young donors (2) Elderly donors	[31]
CD271	BM	3.7		[30]
CD271	BM	8		[29]
CD271	BM	1.9	Organism: mouse	[32]
CD271	CB	Less than 0.5		[30]
CD271	DM	5.5		[33]
CD271	PVC	Less than 0.5		[30]
CD271	WJ	Less than 0.5		[30]
CD271	WJ	Less than 1		[34]
CD271	WJ	2		[29]
CD349	PL	20–58	-Site of isolation: chorion laeve tissue -Expression differences between clones -Loss of MSC markers -Together with negative CD271 expression	[35]
CD349	PL	0.2	-Site of isolation not specified, -Together with Nanog, Oct4 and SSEA4 upregulation	[36]
GD2	BM, adult	(1) ~55 (2) ~35	(1) Passage 2, cell culture in AB-HS (2) Passage 2, cell culture in FBS	[37]
GD2	AT	46.7	–	[38]
GD2	BM	95	Passage 2, cells $CD45^{-}$ $CD105^{+}CD73^{+}$, maintained expression for 8 passages	[39]
GD2	BM, fetal	(1) ~88 (2) ~65	(1) Passage 2, cell culture in AB-HS (2) Passage 2, cell culture in FBS	[37]
GD2	BM	63.4–73.9	-Organism: mouse, -Passage 2, expression differed between mouse strains	[40]
GD2	UC	(1) ~38 (2) ~18	(1) Passage 2, cell culture with AB-HS (2) Passage 2, cell culture in FBS	[37]
Sca-1	BM	(1) 4 (2) 0.5	(1) Compact bone marrow (2) Flushed bone marrow	[41]
SSEA-3	Mouse AT	6.3		[42]
SSEA-3	AT	3.2		[43]
SSEA-3	AT	8.8		[21]

Table 1: Continued.

Marker	MSCs source	% of cells	Comments	Reference
SSEA-3	AT	1.9		[44]
SSEA-3	BM	5.3		[45]
SSEA-3	WJ (explant)	(1) 6.7 (2) 6.1	(1) Explant isolation, passage 0 (2) Enzymatic isolation, passage 0	[34]
SSEA-4	AT	10		[29]
SSEA-4	BM	(1) 5.2 (2) 4	(1) Young donors (2) Elderly donors	[31]
SSEA-4	BM	(1) 72 (2) 79.8	(1) Females (2) Males	[46]
SSEA-4	BM	55		[29]
SSEA-4	DM	5.6		[33]
SSEA-4	WJ	(1) 32.4 (2) 26.1	(1) Explant isolation, passage 0 (2) Enzymatic isolation, passage 0	[34]
SSEA-4	WJ	60		[29]
SSEA-4	WJ	(1) 35% (2) 70%–74%	Used different human platelet lysates: (1) with lower concentration of factors, (2) with higher concentration of factors.	In submission

Note: ∼: approximately, AB-HS: human AB serum, AFC: amniotic fluid, AT: adipose tissue, BM: bone marrow, CB: cord blood, DM: dermis, FBS: fetal bovine serum, IFN: interferon, PL: placenta, PVC: perivascular compartment of umbilical cord, TNF: tumor necrosis factor, UC: umbilical cord, WJ: Wharton Jelly. *Source of MSCs: human, unless otherwise stated.*

response and regulates apoptosis, cell survival, proliferation, and differentiation [84, 85]. CD271+ cells were isolated from fetal peripheral nerves [86] as well as the human adult subventricular zone [87]. CD271 is associated with neural crest-derived stem cells that migrated to different tissues during EMT [88, 89]. Interestingly, CD271 expression could be induced even earlier during development, as it was found in the murine inner cell mass of blastocyst before implantation [90].

Isolated CD271+ cells differentiated differentiation into neurons and glial cells *in vitro* and *in vivo* [86, 87]. Deletion of CD271 within sensory neurons in mice resulted in the loss of neurons that started during embryonic development and continued until adulthood [91], while CD271-depleted mice displayed a reduction in sciatic nerves and abnormal hind limb reflexes [92].

CD271+ cells were found in mesenchymal tissues, indicating a partial neural crest origin of MSCs [93, 94]. Although adult tissues contain more CD271+ cells, the subpopulation derived from fetal and neonatal tissues is more stable and decreases less rapidly with passage number than CD271+ cells in MSCs from adult tissues [30] (Table 1). Described properties of CD271+ MSCs suggest that this marker could indicate the pool of genuine stem cells that differ in embryonic origin. CD271+ MSCs differed from the rest of the heterogenous population; they proliferated more rapidly [31, 47], formed more colonies [30, 47], formed spheres, and expressed pluripotent and neural genes at higher levels [31, 48] (Table 2). Although its potential ectoneural origin, evidences for CD271+ cells from MSCs differentiation toward neurons and glial cells are lacking. Indeed, if those cells did possess this ability, they could provide an alternative source for neuron-like cells in regenerative medicine. However, according to Sowa et al. [93], a huge pool of CD271 cells found within AD-MSCs may not originate from the neural crest.

2.4. CD49F. The CD49f protein, also known as integrin a6 (ITG6), is a transmembrane receptor consisting of two subunits: α and β. Each subunit plays a different function, but the exact roles remain unknown. It has been found on the surface of many different stem cells' populations, such as primordial germ cells, keratinocyte stem cells, hematopoietic stem cells (HSCs), ESCs, cancer stem cells, and MSCs [95]. The principal function of the integrins family is to adhere to the extracellular matrix ligands, such as laminin, collagens, and fibronectin, and together with the tyrosine kinases, provide signals between the external and intracellular environment of the cells. The CD49f protein itself regulates the cells' interaction with the extracellular environment and mediates cell-to-cell adhesion. CD49f is considered to be a highly conservative biomarker of early-stage stem cells that is involved in their self-renewal maintenance.

The amount of CD49f marker in MSCs varies depending on the cells' source (Table 1). The highest number of CD49f-positive cells was found in BM-MSCs. Yang et al. [25] discovered that the younger the MSC cells, the higher the expression of CD49f. Their study revealed that fetal cells expressed 66.5% of the CD49f marker, while adult cells had only 11%. Moreover, during the cell culture and passage number, a gradual decrease of CD49f-positive cells was observed, from 74.8% in passage 2%–4.88% in passage 10. Interestingly, when the CD49f-positive population was sorted by fluorescence-activated cell sorting (FACS), they observed the quick loss of CD49f expression shortly after culture, from 95.2% to 48.7%. The Yang et al. [25] research also revealed better clonogenic potential of CD49f-positive cells and enhanced osteogenic differentiation. However, the

Table 2: Properties of subpopulations separated from MSC tissues.

Marker	Sorting method	Effect	Reference
CD49f	FACS	↑ Clonogenity, ↑ proliferation, ↑ migration, ↑ multilineage differentiation,	[26]
CD49f	FACS	↑ Colony forming, ↑ adipogenic and osteogenic differentiation	[25]
CD49f	FASC	↑ Self-renewal, ↑ spheres formation, ↑ adipogenic and osteogenic differentiation	[27]
CD49f	MASC	↑ Adhesion, ↑ proliferation, ↑ adipogenic and osteogenic differentiation, ↑ migration, ↑ antiapoptotic potential	[28]
CD271	FACS	↑ Clonogenicity, ↑ osteogenic differentiation	[30]
CD271	FACS	↑ Proliferation,	[31]
CD271	FACS	↑ Proliferation, ↓ osteogenic and adipose differentiation	[47]
CD271	MACS	↑ Neuronal and glial differentiation, ↑ migration toward islets and islet-like cell clusters	[32]
CD271	MACS	↑ Pluripotent genes expression	[48]
CD271	MACS	No changes in multipotent differentiation *in vitro*, ↑ osteochondral repair *in vivo*, ↓ angiogenesis *in vitro* and *in vivo*	[49]
CD271	MACS	↑ Adipogenesis, chondrogenesis, osteogenesis	[33]
CD349	FACS	↓ Angiogenic-properties, ↓ vasculogenesis, ↓ re-endothelialization, similar osteogenic differentiation potential	[35]
CD349	FASC	↑ Clonogenicity, ↑ multi-lineage differentiation	[36]
GD2	FACS	↑ Clonogenicity, ↑ proliferation, ↑ adipogenesis, ↑ osteogenesis, ↑ gene expression: LPL, adipsin, collagen I, CBFA1, OC, ↑ content of positive cells: Sca-1+, CD105+, SSEA-1+, Nanog+, ↓ content of positive cells: CD34+, C-kit+, CD45+, CD11b+	[40]
GD2	MACS	↑ Clonogenicity, ↑ colony size, ↑ proliferation, ↑ gene expression: SSEA-4, Oct-4, Sox-2, Nanog, Nestin, GFAP, NSE, ↑ adipogenesis, ↑ osteogenesis	[37]
Sca-1	FACS	↑ Clonogenicity, ↑ gene expression: NANOG, TERT, BMP2, Myf5, ↓ chondrogenesis, ↓ gene expression: Col2a1	[41]
Sca-1	FACS	↑ Clonogenicity	[50]
Sca-1	FCAS	↑ Gene expression: Eng (CD105), ↓ gene expression: IL-6, Pdgfra, Ly6a, Itgb1, Itga5, CD44, Thy1(CD90)	[51]

Table 2: Continued.

Marker	Sorting method	Effect	Reference
SSEA-3	FACS	↑ Differentiation into insulin-producing cells, ↑ pluripotent genes expression	[43]
SSEA-3	FACS	↑ Migration toward injured liver cells, ↑ restoration of liver function in liver fibrosis model, ↑ *in vivo* spontaneous differentiation into hepatocyte	[52]
SSEA-3	FACS	↑ Sphere formation	[22]
SSEA-3	FACS	↑ Sphere formation, ↑ pluripotency, ↑ spontaneous expression and expression after differentiation of markers from three germ layers	[21]
SSEA-3	FACS	Better biodistribution, ↑ motor and cognitive functions of HIE rats	[45]
SSEA-3	FACS, MACS	Similar effects observed in both sorting methods ↑ sphere formation, ↑ pluripotency, ↑ neural differentiation	[42]
SSEA-3	MACS	↓ Apoptosis and senescence after UV or H_2O_2 treatment, ↑ activation of damage repair system of DNA via non-homologous end joining	[53]
SSEA-3	MACS	↑ Pluripotent genes expression	[48]
SSEA-3	MACS	↑ Expression and secretion of growth factors, ↑ pluripotency gene expression, ↑ increased wound healing of skin ulcers	[44]
SSEA-4	FACS	No differences in proliferation, pluripotency genes expression, osteogenic differentiation, adipogenic differentiation	[34]
SSEA-4	FACS	↑ Clonogenicity, ↑ proliferation	[54]
SSEA-4	FACS	↑ Pluripotency and neural gene expression, ↑ viability of spheres, smaller spheres formed, no differences in proliferation and clonogenicity	In submission
SSEA-4	MACS	↑ Adipogenesis	[33]
SSEA-4 CD271	FACS	↑ Proliferation	[31]
SSEA-4 CD271	FACS	↑ Clonogenicity, ↓ adipogenesis	[55]

Note: FACS: fluorescence-activated cell sorting, MACS: magnetic activated cell sorting, HIE: hypoxic-ischemic encephalopathy.

influence of cytokines such as TNF-α on BM-MSC showed that the inflammatory environment downregulated CD49f expression, decreased adhesion ability, disturbed differentiation potential, and increased migration. In the following years, the same team successfully obtained the CD49f-positive cell population from the dermis stem cells. The isolated CD49f-high population was characterized by the presence of fibroblast markers (*Col1a1* and *Vimentin*), the ability to form spheres, and higher differentiation potential towards mesenchymal and neural lineages. Their results also provided evidence that CD49f-high cells isolated from the dermis may have neural-crest origins or may be progenitor stem cells [27].

Zha et al. [28] found that CD49f expression differed between mouse and rat AD-MSCs; mouse AD-MSCs contained 17.7% of CD49f+ cells, while rat AD-MSCs –27.2%. They also observed a gradual loss of the CD49f marker's presence during subsequent passages. After induction of the inflammatory environment and cells incubation with TNF-α and IFN-γ, a reduction in the number of CD49f markers was observed, but the cells adhesion capacity was elevated due to upregulated VCAM-1 expression. Sorted CD49f-positive AD-MSCs were characterized by increased proliferation potential, higher multilineage differentiation ability, and antiapoptotic capabilities compared to unsorted AD-MSCs.

The diversity of CD49f marker presence was also described in the work of Nieto-Nikolau et al. [26], where the different donors of bone marrow stem cells were taken under consideration. In the work of this group, they obtained 22.17%, 25.5%, and 8.65% of CD49f-positive cells isolated from different sources. Moreover, like the previous groups, they also observed a gradual loss of the marker with successive passages and similarly increased clonogenicity, migration, and differentiation potential. In addition, they found

that with the lower the cell confluence expression of CD49f was higher, which may confirm the microenvironmental regulation of this integrin. They also showed that spheroid-derived MSC expressed higher amounts of CD49f together with higher proliferation, migration, and colony-forming efficiency that may be correlated, in their view, with the number of progenitor cells in MSC cultures. Earlier, another group came to similar conclusions; they proved that the sphere-forming MSC cells are rich in CD49f marker together with stemness genes expression of *NANOG*, *SOX2*, and *OCT4* compared to cells cultured in monolayer form. Therefore, CD49f may regulate the sphere-forming ability and stemness maintenance in MSC, and this regulation may be correlated with the activation of the PI3K/AKT signaling pathway [96].

In conclusion, the presented studies consistently show that the expression of the CD49f marker in MSCs is sensitive to environmental changes, such as induction of the inflammatory environment; moreover, it is also regulated by cell growth and confluence and lost during cell senescence. The results of the presented studies are consistent in terms of increased proliferation, differentiation, clonogenicity of CD49f-positive cells, and their ability to form spheres. However, the relationship between CD49f marker expression and elevated pluripotency markers for the maintenance of stemness and regulation of self-renewal needs to be thoroughly investigated.

2.5. GD2. GD2, a neural ganglioside, was identified in cells of the nervous system [39] and in MSCs derived from various sources: bone marrow, umbilical cord, and adipose tissue [37–40]. Its overexpression is characterized by different neuroectoderm-derived tumors related to tumor progression and metastatic potential [97].

The level of expression GD2 in MSCs fluctuated between 18% and 95%, depending on the source, culture conditions, and mouse inbred [37–40]. Martinez et al. [39] demonstrated that both BM-MSCs and AD-MSCs were characterized by the similar expression of GD2 –95%. However, the other research group reported that far less AD-MSCs expressed GD2—only 46.7%. MSCs cultured in AB-HS (human AB serum) were characterized by a higher percentage of $GD2^+$ cells than MSCs cultured in FBS [37]. It's also worth noting that $GD2^+$ percent in ADM-MSCs decreased from 46.7% to 31.4% or 23% when cells were cultured for 30 days in medium coming from cell culture of human glioblastoma multiforme cell line 8MGBA or A375 [38].

Sorted population of murine BM-MSCs $GD2^+$ characterized higher percentage of positive cells of markers: $Sca\text{-}1^+$ (stem cells antigen-1), $CD105^+$, $SSEA\text{-}1^+$, $Nanog^+$, and lower percentage of positive cells: $CD34^+$, $C\text{-}kit^+$, $CD45^+$, and $CD11b^+$ [40]. $GD2^+$ cells from both murine BM-MSCs and umbilical cord MSCs (UC-MSCs) showed higher clonogenicity, proliferation, ability to adipogenesis and osteogenesis [37, 40]. Coexpression of $Sca\text{-}1^+$, $CD105^+$, $SSEA\text{-}1^+$, $Nanog^+$, together with higher clonogenicity and proliferation by GD2+ population suggested that it could be used as a marker for early precursor cells of mouse BM-MSCs [40]. Interestingly, UC-MSCs $GD2^-$ did not display a CFU-F activity [37]. However, more research concerning GD2+ cells within human MSCs are needed to confirm those observations.

2.6. CD349. The CD349, also known as Frizzled-9 (FZD-9), is a member family of seven transmembrane proteins that serve as receptors for Wnt proteins. CD349 is mainly expressed in pericytes, presented on the surface of capillaries and mesenchymal cells surrounding blood vessels [35]. There are also reports that CD349 is expressed on neural progenitor cells in the developing neural tube [98]. It was also shown that CD349 expression may be correlated with SSEA4, Nanog-3, Nestin, and Oct-4 upregulation in placenta-derived MSCs (PL-MSCs), and CD349-positive cells may differentiate into endoderm, mesoderm, and ectoderm cells [99]. Battula et al. [36] also showed that only about 0.2% of PL-MSCs were positive for the CD349 marker, but they had about 60-fold higher clonogenic potential. CD349 marker expression was also found by other groups, in placental decidual MSCs, which may be involved in the vascular niche building [100].

An interesting study was conducted by Tran et al. [35]. They isolated six cell lines from placental chorion leave tissue, described them by surface markers expression, and divided into groups depending on different morphology. The authors examined the CD349 expression, and in the case of two selected populations, they obtained 58% and 20% of CD349-positive cells. They also sorted one of the placental cell populations for CD349-positive and CD349-negative cells and used them in mouse vascular occlusion model experiments. They discovered that the CD349-negative cells more successfully repaired bone injury, recovered blood flow, had better effects on vessel formation, and had a greater ability of re-endothelialization in a mouse model. Interestingly, the CD349-negative population was also shown to upregulate angiogenic factors expression. Tran et al. [35], therefore, suggested that depletion of the CD349 marker may be a promising strategy in angiogenesis and arteriogenesis.

2.7. Sca-1. Sca-1 (stem cell antigen-1) is the mouse's surface protein of *Ly6* gene family [101]. This marker is found on adult cardiac progenitor cells or adult epicardial progenitors and is thought to be of neural crest origin [102]. Confirming these speculations on mice BM-MSC, that population $PDGFR\alpha^+Sca\text{-}1^+CD45^-TER119^-$ expressed markers typical for neural crest such as Twist, CD271, Snail1, Snail2, Sox9 (SRY-Box transcription factor 9), and Mpz (myelin protein zero) [103]. Sca-1 was also shown for murine HSCs, mesenchymal progenitor cells, and murine BM-MSCs [41, 50, 51, 101]. Both mesenchymal progenitor cells and BM-MSCs $Sca\text{-}1^+$ populations exhibited increased clonogenicity [41, 50]. Additionally, a positive population of BM-MSCs exhibited higher gene expression of *Nanog*, *TERT* (*telomerase reverse transcriptase*), *BMP2* (*bone morphogenetic protein 2*), *Myf5* (*myogenic factor 5*), decreased chondrogenesis ability and related to it decreased gene expression of *Col2a1* (*collagen type II alpha 1*). BM-MSCs from compact bone marrow expressed more Sca-1 than those derived from flushed bone marrow. BM-MSCs $Sca\text{-}1^+$ cells showed an increased number of colony-forming units that exhibited greater size at 5% oxygen concentration

Table 3: Expression of markers for more specialized subpopulations in different MSC sources.

Marker	MSC source	% of cells	Comments	Reference
CD142	WJ (explant)	71.2–88	Depending on donors	[109]
CD146	AT	5		[29]
CD146	AT	∼5		[29]
CD146	AT	∼18.9	Semiconfluent culture	[110]
CD146	BM	∼5		[29]
CD146	BM	50.1		[111]
CD146	DM	22		[33]
CD146	DP	38.8		[112]
CD146	WJ	21.8		[29]
CD200	AT	(1) 24% (2) 80%	(1) Subcutaneous fat derived cells (2) Visceral fat derived cells	[113]
CD200	BM	23–63.4	The highest level of CD200 at the density 30×10^3 cells/cm^2	[114]
CD200	PL	(1) ∼70 (2) ∼1.8	Passage 5, (1) fetal PL, (2) maternal PL	[115]
CD317	BM	1–3		[116]
CD317	BM	(1) 28 (2) 1.7	*Two distinct subpopulations: CD317dim (1) and CD317bright (2)*	[117]
Nestin	Kidney	1.1	Nestin-GFP mice	[118]
Nestin	Spleen	0.7	Nestin-GFP mice	[119]
VCAM	AT	0.73	Passage 3	[120]
VCAM	BM	32.04	Passage 3	[120]
VCAM	CV	65.01	Passage 3	[120]
VCAM	CV	62.9		[121]
VCAM	UC	7.44	Passage 3	[120]
VCAM	UC	88	After proinflammatory induction	[122]

Note: ∼: approximately, AT: adipose tissue, BM: bone marrow, CV: chorionic villi, GFP: Green Fluorescence Protein, PL: placenta, UC: umbilical cord, WJ: Wharton Jelly. *Source of MSCs: human, unless otherwise stated.*

than at 21% O_2 concentration, which could be connected with the native location of Sca-1$^+$ cells in the endosteum, where oxygen concentration is lesser. They also observed that the Sca-1 negative population of mouse MSCs did not express Sca-1 at passage 1, but due to positive cell contamination, the Sca-1$^+$ cell number was increased to 90% of the population [41]. BM-MSC-Sca-1$^+$ subpopulation was characterized by a lowered level of CD105, while Sca-1 expression was maintained at a high level for 22 days after sorting [51]. Despite multiple reports of Sca-1 role in murine cells, its human counterpart remains unidentified.

2.8. CD133. CD133 (Prominin) is characteristic of hematopoietic stem cells and neural stem cells (NSCs) and is suggested to identify cancer stem cells [104]. CD133 was found in a small subset of MSCs [29, 105]. CD133+ cells isolated from different sources expressed of some pluripotent genes than heterogenous MSCs population (mostly OCT4 and SOX2) [48]. CD133+ BM-MSCs population was suggested to secrete neuroprotection factors to treat a stroke [106]. However, CD133 properties should be wider confirmed by more research groups to clearly list it as a suitable candidate for genuine stem cell separation.

3. Markers for Specialized Populations within MSCs

Among the populations of MSCs, many subpopulations can be found that share characteristics with other cell types associated with other germ layers. Specific markers may support the targeting of MSCs populations into specialized cells and enhance their differentiation potential [107, 108]. In this section, we will focus on markers predicting therapeutically potential in differentiated tissue such as endothelial, neuronal, or osteocytes. The occurrence and characteristics of described subpopulations are described, respectively, in Table 3 (occurrence) and Table 4 (characteristics).

3.1. CD146. CD146—a melanoma cell adhesion molecule (MCAM) or surface glycoprotein MUC 18—is used as a marker for endothelial cell lineage. CD146 is a transmembrane glycoprotein constitutively expressed on vessel wall of endothelial cells, independently of the vessel type. Studies showed that CD146 was not only an MCAM but also a cellular surface receptor of numerous ligands, participating in several physiological and pathological processes [123].

Table 4: Properties of subpopulations separated from MSC tissues.

Marker	Sorting method	Effect	Reference
CD142	FACS	↑ Gene expression: SPARC, COL4A1, COL1A1, and COL5A1, ↑ "wound healing" potential, ↓ gene expression: MKI67, ↓ proliferation,	[109]
CD146		↑ Proliferation, ↑ immunomodulation, ↑ multilineage differentiation,	[123]
CD146	FACS	No differences in clonogenicity, proliferation, multilineage differentiation, ↑ differentiation in vascular smooth muscle cell	[124]
CD146	FACS	↑ Immunomodulation, ↑ telomere length	[125]
CD146	FACS	↑ Migration towards intervertebral discs, ↑ discogenic differentiation *in vitro*	[126]
CD146	MACS	↑ Adipogenesis, ↑ angiogenesis	[110]
CD146	MACS	↑ Differentiation, ↑ mineralization	[112]
CD200	MoFlo (Dako, Glostrup, Denmark)	↑ Level of αSM-actin protein, ↑ expression of *RUNX2* and *DLX5*, ↑ osteoblastic differentiation	[114]
CD317	FACS	No changes in clonogenicity, smaller cells, ↑ increased IL-7 expression and secretion	[116]
CD317	FACS	↑ Expression of CD54, CXCL10, CXCL11 and CCL2, induction of Th1 phenotype, induction of cutaneous tissue damage of skin explant model of inflammation, no tissue formation when applied in scaffold in immunocompromised mice	[117]
VCAM	EasySep (magnetic separation)	↑ Effective to modulate T helper subsets, ↓ clonogenecity	[120]
VCAM	FACS	↑ Angiogenic potential	[121]

Note: FACS: fluorescence-activated cell sorting, IL: interleukin, MACS: magnetic-activated cell sorting.

CD146 intermediates many activities of various cell types such as epithelial cells, endothelial cells, macrophages, and T cells, as well as is involved in angiogenesis, development, and immune responses [127]. CD146 expression is regulated at areas of cell–cell junction, what suggests its contribution in cell–cell interaction as a mediator [128].

CD146 was detected in various many MSCs sources: bone marrow [129, 130], adipose tissue [131], umbilical cord [125, 129], synovial membrane [132], placenta, dental pulp [112, 123], and intervertebral disc [133]. Petrenko et al. [29] reported that CD146+ cells percentage was approximately in 30% of Wharton jelly MSCs (WJ-MSCs), but below 5% of BM-MSCs and AD-MSCs. In MSCs isolated from dental pulp, marker CD146 was influenced to increase proliferation, immunomodulation, and differentiation of cells. Importantly, the expression level of CD146 in MSCs from dental pulp decreased with passage after the separation [123]. Furthermore, CD146+ subpopulation from BM-MSCs was depended on oxygen levels *in vitro* due to the fact that CD146 expression was absent or very weak near the bone surface in the bone marrow niche *in situ* [130]. Localization within umbilical cord influenced the CD146 presence—the highest levels were observed in Wharton jelly. This study confirmed the potential specificity of CD146 for MSCs. Gene expression analysis revealed that. CD146 was expressed at more than three-fold higher levels in UC-MSCs compared to fibroblasts, whereas common MSC-specific markers (CD73, CD90, CD105) displayed stable expression throughout passaging [125]. The same group showed a markedly higher secretory capacity with significantly greater immunomodulatory and anti-inflammatory

protein production upon inflammatory induction BM-MSCs-CD146+ compared with the BM-MSCs-CD146− [111]. Espagnolle et al. [124] showed that subpopulation CD146+ exhibited no differences in clonogenicity, proliferation, and multilineage differentiation in comparison to population CD146−, while CD146 molecule was associated with a commitment to a vascular smooth muscle cell lineage. CD146+ cells selected from human heterogenous AD-MSCs exhibited more beneficial angiogenic and adipogenic properties [110], confirming benefits in reconstructive and tissue engineering applications for AD-MSC-CD146+ cells.

Additionally, MSCs CD146+ were characterized with higher osteogenic potential—many studies revealed an association of tissue mineralization and bone reconstruction with the presence of CD146. Wrangler et al. [126] suggested that BM-MSCs CD146+ could be suitable for repopulation, whereas BM-MSCs CD146− could represent the primary choice for stimulation of endogenous intervertebral disc cells (IVDs). The CD146+ BM-MSC subpopulation possessed a greater migration potential toward degenerative IVDs, but BM-MSCs CD146− induced a stronger regenerative response. Application route (injection vs. migration) did not influence those effects Moreover, these results were independent of the application route [126]. *In vivo* murine studies defined CD146+ BM-MSCs as capable of bone formation and transendothelial migration [134]. Ye et al. [135] showed an association of CD146 with increased motility dependent on the Wnt signaling.

Moreover, CD146+ cells may promote mineralization and generate dental pulp-like structures, suggesting a role in self-renewal of stem cells and dental pulp regenerative therapy [112]. Interestingly, the CD146 molecule may have an impact on peripheral nerve regeneration. Shen et al. [136] suggested that CD146 not only had a key role in promoting of blood vessel regeneration but also regulated cell migration. Functional assessments showed that knockdown of CD146 decreased proliferation and viability of Schwann cells but increased their migration. Additionally, CD146 was upregulated in Schwann cells and cells associated with blood vessels following mouse peripheral nerve injury [136]. Taking together described CD146+ cells properties and its key role in vascular endothelial cell activity and angiogenesis, this subpopulation could be used in vascular smooth muscle, endothelial, or IVDs regeneration.

3.2. Nestin. Nestin is a class VI intermediate filament protein originally described as a marker of NSCs that is expressed during the development of the central nervous system (CNS). It is essential for stem cell survival, self-renewal, and proliferation, as well as it poses a critical regulator of cell differentiation and migration [137, 138]. *In vivo* study observation reported that NSCs cultures derived from knockout embryos showed reduced self-renewal ability, which was associated with elevated apoptosis, but no defects in cell proliferation or differentiation. In addition, nestin deficiency had no detectable effect on the integrity of the cytoskeleton [139].

MSCs Nestin+ played a key role in supporting niche activity and promote the maintenance of HSCs [140]. This population, together with PDGFR-α and CD51 coexpression, was characterized by fibroblastic CFUs, self-renewing capacity, and forming nonadherent mesenspheres [141]. In the other studies, the fraction of Nestin+ adult human BM-MSC expressed CD105 and CD146, which were capable of forming mesenspheres, while CD105−CD146− or CD105 +CD146− cells did not generate any progeny [142]. Isern et al. [142] used transgenic mice, expressing the regulatory elements of the nestin-promotor (Nestin-GFP), to demonstrate that the MSCs Nestin+ subpopulation originated from the neural crest and had special HSCs niche functions, while the MSCs Nestin—originated from the mesoderm and gave rise to bone and cartilage. An increase in nestin expression *in vitro* was observed after MSCs culture with supplements used for neural cell culture, such as N21 or B27 [20].

Due to the intracellular localization of Nestin, numerous studies used Nestin-GFP+ transgenic mice to separate Nestin+ MSCs from various tissues, such as spleen [119], bone marrow [141–143], kidney [118], and tendon [144]. Nestin-GFP+ cells Nestin+ were isolated from kidney and expressed markers such as NG2, Sca-1, and VCAM. Those cells could differentiate into adipocytes, osteocytes, and chondrocytes under appropriate differentiation conditions. Moreover, the described population was self-renewal and exhibited high clonogenicity [118]. Huang et al. [119] found that Nes-GFP+ cells constituted about 0.68% of the total spleen cell population. Isolated Nes-GFP+ cells exhibited the characteristics of MSCs and were excellent in immunomodulation. Those observations suggested that Nestin would be used for the identification of potential markers of splenic stromal cells. Nestin+ BM-MSCs increased cell chemotaxis in myocardial infarction through paracrine activity and were involved in its regeneration [143]. TSPCs expressed higher levels of nestin than tenocytes, while isolated Nestin+ cells exhibited MSCs features, such as the capacity for colony formation and multipotential differentiation. This data suggested that nestin represented a characteristic marker of TSPCs with strong tenogenic and regenerative potential [144].

In conclusion, the expression of nestin may support the process of tendon regeneration and also affect immunomodulation. In addition, MSCs Nestin+ may maintain HSCs niche and be key in bone marrow regeneration. The problem remains the intracellular location of nestin, which limits the ability to sort human MSCs. The solution may be to find a culture method that targets MSCs to increase Nestin+ cells in a population, such as the addition of neural differentiation supplements.

3.3. CD200 (OX2). CD200, also called OX2, is a membrane glycoprotein [145] responsible for the negative regulation of the number of immune cells, predominantly cells of myeloid origin [115]. That marker was expressed in different cells and tissues, such as lymphocytes and CNS [145]. Overexpression of CD200 was observed in cutaneous squamous cell carcinoma and myelodysplastic syndrome, suggesting that CD200 could also be used as a prognostic tumor marker [146, 147]. CD200-depleted mice developed faster experimental autoimmune encephalomyelitis, while binding between two CD200

receptors increased susceptibility to collagen-induced arthritis [145].

CD200 was also expressed in MSCs. According to the research from 2012, BM-MSCs had the highest level of this receptor, while it remained almost undetectable for UC-MSCs [148]. However, other research has shown BM-MSCs show about 23%–63.4% of positive cells depending on donors [114]. CD200 expression is found in AD-MSCs, but this antigen appeared to be more associated with visceral fat-derived AD-MSC (around 80% positive cells) than subcutaneous fat AD-MSC (24%) [113]. CD200 percentage for human fetal PL-MSCs was calculated as had approximately 70% of positive cells [115], while for human maternal PL-MSCs –1.8%. Additionally, fetal PL-MSC-CD200+ cells increased allograft survival in compared to maternal PL-MSCs [115]. Authors suggested that a higher number of positive CD200 cells could exaggerate better immunosuppressive effects [115]. Pontikoglou et al. [114] observed that BM MSCs CD200+ showed higher levels of αSM-actin (α smooth muscle-actin) protein, increased expression of *RUNX2* (*runt-related transcription factor 2*) and *DLX5* (*distal-less homebox 5*) *and higher* osteoblastic potential. A similar result was received by Rostovskaya et al. [149] on mice BM-MSCs. The $CD200^+$ population of mouse BM-MSCs showed an increased potential of osteogenesis both at the mRNA and protein levels. In addition, they considered that CD200 could be the marker progenitor cells in osteogenesis. CD200 transfection resulted in enhanced osteogenesis and chondrogenesis of BM-MSC, as well as increased clonogenicity and stemness-related genes expression [150], which confirms the connection between CD200 and osteogenesis. CD200+ AD-MSC isolated from visceral fat exhibited reduced adipogenesis, which suggests it as a predictive marker for lowered adipogenic capacity [113]. Based on the literature, CD200 could be associated with immunogenic subpopulation as well as with osteogenic progenitors—however, this link requires further explanation.

3.4. VCAM (CD106). Vascular cell adhesion molecule 1 (VCAM-1)/CD106 is a typical marker on endothelial cells and is also expressed on some stromal cells in particular vascular niches [151]. VCAM-1 is expressed on inflamed vascular endothelium, as well as on dendritic cell and macrophage-like types in both normal tissue and inflammation environment sites. VCAM-1 is important in cell–cell recognition and appears to regulate inflammation-associated vascular adhesion and the trans-endothelial migration of leukocytes, such as macrophages and T cells [152].

VCAM-1 was detected in MSCs isolated from bone marrow, umbilical cord, and placenta chronic villi (CV-MSC), while MSCs from adipose tissue were lacking this marker [120]. Yang et al. [120] proved that VCAM-1 expression on CV-MSCs was regulated in response to propagation and cytokine induction. Moreover, population CV-MSCs VCAM+ displayed a potent angiogenic property through superior angiogenic secretomes, e.g., HGF, IL-8, ANG, ANGPT2, and CXCL1 in comparison with the CV-MSC VCAM− subpopulation. As a result, VCAM+ subpopulation exerted enhanced therapeutic efficacy on regeneration after ischemia. [65]. VCAM-1 plays an important role of immunomodulation—its presence depended on inflammatory cytokines such as INF, TNF, and IL-1 [122, 153]. MSCs treated with the pro-inflammatory cytokines IFNγ, TNFα, and IL-1β increased the VCAM+ subpopulation to 88%. After inflammatory stimulation, VCAM+ cells still showed the capacity to multilineage differentiation potential [122]. V-CAM-1+ cells properties link this subpopulation with immune response.

3.5. CD142. CD142 (factor tissue) is a transmembrane protein with a little tail, which plays a key role in wound healing. The expression of this mark occurs in brain, lung, and epithelial cells of the skin, mucosa, and glomeruli, such as MSCs [154]. Sun et al. [13] observed that the percent of CD142-positive cells fluctuate between 71.2% and 88.6% in WJ-MSCs, depends on donors. Additionally, medium from culture cells $CD142^+$ stimulated "would healing" in scratch test of fibroblast compared to medium from WJ-MSCs $CD142^-$. WJ-MSCs $CD142^+$ also shown higher gene expression of *SPARC* (*secreted protein acidic and cysteine-rich*), *COL4A1* (*collagen type IV alpha 1 chain*), *COL1A1* (*collagen type I alpha 1 chain*), *COL5A1* (*collagen type V alpha 1 chain*) and lower gene expression of *MKI67* (*marker of proliferation Ki-67*) which was related with lower proliferation. Possible procoagulant activity of CD142 may raise concern in the future *in vivo* and clinical studies. However, according to Araldi et al. [155], this is not the only universal procoagulant variable while addiction of heparin could decrease this effect.

3.6. CD317. Another surface antigen indicating a distinct subpopulation is CD317. Identified within BM-MSCs, CD317+ cells did not differentiate toward standard lineages: oste-, chondro, and adipocytes. CD317+ MSC exhibited increased expression and secretion of IL-7, linking this population with enhanced immunomodulatory capacity [116]. Further studies revealed that the immune profile of CD317+ MSCs contrasts with the immunosuppressive function of MSCs. CD317+ subpopulation induced Th1 proinflammatory phenotype *in vitro* as well as promoted cutaneous tissue damage *in vivo* instead of tissue formation [117]. It is suggested that CD317+ subpopulation promoted a proinflammatory response through constitutive interferon signaling [117].

4. Challenges in Cell Separation of Specific Subpopulations

The main challenges in receiving homogenous MSC subpopulations are connected with the efficient process of cell separation. Magnetic-activated cell sorting (MACS) and FACS are the most frequently chosen methods. MACS uses microparticles to detect antigens, while the cells are separated between magnetic columns [156], while in FACS, cells are bound with fluorochrome-conjugated antibodies recognizing specific antigens and then separated with laser. The choice of selection technique is a matter of dispute, as both methods have advantages and limitations (Figure 2). According to Bowles et al. [157], MACS isolated cells with the same efficiency as FACS with reduced cell stress and

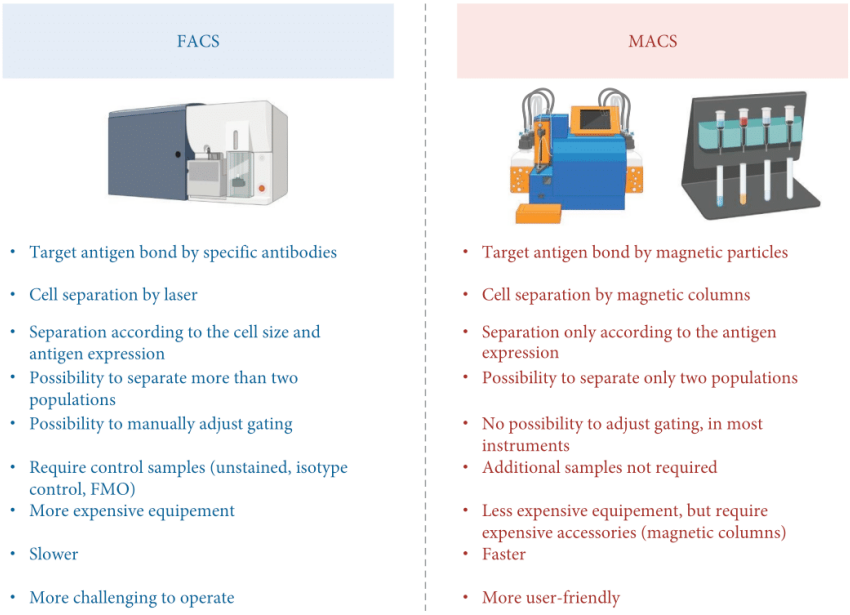

Figure 2: Fluorescence-activated cell sorting (FACS) and magnetic activated cell sorting (MACS)—properties comparison. Abbreviation: FMO: fluorescence minus one.

increased yield. They also observed smaller contamination of unrelated cells in culture after separation, while other authors observed the opposite—FACS sorting resulted in a more homogenous population of microglia [158]. FACS is found as a less variable than MACS [159, 160] and preferred for negative selection—MACS did not sufficiently eliminate labeled cells from population, especially those exhibiting low-level expression of antigen [161]. Sutermaster and Darling [162] described that MACS and FACS outcomes were similar, but MACS required the optimization of antibody and microbead concertation. In our experiences, we observed 13 times better recovery after SSEA-4+ WJ-MSCs with FACS, comparing to MACS (in submission). Given these points, MACS works faster, requires less equipment and probes for controls, and lower machine costs. FACS allows for the selection of multiple surface antigens and also the choice of size.

The above described heterogeneity issue also should be taken into consideration in planning further experiments, especially in the context of tissue complexity. Some authors observed the differences in surface antigens expression from different compartments of the same tissue. Unfortunately, the majority of publications did not provide a specific site of tissue that was used for MSC isolation. This problem is apparent regarding perinatal tissues, e.g., "placental MSC" refers to cells isolated from different parts of the placenta: chorionic plate, chorionic villi, trophoblast or placental amniotic membrane [163, 164]. The lack of more specific information regarding the isolation site could indeed contribute to the observed disproportions in the literature and would hinder the reproduction of experimental protocols in close future.

Reaserchers report that both separation methods not always result in receiving of 100% pure fraction of positive cells. Vaculik et al. [33] scored obtaining 71% SSEA-4+ cells and 82% CD271+ cells after MACS as a great outcome. Fouad et al. [43] reported the enrichment to 82% of SSEA-3+ cells after FACS. The purity issue was observed especially during the sorting of sparse populations—MACS separation allowed to increase SSEA-3+ population from 1.9% to 77% [44]. Unfortunately, most of the scientific articles does not provide values of specific target antigen before and after separation nor calculate the efficiency of the process.

Maintenance of the homogeneity of separated populations is another problem to discuss. Many researchers observed a gradual decrease of surface antigen expression with time of cell culture for SSEA-3 [67], CD271 [55], CD49-F [25, 28], and CD146 [123]. Rosu-Myles et al. [54] observed the decrease of SSEA-4+ number during 28 days (approximately four passages) of culture in both unsorted, positive, and negative subpopulations. On the other side of the coin, researchers also reported the contamination and growing numbers of positive cells in the negative fractions in SSEA-4 [34] and Sca-1 [41] studies. The scale of this problem remains unknown, as a majority of researchers do not report the purity of the received fraction, and they do not conduct the analysis for further passages after the sorting.

5. Mesenchymal Plasticity as a Manifestation of Stochastic Stem Cell Model

The information gathered above attempts to move towards an understanding of MSC cell plasticity, but this concept

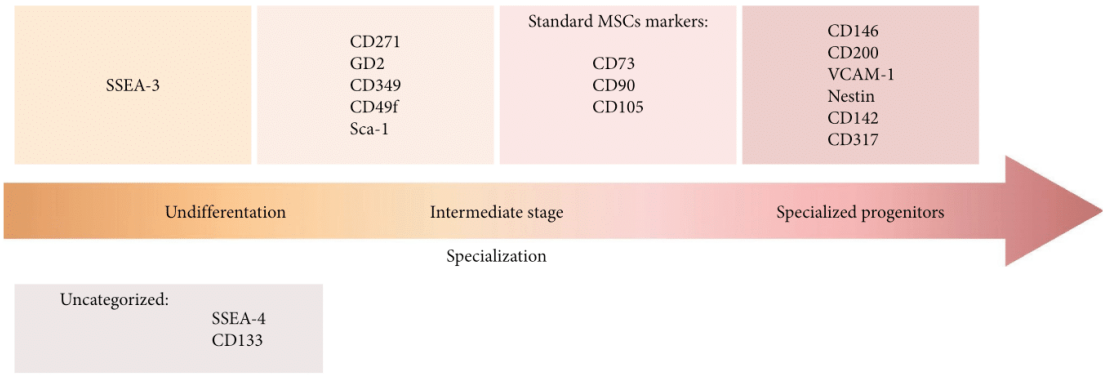

Figure 3: Markers described in the review in a context of cell specialization.

itself remains difficult to explain due to numerous factors that remain vaguely explored. In 1985, Ogawa et al. [165] published a very important experiment, establishing different types of colonies arising from single cells. He proved that two daughter cells can produce completely different lineages within one cell cycle. In 2006, Zipori [166] indicated that the cells tend to change phenotypes even when obtained as clonal populations. Not only phenotype of that cells changed but also properties. Enzyme expression was different among individual cells of the same clone; adipogenesis was an inducible and reversible feature in all of the clones, the same as the capacity to support hemopoiesis. Thus, the authors concluded that mesenchymal cell lines phenotype is very flexible and environmental-dependent. The observed heterogeneity and the presence of a small population of cells with stem potential may be due to the presence of many cell types with different origins. It could also be the possibility that these stem cells are direct descendants that distribute to various organs and tissues during ontogeny and remain there throughout the mammalian life span. Alternatively, these different phenotypes may be derived from a common one universal stem cell. The latter hypothesis was supported by experiments of several research groups. Pittenger et al. [167] proved that cells forming a clone derived from a single cell can differentiate into adipocytes, chondrogenic cells, and osteocytes, confirming the multipotency of mesenchymal cells. Jiang et al. [168, 169] proved the existence of the same population of pluripotent cells in the brain and muscles, calling these cells multipotent adult progenitor cells (MAPCs). At the single-cell level, researchers confirmed the differentiation of MAPCs *in vitro* to derivatives of all three germ layers. Moreover, after implantation into the mouse blastocyst, these cells contributed to the formation of many somatic cells [170]. Such cells were found not only in bone marrow but also in muscles and brain. Zipori [166] suggested that stemness is a state that, theoretically, any cell may enter, and stemness is an unstable state characterized by promiscuous gene expression that puts the cell in a standby state, ready to commit to a variety of different directions. A new concept for the traditional stem cell model, assuming the stem cell to be the origin of an irreversible hierarchy of descending potency for renewal (deterministic model) as opposed to the stem cell state notion in which cells may assume a stem state even when already in a differentiating stage (stochastic model) due to plastic process of epigenetic remodeling.

In 2022, Quesenberry et al. [23] brought the described hypothesis much closer. The presented theory of a "universal stem cell" denies the old, deterministic model in which the fate of the cells is hierarchical and directed. The theory of universal stem cell convinces that differentiation is not ultimately determined into a given cell type, but it occurs as continuum during the cell cycle and depends on numerous factors such as the surrounding environment, paracrine factors, and more general, e.g., sex, disease status, race, or drug therapy. This model explains the phenotypic changes of cells depending on the point in the cell cycle. Possibly, further discoveries on the topic of possessing the genuine stem cell subpopulation change the perspective on the currently used stem cell classification.

6. Further Perspectives

In this review, we have collected available information for markers indicating distinct subpopulations within MSCs. To our surprise, reports differ between research groups, especially in calculations of positive cells expressing described markers. Discrepancies could be a result of different protocols between research groups, which emphasizes the importance of standardization of MSCs studies to minimize variations and make research more comparable.

We presented that some of the markers could indicate the population of genuine stem cells within MSCs, while others could predict a more specialized pool of cells that potentially could be applied in wound healing or to suppress inflammatory (Figure 3). However, more studies are still needed to support those observations, especially as some markers are barely described for human MSCs like CD106 (VCAM), GD2, or CD49F; some markers, like CD349, were only described in MSCs from one tissue. For some of the markers described, there are insufficient data (CD133) or conflicting data (SSEA-4) to properly categorize them. There

is also still a lack of studies linking the described subpopulations to a specific developmental origin. Most evidence is collected for the SSEA family and CD271, whereas this topic remains almost unexplored for Sca-1, GD-2, CD49F, and other markers. However, presented initial attempts linked unique properties with an undifferentiated character of described subpopulations. For more precise competitive analysis, there is a need for publishing also, so-called negative data, which is difficult in academic environment where publications showing statistically significant differences are promoted while the others are rejected. The change of perspective for academic publishing could ultimately provide the evidences for the acceptance or rejection of markers for further therapies.

Last but not least, the majority of presented subpopulations are studied only at *in vitro* level. This is understandable, as there is a need for detailed characteristics of those cells. Several subpopulations were also assessed *in vivo*, but still, there are more research to conclude. To our knowledge, only SSEA-3+ subpopulation was translated to patient studies, and currently, phase I studies are conducted. Taken together, further research on the described subpopulations is essential to progress toward the use of a homogeneous subpopulation that would be focused on treating a specific need rather than using heterogeneous MSCs that currently pose as a therapeutic standard.

Abbreviations

AD-MSCs: Adipose tissue-derived mesenchymal stem/stromal cells
ANG: Angiogenin
ANGPT2: Angiopoietin 2
BDNF: Brain derived neurotrophic factor
BM-MSCs: Bone marrow-derived mesenchymal stem/stromal cells
CFU: Colony forming unit
CIA: Collagen-induced arthritis
CNS: Central nervous system
CV: Placenta chorionic villi
CXCL1: C-X-C motif chemokine ligand 1
DP: Dental pulp
EAE: Experimental autoimmune encephalomyelitis
ECM: Extracellular matrix
EMT: Epithelial-to-mesenchymal transition
ESCs: Embryonic stem cells
FACS: Fluorescence-activated cell sorting
FGF: Fibroblast growth factor
FZD-9: Frizzled-9
GD2: Neural ganglioside
GFP: Green fluorescence protein
HGF: Hepatocyte growth factor
IFNγ: Interferon gamma
IL-1β: Interleukin 1 beta
IL-8: Interleukin 8
IPSCs: Induced pluripotent stem cells
IVD: Intervertebrate discs
ISCT: International Society of Cell & Gene Therapy
HSCs: Hematopoietic stem cells
LPM: Lateral plate mesoderm
MACS: Magnetic-activated cell sorting
MAPCs: Multipotent adult progenitor cells
MCAM: Melanoma cell adhesion molecule
MET: Mesenchymal-to-epithelial transition
MSCs: Mesenchymal stem/stromal cells
MUSE Cells: Multi-lineage differentiating stress enduring cells
NCSCs: Neural crest-derived stem cells
NGF: Nerve growth factor
NSCs: Neural Stem Cells
PL-MSCs: Placenta-derived mesenchymal stem/stromal cells
PNS: Peripheral nervous system
Sca-1+: Stem cells antigen-1
SSEA: Stage-specific embryonic antigen
TNFα: Tumor necrosis factor alpha
UC-MSCs: Umbilical cord-derived mesenchymal stem/stromal cells
VCAM- 1: Vascular cell adhesion molecule 1
WJ-MSCs: Wharton jelly-derived mesenchymal stem/stromal cells.

Data Availability

No underlying data were collected or produced in this study.

Conflicts of Interest

The authors declare that they have no conflicts of interest.

Authors' Contributions

Agnieszka Smolinska and Aleksandra Bzinkowska contributed equally to this work.

Acknowledgments

This work was supported by National Science Centre (grant numbers: NCN 2018/31/B/NZ4/03172, NCN 2022/45/N/NZ3/02564) and ESF, POWR.03.02.00-00-I028/17-00.

References

[1] A. Naji, M. Eitoku, B. Favier, F. Deschaseaux, N. Rouas-Freiss, and N. Suganuma, "Biological functions of mesenchymal stem cells and clinical implications," *Cellular and Molecular Life Sciences*, vol. 76, no. 17, pp. 3323–3348, 2019.

[2] O. Levy, R. Kuai, E. M. J. Siren et al., "Shattering barriers toward clinically meaningful MSC therapies," *Science Advances*, vol. 6, no. 30, 2020.

[3] D. A. Rennerfeldt and K. J. Van Vliet, "Concise review: when colonies are not clones: evidence and implications of intracolony heterogeneity in mesenchymal stem cells," *Stem Cells*, vol. 34, no. 5, pp. 1135–1141, 2016.

[4] M. Liu, H. Lei, P. Dong et al., "Adipose-derived mesenchymal stem cells from the elderly exhibit decreased migration and differentiation abilities with senescent properties," *Cell Transplantation*, vol. 26, no. 9, pp. 1505–1519, 2017.

[5] D. N. Urrutia, P. Caviedes, R. Mardones et al., "Comparative study of the neural differentiation capacity of mesenchymal stromal cells from different tissue sources: an approach for their use in neural regeneration therapies," *PLoS One*, vol. 14, no. 3, Article ID e0213032, 2019.

[6] K. Drela, A. Sarnowska, P. Siedlecka et al., "Low oxygen atmosphere facilitates proliferation and maintains undifferentiated state of umbilical cord mesenchymal stem cells in an hypoxia inducible factor-dependent manner," *Cytotherapy*, vol. 16, no. 7, pp. 881–892, 2014.

[7] K. Drela, L. Stanaszek, K. Snioch et al., "Bone marrow-derived from the human femoral shaft as a new source of mesenchymal stem/stromal cells: an alternative cell material for banking and clinical transplantation," *Stem Cell Research & Therapy*, vol. 11, no. 1, pp. 1–13, 2020.

[8] W. K. Ong, S. Chakraborty, and S. Sugii, "Adipose tissue: understanding the heterogeneity of stem cells for regenerative medicine," *Biomolecules*, vol. 11, no. 7, Article ID 918, 2021.

[9] D. L. Roelen, B. J. van der Mast, P. S. in't Anker et al., "Differential immunomodulatory effects of fetal versus maternal multipotent stromal cells," *Human Immunology*, vol. 70, no. 1, pp. 16–23, 2009.

[10] A. Papait, E. Vertua, M. Magatti et al., "Mesenchymal stromal cells from fetal and maternal placenta possess key similarities and differences: potential implications for their applications in regenerative medicine," *Cells*, vol. 9, no. 1, Article ID 127, 2020.

[11] V. S. Sardesai, A. Shafiee, N. M. Fisk, and R. A. Pelekanos, "Avoidance of maternal cell contamination and overgrowth in isolating fetal chorionic villi mesenchymal stem cells from human term placenta," *Stem Cells Translational Medicine*, vol. 6, no. 4, pp. 1070–1084, 2017.

[12] D. G. Phinney and J. Galipeau, "Manufacturing mesenchymal stromal cells for clinical applications: a survey of good manufacturing practices at U.S. academic centers," *Cytotherapy*, vol. 21, no. 7, pp. 782–792, 2019.

[13] C. Sun, L. Wang, H. Wang et al., "Single-cell RNA-seq highlights heterogeneity in human primary Wharton's jelly mesenchymal stem/stromal cells cultured in vitro," *Stem Cell Research & Therapy*, vol. 11, no. 1, Article ID 149, 2020.

[14] A. Selich, J. Daudert, R. Hass et al., "Massive clonal selection and transiently contributing clones during expansion of mesenchymal stem cell cultures revealed by lentiviral RGB-barcode technology," *Stem Cells Translational Medicine*, vol. 5, no. 5, pp. 591–601, 2016.

[15] C. M. McLeod and R. L. Mauck, "On the origin and impact of mesenchymal stem cell heterogeneity: new insights and emerging tools for single cell analysis," *European Cells and Materials*, vol. 34, pp. 217–231, 2017.

[16] C. Li, H. Zhao, and B. Wang, "Mesenchymal stem/stromal cells: developmental origin, tumorigenesis and translational cancer therapeutics," *Translational Oncology*, vol. 14, no. 1, Article ID 100948, 2021.

[17] G. Sheng, "The developmental basis of mesenchymal stem/stromal cells (MSCs)," *BMC Developmental Biology*, vol. 15, no. 1, Article ID 44, 2015.

[18] C. Coste, V. Neirinckx, A. Sharma et al., "Human bone marrow harbors cells with neural crest-associated characteristics like human adipose and dermis tissues," *PLoS One*, vol. 12, no. 7, Article ID e0177962, 2017.

[19] E. Tomecka, W. Lech, M. Zychowicz et al., "Assessment of the neuroprotective and stemness properties of human Wharton's jelly-derived mesenchymal stem cells under variable (5% vs. 21%) aerobic conditions," *Cells*, vol. 10, no. 4, Article ID 717, 2021.

[20] A. Figiel-Dabrowska, K. Radoszkiewicz, P. Rybkowska, N. E. Krzesniak, D. Sulejczak, and A. Sarnowska, "Neurogenic and neuroprotective potential of stem/stromal cells derived from adipose tissue," *Cells*, vol. 10, no. 6, Article ID 1475, 2021.

[21] F. Ogura, S. Wakao, Y. Kuroda et al., "Human adipose tissue possesses a unique population of pluripotent stem cells with nontumorigenic and low telomerase activities: potential implications in regenerative medicine," *Stem Cells and Development*, vol. 23, no. 7, pp. 717–728, 2014.

[22] Y. Kuroda, M. Kitada, S. Wakao et al., "Unique multipotent cells in adult human mesenchymal cell populations," *Proceedings of the National Academy of Sciences*, vol. 107, no. 19, pp. 8639–8643, 2010.

[23] P. J. Quesenberry, S. Wen, L. R. Goldberg, and M. S. Dooner, "The universal stem cell," *Leukemia*, vol. 36, no. 12, pp. 2784–2792, 2022.

[24] C. Zhang, X. Han, J. Liu et al., "Single-cell transcriptomic analysis reveals the cellular heterogeneity of mesenchymal stem cells," *Genomics, Proteomics & Bioinformatics*, vol. 20, no. 1, pp. 70–86, 2022.

[25] Z. Yang, P. Dong, X. Fu et al., "CD49f acts as an inflammation sensor to regulate differentiation, adhesion, and migration of human mesenchymal stem cells," *Stem Cells*, vol. 33, no. 9, pp. 2798–2810, 2015.

[26] N. Nieto-Nicolau, R. M. de la Torre, O. Fariñas, A. Savio, A. Vilarrodona, and R. P. Casaroli-Marano, "Extrinsic modulation of integrin α6 and progenitor cell behavior in mesenchymal stem cells," *Stem Cell Research*, vol. 47, Article ID 101899, 2020.

[27] Z. Yang, S. Ma, R. Cao et al., "CD49f high defines a distinct skin mesenchymal stem cell population capable of hair follicle epithelial cell maintenance," *Journal of Investigative Dermatology*, vol. 140, no. 3, pp. 544–555.e9, 2020.

[28] K. Zha, X. Li, G. Tian et al., "Evaluation of CD49f as a novel surface marker to identify functional adipose-derived mesenchymal stem cell subset," *Cell Proliferation*, vol. 54, no. 5, pp. 1–15, 2021.

[29] Y. Petrenko, I. Vackova, K. Kekulova et al., "A comparative analysis of multipotent mesenchymal stromal cells derived from different sources, with a focus on neuroregenerative potential," *Scientific Reports*, vol. 10, no. 1, Article ID 4290, 2020.

[30] M. Barilani, F. Banfi, S. Sironi et al., "Low-affinity nerve growth factor receptor (CD271) heterogeneous expression in adult and fetal mesenchymal stromal cells," *Scientific Reports*, vol. 8, no. 1, pp. 1–11, 2018.

[31] H. Kawamura, R. Nakatsuka, Y. Matsuoka et al., "TGF-β signaling accelerates senescence of human bone-derived CD271 and SSEA-4 double-positive mesenchymal stromal cells," *Stem Cell Reports*, vol. 10, no. 3, pp. 920–932, 2018.

[32] A. Brboric, S. Vasylovska, J. Saarimäki-Vire et al., "Characterization of neural crest-derived stem cells isolated from human bone marrow for improvement of transplanted islet function," *Upsala Journal of Medical Sciences*, vol. 124, no. 4, pp. 228–237, 2019.

[33] C. Vaculik, C. Schuster, W. Bauer et al., "Human dermis harbors distinct mesenchymal stromal cell subsets," *Journal of Investigative Dermatology*, vol. 132, pp. 563–574, 2012.

[34] H. He, T. Nagamura-Inoue, H. Tsunoda et al., "Stage-specific embryonic antigen 4 in Wharton's jelly-derived mesenchymal stem cells is not a marker for proliferation and multipotency," *Tissue Engineering Part A*, vol. 20, no. 7-8, pp. 1314–1324, 2014.

[35] T. C. Tran, K. Kimura, M. Nagano et al., "Identification of human placenta-derived mesenchymal stem cells involved in re-endothelialization," *Journal of Cellular Physiology*, vol. 226, no. 1, pp. 224–235, 2011.

[36] V. L. Battula, S. Treml, H. Abele, and H.-J. Bühring, "Prospective isolation and characterization of mesenchymal stem cells from human placenta using a frizzled-9-specific monoclonal antibody," *Differentiation*, vol. 76, no. 4, pp. 326–336, 2008.

[37] J. Xu, W. Liao, D. Gu et al., "Neural ganglioside GD2 identifies a subpopulation of mesenchymal stem cells in umbilical cord," *Cellular Physiology and Biochemistry*, vol. 23, no. 4–6, pp. 415–424, 2009.

[38] L. Kucerova, J. Zmajkovic, L. Toro, S. Skolekova, L. Demkova, and M. Matuskova, "Tumor-driven molecular changes in human mesenchymal stromal cells," *Cancer Microenvironment*, vol. 8, no. 1, pp. 1–14, 2015.

[39] C. Martinez, T. J. Hofmann, R. Marino, M. Dominici, and E. M. Horwitz, "Human bone marrow mesenchymal stromal cells express the neural ganglioside GD2: a novel surface marker for the identification of MSCs," *Blood*, vol. 109, no. 10, pp. 4245–4248, 2007.

[40] J. Xu, W. J. Fan, X. X. Tu et al., "Neural ganglioside GD2(+) cells define a subpopulation of mesenchymal stem cells in adult murine bone marrow," *Cellular Physiology and Biochemistry*, vol. 32, no. 4, pp. 889–898, 2013.

[41] C. Baustian, S. Hanley, and R. Ceredig, "Isolation, selection and culture methods to enhance clonogenicity of mouse bone marrow derived mesenchymal stromal cell precursors," *Stem Cell Research & Therapy*, vol. 6, no. 1, 2015.

[42] Y. Nitobe, T. Nagaoki, G. Kumagai et al., "Neurotrophic factor secretion and neural differentiation potential of multilineage-differentiating stress-enduring (Muse) cells derived from mouse adipose tissue," *Cell Transplantation*, vol. 28, no. 9-10, pp. 1132–1139, 2019.

[43] A. M. Fouad, M. M. Gabr, E. K. Abdelhady et al., "In vitro differentiation of human multilineage differentiating stress-enduring (muse) cells into insulin producing cells," *Journal of Genetic Engineering and Biotechnology*, vol. 16, no. 2, pp. 433–440, 2018.

[44] K. Kinoshita, S. Kuno, H. Ishimine et al., "Therapeutic potential of adipose-derived SSEA-3-positive muse cells for treating diabetic skin ulcers," *Stem Cells Translational Medicine*, vol. 4, no. 2, pp. 146–155, 2015.

[45] T. Suzuki, Y. Sato, Y. Kushida et al., "Intravenously delivered multilineage-differentiating stress enduring cells dampen excessive glutamate metabolism and microglial activation in experimental perinatal hypoxic ischemic encephalopathy," *Journal of Cerebral Blood Flow & Metabolism*, vol. 41, no. 7, pp. 1707–1720, 2021.

[46] M. Selle, J. D. Koch, A. Ongsiek et al., "Influence of age on stem cells depends on the sex of the bone marrow donor," *Journal of Cellular and Molecular Medicine*, vol. 26, no. 5, pp. 1594–1605, 2022.

[47] Y. Mikami, Y. Ishii, N. Watanabe et al., "CD271/p75(NTR) inhibits the differentiation of mesenchymal stem cells into osteogenic, adipogenic, chondrogenic, and myogenic lineages," *Stem Cells and Development*, vol. 20, no. 5, pp. 901–913, 2011.

[48] M. T. González-Garza, D. E. Cruz-Vega, A. Cárdenas-Lopez, R. M. de la Rosa, and J. E. Moreno-Cuevas, "Comparing stemness gene expression between stem cell subpopulations from peripheral blood and adipose tissue," *American Journal of Stem Cells*, vol. 7, no. 2, pp. 38–47, 2018.

[49] N. Kohli, I. R. T. Al-Delfi, M. Snow et al., "CD271-selected mesenchymal stem cells from adipose tissue enhance cartilage repair and are less angiogenic than plastic adherent mesenchymal stem cells," *Scientific Reports*, vol. 9, no. 1, pp. 1–12, 2019.

[50] X. Hu, M. Garcia, L. Weng et al., "Identification of a common mesenchymal stromal progenitor for the adult haematopoietic niche," *Nature Communications*, vol. 7, no. 1, pp. 1–14, 2016.

[51] A. Kayaba, A. Itoh-Nakadai, K. Niibe et al., "Bone marrow PDGFRα+Sca-1(+)-enriched mesenchymal stem cells support survival of and antibody production by plasma cells in vitro through IL-6," *International Immunology*, vol. 30, no. 6, pp. 241–253, 2018.

[52] M. Iseki, Y. Kushida, S. Wakao et al., "Nontumorigenic pluripotent-like stem cells, have liver regeneration capacity through specific homing and cell replacement in a mouse model of liver fibrosis," *Cell Transplantation*, vol. 26, no. 5, pp. 821–840, 2017.

[53] N. Alessio, T. Squillaro, S. Özcan et al., "Stress and stem cells: adult muse cells tolerate extensive genotoxic stimuli better than mesenchymal stromal cells," *Oncotarget*, vol. 9, no. 27, pp. 19328–19341, 2018.

[54] M. Rosu-Myles, J. McCully, J. Fair et al., "The globoseries glycosphingolipid SSEA-4 is a marker of bone marrow-derived clonal multipotent stromal cells in vitro and in vivo." *Stem Cells and Development*, vol. 22, no. 9, pp. 1387–1397, 2013.

[55] Y. Matsuoka, R. Nakatsuka, K. Sumide et al., "Prospectively isolated human bone marrow cell-derived MSCs support primitive human CD34-negative hematopoietic stem cells," *Stem Cells*, vol. 33, no. 5, pp. 1554–1565, 2015.

[56] B. A. Fenderson, E. M. Eddy, and S. Hakomori, "Glycoconjugate expression during embryogenesis and its biological significance," *BioEssays*, vol. 12, no. 4, pp. 173–179, 1990.

[57] J. K. Henderson, J. S. Draper, H. S. Baillie et al., "Preimplantation human embryos and embryonic stem cells show comparable expression of stage-specific embryonic antigens," *Stem Cells*, vol. 20, no. 4, pp. 329–337, 2002.

[58] A. Kallas, M. Pook, M. Maimets, K. Zimmermann, and T. Maimets, "Nocodazole treatment decreases expression of pluripotency markers nanog and Oct4 in human embryonic stem cells," *PLoS One*, vol. 6, no. 4, Article ID e19114, 2011.

[59] J. S. Draper, C. Pigott, J. A. Thomson, and P. W. Andrews, "Surface antigens of human embryonic stem cells: changes upon differentiation in culture," *Journal of Anatomy*, vol. 200, no. 3, pp. 249–258, 2002.

[60] T. Ojima, E. Shibata, S. Saito et al., "Glycolipid dynamics in generation and differentiation of induced pluripotent stem cells," *Scientific Reports*, vol. 5, no. 1, pp. 1–13, 2015.

[61] R.-J. Lin, M.-W. Kuo, B.-C. Yang et al., "B3GALT5 knockout alters gycosphingolipid profile and facilitates transition to human naïve pluripotency," *Proceedings of the National Academy of Sciences*, vol. 117, no. 44, pp. 27435–27444, 2020.

[62] K. Hamamura, H. Hotta, Y. Murakumo, H. Shibuya, Y. Kondo, and K. Furukawa, "SSEA-3 and 4 are not essential for the induction or properties of mouse iPS cells," *Journal of Oral Science*, vol. 62, no. 4, pp. 393–396, 2020.

[63] T. Tian, R.-Z. Zhang, Y.-H. Yang, Q. Liu, D. Li, and X.-R. Pan, "Muse cells derived from dermal tissues can differentiate into melanocytes," *Cellular Reprogramming*, vol. 19, no. 2, pp. 116–122, 2017.

[64] Z. Leng, D. Sun, Z. Huang et al., "Quantitative analysis of SSEA3+ cells from human umbilical cord after magnetic sorting," *Cell Transplantation*, vol. 28, no. 7, pp. 907–923, 2019.

[65] F. Amiri, R. Halabian, M. Salimian et al., "Induction of multipotency in umbilical cord-derived mesenchymal stem cells cultivated under suspension conditions," *Cell Stress Chaperones*, vol. 19, no. 5, pp. 657–666, 2014.

[66] D. Aprile, N. Alessio, T. Squillaro, G. Di Bernardo, G. Peluso, and U. Galderisi, "Role of glycosphingolipid SSEA-3 and FGF2 in the stemness and lineage commitment of multilineage differentiating stress enduring (MUSE) cells," *Cell Proliferation*, vol. 56, no. 1, Article ID e13345.

[67] A. M. Fouad, M. M. Gabr, E. K. Abdelhady, S. A. Rashed, S. M. Khater, and M. M. Zakaria, "Down-regulation of pluripotency and expression of SSEA-3 surface marker for mesenchymal Muse cells by in vitro expansion passaging," *Egyptian Journal of Basic and Applied Sciences*, vol. 6, no. 1, pp. 68–72, 2019.

[68] X. Chen, X.-Y. Yin, Y.-Y. Zhao et al., "Human Muse cells-derived neural precursor cells as the novel seed cells for the repair of spinal cord injury," *Biochemical and Biophysical Research Communications*, vol. 568, pp. 103–109, 2021.

[69] Y. Yamada, S. Minatoguchi, H. Kanamori et al., "Stem cell therapy for acute myocardial infarction—focusing on the comparison between Muse cells and mesenchymal stem cells," *Journal of Cardiology*, vol. 80, no. 1, pp. 80–87, 2022.

[70] T. Yamashita, Y. Kushida, S. Wakao et al., "Therapeutic benefit of Muse cells in a mouse model of amyotrophic lateral sclerosis," *Scientific Reports*, vol. 10, no. 1, 2020.

[71] K. Hosoyama, S. Wakao, Y. Kushida et al., "Intravenously injected human multilineage-differentiating stress-enduring cells selectively engraft into mouse aortic aneurysms and attenuate dilatation by differentiating into multiple cell types," *The Journal of Thoracic and Cardiovascular Surgery*, vol. 155, no. 6, pp. 2301–2313.e4, 2018.

[72] H. Uchida, K. Niizuma, Y. Kushida et al., "Human muse cells reconstruct neuronal circuitry in subacute lacunar stroke model," *Stroke*, vol. 48, no. 2, pp. 428–435, 2017.

[73] H. Katagiri, Y. Kushida, M. Nojima et al., "A distinct subpopulation of bone marrow mesenchymal stem cells, muse cells, directly commit to the replacement of liver components," *American Journal of Transplantation*, vol. 16, no. 2, pp. 468–483, 2016.

[74] Y. Yamada, S. Wakao, Y. Kushida et al., "S1P-S1PR2 axis mediates homing of muse cells into damaged heart for long-lasting tissue repair and functional recovery after acute myocardial infarction," *Circulation Research*, vol. 122, no. 8, pp. 1069–1083, 2018.

[75] T. Abe, D. Aburakawa, K. Niizuma et al., "Intravenously transplanted human multilineage-differentiating stress-enduring cells afford brain repair in a mouse lacunar stroke model," *Stroke*, vol. 51, pp. 601–611, 2020.

[76] T. Noda, K. Nishigaki, and S. Minatoguchi, "Safety and efficacy of human muse cell-based product for acute myocardial infarction in a first-in-human trial," *Circulation Journal*, vol. 84, pp. 1189–1192, 2020.

[77] S. Shimizu N. Matsuyama, K. Ueda, T. Suzuki et al., "Protocol: safety and tolerability of a multilineage-differentiating stress-enduring cell-based product in neonatal hypoxic-ischaemic encephalopathy with therapeutic hypothermia (SHIELD trial): a clinical trial protocol open-label, non-randomised, dose-escalation trial," *BMJ Open*, vol. 12, Article ID 57073, 2022.

[78] C. Soliman, J. X. Chua, M. Vankemmelbeke et al., "The terminal sialic acid of stage-specific embryonic antigen-4 has a crucial role in binding to a cancer-targeting antibody," *Journal of Biological Chemistry*, vol. 295, no. 4, pp. 1009–1020, 2020.

[79] A. Kaminska, A. Wedzinska, M. Kot, and A. Sarnowska, "Effect of long-term 3D spheroid culture on WJ-MSC," *Cells*, vol. 10, no. 4, Article ID 719, 2021.

[80] T. J. Block, M. Marinkovic, O. N. Tran et al., "Restoring the quantity and quality of elderly human mesenchymal stem cells for autologous cell-based therapies," *Stem Cell Research & Therapy*, vol. 8, no. 1, Article ID 239, 2017.

[81] S. M. Mihaila, A. M. Frias, R. P. Pirraco et al., "Human adipose tissue-derived SSEA-4 subpopulation multi-differentiation potential towards the endothelial and osteogenic lineages," *Tissue Engineering Part A*, vol. 19, no. 1-2, pp. 235–246, 2013.

[82] M. V. Chao and M. Bothwell, "Neurotrophins: to cleave or not to cleave," *Neuron*, vol. 33, no. 1, pp. 9–12, 2002.

[83] P. A. Barker, "p75NTR is positively promiscuous: novel partners and new insights," *Neuron*, vol. 42, no. 4, pp. 529–533, 2004.

[84] P. Ruggeri, R. A., L. Cappabianca et al., "Neurotrophin and neurotrophin receptor involvement in human neuroblastoma," *InTech*, 2013.

[85] G. Calabrese, R. Giuffrida, D. Lo Furno et al., "Potential effect of CD271 on human mesenchymal stromal cell proliferation and differentiation," *International Journal of Molecular Sciences*, vol. 16, no. 12, pp. 15609–15624, 2015.

[86] S. J. Morrison, P. M. White, C. Zock, and D. J. Anderson, "Prospective identification, isolation by flow cytometry, and in vivo self-renewal of multipotent mammalian neural crest stem cells," *Cell*, vol. 96, no. 5, pp. 737–749, 1999.

[87] M. E. van Strien, J. A. Sluijs, B. A. Reynolds, D. A. Steindler, E. Aronica, and E. M. Hol, "Isolation of neural progenitor cells from the human adult subventricular zone based on expression of the cell surface marker CD271," *Stem Cells Translational Medicine*, vol. 3, no. 4, pp. 470–480, 2014.

[88] E. Dupin and L. Sommer, "Neural crest progenitors and stem cells: from early development to adulthood," *Developmental Biology*, vol. 366, no. 1, pp. 83–95, 2012.

[89] A. Vidal and T. Redmer, "Decoding the role of CD271 in melanoma," *Cancers (Basel)*, vol. 12, no. 9, Article ID 2460, 2020.

[90] I. Moscatelli, E. Pierantozzi, A. Camaioni, G. Siracusa, and L. Campagnolo, "p75 neurotrophin receptor is involved in proliferation of undifferentiated mouse embryonic stem cells," *Experimental Cell Research*, vol. 315, no. 18, pp. 3220–3232, 2009.

[91] Z. Chen, C. R. Donnelly, B. Dominguez et al., "p75 is required for the establishment of postnatal sensory neuron diversity by potentiating ret signaling," *Cell Reports*, vol. 21, no. 3, pp. 707–720, 2017.

[92] E. Bogenmann, P. S. Thomas, Q. Li et al., "Generation of mice with a conditional allele for the p75NTR neurotrophin receptor gene," *Genesis*, vol. 49, no. 11, pp. 862–869, 2011.

[93] Y. Sowa, T. Imura, T. Numajiri et al., "Adipose stromal cells contain phenotypically distinct adipogenic progenitors derived from neural crest," *PLoS One*, vol. 8, no. 12, Article ID e84206, 2013.

[94] S. Wislet-Gendebien, E. Laudet, V. Neirinckx et al., "Mesenchymal stem cells and neural crest stem cells from adult bone marrow: characterization of their surprising similarities and differences," *Cellular and Molecular Life Sciences*, vol. 69, no. 15, pp. 2593–2608, 2012.

[95] P. H. Krebsbach and L. G. Villa-Diaz, "The role of integrin α6 (CD49f) in stem cells: more than a conserved biomarker," *Stem Cells and Development*, vol. 26, no. 15, pp. 1090–1099, 2017.

[96] K.-R. Yu, S.-R. Yang, J.-W. Jung et al., "CD49f enhances multipotency and maintains stemness through the direct regulation of OCT_4 and SOX_2," *Stem Cells*, vol. 30, no. 5, pp. 876–887, 2012.

[97] P. Zhang, Y. Ohkawa, S. Yamamoto et al., "St8sia1-deficiency in mice alters tumor environments of gliomas, leading to reduced disease severity," *Nagoya Journal of Medical Science*, vol. 83, no. 3, pp. 535–549, 2021.

[98] T. J. Van Raay, Y. K. Wang, M. R. Stark et al., "Frizzled 9 is expressed in neural precursor cells in the developing neural tube," *Development Genes and Evolution*, vol. 211, no. 8-9, pp. 453–457, 2001.

[99] V. L. Battula, P. M. Bareiss, S. Treml et al., "Human placenta and bone marrow derived MSC cultured in serum-free, b-FGF-containing medium express cell surface frizzled-9 and SSEA-4 and give rise to multilineage differentiation," *Differentiation*, vol. 75, no. 4, pp. 279–291, 2007.

[100] G. D. Kusuma, U. Manuelpillai, M. H. Abumaree, M. D. Pertile, S. P. Brennecke, and B. Kalionis, "Mesenchymal stem cells reside in a vascular niche in the decidua basalis and are absent in remodelled spiral arterioles," *Placenta*, vol. 36, no. 3, pp. 312–321, 2015.

[101] C. Holmes and W. L. Stanford, "Concise review: stem cell antigen-1: expression, function, and enigma," *Stem Cells*, vol. 25, no. 6, pp. 1339–1347, 2007.

[102] K. E. Hatzistergos, S. Selem, W. Balkan, and J. M. Hare, *Cardiac Stem Cells: Biology and Therapeutic Applications*, Elsevier Inc, 2019.

[103] S. Morikawa, Y. Mabuchi, K. Niibe et al., "Development of mesenchymal stem cells partially originate from the neural crest," *Biochemical and Biophysical Research Communications*, vol. 379, no. 4, pp. 1114–1119, 2009.

[104] P. M. Glumac and A. M. LeBeau, "The role of CD133 in cancer: a concise review," *Clinical and Translational Medicine*, vol. 7, no. 1, Article ID 18, 2018.

[105] M. Doshmanziari, S. Shirian, M.-R. Kouchakian et al., "Mesenchymal stem cells act as stimulators of neurogenesis and synaptic function in a rat model of Alzheimer's disease," *Heliyon*, vol. 7, no. 9, Article ID e07996, 2021.

[106] B. Bakondi, I. S. Shimada, A. Perry et al., "CD133 identifies a human bone marrow stem/progenitor cell sub-population with a repertoire of secreted factors that protect against stroke," *Molecular Therapy*, vol. 17, no. 11, pp. 1938–1947, 2009.

[107] Y.-S. Fu, Y.-T. Shih, Y.-C. Cheng, and M.-Y. Min, "Transformation of human umbilical mesenchymal cells into neurons in vitro," *Journal of Biomedical Science*, vol. 11, no. 5, pp. 652–660, 2004.

[108] M. Khaki, A. H. Salmanian, H. Abtahi, A. Ganji, and G. Mosayebi, "Mesenchymal stem cells differentiate to endothelial cells using recombinant vascular endothelial growth factor-A," *Reports of Biochemistry and Molecular Biology*, vol. 6, no. 2, pp. 144–150, 2018.

[109] C. Sun, L. Wang, H. Wang et al., "Single-cell RNA-seq highlights heterogeneity in human primary Wharton's jelly mesenchymal stem/stromal cells cultured in vitro," *Stem Cell Research & Therapy*, vol. 11, no. 1, pp. 1–16, 2020.

[110] A. T. Lauvrud, P. Kelk, M. Wiberg, and P. J. Kingham, "Characterization of human adipose tissue-derived stem cells with enhanced angiogenic and adipogenic properties," *Journal of Tissue Engineering and Regenerative Medicine*, vol. 11, no. 9, pp. 2490–2502, 2017.

[111] A. C. Bowles, D. Kouroupis, M. A. Willman, C. Perucca Orfei, A. Agarwal, and D. Correa, "Signature quality attributes of CD146+ mesenchymal stem/stromal cells correlate with high therapeutic and secretory potency," *Stem Cells*, vol. 38, no. 8, pp. 1034–1049, 2020.

[112] M. Matsui, T. Kobayashi, and T. W. Tsutsui, "CD146 positive human dental pulp stem cells promote regeneration of dentin/pulp-like structures," *Human Cell*, vol. 31, no. 2, pp. 127–138, 2018.

[113] W. K. Ong, C. S. Tan, K. L. Chan et al., "Identification of specific cell-surface markers of adipose-derived stem cells from subcutaneous and visceral fat depots," *Stem Cell Reports*, vol. 2, no. 2, pp. 171–179, 2014.

[114] C. Pontikoglou, A. Langonné, M. A. Ba et al., "CD200 expression in human cultured bone marrow mesenchymal stem cells is induced by pro-osteogenic and pro-inflammatory cues," *Journal of Cellular and Molecular Medicine*, vol. 20, no. 4, pp. 655–665, 2016.

[115] Y. Zhu, Y. Yang, Y. Zhang et al., "Placental mesenchymal stem cells of fetal and maternal origins demonstrate different therapeutic potentials," *Stem Cell Research & Therapy*, vol. 5, no. 2, 2014.

[116] S. James, J. Fox, F. Afsari et al., "Multiparameter analysis of human bone marrow stromal cells identifies distinct immunomodulatory and differentiation-competent subtypes," *Stem Cell Reports*, vol. 4, no. 6, pp. 1004–1015, 2015.

[117] A. G. Kay, J. M. Fox, J. P. Hewitson et al., "CD317-positive immune stromal cells in human, mesenchymal stem cell," *Populations Frontiers in Immunology*, vol. 13, 2022.

[118] M. H. Jiang, G. Li, J. Liu et al., "Nestin+ kidney resident mesenchymal stem cells for the treatment of acute kidney ischemia injury," *Biomaterials*, vol. 50, pp. 56–66, 2015.

[119] J. Huang, R. Deng, W. Li, M. Jiang, A. P. Xiang, and X. Zhang, "$Nestin^+$ mesenchymal precursors generate distinct spleen stromal cell subsets and have immunomodulatory function," *International Journal of Molecular Sciences*, vol. 23, no. 19, Article ID 11819, 2022.

[120] Z. X. Yang, Z.-B. Han, Y. R. Ji et al., "CD106 identifies a subpopulation of mesenchymal stem cells with unique immunomodulatory properties," *PLoS One*, vol. 8, no. 3, Article ID 12, Article ID e59354, 2013.

[121] W. Du, X. Li, Y. Chi et al., "VCAM-1+ placenta chorionic villi-derived mesenchymal stem cells display potent pro-angiogenic activity," *Stem Cell Research & Therapy*, vol. 7, no. 1, pp. 1–13, 2016.

[122] Y. Wei, L. Zhang, Y. Chi et al., "High-efficient generation of VCAM-1+ mesenchymal stem cells with multidimensional superiorities in signatures and efficacy on aplastic anaemia mice," *Cell Prolif.*, vol. 53, no. 8, pp. 1–14, 2020.

[123] L. Ma, Z. Huang, D. Wu, X. Kou, X. Mao, and S. Shi, "CD146 controls the quality of clinical grade mesenchymal stem cells from human dental pulp," *Stem Cell Research & Therapy*, vol. 12, no. 1, pp. 1–16, 2021.

[124] N. Espagnolle, F. Guilloton, F. Deschaseaux, M. Gadelorge, L. Sensébé, and P. Bourin, "CD146 expression on mesenchymal stem cells is associated with their vascular smooth muscle commitment," *Journal of Cellular and Molecular Medicine*, vol. 18, no. 1, pp. 104–114, 2014.

[125] D. Kouroupis, S. M. Churchman, D. McGonagle, and E. A. Jones, "The assessment of CD146-based cell sorting and

telomere length analysis for establishing the identity of mesenchymal stem cells in human umbilical cord," *F1000Research*, vol. 3, Article ID 126, 2014.

[126] S. Wangler, U. Menzel, Z. Li et al., "CD146/MCAM distinguishes stem cell subpopulations with distinct migration and regenerative potential in degenerative intervertebral discs," *Osteoarthritis and Cartilage*, vol. 27, no. 7, pp. 1094–1105, 2019.

[127] A. S. Leroyer, M. G. Blin, R. Bachelier, N. Bardin, M. Blot-Chabaud, and F. Dignat-George, "CD146 (cluster of differentiation 146): an adhesion molecule involved in vessel homeostasis," *Arteriosclerosis, Thrombosis, and Vascular Biology*, vol. 39, no. 6, pp. 1026–1033, 2019.

[128] N. Bardin, F. Anfosso, J.-M. Massé et al., "Identification of CD146 as a component of the endothelial junction involved in the control of cell–cell cohesion," *Blood*, vol. 98, no. 13, pp. 3677–3684, 2001.

[129] D. Baksh, R. Yao, and R. S. Tuan, "Comparison of proliferative and multilineage differentiation potential of human mesenchymal stem cells derived from umbilical cord and bone marrow," *Stem Cells*, vol. 25, no. 6, pp. 1384–1392, 2007.

[130] A. Tormin, O. Li, J. C. Brune et al., "CD146 expression on primary nonhematopoietic bone marrow stem cells is correlated with in situ localization," *Blood*, vol. 117, no. 19, pp. 5067–5077, 2011.

[131] X. Li, W. Guo, K. Zha et al., "Enrichment of $CD146^+$ adipose-derived stem cells in combination with articular cartilage extracellular matrix scaffold promotes cartilage regeneration," *Theranostics*, vol. 9, no. 17, pp. 5105–5121, 2019.

[132] K. B. Van Landuyt, E. A. Jones, D. McGonagle, F. P. Luyten, and R. J. Lories, "Flow cytometric characterization of freshly isolated and culture expanded human synovial cell populations in patients with chronic arthritis," *Arthritis Research & Therapy*, vol. 12, no. 1, Article ID R15, 2010.

[133] S. Huang, V. Y. L. Leung, D. Long et al., "Coupling of small leucine-rich proteoglycans to hypoxic survival of a progenitor cell-like subpopulation in Rhesus Macaque intervertebral disc," *Biomaterials*, vol. 34, no. 28, pp. 6548–6558, 2013.

[134] L. Harkness, W. Zaher, N. Ditzel, A. Isa, and M. Kassem, "CD146/MCAM defines functionality of human bone marrow stromal stem cell populations," *Stem Cell Research & Therapy*, vol. 7, no. 1, pp. 1–14, 2016.

[135] Z. Ye, C. Zhang, T. Tu et al., "Wnt5a uses CD146 as a receptor to regulate cell motility and convergent extension," *Nature Communications*, vol. 4, no. 1, pp. 1–11, 2013.

[136] Y. Shen, J. Zhu, Q. Liu, S. Ding, X. Dun, and He J. Up-Regulation, "Up-regulation of CD146 in schwann cells following peripheral nerve injury modulates schwann cell function in regeneration," *Frontiers in Cellular Neuroscience*, vol. 15, Article ID 743532, 2021.

[137] U. Lendahl, L. B. Zimmerman, and R. D. G. McKay, "CNS stem cells express a new class of intermediate filament protein," *Cell*, vol. 60, no. 4, pp. 585–595, 1990.

[138] A. Bernal and L. Arranz, "Nestin-expressing progenitor cells: function, identity and therapeutic implications," *Cellular and Molecular Life Sciences*, vol. 75, no. 12, pp. 2177–2195, 2018.

[139] E. Park and A. N. Patel, "Changes in the expression pattern of mesenchymal and pluripotent markers in human adipose-derived stem cells," *Cell Biology International*, vol. 34, no. 10, pp. 979–984, 2010.

[140] S. Méndez-Ferrer, T. V. Michurina, F. Ferraro et al., "Mesenchymal and haematopoietic stem cells form a unique bone marrow niche," *Nature*, vol. 466, no. 7308, pp. 829–834, 2010.

[141] S. Pinho, J. Lacombe, M. Hanoun et al., "PDGFRα and CD51 mark human $Nestin^+$ sphere-forming mesenchymal stem cells capable of hematopoietic progenitor cell expansion," *Journal of Experimental Medicine*, vol. 210, no. 7, pp. 1351–1367, 2013.

[142] J. Isern, B. Martín-Antonio, R. Ghazanfari et al., "Self-renewing human bone marrow mesenspheres promote hematopoietic stem cell expansion," *Cell Reports*, vol. 3, no. 5, pp. 1714–1724, 2013.

[143] D. Lu, Y. Liao, S.-H. Zhu et al., "Bone-derived Nestin-positive mesenchymal stem cells improve cardiac function via recruiting cardiac endothelial cells after myocardial infarction," *Stem Cell Research & Therapy*, vol. 10, no. 1, pp. 1–15, 2019.

[144] Z. Yin, J.-J. Hu, L. Yang et al., "Single-cell analysis reveals a nestin+ tendon stem/progenitor cell population with strong tenogenic potentiality," *Sci Adv.*, vol. 2, no. 11, pp. 1–15, 2016.

[145] R. M. Hoek, S. R. Ruuls, C. A. Murphy et al., "Down-regulation of the macrophage lineage through interaction with OX_2 (CD200)." *Science*, vol. 290, no. 5497, pp. 1768–1771, 2000.

[146] L. Li, Y. L. Tian, C. F. Shi, H. Zhang, and Z. Zhou, "Over-expression of CD200 predicts poor prognosis in cutaneous squamous cell carcinoma," *Medical Science Monitor*, vol. 22, pp. 1079–1084, 2016.

[147] J.-X. Chen, L.-P. Mei, B.-G. Chen et al., "Over-expression of CD200 predicts poor prognosis in MDS," *Leukemia Research*, vol. 56, pp. 1–6, 2017.

[148] M. Pietilä, S. Lehtonen, E. Tuovinen et al., "CD200 positive human mesenchymal stem cells suppress TNF-alpha secretion from CD200 receptor positive macrophage-like cells," *PLoS One*, vol. 7, no. 2, Article ID e31671, 2012.

[149] M. Rostovskaya, K. Anastassiadis, and X.-M. Shi, "Differential expression of surface markers in mouse bone marrow mesenchymal stromal cell subpopulations with distinct lineage commitment," *PLoS One*, vol. 7, no. 12, Article ID 51221, 2012.

[150] H. J. Kim, K.-W. Kim, Y.-R. Kwon, B.-M. Kim, and Y.-J. Kim, "Forced expression of CD200 improves the differentiation capability and immunoregulatory functions of mesenchymal stromal cells," *Biotechnology Letters*, vol. 40, no. 9-10, pp. 1425–1433, 2018.

[151] N. M. Castrechini, P. Murthi, N. M. Gude et al., "Mesenchymal stem cells in human placental chorionic villi reside in a vascular Niche," *Placenta*, vol. 31, no. 3, pp. 203–212, 2010.

[152] C. Cerutti and A. J. Ridley, "Endothelial cell–cell adhesion and signaling," *Experimental Cell Research*, vol. 358, no. 1, pp. 31–38, 2017.

[153] C.-M. Wang, Z. Guo, Y.-J. Xie et al., "Co-treating mesenchymal stem cells with IL-1β and TNF-α increases VCAM-1 expression and improves post-ischemic myocardial function," *Molecular Medicine Reports*, vol. 10, no. 2, pp. 792–798, 2014.

[154] M. Hoffman, "The tissue factor pathway and wound healing," *Seminars in Thrombosis and Hemostasis*, vol. 44, no. 2, pp. 142–150, 2018.

[155] R. P. Araldi, B. C. Prezoto, V. Gonzaga et al., "Advanced cell therapy with low tissue factor loaded product NestaCell® does not confer thrombogenic risk for critically ill COVID-19 heparin-treated patients," *Biomedicine & Pharmacotherapy*, vol. 149, Article ID 112920, 2022.

[156] S. Miltenyi, W. Müller, W. Weichel, and A. Radbruch, "High gradient magnetic cell separation with MACS," *Cytometry*, vol. 11, pp. 231–238, 1990.
[157] K. R. Bowles, J. T. C. W., L. Qian, B. M. Jadow, A. M. Goate, and W. Hu, "Reduced variability of neural progenitor cells and improved purity of neuronal cultures using magnetic activated cell sorting," *PLoS One*, vol. 14, no. 3, Article ID e0213374, 2019.
[158] J. Pan and J. Wan, "Methodological comparison of FACS and MACS isolation of enriched microglia and astrocytes from mouse brain," *Journal of Immunological Methods*, vol. 486, Article ID 112834, 2020.
[159] C. R. Muratore, P. Srikanth, D. G. Callahan, T. L. Young-Pearse, and M. Dottori, "Comparison and optimization of hiPSC forebrain cortical differentiation protocols," *PLoS One*, vol. 9, no. 8, Article ID e105807, 2014.
[160] C. Cheng, D. M. Fass, K. Folz-Donahue, M. E. MacDonald, and S. J. Haggarty, "Highly expandable human iPS cell-derived neural progenitor cells (NPC) and neurons for central nervous system disease modeling and high-throughput screening," *Current Protocols in Human Genetics*, vol. 92, no. 1, pp. 1–21, 2017.
[161] C. Y. Fong, G. S. L. Peh, K. Gauthaman, and A. Bongso, "Separation of SSEA-4 and TRA-1-60 labelled undifferentiated human embryonic stem cells from a heterogeneous cell population using magnetic-activated cell sorting (MACS) and fluorescence-activated cell sorting (FACS)," *Stem Cell Reviews and Reports*, vol. 5, no. 1, pp. 72–80, 2009.
[162] B. A. Sutermaster and E. M. Darling, "Considerations for high-yield, high-throughput cell enrichment: fluorescence versus magnetic sorting," *Scientific Reports*, vol. 9, no. 1, pp. 1–9, 2019.
[163] A. R. Silini, R. Di Pietro, I. Lang-Olip et al., "Perinatal derivatives: where do we stand? a roadmap of the human placenta and consensus for tissue and cell nomenclature," *Frontiers in Bioengineering and Biotechnology*, vol. 8, Article ID 610544, 2020.
[164] R. Hass, C. Kasper, S. Böhm, and R. Jacobs, "Different populations and sources of human mesenchymal stem cells (MSC): a comparison of adult and neonatal tissue-derived MSC," *Cell Communication and Signaling*, vol. 9, no. 1, pp. 1–14, 2011.
[165] M. Ogawa, P. Pharr, and T. Suda, "Stochastic nature of stem cell functions in culture," *Progess Clin Biol Res.*, vol. 184, pp. 11–19, 1985.
[166] D. Zipori, "The stem state: mesenchymal plasticity as a paradigm," *Current Stem Cell Research & Therapy*, vol. 1, no. 1, pp. 95–102, 2006.
[167] M. F. Pittenger, A. M. Mackay, S. C. Beck et al., "Multilineage potential of adult human mesenchymal stem cells," *Science*, vol. 284, no. 5411, pp. 143–147, 1999.
[168] Y. Jiang, B. Vaessen, T. Lenvik, M. Blackstad, M. Reyes, and C. M. Verfaillie, "Multipotent progenitor cells can be isolated from postnatal murine bone marrow, muscle, and brain," *Experimental Hematology*, vol. 30, no. 8, pp. 896–904, 2002.
[169] Y. Jiang, B. N. Jahagirdar, R. L. Reinhardt et al., "Pluripotency of mesenchymal stem cells derived from adult marrow," *Nature*, vol. 418, no. 6893, pp. 41–49, 2002.
[170] C. D. Keene, X. R. Ortiz-Gonzalez, Y. Jiang, D. A. Largaespada, C. M. Verfaillie, and W. C. Low, "Neural differentiation and incorporation of bone marrow-derived multipotent adult progenitor cells after single cell transplantation into blastocyst stage mouse embryos," *Cell Transplantation*, vol. 12, no. 3, pp. 201–213, 2003.

12. Pisemne oświadczenia autorów prac tworzących zbiór

PLATFORMA BADAŃ TRANSLACYJNYCH
W ZAKRESIE MEDYCYNY REGENERACYJNEJ

Instytut Medycyny Doświadczalnej i Klinicznej
im. M. Mossakowskiego PAN
02-106 Warszawa, ul. Pawińskiego 5

Mgr Agnieszka Smolińska

E-mail: asmolinska@imdik.pan.pl

22.02.2024 r., Warszawa

Oświadczenie kandydata

Niniejszym poświadczam swój wkład w postanie następujących publikacji:

1. **Kaminska, A.**; Wedzinska, A.; Kot, M.; Sarnowska, A. *Effect of Long-Term 3D Spheroid Culture on WJ-MSC*. Cells 2021, 10, 719. Doi: 10.3390/ cells10040719,

Wkład obejmuje:
Planowanie i wykonywanie większości doświadczeń, przeprowadzenie izolacji i dalszej hodowli komórek macierzystych, wykonanie testów fizjologicznych, oznaczenie ekspresji genów, wykonanie barwień immunocytochemicznych, przeprowadzenie analizy statystycznej otrzymanych wyników, przygotowanie pierwotnej wersji manuskryptu, wraz z rycinami oraz dyskusji z recenzentami pracy przed jej publikacją.

2. **Smolinska, A.**; Chodkowska, M., Kominek, A.; Janiec, J.; Piwocka, K.; Sulejczak, D.; Sarnowska, A,. *Stemness properties of SSEA-4+ subpopulation isolated from heterogenous Wharton jelly mesenchymal stem/stromal cells*. Frontiers of Cell and Developmental Biology 2024, Doi: 10.3389/fcell.2024.1227034,

Wkład obejmuje:
Planowanie i wykonywanie większości doświadczeń, przeprowadzenie izolacji i dalszej hodowli komórek macierzystych, oznaczenie ekspresji genów, wykonanie barwień immunocytochemicznych, oznaczenie sekretomu, przeprowadzenie analizy statystycznej otrzymanych wyników oraz przygotowanie pierwotnej wersji manuskryptu, wraz z rycinami oraz dyskusji z recenzentami pracy przed jej publikacją.

3. **Smolinska, A.**, Bzinkowska, A; Rybkowska, P.; Chodkowska, M.; Sarnowska, A.. *Promising markers in the context of mesenchymal stem/stromal cells subpopulations with unique properties*. Stem Cells International 2023, Doi: 10.1155/2023/1842958,

Wkład obejmuje:
Przygotowanie pierwszej wersji manuskryptu i rycin, rozdzielenie pracy między innymi współautorami, przygotowanie następujących rozdziałów: *Introduction*, fragmenty *Markers for Stem Population within MSCs* dotyczące SSEA-3, SSEA-4, CD271, CD133, fragmenty *Markers for Specialized Populations within MSCs* dotyczące CD142, CD317, *Challenges in Cell Separation of Specific Subpopulations*, *Further Perspectives*; redakcja manuskryptu, dyskusja z recenzentami pracy przed jej publikacją.

Agnieszka Smolińska

PLATFORMA BADAŃ TRANSLACYJNYCH
W ZAKRESIE MEDYCYNY REGENERACYJNEJ

Instytut Medycyny Doświadczalnej i Klinicznej
im. M. Mossakowskiego PAN
02-106 Warszawa, ul. Pawińskiego 5

Dr hab. Anna Sarnowska

E-mail: asarnowska@imdik.pan.pl

22.02.2024 r., Warszawa

Oświadczenie współautora

Niniejszym poświadczam swój wkład w postanie następujących publikacji:

1. Kaminska, A.; Wedzinska, A.; Kot, M.; **Sarnowska, A.** *Effect of Long-Term 3D Spheroid Culture on WJ-MSC*. Cells 2021, 10, 719. Doi: 10.3390/ cells10040719,

Wkład obejmuje:

Sformułowanie koncepcji pracy, planowanie doświadczeń, nadzór merytoryczny nad realizacją działań badawczych, analiza wyników, nadzór nad pisaniem manuskryptu oraz jego końcowa akceptacja, odpowiedzi na uwagi redakcyjne, prowadzenie korespondencji z redakcją.

2. Smolinska, A.; Chodkowska, M., Kominek, A.; Janiec, J.; Piwocka, K.; Sulejczak, D.; **Sarnowska, A,**. *Stemness properties of SSEA-4+ subpopulation isolated from heterogenous Wharton jelly mesenchymal stem/stromal cells*. Frontiers of Cell and Developmental Biology 2024. Doi: 10.3389/fcell.2024.1227034,

Wkład obejmuje:

Sformułowanie koncepcji pracy, planowanie doświadczeń, nadzór merytoryczny nad realizacją działań badawczych, analiza wyników, nadzór nad pisaniem manuskryptu oraz jego końcowa akceptacja, odpowiedzi na uwagi redakcyjne, prowadzenie korespondencji z redakcją.

3. Smolinska, A., Bzinkowska, A; Rybkowska, P.; Chodkowska, M.; **Sarnowska, A.**. *Promising markers in the context of mesenchymal stem/stromal cells subpopulations with unique properties*. Stem Cells International 2023, Doi: 10.1155/2023/1842958,

Wkład obejmuje:

Nadzór nad pisaniem manuskryptu oraz jego końcowa akceptacja, przygotowanie podrozdziału: *Mesenchymal Plasticity as a Manifestation of Stochastic Stem Cell Model*, odpowiedzi na uwagi redakcyjne, prowadzenie korespondencji z redakcją.

Wyrażam zgodę na wykorzystanie publikacji w postępowaniu doktorskim mgr Agnieszki Smolińskiej.

Anna Sarnowska

PLATFORMA BADAŃ TRANSLACYJNYCH
W ZAKRESIE MEDYCYNY REGENERACYJNEJ

Instytut Medycyny Doświadczalnej i Klinicznej
im. M. Mossakowskiego PAN
02-106 Warszawa, ul. Pawińskiego 5

Mgr inż. Magdalena Chodkowska

E-mail: mchodkowska@imdik.pan.pl

22.02.2024 r., Warszawa

Oświadczenie współautora

Niniejszym poświadczam swój wkład w postanie następujących publikacji:

1. Smolinska, A.; **Chodkowska, M.,** Kominek, A.; Janiec, J.; Piwocka, K.; Sulejczak, D.; Sarnowska, A,. *Stemness properties of SSEA-4+ subpopulation isolated from heterogenous Wharton jelly mesenchymal stem/stromal cells*. Frontiers of Cell and Developmental Biology 2024
Doi: 10.3389/fcell.2024.1227034,

Wkład obejmuje:

Przeprowadzenie izolacji i dalszej hodowli komórek macierzystych pozyskanych z tkanki tłuszczowej, asystowanie przy przeprowadzanych doświadczeniach.

2. Smolinska, A., Bzinkowska, A; Rybkowska, P.; **Chodkowska, M.**; Sarnowska, A.. *Promising markers in the context of mesenchymal stem/stromal cells subpopulations with unique properties*. Stem Cells International 2023, Doi: 10.1155/2023/1842958,

Wkład obejmuje:

Przygotowanie następujących rozdziałów: fragmenty *Markers for Stem Population within MSCs* dotyczące GD2 i Sca-1, fragment *Markers for Specialized Populations within MSCs* dotyczący CD200, CD317, zgłaszanie uwag do manuskryptu.

Wyrażam zgodę na wykorzystanie publikacji w postępowaniu doktorskim mgr Agnieszki Smolińskiej.

Magdalena Chodkowska

Magdalena Chodkowska

PLATFORMA BADAŃ TRANSLACYJNYCH
W ZAKRESIE MEDYCYNY REGENERACYJNEJ

Instytut Medycyny Doświadczalnej i Klinicznej
im. M. Mossakowskiego PAN
02-106 Warszawa, ul. Pawińskiego 5

Mgr inż. Aleksandra Bzinkowska (panieńskie: Wędzińska)

E-mail: abzinkowska@imdik.pan.pl

19.02.2024 r., Warszawa

Oświadczenie współautora

Niniejszym poświadczam swój wkład w postanie następujących publikacji:

1. Kaminska, A.; **Wedzinska, A**.; Kot, M.; Sarnowska, A. *Effect of Long-Term 3D Spheroid Culture on WJ-MSC*. Cells 2021, 10, 719. Doi: 10.3390/ cells10040719,

Wkład obejmuje:

Przeprowadzenie izolacji i dalszej hodowli komórek macierzystych, asystowanie przy wykonywanych doświadczeniach, wykonanie testów fizjologicznych.

2. Smolinska, A., **Bzinkowska, A**; Rybkowska, P.; Chodkowska, M.; Sarnowska, A.. *Promising markers in the context of mesenchymal stem/stromal cells subpopulations with unique properties*. Stem Cells International 2023, Doi: 10.1155/2023/1842958,

Wkład obejmuje:

Przygotowanie pierwszej wersji manuskryptu i rycin, rozdzielenie pracy między innymi współautorami, przygotowanie następujących podrozdziałów: *Introduction*, *Markers for Specialized Populations within MSCs* dotyczące CD146, Nestyny i VCAM, oraz *Further Perspectives*, redakcja manuskryptu, dyskusja z recenzentami pracy przed jej publikacją.

Wyrażam zgodę na wykorzystanie publikacji w postępowaniu doktorskim mgr Agnieszki Smolińskiej.

Aleksandra Bzinkowska

Bzinkowska

PLATFORMA BADAŃ TRANSLACYJNYCH
W ZAKRESIE MEDYCYNY REGENERACYJNEJ

Instytut Medycyny Doświadczalnej i Klinicznej
im. M. Mossakowskiego PAN
02-106 Warszawa, ul. Pawińskiego 5

Mgr Paulina Rybkowska

E-mail: prybkowska@imdik.pan.pl

19.02.2024 r., Charlottesville, Stany Zjednoczone

Oświadczenie kandydata

Niniejszym poświadczam swój wkład w postanie następujących publikacji:

1. Smolinska, A., Bzinkowska, A; **Rybkowska, P.**; Chodkowska, M.; Sarnowska, A.. *Promising markers in the context of mesenchymal stem/stromal cells subpopulations with unique properties*. Stem Cells International 2023, Doi: 10.1155/2023/1842958,

Wkład obejmuje:
Przygotowanie następujących rozdziałów: fragmenty *Markers for Stem Population within MSCs* dotyczące CD49-F i CD349zgłaszanie uwag do manuskryptu.

Wyrażam zgodę na wykorzystanie publikacji w postępowaniu doktorskim mgr Agnieszki Smolińskiej.

Paulina Rybkowska

Paulina Rybkowska

ZAKŁAD BIOINŻYNIERII KOMÓREK MACIERZYSTYCH

Instytut Medycyny Doświadczalnej i Klinicznej
im. M. Mossakowskiego PAN
02-106 Warszawa, ul. Pawińskiego 5

Dr hab. Marta Kot

E-mail: mkot@imdik.pan.pl

19.02.2024 r., Warszawa

Oświadczenie współautora

Niniejszym poświadczam swój wkład w postanie następujących publikacji:

1. Kaminska, A.; Wedzinska, A.; **Kot, M.**; Sarnowska, A. *Effect of Long-Term 3D Spheroid Culture on WJ-MSC*. Cells 2021, 10, 719. Doi: 10.3390/ cells10040719,

Wkład obejmuje:

Nadzór nad eksperymentami związanymi z oznaczeniem ekspresji genów, przeprowadzenie analizy statystycznej wyników dotyczących ekspresji genów oraz zgłoszenie uwag do manuskryptu.

Wyrażam zgodę na wykorzystanie publikacji w postępowaniu doktorskim mgr Agnieszki Smolińskiej.

dr hab. n. med.
Marta Kot
Marta Kot

ZAKŁAD FIZJOLOGII DOŚWIADCZALNEJ

Instytut Medycyny Doświadczalnej i Klinicznej
im. M. Mossakowskiego PAN
02-106 Warszawa, ul. Pawińskiego 5

Dr hab. Dorota Sulejczak

E-mail: dsulejczak@imdik.pan.pl

22.02.2024 r., Warszawa

Oświadczenie współautora

Niniejszym poświadczam swój wkład w postanie następujących publikacji:

1. Smolinska, A.; Chodkowska, M., Kominek, A.; Janiec, J.; Piwocka, K.; **Sulejczak, D**.; Sarnowska, A,. *Stemness properties of SSEA-4+ subpopulation isolated from heterogenous Wharton jelly mesenchymal stem/stromal cells*. Frontiers of Cell and Developmental Biology 2024, Doi: 10.3389/fcell.2024.1227034,

Wkład obejmuje:

Oznaczenie sekretomu i analiza uzyskanych wyników.

Wyrażam zgodę na wykorzystanie publikacji w postępowaniu doktorskim mgr Agnieszki Smolińskiej.

KIEROWNIK
Zakładu Farmakologii Doświadczalnej
Dr hab. Dorota Gołąbek-Sulejczak

Dorota Sulejczak

PRACOWNIA CYTOMETRII

Instytut Biologii Doświadczalnej im. Marcelego Nenckiego PAN

02-093 Warszawa, ul. Pasteura 3

Mgr Jakub Janiec

E-mail: kubaj8@gmail.com

22.02.2024 r., Warszawa

Oświadczenie współautora

Niniejszym poświadczam swój wkład w postanie następujących publikacji:

1. Smolinska, A.; Chodkowska, M., Kominek, A.; **Janiec, J.;** Piwocka, K.; Sulejczak, D.; Sarnowska, A,. *Stemness properties of SSEA-4+ subpopulation isolated from heterogenous Wharton jelly mesenchymal stem/stromal cells*. Frontiers of Cell and Developmental Biology 2024, Doi: 10.3389/fcell.2024.1227034,

Wkład obejmuje:

Przeprowadzenie sortowania komórkowego.

Wyrażam zgodę na wykorzystanie publikacji w postępowaniu doktorskim mgr Agnieszki Smolińskiej.

Jakub Janiec

PRACOWNIA CYTOMETRII

Instytut Biologii Doświadczalnej im. Marcelego Nenckiego PAN

02-093 Warszawa, ul. Pasteura 3

Mgr Agata Kominek

E-mail: akominek@nencki.edu.pl

22.02.2024 r., Warszawa

Oświadczenie współautora

Niniejszym poświadczam swój wkład w postanie następujących publikacji:

2. Smolinska, A.; Chodkowska, M., **Kominek, A.**; Piwocka, K.; Sulejczak, D.; Sarnowska, A,. *Stemness properties of SSEA-4+ subpopulation isolated from heterogenous Wharton jelly mesenchymal stem/stromal cells*. Frontiers of Cell and Developmental Biology 2024 Doi: 10.3389/fcell.2024.1227034,

Wkład obejmuje:

Przeprowadzenie sortowania komórkowego, pomoc w odpowiedzi na pytania recenzentów.

Wyrażam zgodę na wykorzystanie publikacji w postępowaniu doktorskim mgr Agnieszki Smolińskiej.

A. Kominek

Agata Kominek

22.02.2024 r., Warszawa

Oświadczam, że udział dr hab. K. Piwockiej w publikacji Smolinska, A.; Chodkowska, M., Kominek, A.; Janiec, J.; **Piwocka, K.**; Sulejczak, D.; Sarnowska, A,. *Stemness properties of SSEA-4+ subpopulation isolated from heterogenous Wharton jelly mesenchymal stem/stromal cells*. Frontiers of Cell and Developmental Biology 2024, Doi: 10.3389/fcell.2024.1227034,

Obejmował nadzór nad przeprowadzeniem sortowania komórkowego.

Mgr Agnieszka Smolińska

A Smolińska